72-1029

TRANSNUCLEAR WEST

May 18, 2001
DCS-TNW0105-12
RMG-01-019

Mr. Timothy Kobetz
Project Manager, Spent Fuel Project Office
U.S. Nuclear Regulatory Commission
11555 Rockville Pike
Rockville, MD 20852

Subject: Response to Request for Additional (RAI) Information and Submittal of Revision 1 of Advanced NUHOMS® Storage System Application (TAC No. L23203).

References:
1. Request for Additional Information Regarding Approval of Advanced NUHOMS® Storage System (TAC No. L23203), March 5, 2001.
2. Application for Approval of Advanced NUHOMS® Storage System Application, dated September 29, 2000 (TAC No. L23203).

Dear Mr. Kobetz:

Transnuclear West Inc., (TN West) herewith submits the responses to the RAI (Reference 1) and Revision 1 of the proprietary version of the Advanced NUHOMS® Storage System Application. This package includes:

1. Affidavit for withholding proprietary Information
2. Responses to the RAI (except Question 3-6)
3. Response to RAI Question 3-6
4. Verification and Validation Report for LS-DYNA Version 950 (c), Revision 1 (Proprietary)
5. "Sensitivity and Parametric Evaluations of Significant Aspects of Burnup Credit for PWR Spent Fuel Packages"; Report ORNL/TM-12973
6. Advanced NUHOMS SAR, Revision 1 (Proprietary).

This submittal includes proprietary documents. The proprietary material may not be used for any purpose other than to support your staff's review of the application. In accordance with 10 CFR 2.790, we are providing an affidavit specifically requesting that you withhold this proprietary information from public disclosure.

NMSS01 Prop

Transnuclear West Inc.
39300 Civic Center Drive, Suite 280, Fremont, CA 94538
Phone: 510-795-9800 • Fax: 510-744-6002

Revision 1 of the SAR reflects the changes resulting from the subject RAI responses. TN West has also revised AHSM and DSC drawings included in SAR section 1.5.2 as discussed in response to RAI Question 1-1. In addition, this revision updates the shielding and criticality analysis presented in the SAR to address the effect of uncertainty (manufacturing tolerance) in initial enrichment of SC and MOX fuel. Revision 1 supercedes the previous version submitted with Reference 2 in its entirety.

Also enclosed herewith is the Revision 1 of the non-proprietary version of the Advanced NUHOMS® Storage System Application.

Please contact Mr. U. B. Chopra (510-744-6053) or me (510-744-6020) if you require any additional information in support of this submittal.

Sincerely,

Robert M. Grenier
President and Chief Operating Officer

Docket 72-1029

Enclosures:
1. Responses to the RAI and Revision 1 of the proprietary version of the Advanced NUHOMS® Storage System Application (10 copies).
2. Responses to the RAI and Revision 1 of the non-proprietary version of the Advanced NUHOMS® Storage System Application (4 copies).

cc: File: SCE-01-0007.01

TRANSNUCLEAR WEST

ATTACHMENT 1

AFFIDAVIT

AFFIDAVIT PURSUANT
TO 10 CFR 2.790

Transnuclear West Inc.)
State of California) SS.
County of Alameda)

I, Robert M. Grenier, depose and say that I am President and Chief Operating Officer of Transnuclear West Inc., duly authorized to make this affidavit, and have reviewed or caused to have reviewed the information which is identified as proprietary and referenced in the paragraph immediately below. I am submitting this affidavit in conformance with the provisions of 10 CFR 2.790 of the Commission's regulations for withholding this information.

The information for which proprietary treatment is sought is contained in the documents included in Attachment 4 and 6 of this submittal and as listed below:

- Verification and Validation Report for LS-DYNA Version 950 (c), Revision 1.
- Advanced NUHOMS SAR, Revision 1 (Proprietary).

These sections of the document have been appropriately designated as proprietary.

I have personal knowledge of the criteria and procedures utilized by Transnuclear West Inc. in designating information as a trade secret, privileged or as confidential commercial or financial information.

Pursuant to the provisions of paragraph (b) (4) of Section 2.790 of the Commission's regulations, the following is furnished for consideration by the Commission in determining whether the information sought to be withheld from public disclosure, included in the above referenced document, should be withheld.

1) The information sought to be withheld from public disclosure is design drawings and supporting analysis of NUHOMS® Cask, which is owned and has been held in confidence by Transnuclear West Inc.

2) The information is of a type customarily held in confidence by Transnuclear West Inc. and not customarily disclosed to the public. Transnuclear West Inc. has a rational basis for determining the types of information customarily held in confidence by it.

3) The information is being transmitted to the Commission in confidence under the provisions of 10 CFR 2.790 with the understanding that it is to be received in confidence by the Commission.

4) The information, to the best of my knowledge and belief, is not available in public sources, and any disclosure to third parties has been made pursuant to regulatory provisions or proprietary agreements which provide for maintenance of the information in confidence.

5) Public disclosure of the information is likely to cause substantial harm to the competitive position of Transnuclear West Inc. because:

a) A similar product is manufactured and sold by competitors of Transnuclear West Inc.

b) Development of this information by Transnuclear West Inc. required thousands of man-hours and hundreds of thousands of dollars. To the best of my knowledge and belief, a competitor would have to undergo similar expense in generating equivalent information.

c) In order to acquire such information, a competitor would also require considerable time and inconvenience related to the development of a design and analysis of a dry spent fuel storage system.

d) The information required significant effort and expense to obtain the licensing approvals necessary for application of the information. Avoidance of this expense would decrease a competitor's cost in applying the information and marketing the product to which the information is applicable.

e) The information consists of description of the design and analysis of a dry spent fuel storage and transportation system, the application of which provides a competitive economic advantage. The availability of such information to competitors would enable them to modify their product to better compete with Transnuclear West Inc., take marketing or other actions to improve their product's position or impair the position of Transnuclear West's product, and avoid developing similar data and analyses in support of their processes, methods or apparatus.

f) In pricing Transnuclear West's products and services, significant research, development, engineering, analytical, licensing, quality assurance and other costs and expenses must be included. The ability of Transnuclear West's competitors to utilize such information without similar expenditure of resources may enable them to sell at prices reflecting significantly lower costs.

Further the deponent sayeth not.

MGC1 SHANNON L. CHRISTENSEN MGC1
COMM. # 1264196
NOTARY PUBLIC-CALIFORNIA
ALAMEDA COUNTY
COMM. EXP. MAY 18, 2004

Robert M. Grenier
President and Chief Operating Officer
Transnuclear West Inc.

Subscribed and sworn to me before this 18th day of May, 2001, by Robert M. Grenier.

Shannon L. Christensen
Notary Public

TRANSNUCLEAR WEST

ATTACHMENT 2

RAI RESPONSES

Attachment 2

RESPONSE TO REQUEST FOR ADDITIONAL INFORMATION
TRANSNUCLEAR WEST INC., TAC NO. L23203

Chapter 1 General Information

Question 1-1

Specify which transfer casks will be used to perform on-site transfer of the dry shielded canister (DSC).

Section 1.2.1.3.1 of the Safety Analysis Report (SAR) states that "the OS-197, MP-187, or any other NRC licensed transfer or transportation cask of sufficient size and payload capacity is acceptable for use with the Advanced NUHOMS® System subject to a site specific safety evaluation prior to the first usage." However, the SAR does not provide a methodology used to evaluate that the transfer or transportation cask has the appropriate shielding, heat transfer, structural integrity, and criticality characteristics to be used with the DSC-24PT. The application references previous evaluations of the OS-197 and MP-187 performed for the Standardized NUHOMS® System and the Rancho Seco site-specific application but does not demonstrate that those evaluations bound the DSC-24PT1.

This information is required by the staff to assess compliance with 10 CFR 72.24(c)(3), to assess whether all structures, systems, and components important to safety will satisfy the design bases with an adequate margin of safety.

Response Question 1-1

The SAR has been revised to specify that only the OS-197 transfer cask will be used for onsite transfer of the 24PT1-DSC. SAR Sections 1.1, 1.2 and 1.2.1.3.1 have been revised to delete references to transfer casks other than the OS-197. See responses to RAI Questions 4-1, 5-2, 6-2, 6-3 and 12-1 for specific changes regarding transfer cask configuration for the associated SAR Chapters. In addition, a review of the entire SAR was performed and SAR Sections 3.1, 3.6, 9.1, 9.2 and 12.1.1 were also revised to remove reference to alternate casks.

TN West has revised the AHSM and DSC drawings included in SAR section 1.5.2 to enhance fabricability, correct minor interference errors, and provide clarification to the notes shown on these drawings. A brief description of the changes implemented and a justification for each change is provided herewith. Change number 6 addresses RAI Question 7-1; all other changes were initiated as a result of TN West internal review.

BRIEF DESCRIPTION OF CHANGES IMPLEMENTED TO DSC DRAWINGS NUH-05-4010 and NUH-05-4010NP:

1. Editorial changes to notes to clarify the intent/ meaning of note. Added notes as required by the inclusion of additional details. Permitted the substitution of alternate material specifications and fabrication of grapple ring and grapple plate from a single forging/plate.
2. Revised the Vent and Siphon block configuration and increased siphon tube to 1 1/4" diameter to provide larger passages for better draining and drying of cavity.
3. Reduced size of lifting lug to remove interference with top spacer disc.
4. Revised guide sleeve poison length and location to cover active fuel length under all drop conditions. Added bottom spacer plate for interface with bottom spacer disc.
5. Clarified threaded lengths for support rods
6. Added alternate details for bottom closure to provide options for fabrication. Revised weld detail for inner bottom cover to shell.
7. Revised the minimum thickness of the outer top cover from 1.24" to 1.31".

BRIEF DESCRIPTION OF CHANGES IMPLEMENTED TO AHSM DRAWINGS NUH-03-4011 and NUH-03-4011NP:

8. Editorial changes were made to the notes. Detailed changes are shown on attached sheets.
9. Corrected the material specification for the support rail plate in the DSC Support Structure.
10. Increased width and radius of rear wall recess and extended the length of the heat shields.
11. Clarified primary reinforcement requirements for the door and added flag note to permit a composite door structure using the 1/2" plate (in lieu of reinforcement behind the plate).
12. Added flag note to the DSC Support Structure to permit construction holes in the interior stiffeners.

REASON FOR CHANGE & TECHNICAL JUSTIFICATION:

1. Editorial changes to clarify the meaning of notes. Added Note 9 to specify that the weld contours shown on the drawing are permissive and not required by the design. Removed over specification from notes and added notes 37 through 45 to clarify the added details.
2. Vent and siphon block passages were revised to give additional flow capacity and restore the intent of the dog leg to minimize shine paths.
3. There was a minor interference between the bottom of the lifting lug and the top spacer disc in the worst-case tolerance condition. Removing a small amount from the bottom of the lug resolves this issue.
4. Guide sleeve details were reviewed and revised to provide adequate support for

the ends of the guide sleeve and to locate poison plates where they covered the worst case location for the active fuel to be in compliance with the criticality calculations.

5. Fixed the potential interference between support rods and the threaded portions of the top and bottom spacer sleeves.
6. Added alternate details for the bottom closure to allow flexibility for fabricator to pick a solution that best meets the shop capabilities. Increased the thickness of the inner bottom cover plate to 1.24" min./ 2.0" max. to ensure that the plate will carry the defined ASME loads without assistance from the bottom shield plug. This permits the classification of the shield plug and outer bottom cover plate as ASTM materials. Also, permitted the use of a forging for the inner bottom cover plate to move the Class C tee joint weld to a Class B circumferential weld that is easier to inspect than the existing joint. Because of the increased plate thickness revised the weld callout for the Tee (existing) joint to allow any of the configurations permitted by Figure-NB-4243-1 of the ASME code. This will allow fabricator to minimize the weld volume if this detail is used.
7. The outer top cover plate thickness assumed in the supporting calculations is 1.31".
8. Editorial changes clarify the meaning of notes.
9. The material specification is corrected for the support rail plate to reflect the finish product. Nitronic® 60 is a brand name material that initially complies to ASTM A240, after it is cold rolled to meet the specified hardness it no longer meets all ASTM A240 properties. Therefore, specifying just the brand name and desired hardness is sufficient.
10. The rear wall recess is increased to simplify fabrication and improve clearance to the DSC. The change results in a consistent cross-section along the full length of the AHSM cavity. The heat shield is increased in length through this area. The net affect is an improvement in thermal performance of the AHSM. This change does not affect the reported results in the SAR based on a review of the shielding, thermal and structural calculations.
11. The flag note permits the 1/2" door plate to act as a tension element in a composite design. Such a design eliminates the primary reinforcement on the inner face.
12. The design of the DSC Support Structure requires only one crossbeam (in its installed configuration). Temporary crossbeam bracing at the other three rail stiffener locations is desirable to facilitate fabrication and installation. The bracing permits shop control and accuracy in the alignment of the rails and provides a means of maintaining rail alignment during shipment and installation of the DSC Support Structure. The bracing may be welded or bolted to the stiffeners. Bolted braces would be completely removed just leaving holes in the stiffeners. Welded bracing would be cut and the welds and/or ends of welded bracing could remain in place.

Chapter 2 Principle Design Criteria

Question 2-1

Remove the statement in Sections 2.1.1 and 3.1.1.1, that refer to the storage of 'Greater than Class C' (GTCC) waste inside an advanced NUHOMS® Systems (AHSM).

Approval to store GTCC will not be addressed in a Certificate of Compliance, issued in accordance with 10 CFR Part 72, for the Advanced NUHOMS® Storage System. This changes is required by the staff to confirm compliance with 10 CFR 72.2.

Response to Question 2-1

SAR Sections 2.1.1 and 3.1.1.1 have been revised to delete reference to storage of GTCC waste.

Question 2-2

Discuss design features of the Advanced NUHOMS® system to enhance decontamination and decommissioning.

The SAR did not contain sufficient detail with regard to decontamination and decommissioning of the Advanced NUHOMS® System. Include a discussion of the effect of the contamination limits stated in Section 12.5.2.4.b on potential off-site releases such as through the outlet vent at the top of the AHSM. The discussion should also include a statement on what affect the contamination level will have on the ability to decontaminate and decommission the concrete AHSM, the ISFSI pad, and the surrounding soils. Consideration of decontamination and decommissioning activities is required under 10 CFR 72.130 and 72.236(i).

Response to Question 2-2

The NUHOMS® system incorporates several design features to limit contamination of the NUHOMS® system components. These include:

- The transfer cask and dry shielded canister are designed and fabricated to limit contamination by specification of appropriate surface finishes.
- The dry shielded canister outer surface is also isolated from the spent fuel pool by filling the annular gap between the canister and the cask with clean water and sealing this volume at the top with an inflatable seal. This limits the ingress of pool water and contamination of the canister outer surface.

By limiting contamination of the 24PT1-DSC outer surface, contamination of the horizontal storage module is virtually eliminated. Contamination that may be present on the canister surface will be protected by the AHSM from direct exposure to the elements (wind, rain, etc.) and will therefore limit any potential release of removable

contamination. The probability of any removable contamination being entrapped in the AHSM air flow path and released outside the AHSM is considered extremely small given the low flow velocities characteristic of natural ventilation cooling. The effect of the contamination limits specified in SAR Section 12.5.2.4.c is addressed in the response to RAI Question 12-5.

The effect of these limits on decommissioning of the Advanced NUHOMS® system components is negligible. However, additional decontamination at the time of decommissioning may be required to allow free release of the canister (canister decommissioning is likely to occur offsite at a DOE facility), AHSM, ISFSI pad and surrounding soil. The spread of contamination from the canister surface, if any should occur, to the AHSM, ISFSI pad and surrounding soil is limited to very small areas of the ASHM internal surface. Performance of final decontamination for free release at the time of decommissioning is considered more appropriate since these decontamination activities will be performed under minimal radiation field conditions and would therefore be consistent with ALARA practices.

Chapter 3 Structural

Question 3-1

Justify the 392 degrees F maximum concrete temperature for accident conditions given in Table 4.1-5. This temperature exceeds the allowable range of 0 - 350 degrees F stated in the table.

Note 2 in Table 4.1-5 states testing will be performed to document that concrete compression strength will be greater than that assumed in structural analyses. The tests are to be on the exact concrete mix and are to acceptably demonstrate the level of strength reduction which needs to be applied, and to show that the increased temperatures do not cause deterioration of the concrete either with or without load. However, there is no discussion of what type of testing will be performed and why the testing is sufficient to confirm performance of the AHSM. The test details are required for the staff to assess compliance with 10 CFR 72.146 (b).

Response to Question 3-1

As described in the SAR, the following acceptance criteria apply to the concrete materials used in the construction of the AHSM:

- Satisfy ASTM C 33 requirements and other requirements referenced in ACI 349 for aggregates, and
- Have demonstrated a coefficient of thermal expansion (tangent in temperature range of 70°F to 100°F) no greater than 6x10-6 in/in/°F, or be one, or a mixture of the following minerals: limestone, dolomite, marble, basalt, granite, gabbro, or rhyolite.
- If concrete temperatures of general or local areas in normal conditions do not exceed 200°F and in off-normal conditions do not exceed 225°F, in addition to the above list of acceptable aggregates, quartz sands and sandstone sands are also acceptable as a fine aggregate only.

The calculated temperatures within the concrete AHSM demonstrate that the concrete meets ACI 349 and NUREG 1536 temperature criteria for all normal and off-normal cases. There are three areas of the AHSM predicted to experience temperatures in excess of 350°F during a 40 hour duration blocked vent accident that require evaluation for acceptability to ACI 349-97 criteria, as modified by NUREG 1536. The subject areas are as follows:

1. An area of 101" (along the 24PT1-DSC longitudinal axis) x 36" x 2.2" deep on each of the side walls. These areas are centered about the 24PT1-DSC centroid projected horizontally onto the two side walls.
2. An area of 85" (along the 24PT1-DSC longitudinal axis) x 52" x 4" deep immediately above the heat shield opening into the vent system. This area is centered about the 24PT1-DSC centroid projected onto the roof. This area is the

top part of the base block with vent openings, which is not required for transferring structural loads.

3. An area 6"x 2"x 1.5"deep located on the top surface of the front vent shielding block under the longitudinal axis of the 24PT1-DSC. Other areas of the shield block that are less than 350°F provide support for the 24PT1-DSC support structure steel.

The proposed elevated temperature testing for the AHSM design mix for the storage block will satisfy the following:

- A minimum of two sets of five 6" x 12" cylinders shall be made from a test batch,
- One set of cylinders will be used as the control (room temperature) set; the second set will be heated to 400 °F at a rate similar to that predicted by the thermal analysis for the high temperature areas. The maximum temperature will be held at a steady state for a time of at least 36 hours to exceed the anticipated effects of the blocked vent case,
- The heated cylinders shall be examined for soundness prior to strength tests. The concrete shall not show signs of spalling, cracks and/or loss of cement bond to aggregate due to the elevated temperatures.
- Each set of cylinders will be broken using standard compressive strength test methods,
- The average test results for the high temperature set, reduced by two standard deviations, shall not be less than 4,500 psi. Computation of the standard deviation shall be consistent with applicable methods within ACI 214. If a proposed design mix does not have sufficient test data to compute a standard deviation, then an equivalent standard deviation shall be computed consistent with trial batch requirements specified within ACI 318.

The above tests are for concrete cylinders heated without load. Since the normal condition compressive stress in the volumes of concrete that exceed 350°F during accident conditions is relatively low, testing cylinders under load is not necessary to simulate service conditions. Relevant published test reports [3-1.1] indicate that testing cylinders under load produces higher compressive strength test results than identical cylinders tested without load. Therefore, heating and testing unrestrained cylinders (without load) is adequate and conservative.

This testing will be re-performed if the concrete mix is changed by the concrete fabricator or as a result of a change in concrete fabricators.

As an alternative to the above testing requirements, the AHSM structural analysis may be revised by defining the volume of concrete exceeding 350°F as *non-structural* and excluding these areas from the blocked vent accident structural analyses (or modeling the areas with negligible structural properties). The location of primary reinforcement within these volumes would be adjusted to provide appropriate reinforcement for the reduced thickness *structural* concrete. Standard temperature and shrinkage reinforcement would then be provided for the *non-structural* concrete in order to ensure integrity for shielding.

Implementation of this design alternative would eliminate the need to perform elevated temperature testing of concrete since the *structural* concrete would be at or below 350°F.

SAR Table 4.1-5, Note 2 has been revised to incorporate a summary of the above discussion.

[3-1.1] M. S. Abrams, Compressive Strength of Concrete at Temperatures to 1600°F, ACI Special Publication SP25 (Paper SP 25-2), American Concrete Institute, Detroit, MI (1971).

Question 3-2

Justify the use of the selected friction coefficients between the AHSM and the storage pad.

The friction coefficients determine the AHSM rocking/tipping and sliding responses. The AHSM sliding analyses are performed using a range of friction coefficients between the cask and pad surfaces. The range varies between 0.3 and 0.7. However, it is not clear why these values were selected or if they are conservative. This information is required by the staff to assess compliance with 10 CFR 72.122(b)(2).

Response to Question 3-2

The selected range of friction coefficients is judged to be broad enough to adequately represent concrete sliding behavior considering potential variations in concrete-to-concrete surface conditions. The lower bound is intended to maximize sliding response while the upper bound is intended to maximize rocking response. The basis for the selected range is as follows:

- Available results of tests performed to determine the friction coefficient between concrete and steel surfaces show static friction coefficients of approximately 0.39 to 0.58 [3-2.1]. The data presented in [3-2.1] is for coated steel plates resting on a broom finished concrete pad. The friction coefficient for concrete-to-concrete is expected to be higher than for steel-to-concrete. Based on these considerations a reasonable "best estimate" approximation of the static coefficient of friction for concrete-to-concrete is judged to be 0.6. Also, the range is broadened from 0.6 to 0.7 to cover possible uncertainties.

- A reduction factor of 2/3 of the static value is taken as the dynamic friction coefficient, which yields a 0.4 friction coefficient (2/3x0.6). An additional reduction of 25% is taken to cover other possible uncertainties (e.g. wet conditions [3-2.2]), thus broadening the range to 0.3.

To demonstrate that the sliding displacements do not change significantly, TNW has performed two additional LS-DYNA analyses using 0.2 and 0.8 friction coefficients. These analyses further broaden the range of friction coefficients to 0.2 at the lower end and 0.8 at the upper end. Although the 0.2 friction coefficient is considered unrealistically low for concrete-to-concrete (typically applicable for steel-to-steel

surfaces) it is provided here to represent a bounding result. This lower value is also not supported by available test data of steel-to-concrete friction tests as reported in [3-2.1].

The maximum sliding displacement obtained from the 0.2 analysis case is 47.9 inches. This compares with a maximum of 41.9 inches for the 0.3 case. This comparison indicates that a change in friction coefficient from 0.3 to 0.2 causes only a 14% change in maximum sliding displacement response.

The 0.8 friction coefficient case is reported as an upper bound static coefficient of friction in [3-2.2], validating the use of 0.7 as a reasonable upper bound for dynamic friction value. The analysis for the 0.8 case yields a maximum sliding displacement of 35.1 inches, compared with 39.3 for the 0.7 case. As in the 0.7 friction case, the rocking uplift for the 0.8 friction case remains negligibly small. These two cases are included in revised SAR Table 11.2-2.

The calculated sliding displacement remains substantially less than the 120 inches space allowed in the ISFSI design for sliding of the AHSM.

No changes to the SAR have been made with respect to this RAI Question response.

[3-2.1] Duke Power Co., McGuire Nuclear Station, "Steel on Concrete-Coefficient of Friction Testing for Dry Cask Storage Project," dated January 20, 1999
[3-2.2] PCI Design Handbook, Fifth Edition, Precast/Prestressed Concrete Institute.

Question 3-3

Provide the following clarifications for Table 11.2-2 of the SAR.

For Case 2, evaluate how a group of three AHSMs would respond to a design basis earthquake when only one is loaded with a 24PT1-DSC.

Explain why Cases 3 and 4 are more sensitive to the friction coefficient than Cases 1 and 2. For Cases 3 and 4 when the friction coefficient changes from 0.7 to 0.3 the X-displacement increases from 11.9 inches to 32.4 inches, however, similar friction coefficient changes for Cases 1 and 2 only result in an increase from 39.3 inches to 41.9 inches.

This information is required by the staff to assess compliance with 10 CFR 72.122(b)(2).

Response to Question 3-3

An additional analysis has been performed as requested using the Case 2 analysis model with only one AHSM loaded with a 24PT1-DSC. The resulting maximum sliding displacements are summarized in SAR Table 11.2-2 as Analysis Case 13. As shown in SAR Table 11.2-2, the maximum sliding displacements for the fully loaded (3 AHSMs loaded with 24PT1-DSCs, Case 2) and one AHSM loaded case (Cases 13) are essentially the same.

For completeness, an additional analysis using Case 11 analysis model (AHSMs loaded with one 24PT1-DSC, 0.7 friction coefficient with construction tolerances) was also analyzed with a 0.3 coefficient of friction. The resulting and maximum displacements are summarized in SAR Table 11.2-2 analysis Case 14. As shown in SAR Table 11.2-2, the maximum sliding displacement (ΔX_{max}) for the fully loaded AHSMs is slightly larger than for the one AHSM loaded case (Cases 2 and 14, respectively) and, thus, is controlling.

Based on the analyses performed, it is concluded that the effect of one AHSM loaded versus a fully loaded group of three AHSMs with a 0.3 friction factor does not significantly affect the AHSM sliding displacement response.

In the analyses results reported in Table 11.2-2 of the SAR, Case 1 and Case 2 used time history set 1 (TH1), whereas Case 3 and Case 4 used time history set 2 (TH2). These two time histories sets were developed from different recordings of large magnitude earthquakes using spectral matching techniques that preserve the time domain characteristics of the natural record. Time history set 1, TH1, was developed using the Magnitude 7.6, 1999 Taiwan, Chi-Chi earthquake. Time history set 2, TH2, was developed using the Magnitude 7.4 1978 Tabas earthquake. Since the starting seeds used for the spectral matching are different, the resulting time histories will have different characteristics.

The X-direction component (H1) for time history sets TH1 and TH2 are shown in SAR Figures 11.2-2 and 11.2-5, respectively. It can be observed from SAR Figure 11.2-2 that the TH1 displacement time history is asymmetric or one-sided, e.g., the maximum displacements generally occur on one side of the time history baseline. This characteristic of the record produces a ratcheting effect in the sliding response of the AHSM, e.g., a continuous monotonic increase with time in sliding displacement of the AHSM in a single direction. These responses are shown in SAR Figure 11.2-11 (Case 1, 0.7 friction coefficient) and SAR Figure 11.2-16 (Case 2, 0.3 friction coefficient). As expected, Case 2 (with the lower, 0.3 friction coefficient case) exhibits more back-and-forth sliding and a larger maximum sliding displacement. However, the ratcheting effect is more pronounced for the higher friction coefficient case (Case 1, with 0.7 friction coefficient). The end result is that the maximum sliding displacements are not significantly different between Case 1 and Case 2 (39.3 inches for the 0.7 case versus 41.9 inches for the 0.3 case).

The X-direction component (H1) displacement time history TH2 (used for Case 3 and Case 4) is shown in SAR Figure 11.2-5. Time history set TH2 does not exhibit the same characteristics as TH1, e.g., the positive versus negative direction displacements are about the same magnitude. The resulting sliding displacements for time history TH2 are shown in SAR Figure 11.2-17 (Case 3, 0.7 friction coefficient) and SAR Figure 11.2-18 (Case 4, 0.3 friction coefficient). It can be observed that for this time history the sliding response is primarily a function of the friction coefficient, e. g., a larger sliding displacement is obtained for the 0.3 friction case than for the 0.7 friction case. The lack of a significant ratcheting effect does not mask the effect of the friction coefficient, as is the case for time history TH1.

Question 3-4

Discuss why the three sets of time histories each have a total duration of 40 seconds.

The discussion should include statements on what the affects a longer duration would have on the time histories or a statement stating why 40 seconds is sufficient for the time histories. This information is required by the staff to assess compliance with 10 CFR 72.122(b)(2).

Response to Question 3-4

The design ground motions for the Advanced NUHOMS® System are based on NRC R.G. 1.60 spectrum shape anchored to ZPA accelerations of 1.5g (horizontal) and 1.0g (vertical). These high ZPA acceleration levels and spectral characteristics suggest ground motions representative of large magnitude earthquakes ($M \geq 7.5$) and close epicentral distances (≤ 10 km).

The selected recorded motions used as starting seed for spectral matching generally reflect the magnitude, distance implied by the target spectrum. Given that the spectral matching procedure used for generation of the time histories preserves the time domain characteristics of the recorded motion, the duration of the matched time histories is consistent with the recorded durations.

To assess the reasonableness and adequacy of the duration of the input "design" ground motions, the 5% to 75% Husid durations of Arias Intensities are used as a measure of comparison and benchmarking with durations predicted by empirical models based on Western US recorded motions [3-4.1]. The 5% to 75% Arias Intensity is a measure of the duration of strong shaking of significance to stiff structures. The method for ensuring the time histories have sufficient duration is described in Reference [3-4.2]. Table 3-4.1 shows the 5% to 75% duration for ground motions based on the Western US empirical model, for magnitude 7.5 and above. Table 3-4.2 shows the 5% to 75% Arias Intensity duration for the spectrally matched time histories used for design of the Advanced NUHOMS® System. It can be observed that the strong motion durations are consistent with or conservatively exceed those of the empirical model and thus represent large magnitude earthquakes. Additionally the total duration of 40 seconds provides additional margin of conservatism for non-linear sliding response.

Table 3-4.1: 5% to 75% Husid Durations of Arias Intensity - Empirical Model

Magnitude	Component	Site Condition	Rupture Distance (km)	Strong Motion Duration Median (sec)		
				-1 σ	Median	+1σ
7.5	H	Rock	0 – 10	5.21	9.16	16.12
7.5	V	Rock	0 – 10	5.04	8.13	13.11
7.75	H	Rock	0 – 10	6.47	11.38	20.00
7.75	V	Rock	0 – 10	5.91	9.53	15.38
7.50	H	Soil	0 – 10	5.57	9.98	17.55
7.50	V	Soil	0 – 10	5.73	9.24	14.90
7.75(1)	H	Soil	0 – 10	6.93	12.19	21.45
7.75(1)	V	Soil	0 – 10	6.60	10.65	17.17

Notes :

1. Extrapolated data

Table 3-4.2: 5% to 75% Husid Durations of Arias Intensity – Advanced NUHOMS Time Histories

Time History Set	Component	Strong Motion Duration Based on Arias Intensity (sec)
TH1	H1	16.67
	H2	21.32
	V	19.33
TH2	H1	13.74
	H2	12.88
	V	13.25
TH3	H1	9.82
	H2	12.53
	V	11.16

Notes:

1. TH1 is based on the 1999 Taiwan Chi-Chi earthquake M=7.6
2. TH2 is based on the 1978 Tabas earthquake M=7.4
3. TH3 is based on the 1992 Landers/Lucern M=7.3

As additional information to address an example of a Western US ISFSI site with a seismic time history of 80 seconds total duration, a specific LS-DYNA analysis has been performed.

Consistent with the criteria specified in Section 12.4.2.2 of the Advanced NUHOMS® SAR, the time histories provided correspond to the amplified response spectra obtained at the center of gravity elevation of the AHSM, and include the effects of soil-structure interaction (SSI) of the ISFSI pad. The details of the SSI analysis is provided in the response to RAI Question 3-6. A seismic time history of 80 seconds duration was developed for the response spectra of the AHSM center of gravity (cg) shown in Figures 6-9a to 6-9c provided in the response to RAI Question 3-6 (Attachment 3). Time histories were not directly used from the SSI analysis because the AHSM cg response spectra are the results of an envelope of various soil cases and nodal locations. Also, the SSI analysis used a seismic input of 40 seconds duration due to the limitations of the SASSI program. Development of the time history followed the criteria given by the Standard Review Plan [3-4.3], Section 3.7 for response spectra enveloping, strong motion duration, statistical correlation and power spectral density enveloping. The time history components combined two records from the Taiwan 1999 (Chi-Chi) earthquake as the seeds to obtain a total duration of 80 seconds. The acceleration time history plots are shown in Figure 3-4.1. Amplified peak accelerations are 0.77g on the horizontal directions and 0.55g in the vertical direction.

The LS-DYNA analysis is performed using the same model described in Chapter 11 of Advanced NUHOMS® SAR. A 0.3 value for the static and dynamic coefficient of friction is selected as a reasonable lower bound to maximize sliding displacements.

The results of the analysis indicate that maximum sliding displacements are on the order of 13.7 inches (1.1 ft) in the X-direction and 19.1 inches (1.6 ft) in the Y-direction. The maximum vertical relative displacement is negligible (0.01 inches). These maximum values are significantly less than the maximum sliding displacements obtained from all the analyses cases considered in the SAR (on the order of 48 inches, SAR Table 11.2-2). Furthermore, they are bounded with significant margin by the clear distance of 10 ft. allowed for sliding around the row of AHSMs.

No changes to the SAR have been made with respect to this RAI Question response.

[3-4.1] Silva, W.J., N. Abrahamson, G. Toro, C. Costantino (1997). "Description and validation of the stochastic ground motion model." Submitted to Brookhaven National Laboratory, Associated Universities, Inc. Upton, New York.

[3-4.2] Kennedy, R.P., Short, S.A., Merz, K.L., Tokarz, F.J., Idriss, I.M., Power, M.S., and Sadigh, K. (1984). "Engineering characterization of ground motion, Task I: Effects of characteristics of free-field motion on structural response." Prepared for U.S. Nuclear Regulatory Commission. NUREG/CR-3805, vol.1.

[3-4.3] NUREG-0800, "Standard Review Plan for the Review of Safety Analysis Reports for Nuclear Power Plants," Sections 3.7.1 and 3.7.2, Revision 2.

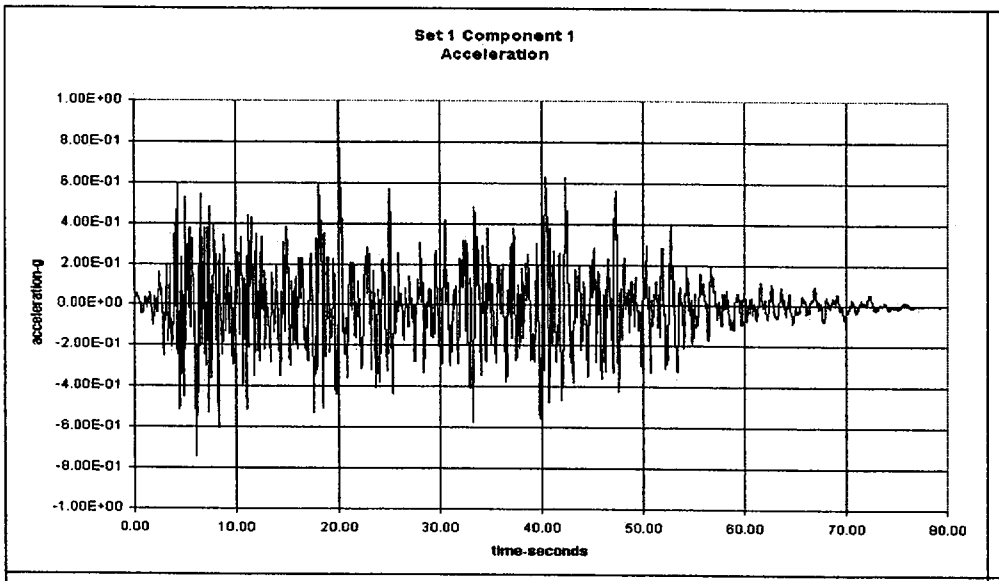

Horizontal Acceleration Time History Component S1H1

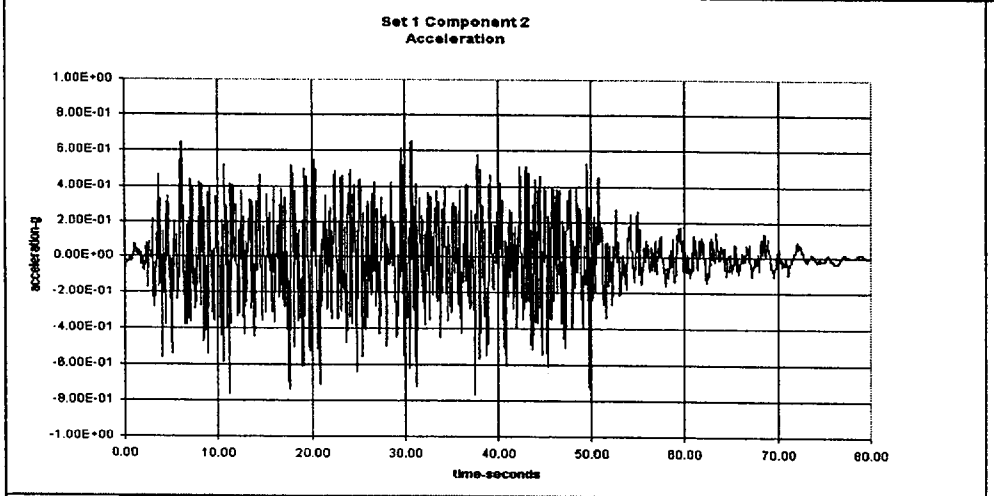

Horizontal Acceleration Time History Component S1H2

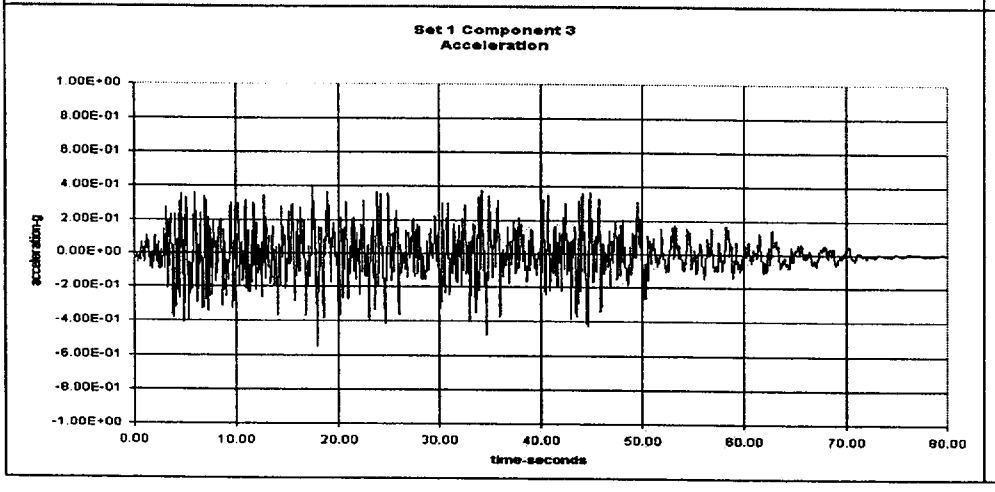

Horizontal Acceleration Time History Component S1V

Figure 3-4.1 - 80 Second Acceleration Time Histories

Question 3-5

Justify the use of a short term fuel cladding temperature limit of 1058 degrees F for stainless steel cladding in lieu of 806 degrees F as previously approved by the staff, or revise the allowable maximum temperature for the stainless steel cladding to 806 degrees F.

Section 3.5.1.2.1 of the SAR references EPRI TR-106440 "Evaluation of Expected Behavior of LWR Stainless Steel Fuel in Long-Term Dry Storage" as the basis of the long term cladding temperature limit. However, this reference also states that dry storage at temperatures above 806°F should be discouraged because of the increased potential to sensitize the stainless steel.

The justification should address the effect of sensitization on the stainless steel cladding integrity and retrievability of the fuel assembly at temperatures above the short term allowable fuel cladding temperature limits for stainless steel cladding of 806 degrees F.

Reference 3.33 of the SAR should also be provided along with a discussion on how the methods and data encompassed can be used to address the conclusions in Reference 3.30 of the SAR, specifically, that stress rupture by the development of a micron-sized pinhole leak is a possible failure mechanism for stainless steel cladding at temperatures above 806 degrees F. Issues that should be addressed include:

The fuel cladding material's microstructural properties and characterization after sensitization.

The material operating environment including maximum fuel rod internal pressure.

Fuel rod cladding susceptibility to the failure mechanism described in Reference 3.30 of the SAR during short term events.

Data and calculational methods, including applicable assumptions and codes, which address this failure mechanism.

This information is required by the staff to assess compliance with 10 CFR 72.236(f).

Response to Question 3-5

The Westinghouse 14x14 Stainless Steel Clad Fuel temperature limit has been revised to reflect a conservative maximum temperature of 806 °F. This temperature limit is based on EPRI TR-106440 for the sensitization of stainless steel at elevated temperatures in a non-inert environment. The 24PT1-DSC is inerted with helium for storage and transfer, so the use of non-inert temperature limit is conservative.

Since the Westinghouse 14x14 Stainless Steel Clad Fuel temperature limit has been revised to 806 °F, therefore the issues identified in this RAI Question related to stainless steel clad fuel temperature effects need not be evaluated further.

SAR Sections 3.5.1.2.2, Table 3.5-2, Table 4.1-4, Table 4.1-5, Table 4.4-7, Section 4.7.1 and Table 4.7-1 have been revised to reflect the 806 °F cladding temperature limit. SAR Reference 3.33 and associated data in Table 3.5-1 have been deleted.

In addition, SAR Table 4.4-7 has been revised to correct the maximum fuel clad temperature reported (for the 14 kW vacuum drying case).

Question 3-6

Provide a soil-structure interaction analysis that would be typical for a site deploying the Advanced NUHOMS® System.

The design basis response spectra of the Advanced NUHOMS® System design is based on the standard spectrum shape in NRC Regulatory Guide 1.60, "Design Response Spectra for Seismic Design of Nuclear Power Plants," Revision 1, 1973, anchored at 1.5g zero period acceleration for the horizontal direction. The vertical design spectrum is set at 2/3 of the horizontal over the entire frequency range. The horizontal and vertical spectra are specified at the top of the basemat.

Nonlinear analyses were performed in Chapter 11 of the SAR to determine the maximum sliding and rocking/tipping response of the AHSM during a design basis seismic event. These analyses were based on acceleration time histories from the Taiwan earthquake in 1999, the Landers/Lucern earthquake in 1992, and the Tabas earthquake in 1978. However, the staff requires the analysis including the soils and structure interactions, the methodologies and computer model, and the specific acceleration histories that envelope the parameters of a typical site. This is required for the staff to assess compliance with 10 CFR 72.122(b).

Note: The above question was restated in accordance with a communication from Mr. Steve Baggett (NRC) to Mr. U. B. Chopra (TN-West) via e-mail dated 4/18/01, 9:57 am, subject: "Reference RAI 3-6 for the Advanced NUHOMS design".

Response to Question 3-6

See Attachment 3 to the RAI Question Response transmittal letter for the response to this RAI.

Question 3-7

Demonstrate that the LS-DYNA computer program has been benchmarked against actual test data using a quality assurance program in accordance with 10 CFR Part 72, Subpart G, or justify the use of this program for non-linear seismic stability analyses.

This is required for the staff to assess compliance with 10 CFR 72.122(b).

Response to Question 3-7

The TN West Report documenting the Verification and Validation of the LS-DYNA program (TNW File No. QA040.0227, Revision 1) is provided as Attachment 4. Proprietary and non-proprietary copies of this report are provided. No revision of the SAR is required due to this RAI Question response.

Chapter 4 Thermal

Question 4-1

Specify which transfer casks will be used to perform on-site transfer of the dry shielded canister (DSC) and provide an analysis for each of the transfer cask designs to be used with the Advanced NUHOMS® System and provide design details or demonstrate why a previous analysis of the transfer casks bound its use with the 24PT1-DSC.

Section 1.2.1.3.1 of the SAR states that any NRC licensed transfer cask of sufficient size and payload capacity is acceptable for use. That statement has not been supported. The maximum heat load specified for the 24PT1-DSC is 14 kW. A previous calculation using a higher heat load for a different system may be bounding to determine the effects of that heat load on a transfer cask. However, the review is also focused on the response of the 24PT1-DSC components important to safety and the fuel cladding when subjected to the heat load and heat transfer characteristics associated with the system and particular transfer cask used. Additionally, Section 4 of the SAR provides an example which demonstrates that the MP 187 is not allowed for the content heat load in excess of 13.5 kW. This information is required by the staff to assess whether the system design can perform its function when subjected to the licensed content heat load under normal and accident conditions per 10 CFR 72.128(a).

Response to Question 4-1

See response to RAI Question 1-1. SAR Sections 4., 4.1.2 and 4.4.3.1 have been revised to remove references to casks other than the OS-197.

Question 4-2

Justify the assumption stated in Section 4.4.2.2 that the side and back surfaces of the AHSM should be modeled as adiabatic in order to simulate adjacent modules.

Applying the heat load generated in adjacent modules may be the more appropriate approach. The results of this calculation based on actual system arrangement will be used to determine compliance to 72.128(a).

Response to Question 4-2

Two adjacent modules with the same design basis heat load back to back or side to side result in no heat transfer between the modules due to symmetry of the heat loads and boundary conditions. Therefore, an adiabatic boundary condition is appropriate.

The thermal analysis of the AHSM and 24PT1-DSC shell is performed by using conservative assumptions. The use of side and back surfaces of the AHSM as adiabatic boundary conditions produces maximum component temperatures. This analysis is used to obtain maximum AHSM and 24PT1-DSC temperatures. To maximize the gradients in the AHSM concrete, for structural analysis of the AHSM, a module containing a design

basis heat load is modeled with adjacent modules empty. The maximum temperature cases are used to qualify materials and establish code allowables while the maximum gradient cases are used to calculate thermal stresses.

No SAR change has been made.

Question 4-3

When reformatting the SAR, ensure proper pagination.

Note that there are two pages identified as 4.1-3.

Response to Question 4-3

The pagination has been corrected in the section specified. Pagination of the remainder of the SAR was verified to be correct.

Question 4-4

Clarify actual Pu enrichments in mixed oxide (MOX) fuel descriptions.

Fissile Pu enrichments listed on Page 5.2-2 (2.78, 3.05, 3.25 w/o) are different from those listed as footnote (1) of Table 2.1-2 (2.81, 3.1, 3.31 fissile Pu w/o), and Table 6.2-2 (2.84, 3.1, 3.31- fissile Pu w/o = 3.30, 3.65, 3.85 - total Pu w/o). Also, include the minimum fissile Pu enrichments in Table 12.2-1. Information must be presented accurately and in sufficient detail for the staff to assess compliance with 10 CFR 72.24(c)(3).

Response to Question 4-4

The MOX fuel assemblies each contain fuel rods with different plutonium enrichments. Minimum enrichments are used for shielding analyses and maximum enrichments are used for criticality analyses. The corrected Pu enrichments are shown below.

Number of Fuel Rods	Minimum Fissile Pu Weight Percent	Maximum Fissile Pu Weight Percent	Total Pu Weight Percent
64	2.78	2.84	3.30
92	3.05	3.10	3.65
24	3.25	3.31	3.85

Maximum Fissile Pu Weight Percent values presented in Table 2.1-2 of the SAR have been revised. The enrichments specified in SAR Section 5 on page 5.2-2 of the SAR have been clarified by specifying them as minimum enrichments and providing the corresponding maximum enrichments. The minimum Fissile Pu enrichments, specified on page 5.2-2 of the SAR for use in the shielding analyses, as modified to address

enrichment uncertainty (see RAI Question 4-6 response), have also been included in Table 12.2-1. Figure 6.3-6 and Table 12.2-1 of the SAR have been revised to clarify that the Pu weight % specified is Fissile Pu weight %. The Fissile Pu Weight Percent values in SAR Table 6.2-2 are correct as presented.

Question 4-5

Include a discussion of MOX fuel He production effects on maximum nominal operating pressure and cladding failure.

Section 4.4.8 of the SAR refers to Table 4.4-9 and states that based on the information listed, the UO2 assemblies are bounding for the analysis. However, the SAR does not include a discussion of the MOX rod void volume, a plot of gas generation over time, including He, and cladding strength which would provide a complete characterization of the condition of the contents stored. This information is required by the staff to assess whether the fuel cladding is protected against degradation that could lead to gross ruptures in accordance with 10 CFR 71.122(h)(1).

Response to Question 4-5

A comparison of stainless steel clad fuel (SC) and mixed oxide fuel (MOX) parameters affecting the canister pressure analysis (fill pressure, fuel rod void volume, fission gas generation during operation and during fuel decay, and fuel cladding material strength) have been added to SAR Section 4.4.8 to clarify the basis for performance of the pressure analysis based on SC fuel only.

Question 4-6

Clarify that a maximum heat load of 14 kW bounds the allowed contents of the 24PT1-DSC.

Section 1.2.1.1 of the SAR states that the 24PT1-DSC is designed for a maximum heat load of 14 kW. However, the staff found that the maximum heat load, based on allowable contents, is 16 kW. This information is required by the staff to assess compliance with 10 CFR 72.24(d)(1).

Response to Question 4-6

The maximum heat load is specified in SAR Section 12.2.1.c as a specific limitation to be confirmed by a licensee prior to storage of fuel in the 24PT1-DSC. However, to eliminate the need for further analysis to determine the heat load, Table 12.2-4, Fuel Qualification Table, has been added to the SAR to specify burnup/enrichment/cooling time limits to ensure a heat load of $\leq$ 14 kW per 24PT1-DSC.

In conjunction with this fuel qualification table, the fuel enrichment specification in SAR Tables12.2-1, 12.2-2 and 12.2-4 have been revised to accommodate an uncertainty in the

enrichment specified. Revisions to enrichment values specified in SAR Sections 1.2.3, 2.1.1, Tables 2.1-1 and 2.1-2 have been revised. An analysis of the effects of these uncertainties have been added to the SAR in Sections 5.2.3 and 6.4.4. The effect of these uncertainties on criticality analysis results is addressed in SAR Sections 6.1 and 6.4.3.

Question 4-7

Justify the statement in Section 4.4.5 of the SAR that the conservative modeling approach precludes the necessity to perform thermal testing.

Section 4.4.5 of the SAR states that detailed, conservative evaluations were performed for heat transfer from the AHSM, OS 197 transfer cask and the 24PT1-DSC. However, as noted in RAI question 4-6 those evaluations could not be confirmed by the staff. In addition, the SAR did not provide design details for all transfer casks intended to be used with the 24PT1-DSC. This information is required by the staff to assess compliance with 10 CFR 72.128(a)(4).

Response to Question 4-7

Additional constraints have been imposed in new SAR Table 12.2-4 to ensure that the maximum heat load is maintained $\leq$ 14 kW, see RAI Question 4-6 response. The response to RAI Question 4-1 addresses the use of a single transfer cask (OS-197).

Question 4-8

Separately tabulate and provide all assumptions, including initial and boundary conditions, when describing component temperatures under normal, off-normal, and accident conditions.

Tables 4.1-3, 4, and 5, of the SAR assume different heat load assumptions that vary between 14 kW and 24 kW. As discussed in RAI question 4-6, it is not clear that assuming a 14 kW heat load is conservative. This information is required by the staff to assess compliance with 10 CFR 72.24(d)(1).

Response to Question 4-8

SAR Table 4.1-1 provides the ambient temperature and solar insolation values used for Normal, Off-Normal, Long Term Average, Accident and Fuel Building conditions. In accordance with Section 1.2.1.1, the maximum total decay heat load authorized for the 24PT1-DSC is 14.0 kW. Analyses at higher heat loads demonstrate the robustness of the system and may be utilized in future amendments to qualify higher heat load fuel.

SAR Table 4.1-6 is added to provide a summary of the limiting 24PT1-DSC heat loads and the corresponding ambient temperatures and insolation values assumed in the analysis of each major system component. Heat loads specified in SAR Tables 4.1-3, 4.1-4, 4.1-5 and 4.4-6 are deleted and a reference is provided to SAR Table 4.1-6.

Question 4-9

Explain why direct engulfment of the AHSM is unlikely and justify why any fire while the DSC is loaded in the AHSM is bounded by an engulfing fire around the transfer cask.

Section 11.2.4.1 of the SAR includes a discussion of the fire accident. A fire at the inlet of the AHSM may have a greater impact on the 24PT1-DSC than a fire engulfing the transfer cask and, therefore, should be addressed to determine reasonable assurance of adequate safety under normal and accident conditions. This information is required by the staff to assess compliance with 10 CFR 72.128(a).

Response to Question 4-9

Direct engulfment of the AHSM is unlikely because the source of combustible materials near the AHSM is limited to the quantity of fuel and hydraulic fluid associated with vehicles and equipment supporting Advanced NUHOMS® system operation and expansion. The most likely ignition sources would be associated with operation of manned equipment. Plant personnel are likely to be present should a fire occur and will ensure prompt detection and extinguishment of any fire. Therefore, the likelihood of an ignition source being present in the vicinity of the combustibles with the combustibles in an ignitable configuration (fuel/fluid leak) without plant personnel in the vicinity is extremely small. The AHSM inlet is 24" above the ground, precluding the flow of combustible liquid into the AHSM. Any flames or products of combustion would tend to rise rapidly and would have to pass through more than 8 feet of concrete ducting before reaching the canister. The high thermal mass of the concrete would absorb most of the associate heat. Therefore, the smaller, lower thermal mass, more accessible transfer cask represents the bounding fire case.

SAR Section 4.6.4 has been revised to provide additional discussion of the effects of a fire on the 24PT1-DSC stored in an AHSM.

Chapter 5 Shielding

Question 5-1

Describe how ^{59}Co impurities in the fuel assembly structural material and cladding were modeled in determining bounding source terms. Section 5.2 "Source Specification" does not detail how this material was accounted for in the design basis bounding source term for the stainless steel fuel cladding, fuel hardware, and Inconel materials described in Tables 5.2-2 through 5.2-6.

Independent NRC staff calculations using ^{59}Co impurity levels described in EPRI TR-104329 "Evaluation of Shielding Analysis Methods in Spent Fuel Cask Environments" show that this impurity may be important and could lead to significant non - conservatism in both the shielding and thermal source terms.

Alternatively, provide references which characterize the ^{59}Co impurity levels of the materials used to generate the design basis source term and compare those to the impurity levels described in EPRI TR 104329. This information is required under 10 CFR 72.236(d) and (f).

Response to Question 5-1

Additional text has been added to SAR Section 5.2 "Source Specification" to describe how all of the light elements, including ^{59}Co, are modeled in determining bounding source terms. Table 5.2-18 has also been added to provide the required elemental composition, including ^{59}Co.

Question 5-2

Provide shielding analyses for all loading and unloading configurations that will exist during operations involving the Advanced NUHOMS® System. Include descriptions and shielding analyses of each transfer cask that will be qualified to transfer or transport the 24PT1-DSC during the four "Loading Stages" described in Section 5.3.1.2.

Alternatively, provide a table describing and comparing the characteristics of each transfer cask qualified to transfer or transport the 24PT1-DSC. Include a discussion which contrasts each cask characteristic and describes how the analysis in Section 5.3.1.3 (shown by Table 5.1-1, Figure 5.1-4, and Figures 5.4-4 through 5.4-7) is conservative or bounding. Provide reference for the OS197 transfer cask (as stated in Section 5.3) as the analyzed condition and compare any applicable characteristics such as material types, shielding thickness, streaming paths, neutron absorbing materials and other applicable characteristics described in NUREG 1536 for any requested alternative transfer casks.

Update the remaining sections of the SAR (including providing specific reference to allowable transfer cask designs) which detail the allowable transfer casks used in the Advanced NUHOMS® System (including Section 12.4.3.3) as appropriate. Figures which

describe allowable transfer casks should reference specific casks (either submitted in response to this question or already documented at the NRC) and not general designs such as Figure 5.1-4.

Section 5 of the SAR does not describe all of the transfer casks that will be used in the operation of the Advanced NUHOMS® System. Further, the analysis does not explicitly state that the OS197 transfer cask is the basis for the transfer condition model or provide references to the applicable documents which contain OS197 specifications. The staff does not accept the use of transfer casks which are not analyzed and qualified for the Advanced NUHOMS® System. This information is required to show compliance with 72.236(d).

Response to Question 5-2

As discussed in the response to RAI Question 1-1, the SAR has been revised to limit the transfer casks for use with the Advanced NUHOMS® system to the OS-197 transfer cask. The shielding analysis presented in Chapter 5 of the SAR is based on the OS-197 transfer cask. Revisions to SAR Sections 5., 5.1, 5.3.1, 5.5, Table 5.1-1 and Figure 5.1-4 have been made to clearly specify the OS-197 cask configuration in the shielding analysis.

Question 5-3

Clarify the particle transport model discussed in Section 5.4.1. Further describe the discrete ordinates method and limitations and how the DORT-PC computer code used addresses these limitations. Provide an in depth discussion and documentation (including benchmarking, verification, and validation) of reference 5.2 and how the analysis in Sections 5.3 and 5.4 addresses the limitations of the discrete ordinates method including:

1. *The ability to solve mixed problem geometries such as mixed rectangular and cylindrical geometry systems encountered in the cylindrical DSC and the rectangular AHSM.*

2. *Problems with irregular boundaries and material distributions.*

3. *Production of spurious oscillations in the spatial distribution of the calculated flux density (also known as the ray effect) as an inherent consequence of the angular discretization. Discuss whether penetration through large non-scattering regions are encountered (where this effect may be particularly important).*

4. *How the code in reference 5.2 addresses multidimensional situations in which the flux density is anisotropic and in which the medium is many mean-free paths in size.*

5. *Numerical truncation errors introduced through the discretization of the spatial and angular variables and the required mesh fineness of the angular and spatial meshes which are required to obtain flux densities that are independent of the mesh size, particularly for large system models.*

6. *How modeling of streaming effects may be effected by the problems discussed in (a) - (e).*

How the three models described in Sections 5.3 and 5.4 adequately address (a) - (f).

The staff notes that although reference 5.2 is distributed by ORNL/RSIC, no documentation is provided with respect to benchmarking, verification, and validation; and that similar code packages (e.g. CCC-650) may have more applicability as "industry standards." This information is required by the staff to assess compliance with 72.24 and 72.236(d).

Response to Question 5-3

The DORT computer code has been benchmarked, verified and validated in accordance with TN West's QA program requirements for use of computer software in support of safety related analyses. This included a verification of the operation of the code on the software/hardware platform used by replicating the results of sample problems provided in the user's manual. Benchmarking and validation was performed by comparison of results with a previously benchmarked/validated ANISN model. Figures 5.4-8 though 5.4-12 have been added to the SAR to provide a simplified depiction of the shielding analysis models used. A non-proprietary version of these figures is also included in these RAI responses (5-3, 5-5) to facilitate the review of these responses.

1. Limitations of the DORT computer code preclude explicit modeling of combinations of rectangular and cylindrical geometry systems encountered in the cylindrical 24PT1-DSC and the rectangular AHSM in a single DORT model. Nevertheless, DORT allows the description of cylindrical shapes in "R-Z" mode and rectangular shapes in "X-Z" mode. It is possible to conservatively model this rectangular problem by breaking the AHSM geometry into smaller parts and then modeling these parts using "R-Z" or "X-Z" geometry.

For the doses at the top and bottom of the AHSM, the AHSM geometry is split into two parts, an upper half and a lower half, by a horizontal plane through the 24PT1-DSC longitudinal axis, shown in Figure 5-3.1 along line A-A'. These two halves are rectangular in shape, however an "R-Z" model of the rectangular shape is developed by setting the AHSM outer surface radius equal to the distance between the 24PT1-DSC centerline and the AHSM outer surface along line C-C' in Figure 5-3.1. This ensures that the DORT model AHSM surface represents the nearest point on the roof and the floor, as appropriate for the respective model (See Figure 5-3.2).

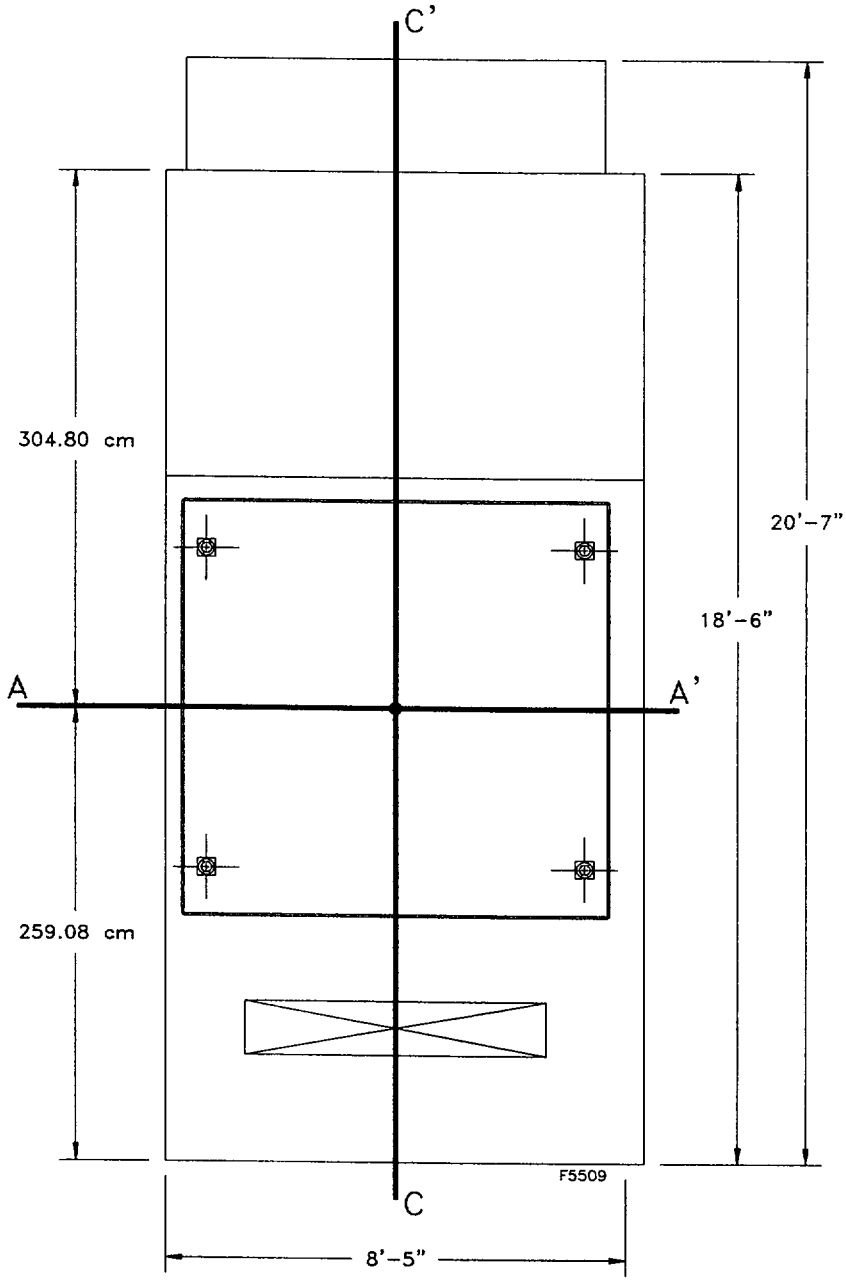

Figure 5-3.1 - AHSM Front View

The rectangle shown in Figure 5-3.2 represents the outer edge of the AHSM halves described above. The radial dimensions are determined from the center of the ASHM door to the roof and floor surface along line C-C' in Figure 5-3.1. Two models are created, one for each half of the AHSM. These models are identified as the "roof" and "floor" models and represent the AHSM geometry above and below the horizontal plane through the 24PT1-DSC longitudinal axis. These models are conservative because they model the thinnest roof and floor shielding. These models are used to estimate dose rates along lines AA', CC' and EE' shown in Figures 5-3.1

and 5-3.3. The DORT models are shown in Figures 5-3.3, 5-3.4, 5-3.5 and 5-3.6. The results calculated with these two models match at the 24PT1-DSC longitudinal centerline.

Assuming that dose rates obtained along lines AA', CC' and EE ' from the models described above are constant over the corresponding surfaces would be too conservative since these lines are aligned with the 24PT1-DSC centerline which results in the peak doses for the entire surface.

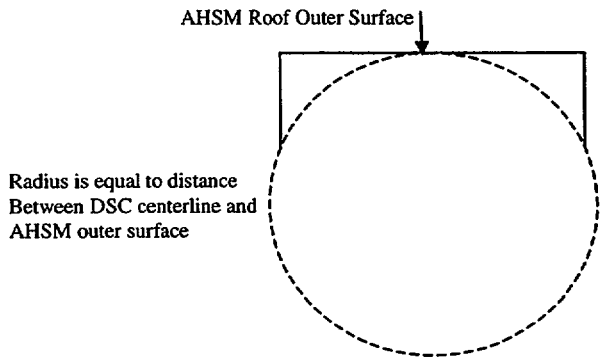

Figure 5.3-2 - Approximation of AHSM Rectangular Geometry in DORT Roof models

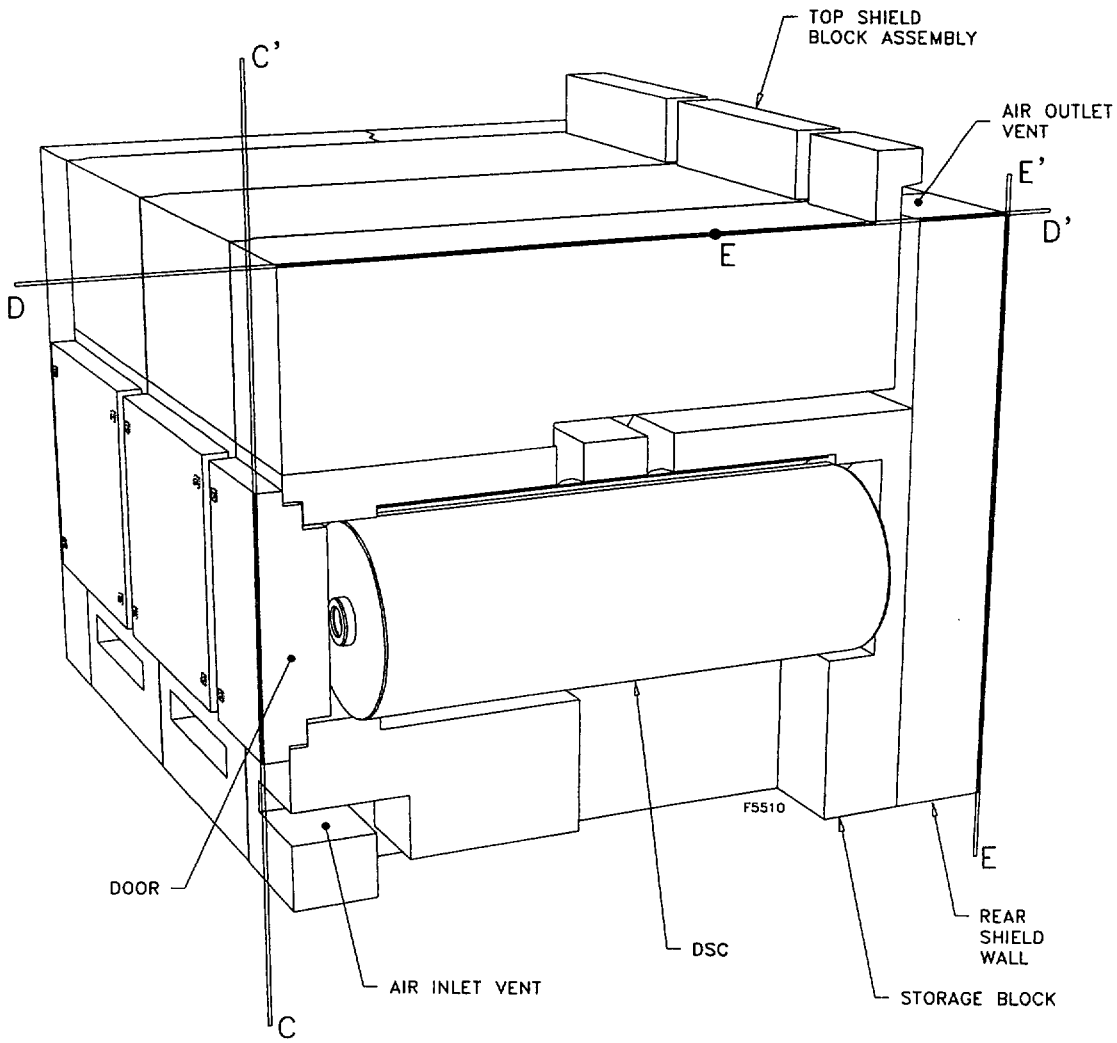

Figure 5-3.3 – AHSM Side View Cross Section

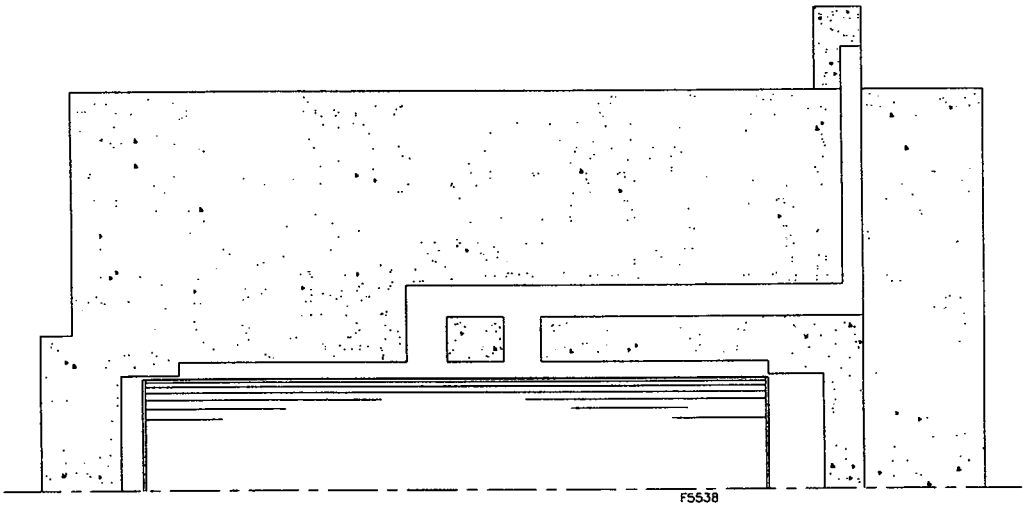

Figure 5-3.4 - AHSM "Roof" Model

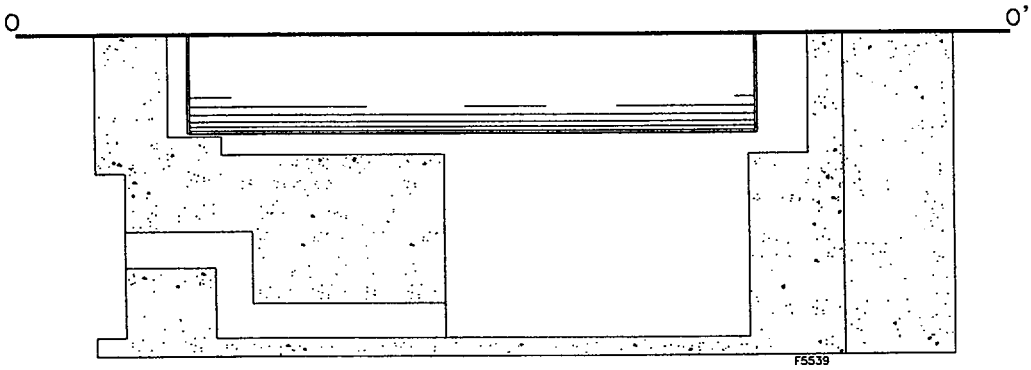

Figure 5-3.5 - AHSM "Floor" Model

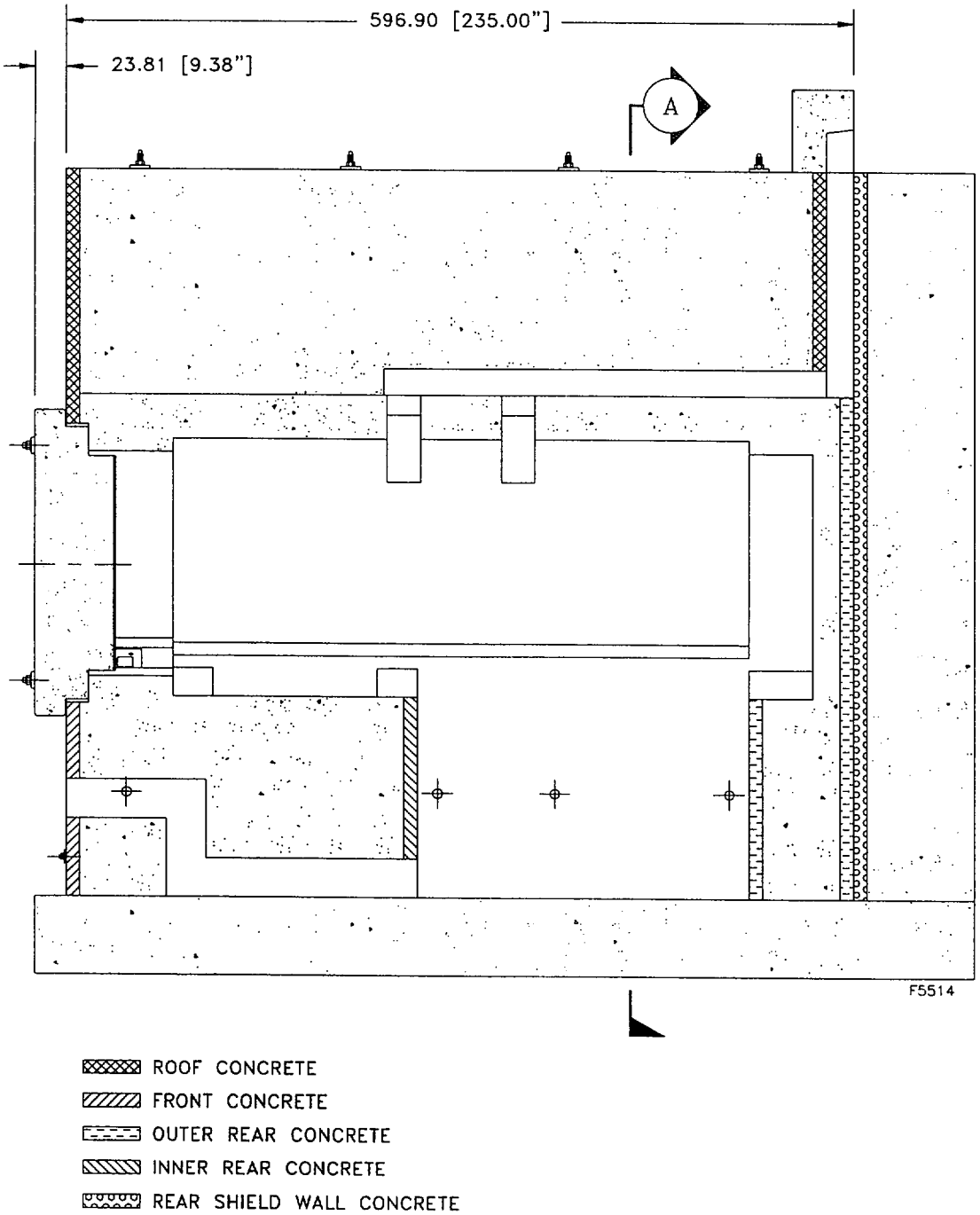

Figure 5-3.6 - AHSM "X-Z" Model

To reduce conservatism and to estimate the shape of the dose rate distribution functions along the AHSM side and front an "X-Z" model is created. This model is shown in Figure 5-3.6. The variation of dose rate along these surfaces is approximated by a Gaussian distribution. As can be seen from Figure 5-3.6, the thickest layer of concrete a particle encounters is in the direction from the 24PT1-

DSC towards the AHSM roof. The shape of the dose rate distribution function on the AHSM roof is determined using an "X-Z" model. This model is used to reshape dose rate distributions on the AHSM front and roof calculated with the two "R-Z" models. This approach appropriately models the geometry of the AHSM.

2. DORT computer code limitations also preclude detailed modeling of irregular boundaries and material distributions. However these irregularities do not affect the overall dose rates. They have only small impact on the dose rates at the surface in localized areas. For example the four cask trunnions are not modeled at all (see response to RAI Question 5-8). Not modeling the trunnions is conservative because they would provide additional shielding in the area adjacent to the trunnions but their presence would have a negligible effect on dose rate distribution at 1 or 3 feet away. Irregularities as described above in this example are neglected in such a way that the model underestimates the actual shielding available. Some irregularities like relief valves may create local 'hot' spots, but these potential hot spots are very localized and do not change the radiation field around the 24PT1-DSC and Transfer Cask as a whole.

3. Schematically the ray effect can be illustrated as shown in Figure 5-3.7, below.

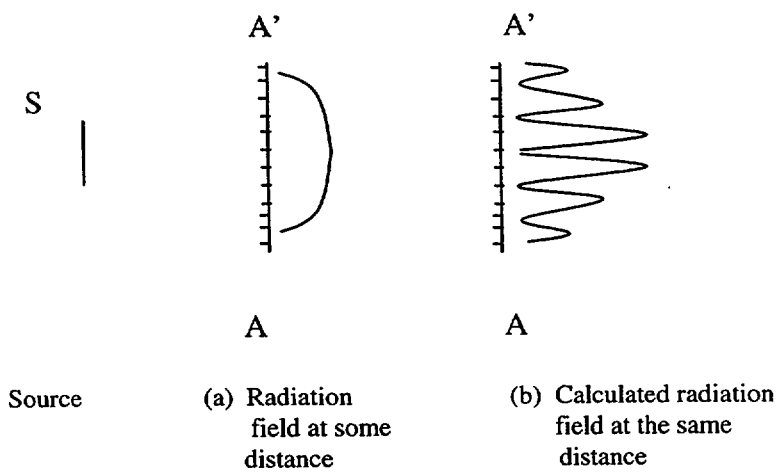

Figure 5-3.7 - Discrete Ray Effect

Figure 5-3.7 depicts the case where the radiation field from source *S* is considered along line AA' at some arbitrary distance. At (a) a real radiation field is depicted. Due to angular discretization the calculated distribution might look like (b). This effect is especially pronounced if the only separation between a source and the area of interest is media with large mean free paths (e.g., air). Even though there are cavities inside of the AHSM (see Figure 5-3.3) most of the points on the AHSM surfaces are separated from the source by very thick layers of concrete. The only place to expect the ray effect is in areas near the air inlet or outlet. As can be seen from Figure 5-3.3 particles streaming through the air vents must experience at least

three collisions before reaching the surface. This leaves little, if any, room for the ray effect. In addition, upward and downward biased quadratures with 420 and 400 directions are used to reduce the possibility of this effect when calculating dose rates on the front and rear surfaces of the AHSM (or Transfer Cask).

Finally, applying small size meshes as along AA' and plotting dose rates would reveal any ray effects. Two examples of dose rate plots are shown in Figures 5-3.8 and 5-3.9 below. The dose rates in these figures show very smooth behavior; no erratic changes, spikes or jumps are observed even in front of the air vents. Any changes are strongly correlated with material type change, geometry change or both.

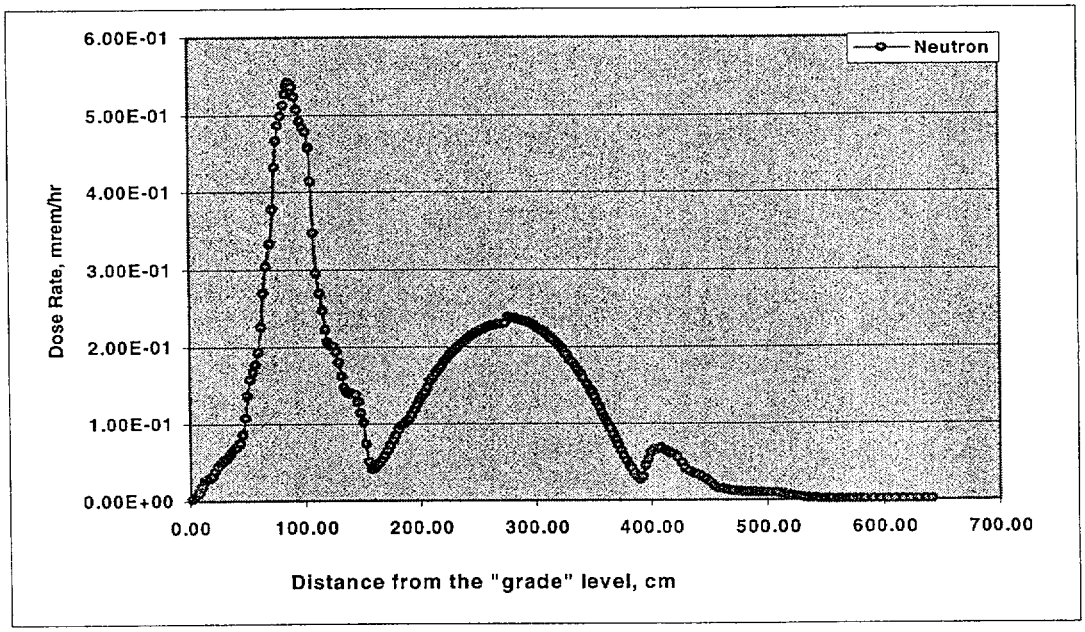

Figure 5-3.8 - Neutron Dose Rates on AHSM Front Surface

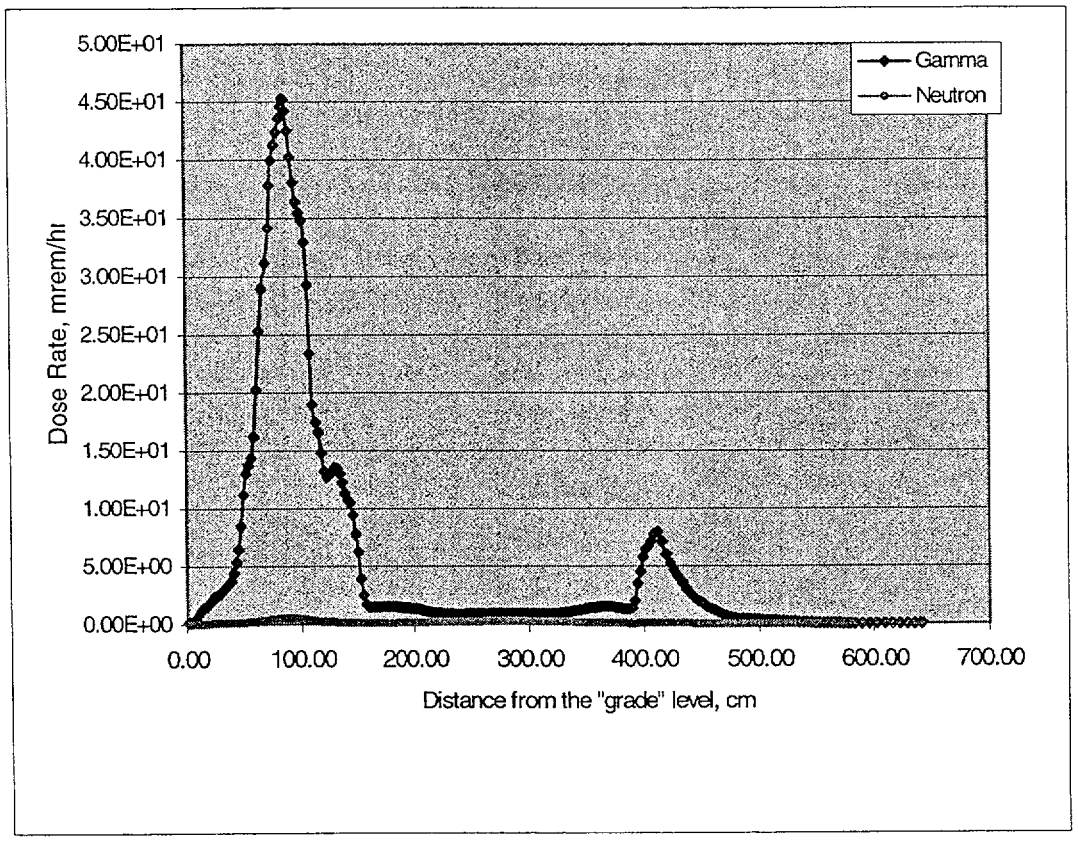

Figure 5-3.9 - Neutron and Gamma Dose Rates on AHSM Front Surface

The 276 cm distance on the above Figures corresponds to the AHSM door center. Dose rates below this point are calculated with the "floor" model, dose rates above this point are obtained with the "roof" model. As can be seen in the figures above, the models are in a very good agreement at the center of the door.

4&5. Some aspects of the theoretical foundation of the discrete-ordinate method are provided in SAR Reference 5.2. Mathematical and physical considerations for simplifications used to solve the transport equation written in the finite difference form are also provided in this reference. The version of DORT provided in the CCC 650 code package is a simple replica of that in Reference 5.2. DORT distributed with the CCC 650 code package has enhanced capabilities related to data storage and manipulation (for example DORT in Reference 5.2 limits fast memory objective to 1Mb but the parameter used to describe this variable is present in both CCC packages).

Table 5-3.1 and Table 5-3.2 are macroscopic cross sections of neutron and gamma interactions in some materials used. The tables provide guidance for choosing the size of finite meshes. Because most of the intensity of a gamma source is concentrated between 1 and 2 MeV the mesh size of 3.0 cm (approximately half a mean free path) in the fuel region is appropriate.

Table 5-3.1. Neutron Macroscopic Cross Sections in Different Materials

Energy		Concrete		Air		SS-304		Lead Plug		In-core Region	
Mev	Gr. #	x-sect., cm^{-1}	mfp., cm	x-sect., cm^{-1}	mfp., cm	x-sect., cm^{-1}	mfp., cm	x-sect., cm^{-1}	mfp., cm	x-sect., cm^{-1}	mfp., cm
4.17E-07	22	0.554621	1.80303	0.000453	2206.31	1.11696	0.895287	0.367537	2.72081	2.7526	0.3633
1.12E-06	21	0.374645	2.66919	0.000406	2462.17	0.955357	1.04673	0.367669	2.71984	1.2114	0.8255
3.06E-06	20	0.37275	2.68276	0.000401	2494.44	0.936653	1.06763	0.371987	2.68827	1.1405	0.8768
1.07E-05	19	0.371236	2.6937	0.000397	2517.07	0.924401	1.08178	0.369317	2.7077	1.2288	0.8138
2.90E-05	18	0.370142	2.70167	0.000394	2537.76	0.917098	1.0904	0.369152	2.70891	1.2133	0.8242
1.01E-04	17	0.369124	2.70912	0.000391	2560.14	0.912799	1.09553	0.369152	2.70891	1.2554	0.7965
5.83E-04	16	0.367333	2.72233	0.000375	2669.28	0.888237	1.12583	0.368789	2.71158	1.1403	0.8770
3.33E-03	15	0.397722	2.51432	0.000345	2902.66	0.770032	1.29865	0.365856	2.73332	1.0483	0.9539
0.111	14	0.340036	2.94087	0.000264	3785.89	0.791259	1.26381	0.353529	2.82862	0.9198	1.0871
0.55	13	0.351613	2.84404	0.000163	6146.13	0.317619	3.14843	0.246023	4.06466	0.5449	1.8352
1.11	12	0.273412	3.65748	0.000101	9913.16	0.240246	4.1624	0.190304	5.25475	0.3539	2.8257
1.83	11	0.202515	4.93791	9.78E-05	10224.4	0.247636	4.03819	0.176293	5.67237	0.2661	3.7575
2.35	10	0.161852	6.17848	7.20E-05	13889.1	0.278292	3.59335	0.192806	5.18656	0.2139	4.6744
2.46	9	0.104616	9.55877	5.57E-05	17962.5	0.290527	3.44202	0.214556	4.66079	0.1754	5.7005
3.01	8	0.129925	7.69675	6.22E-05	16085.4	0.297668	3.35945	0.23338	4.28486	0.1875	5.3321
4.06	7	0.180413	5.54284	8.53E-05	11723.6	0.302938	3.30101	0.249623	4.00604	0.2155	4.6411
4.96	6	0.13817	7.23746	7.31E-05	13686	0.318535	3.13937	0.248245	4.02828	0.1755	5.6992
6.36	5	0.117598	8.50355	6.23E-05	16047.4	0.315963	3.16493	0.230852	4.33178	0.1541	6.4902
8.18	4	0.102732	9.73407	5.80E-05	17245.5	0.304386	3.2853	0.191827	5.21303	0.1351	7.4004
10	3	0.106341	9.40371	5.71E-05	17516.6	0.278948	3.5849	0.164368	6.08391	0.1261	7.9324
12.2	2	0.112431	8.89434	6.44E-05	15516.5	0.252216	3.96486	0.162463	6.15525	0.1228	8.1440
15	1	0.117272	8.52718	7.14E-05	13997.2	0.225212	4.44026	0.170746	5.85665	0.1177	8.4942

The neutron cross section sets shown here are for the case of DSC filled with water. The values will decrease (mfp increases) in dry cask.

Table 5-3.2. Gamma Macroscopic Cross Sections in Different Materials

Energy		Concrete		Air		SS-304		Lead Plug		In-core Region	
Mev	Gr. #	x-sect., cm^{-1}	mfp., cm	x-sect., cm^{-1}	mfp., cm	x-sect., cm^{-1}	mfp., cm	x-sect., cm^{-1}	mfp., cm	x-sect., cm^{-1}	mfp., cm
0.05	40	7.56069	0.132263	0.000637	1569.81	178.309	0.005608	545.092	0.001835	89.5280	0.0112
0.1	39	0.515942	1.9382	0.000179	5587.09	5.90219	0.169429	46.968	0.021291	7.4643	0.1340
0.2	38	0.325435	3.07281	0.000147	6821.75	1.56637	0.638419	25.7286	0.038867	3.8832	0.2575
0.3	37	0.26439	3.78229	0.000124	8072.07	0.948611	1.05417	6.71593	0.1489	1.3835	0.7228
0.4	36	0.2319	4.3122	0.000109	9142.61	0.781874	1.27898	3.21073	0.311456	0.7235	1.3821
0.6	35	0.200828	4.97939	9.50E-05	10530.2	0.659843	1.51551	1.76231	0.567437	0.4370	2.2881
0.8	34	0.173034	5.77921	8.19E-05	12208.3	0.562068	1.77914	1.11088	0.900187	0.2987	3.3474
1	33	0.153789	6.50242	7.28E-05	13730.8	0.49753	2.00993	0.851357	1.1746	0.2388	4.1882
1.33	32	0.135542	7.37779	6.42E-05	15576.3	0.437638	2.28499	0.68247	1.46527	0.1964	5.0913
1.66	31	0.119206	8.38884	5.64E-05	17725.3	0.385695	2.59272	0.573669	1.74317	0.1666	6.0034
2	30	0.107384	9.31237	5.07E-05	19725.7	0.35026	2.85502	0.521922	1.916	0.1500	6.6652
2.5	29	0.096597	10.3523	4.54E-05	22021	0.319466	3.13022	0.487841	2.04985	0.1375	7.2750
3	28	0.087238	11.463	4.07E-05	24540.8	0.294475	3.39587	0.470141	2.12702	0.1286	7.7753
4	27	0.077705	12.8692	3.59E-05	27860.8	0.271149	3.68801	0.46612	2.14537	0.1218	8.2082
5	26	0.06926	14.4384	3.15E-05	31769.5	0.253002	3.95254	0.471822	2.11944	0.1173	8.5239
6.5	25	0.06256	15.9846	2.79E-05	35861.8	0.240896	4.15117	0.482897	2.07083	0.1147	8.7147
8	24	0.057344	17.4387	2.50E-05	40002.7	0.233465	4.2833	0.50142	1.99434	0.1142	8.7602
10	23	0.05402	18.5116	2.29E-05	43573.6	0.233505	4.28256	0.532238	1.87886	0.1166	8.5770

The gamma and cross section sets shown here are for the case of DSC filled with water. The values will decrease (mfp increases) in dry cask.

A 1D ANISN run was prepared to evaluate the transport of gamma radiation through a concrete cylinder to assess spectral distribution of the dose rate. The thickness of the shell is equal to the thickness of the AHSM roof slab. Spectral distributions of gamma and neutron dose rate within and on the outer surface of the shell are shown in Figures 5.3-10 and 5.3-11 below.

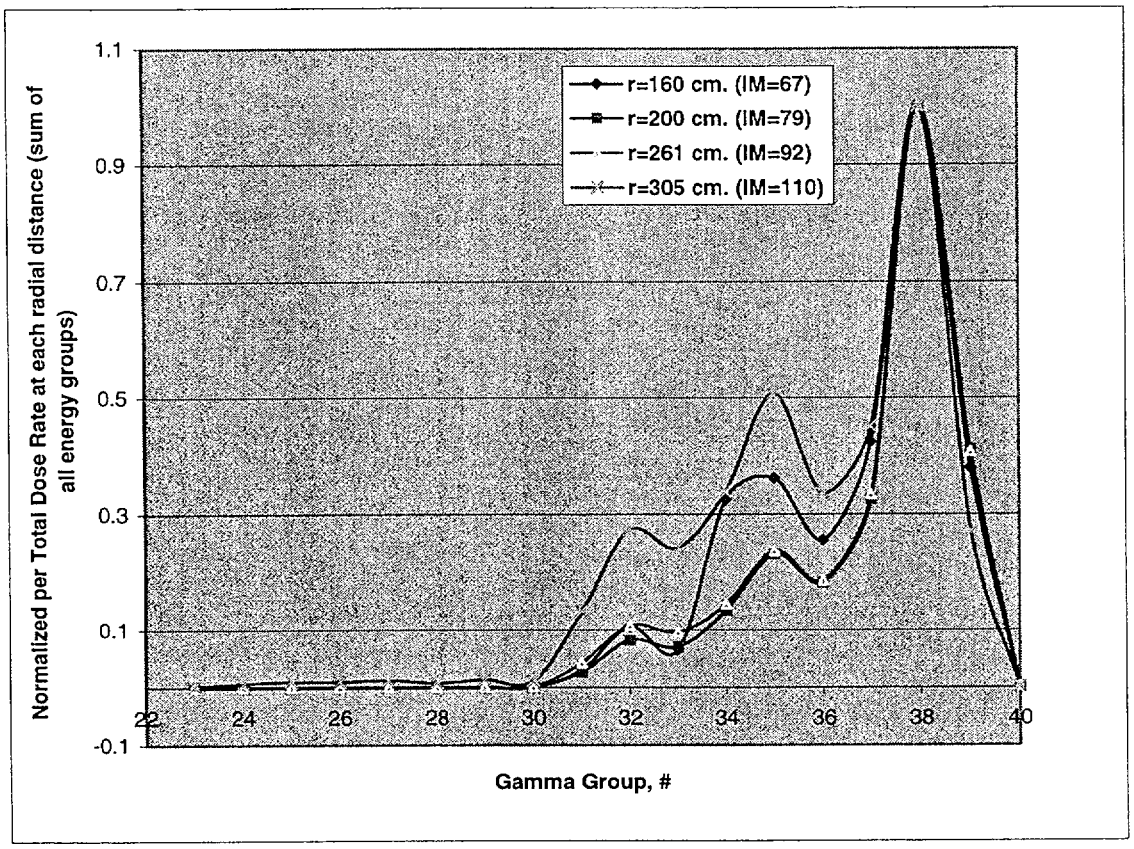

Figure 5-3.10 - Normalized Gamma Dose Rates at Different "IM" Layers in ANISN AHSM Model (Roof Block Starts at r=98 cm and ends at r~300 cm)

As can be seen from Figure 5-3.10, most of the gamma dose rate on the AHSM roof is distributed between groups 32-39. The photon mean free path in concrete is between ~7.4 and 1.9 cm. for these energy groups.

There are two inputs for the "roof" and "floor" AHSM models to calculate the dose rate on the front and rear AHSM surfaces. To calculate dose rates on the front, finer meshes are used in the regions where the front door and 24PT1-DSC bottom shield plugs and plates are located while a mesh size on the order of one mfp is used within an AHSM rear wall. The axial mesh size in the 24PT1-DSC shield plugs and plates is 0.25-0.7 cm. (a few nodes have mesh sizes of between 0.7 and 1.0 cm.). The AHSM door axial mesh is 0.3-1.0 cm. (a few nodes have mesh sizes of 1.16 cm.). A similar approach is used when the dose rate is calculated in the rear parts of the AHSM. Finer meshes are used within rear regions of the AHSM and coarser meshes are used in regions near the front of the AHSM . The mesh size in the radial direction is about 2.33 cm. in both cases.

Special runs are performed to calculate dose rates on the roof. A mesh size between 1.00 and 2.33 cm. is employed in the radial direction in these runs.
The ANISN run shows that spectral distribution of neutron dose on the roof of the AHSM is mostly concentrated within the last, 22-nd, group. The spectral distribution of neutron dose rates on the AHSM roof is shown in Figure 5-3.11 below.

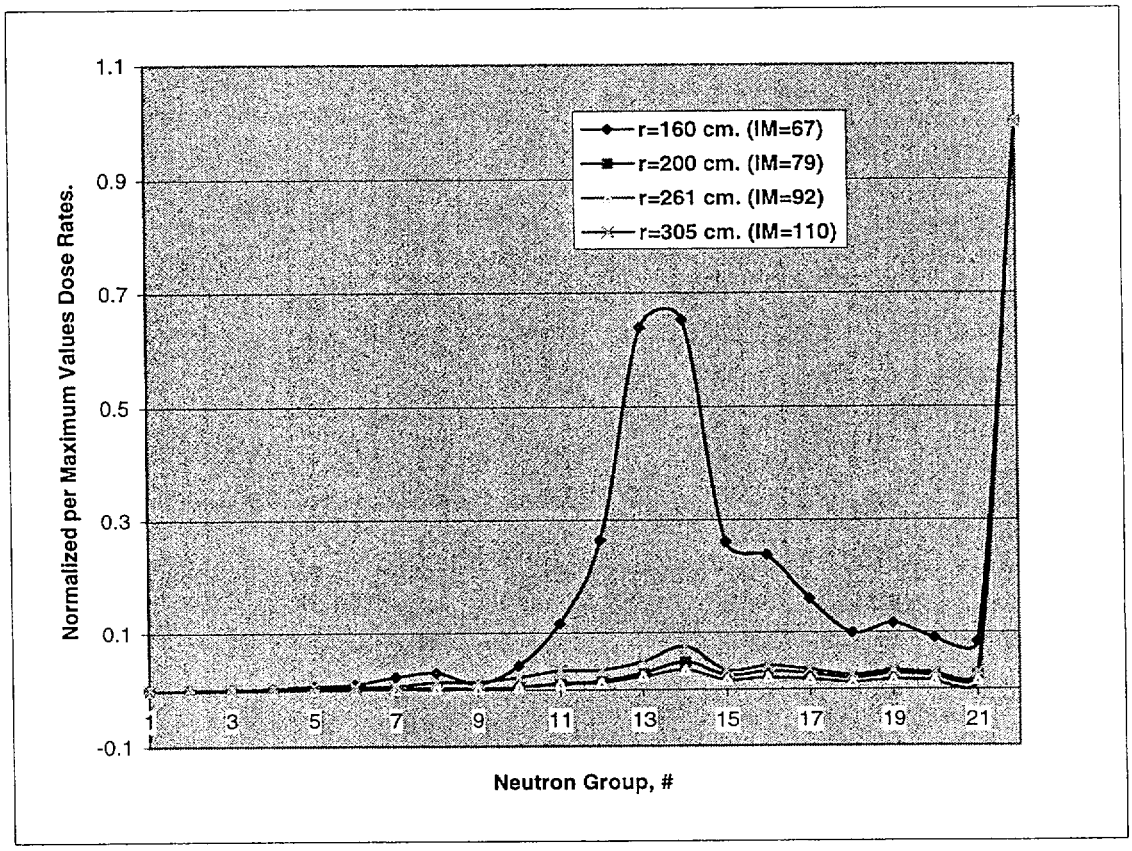

Note: The peak for r = 160 cm is associated with the source term spectrum which is attenuated as neutrons are thermalized for larger distance r into the roof

Figure 5-3.11 - Normalized Neutron Dose Rates at Different "IM" Layers in ANISN AHSM Model (Roof Block Starts at r=98 cm. and ends at ~300 cm.)

As can be seen from the discussion and analysis of Figures 5-3.10 and 5-3.11 and Tables 5-3.1 and 5-3.2; one mean free path or less finite mesh size is used in the DORT models. In most cases such spatial discretization along with fine angular discretization is sufficient. Upward and downward biased quadrature sets with 420 and 400 directions are used to calculate dose rates on the front and rear surfaces of the AHSM. Symmetric quadrature with mm=320 is used to calculate dose rates on the roof. The directional dependence of scattering cross sections is approximated with Legandre polynomials of the third order.

Finally, even finer spatial mesh sizes were used in several trial runs. No change in calculated dose rate values were observed. To keep the duration of computer runs within a manageable time frame the discretization scheme described earlier is used.

6&7. See responses to 1 through 5 above.

Question 5-4

Submit reference 5.7, which is used to describe the "Normalized Conservative Burn-up Shape on WE 14 x 14 Fuel Assembly" shown in Table 5.4-1. This information is required by the staff to assess compliance with 72.236(d).

Response to Question 5-4

Attachment 5 provides a copy of Reference 5.7 of the SAR, as requested. Reference 5.7 in SAR Section 5.5.1 has been revised to identify the associated ORNL document number.

Question 5-5

Provide concise figures which describe the DORT shielding model used. The figures should show clear descriptions of materials and thicknesses including boundaries and should contain dimensions and thickness that relate the model Figures (5.4-1 through 5.4-7) to the drawings shown in Section 1. The figures should also clarify what the letters and numbers (including bold or not bold fonts) shown in the model figures (5.4-1 through 5.4-7) physically mean. Further, the figures should show where dose rate measurements are taken and where and how the material "fluxdosium" is located. The figures should also address generic statements made in the SAR when addressing questions 5-2, 5-3, and 5-6 through 5-10 and should provide clear and concise comparison capabilities between the design basis drawings in Section 1 and the model figures 5.4-1 through 5.4-7.

The staff cannot determine the adequacy of the model based on Figures 5.4-1 through 5.4-7 alone. This information is required by the staff to assess compliance with 72.24, 72.236(b) and 72.236(d).

Response to Question 5-5

Figures 5-3.4 through 5-3.6, of the RAI Question 5-3 response above, provide detailed descriptions of the DORT AHSM models used. A Proprietary version of these figures along with Figures 5-5.1 and 5-5.2 have been incorporated into the SAR as Figures 5.4-8 through 5.4-12 to provide a simplified depiction of the shielding analysis models.

Figure 5-5.1 provides a description of the DORT OS-197 transfer cask model used.

SAR Figures 5.4-1 through 5.4-7 are the DORT printouts of the geometry models used. The number of lines and the number of symbols in a line correspond to the number of fine meshes in axial and radial directions. Each symbol is assigned a number which

represents the material comprising a finite cell. The materials associated with the symbols used in SAR Figures 5.4-1 through 5.4-7 are provided below:

SAR Figures 5.4-1 through 5.4-3 (AHSM models):

Fluxdosium – 1
Stainless Steel 304 – 2
Carbon Steel – 3
Concrete – 4
Air – .
Front Concrete – 6
Roof Concrete – 7
Inside Concrete – 8
Rear Concrete – 9
Inner Rear Concrete – a
Outer Rear Concrete – b
Bottom Nozzle – c
In-core – d
Plenum – e
Top Nozzle – f
Rear shield wall concrete – g

The SAR has been revised to add the appropriate note to Figures 5.4-1 through 5.4-3.

SAR Figures 5.4-4 through 5.4-7 (OS-197 transfer cask):

Fluxodium – 1
Stainless Steel 304 – 2
Carbon Steel – 3
Lead – 4
Air - .
Water - ,
Bottom Nozzle – 7
In-Core – 8
Plenum – 9
Top Nozzle – a
BISCO NS-3 - b

The above notes are included in Figure 5.4-4 for the cask models.

Notes explaining the meaning of bold face symbols and figures are provided at the bottom of SAR Figure 5.4-1 through Figure 5.4-4.

Table 5-5.1 lists details and associated materials used in the shielding analysis. Since the radiation shielding property of different types of steel are identical we assumed that there are two types of steel: carbon and stainless steel (SS).

Table 5-5.1 - DCS/TC Hardware Parts and Materials Nomenclature

Item #	Item Name	Material
1	1" THK. TC Bottom Cover Plate	Carbon Steel
2	Inner and Outer Shell Assembly	SS
3	¾" THK. Neutron Shield Plate	SS
4	0.59" THK. Carbon Steel Shield Plate	Carbon Steel
5	1.88" THK. NS3 Shield Plate	NS3
6	2" THK. TC Bottom End Plate	Carbon Steel
7	TC Bottom Support Ring	SS
8	DSC 1.38" THK. Grapple Ring	Carbon Steel
9	DSC Grapple Support Ring	Carbon Steel
10	½" THK Neutron Shield Panel Support Ring	SS
11	3/16" THK. Neutron Shield Panel	SS
12	Neutron Shielding Material	Water
13	Structural TC Shell, 1 ½" THK. Thickened to 2" after 341.25 cm.	Carbon Steel
14	3.54" THK. Lead Gamma Shield	Lead
15	½" THK. Inner Liner Plate	Carbon Steel
16	¼" THK. Plate for Top Cover	SS
17	2" THK. Neutron Shield Plate (Part of TC Top Cover Plate)	NS3
18	¼" THK. Plate for TC Top Cover	SS
19	3" THK. TC Top Cover Plate	Carbon Steel
20	TC Top Support Ring	SS
21	1.85" THK. Outer Bottom Cover Plate	Carbon Steel
22	6.12" THK. Bottom Shield Plug	SS
23	¾" THK. Inner Bottom Cover Plate	Carbon Steel
24	1.38" THK. Outer Top Cover Plate	Carbon Steel
25	1.14" THK. Inner Top Cover Plate	SS
26	7.62" THK. Top Shield Plug	SS
27	Support Ring	Carbon Steel
28	DSC Spacer Disk #25 and #26	Carbon Steel
29	DSC Spacer Disk # 24	Carbon Steel

The AHSM concrete sections contain various layers of rebar within surface layers of the AHSM. The densities of concrete elements in the 4" thick layer, where the rebar is smeared, are recalculated. The mean free path difference for photons is between ~0.01-0.1 cm. in the different types of concrete. The concrete layers with different densities are shown in Figure 5-5.2.

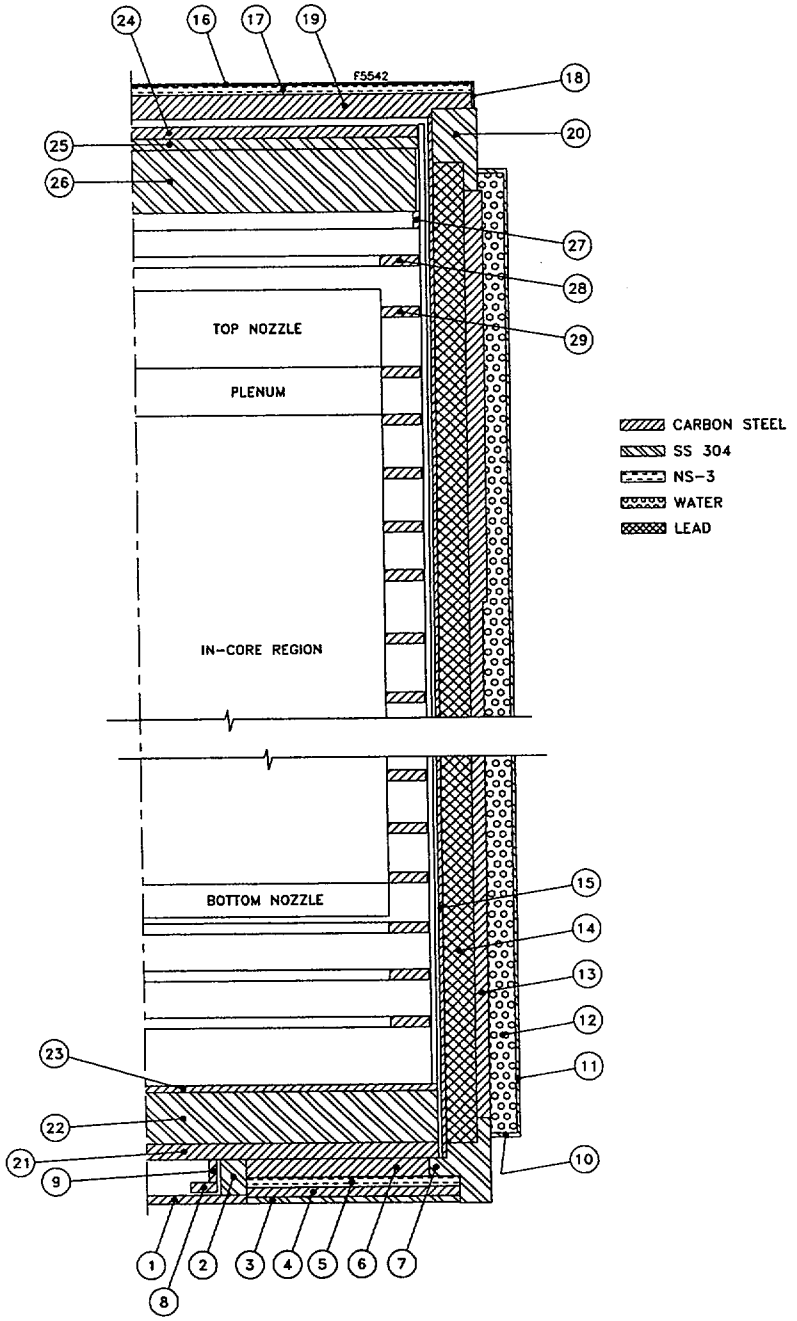

Figure 5-5.1 - 24PT1-DSC inside of Transfer Cask at Transfer Storage Stage
(See Table 5-5.1 for a Description of the item numbers identified above)

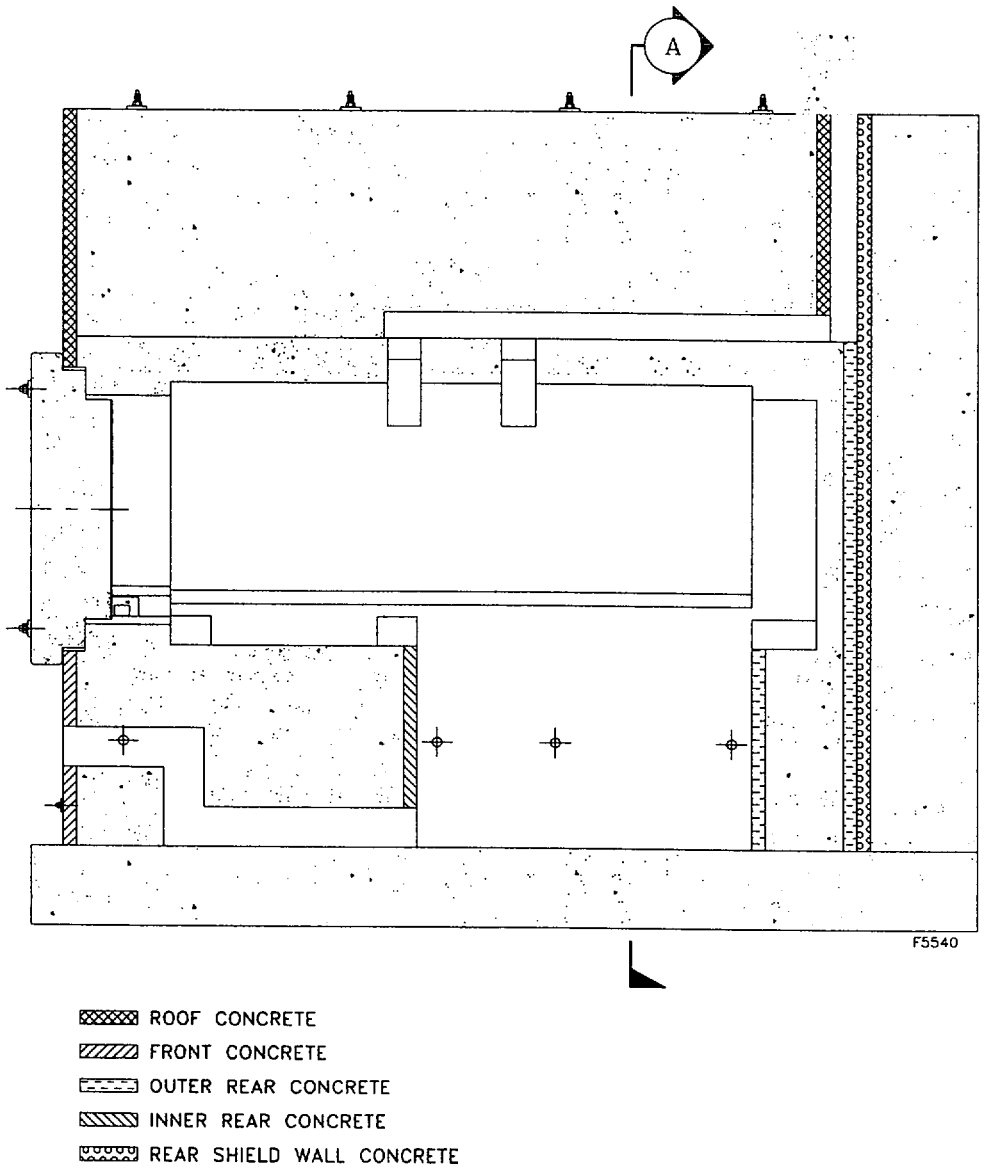

Figure 5-5.2 - AHSM Cross Section View in Vertical Elevation

The material "fluxdosium", used in the calculation of dose rates, is a fictitious material. DORT provides a general formula for the calculation of energy dependent reaction rates. This formula is:

$$A_{i,j} = t \times d_{i,j} \times C_{i,j}^{r,s} \times \sum_{g} \Phi_{i,j}^{g} \times \sigma_{r,s}^{g} \qquad \text{Equation (1)}$$

where:

i,j	- mesh cell index
g	-energy group number
r	-material number
s	-cross section table position number
t	-arbitrary multiplier
d	-density factor if used, if not used it is set equal to 1
σ	-cross section
Φ	-Flux
C	-the number density of the material |r| in cell *i,j*

The parameters for the equation above are described in a so called "activity table". Arrays 25$$, 26$$ and 27** are used to specify the table as following

Array	25$$	26$$	27**
Parameter name	ICMAT	ICPOS	ACMUL
Corresponding Factor in Equation (1)	*r*	*s*	*t*

ICMAT	-material to be used in activity calculation
ICPOS	-cross section table position for activity
ACMUL	-activity multiplier

If we are interested in dose rates we need to replace σ in the equation above with flux-to-dose conversion factors and set *t, d* and *C* to 1. If we use r = -1, per the DORT manual if $r<0$ then $C=1$. Then equation (1) can be written as

$$A_{i,j} = \sum_{g} \Phi_{i,j}^{g} \times \sigma_{r,s}^{g} \qquad \text{Equation (2)}$$

DORT calculates fluxes in each space cell. As can be seen from Equation (2), in order to calculate (or more correctly speaking to output) a reaction rate for material |r| in a space cell i,j one needs to know group flux $\Phi_{i,j}^{g}$. In order to calculate the group flux the materials filling each cell and their groupwise macroscopic cross sections are required. If one is interested in a reaction rate of material |r| knowledge of that material's cross sections is required but material |r| itself need not to be physically present in the cell i,j..

In order to obtain an activity value equal to the dose rate, the cross section in Equation (2) should be replaced with flux-to-dose conversion factors. To accomplish this with GIP, a fictitious material "Fx77" is created. It has a "density" equal to one as can be found from array 12** of the GIP inputs. "Microscopic cross sections" of "Fx77" are equal to ANSI

Standard 6.1.1 flux-to dose conversion factors. These factors for 22 neutron and 18 gamma energy groups are input in array 14** of the GIP inputs. Array 11$$ of the GIP input files indicates that "Fluxdosium" consists of "Fx77". GIP prepares "macroscopic cross section" table for "Fluxdosium" which in fact are groupwise flux to dose conversion factors for that particular "element". So if dose rate is needed in any spatial location one should use " Fluxdosium" for the activity calculation. Setting array 25$$ in a DORT input as

```
25$$ f-1
```

means that material 1 (which in our case is "fluxdosium") will be used in activity calculations in every spatial cell i,j.

Question 5-6

Justify the statement in Section 5.3.1.1 that overestimating the cross-sectional area of the air vents always leads to conservative streaming estimates. Include discussion of how overestimation of these areas is balanced by the limitations of the discrete ordinates method described in question 5-3.

This information is required by the staff to assess compliance with 72.24, 72.236(b) and 72.236(d).

Response to Question 5-6

The AHSM inlet is a square with dimensions of 5.5'×1'. It is not possible to model such a shape in the "floor" model. To account for the streaming effect through the vent, the air inlet is modeled as shown with dotted concentric circles in Figure 5-6.1, below. The difference between radii is equal to 1', the height of the inlet. Because of the huge amount of concrete in the front of the AHSM the dose rate will have its maximum at the center of the inlet and is substantially lower outside the inlet.

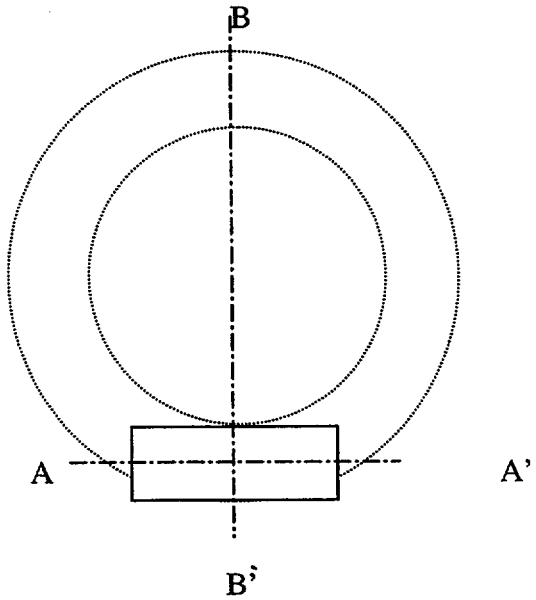

Figure 5-6.1 - Portion of AHSM Geometry Containing Air Vent Inlet.

The width of the inlet is significantly larger than its height. Therefore, the dose rate values in front of the vent along line BB' can be estimated with the "roof" model. The deficiency of the model is that it does not provide a distribution along the horizontal dimension, along line AA'. It inherently assumes that the distribution is not dependent on the horizontal coordinate of the point within the inlet or on the front of the module. Looking at Figures 5-3.8 and 5-3.9 of the response to RAI Question 5-3, it is clear that the dose rate in front of the inlet is caused largely by streaming through the vent. Therefore, based on the geometry of the model discussed above, the streaming would be overestimated. This is the basis for the statement in Section 5.3.1.1 that prompted this question. The assumption that the dose rate is not dependent on the horizontal coordinate is extremely conservative. To reduce this conservatism, a Gaussian function is used to reshape the dose rate distribution on the front and roof of the AHSM in the horizontal dimension. Parameters of the Gaussian function are extracted with a regression analysis of the dose rate distribution function on the AHSM roof. This distribution passes through the same point E in Figure 5-3.3 of the response to RAI Question 5-3. It is obtained from the "X-Z" model and approximated with a Gaussian function. The shape function preserves dose rate values along CC' shown on Figure 5-3.3 but still gives conservative values in the directions perpendicular to CC'. This conservatism is transferred to the final estimate of the average dose rate.

No changes to the SAR have been made with respect to this RAI Question response.

Question 5-7

Clarify the statement in Section 5.3.1.1 that "since the AHSM possesses limited azimuthal cylidrical symmetries, all approximations result in an overestimate of the dose rates on the AHSM surfaces." Justify this statement in relation to question 5-3.

This information is required by the staff to assess compliance with 72.24, 72.236(b) and 72.236(d).

Response to Question 5-7

See response to RAI Question 5-3, part 1, above.

Question 5-8

Clarify the statement in Section 5.3.1.3 of the SAR that "The non-symmetric regions such as the 24 Neutron Shield Panel support angles, the 4 trunnions, relief valves, clevises, eyebolts, etc are modeled such that the dose rate on the surfaces of the cask is overestimated." Describe how these devices are modeled and why resultant dose rates are overestimated.

This information is required by the staff to assess compliance with 72.24, 72.236(b) and 72.236(d).

Response to Question 5-8

Additional discussion has been added to Section 5.3.1.3 of the SAR to describe how the non-symmetric features of the OS-197 cask are modeled and why the resultant dose rates are overestimated.

With the exception of the 24 neutron shield support angles and the trunnions the balance of the items listed as non-symmetric regions are local features that increase the amount of shielding in a small area without replacing any of the shielding material which is included in the model.

The 24 neutron shield support angles provide support for the skin, which contains the water for the neutron shield. The steel that forms these angles is not smeared with the water in the neutron shield; rather it is modeled as water. This is conservative for gamma radiation because water is less than one-seventh the density of steel. The density of the neutron shield water used in the cask DORT models is 0.96 g/cm^3. The resultant reduction in the hydrogen density as compared to full density water results in the water attenuating the neutron dose rate at about the same rate as that for full density steel.
The trunnions penetrate the neutron shield, which locally changes the shielding configuration of the neutron shield. The trunnions are thick steel structures filled with

NS-3 neutron shielding material. These structures provide much more gamma and neutron shielding than the water that they replace

Question 5-9

Clarify the statement in Section 5.3.2 that "...when the source is smeared into a cylinder, the source is moved closer to the surface of the source region. This results in less self-shielding of the source in the model as compared to the actual geometry, which results in an overestimate of the surface dose rates."

Provide a sensitivity analysis that compares the tradeoff between moving the source out closer to the surface of the DSC and the increased material density of the smeared source, which provides more self-shielding compared to helium. This information is required by the staff to assess compliance with 72.24, 72.236(b) and 72.236(d).

Response to Question 5-9

As mentioned in the answer to RAI Question 5-3, item 2 an equivalent cylinder is used to model the non-uniform material distributions associated with fuel assembly components and 24PT1-DSC spacer discs and guide sleeves. The size of the equivalent cylinder is calculated by determining the volume occupied and enclosed by the 24 fuel assemblies, including the guide sleeves, absorber sheets, and oversleeves, in the loaded 24PT1-DSC. The cross sectional area considered for this calculation is shown in Figure 5-9.1 in the lower left quadrant bounded by the outer boundary of the fuel assemblies.

The cylinder with the equivalent radius (r_{eq}), when compared to Figure 5-9.1 indicates that the equivalent cylinder would encompass substantial void regions. Smearing all encompassed elements inside of the entire volume of the cylinder would reduce the density of any element.

As for source points, they are localized within the squares representing the fuel assemblies shown on Figure 5-9.1. When the source points are smeared throughout the cylinder, most of them will move closer to the surface of the cylindrical region.

Reduced material densities and more source points closer to the surface of the equivalent cylinder will result in less self shielding and an overestimate of the surface dose rates. Therefore, a sensitivity analysis comparing the tradeoff between the source location and the shielding material density is not considered necessary.

No changes to the SAR have been made with respect to this RAI Question response.

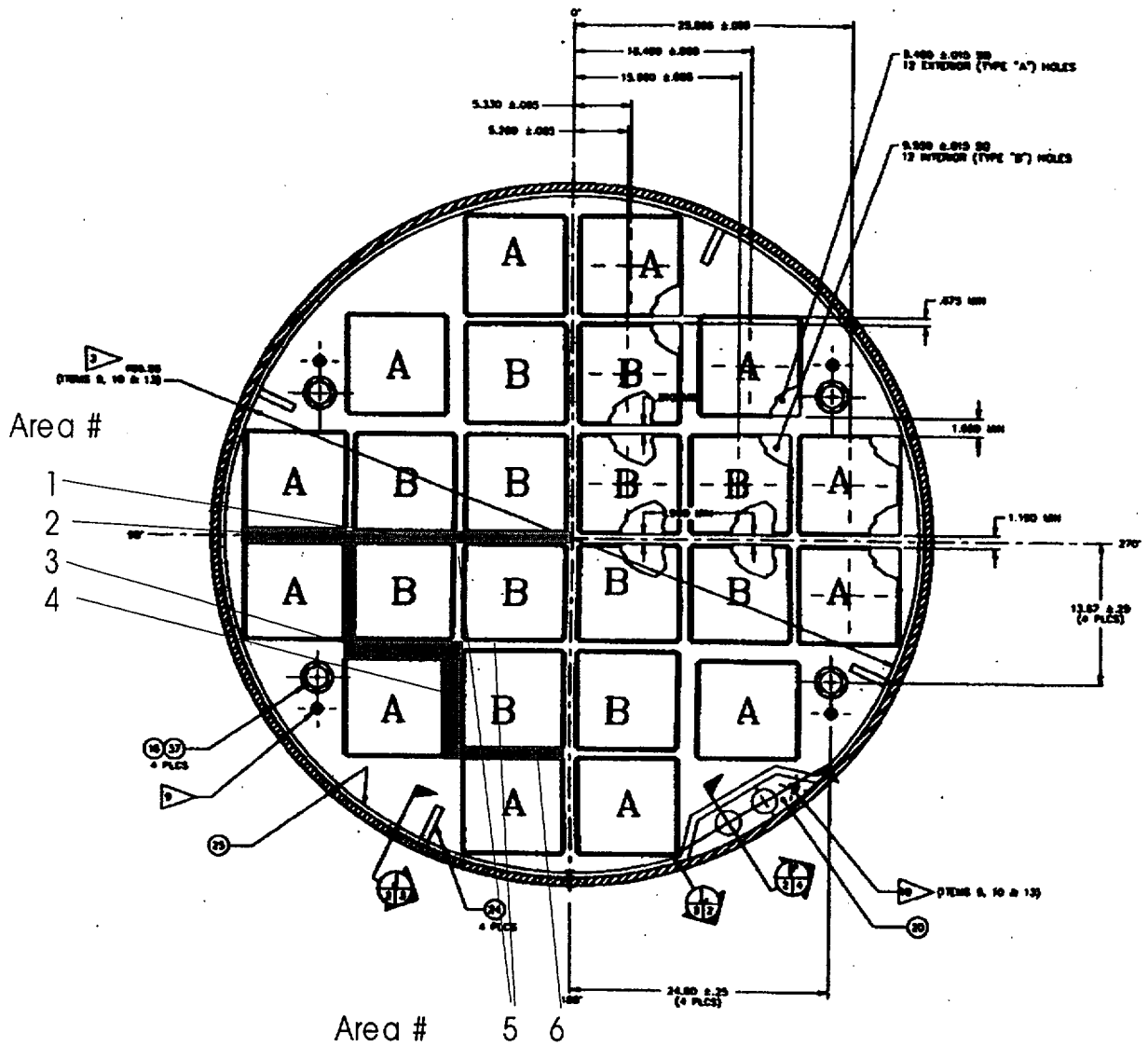

Figure 5-9.1 - Cross section view of 24PT1-DSC loaded with 24 FAs.

Question 5-10

Clarify the statement made in Section 5.3.2 that "For dose rate evaluations made on surfaces that are perpendicular to the spacer disks, credit is taken for the presence of the carbon steel spacer discs..." The staff assumes that the words parallel and perpendicular should be switched. In addition, clarify the statement "For the AHSM evaluation, no credit for the shielding properties of the spacer discs, fuel grid spacers and hold-down springs."

Provide a table which lists the various configurations of the Advanced NUHOMS® System (wet loading, dry transfer, AHSM evaluation) and the type of dose rate evaluation (axial or radial) and the amount of credit taken for the presence of the carbon steel spacer discs, fuel grid spacers, and hold down springs. Relate this table to the figures submitted in response to question 5-5.

This information is required by the staff to assess compliance with 72.24, 72.236(b) and 72.236(d).

Response to Question 5-10

The statement in SAR Section 5.3-2 is incorrect and TN West concurs that the words "parallel" and "perpendicular" should be switched as noted in RAI Question 5-10.

The shielding analysis is performed for two configurations. One configuration consists of the 24PT1-DSC inside the OS-197 Transfer Cask (TC).

There are four stages associated with handling while the 24PT1-DSC is located in the transfer cask. These stages are: Decontamination, Wet Welding, Dry Welding and Transfer/Storage. The definition of these stages is:

1) Cask decontamination. The 24PT1-DSC and the TC are assumed to be completely filled with water, including the region between them referred to as the "cask/DSC annulus." The 24PT1-DSC inner cover plate is assumed to be in place and the temporary shielding has not yet been installed.
2) Wet welding and 24PT1-DSC draining. The water level in the 24PT1-DSC cavity is assumed to be lowered four inches below the bottom of the top shield plug. Temporary shielding consisting of three inches of NS3 and one inch of steel is assumed to cover the 24PT1-DSC top shield plug. The annulus is assumed to remain completely filled with water.
3) Dry welding. The 24PT1-DSC cavity is assumed to be completely dry, the 24PT1-DSC top cover plate has been installed, and temporary shielding consisting of three inches of NS3 and one inch of steel covers the 24PT1-DSC. The annulus is assumed to remain completely filled with water.
4) Transfer-Storage. The 24PT1-DSC cavity and the cask/DSC are completely dry. The 24PT1-DSC inner and outer top cover plates are installed. The top end of the TC is sealed by a 3" thick carbon steel cover plate and a 2" thick NS3 shield. A ¼" thick stainless steel plate covers the NS3 shield.

Two sets of material densities are used at the four stages defined above. These are designated as "dry radial" and "wet axial" densities. For dose rate evaluations made for surfaces that are parallel to the spacer disks (surfaces that are perpendicular to the 24PT1-DSC axial centerline), it is permissible to take credit for the presence of the carbon steel spacer disks and the fuel grid spacers and hold down springs by smearing them in the 24PT1-DSC material regions. Only a part of the spacer disks inside of the equivalent cylinder, defined in the answer to RAI Question 5-9, is smeared. For the purpose of this evaluation these number densities are identified as "axial." For dose rate evaluations made for surfaces that are perpendicular to the spacer disks (parallel to the 24PT1-DSC axial centerline), a considerable fraction of the radiation will travel between the spacer disks, without being attenuated by the spacer disks. Therefore, the spacer disks and fuel grid spacers and hold down springs are not included in these number densities. For the purpose of this evaluation these number densities are identified as "radial." Because the 24PT1-DSC is filled with water at Decontamination and Wet Welding and drained at Dry Welding and Transfer Storage, material densities for these stages are classified as "wet" and "dry", respectively.

The second configuration analyzed is the 24PT1-DSC inside of the AHSM. Dry radial densities are employed in this configuration. Spacer disks are not included in this configuration at all, neither inside nor outside of the "equivalent" cylinder. This provides additional conservatism.

A summary of the configurations analyzed and the credit taken for carbon steel spacer discs is provided below:

Configuration	**Dose Rate Evaluation**	
	Radial	**Axial**
24PT1-DSC in Cask[1]	Cask Side[2]	Cask Top and Bottom Ends[3]
24PT1-DSC in AHSM	AHSM Top, Bottom and Sides[2]	AHSM Front and Back[2]

1 – Cask decontamination, Wet welding and 24PT1-DSC draining, Dry welding and Transfer-Storage configurations
2 – No credit taken for carbon steel spacer discs
3 – Credit taken for carbon steel spacer discs

A revision to SAR Section 5.3.2 to clarify the discussion regarding orientations in which the spacer discs are included in the material densities has been provided.

Chapter 6 Criticality

Question 6-1

Describe the calculational model used for the infinite array of casks which is found on page 6.3-2 of the SAR. Also justify in the SAR that this model is bounding for all actual storage, loading/unloading, and transfer configurations.

The model used for this scenario was not described in sufficient detail. It is not clear whether the casks are an infinite array of canisters in transfer casks or if the array consists of canisters in their typical storage configurations out of the transfer casks. This information is required for the staff to assess compliance with the nuclear criticality safety requirements specified in 10 CFR 72.124 and 72.236(c).

Response to Question 6-1

Additional discussion has been added to SAR Section 6 to demonstrate that the analyses performed are representative of an infinite array of flooded 24PT1-DSCs in flooded MP187 transfer casks. The AHSM storage configuration is bounded by this transfer cask configuration since the canister in the storage configuration is not flooded. The reactivity of the system is highly dependent on the internal moderator density, with the maximum reactivity occurring at maximum internal moderator density.

Question 6-2

Provide a reference for the transfer cask used in the criticality safety analysis in Chapter 6 of the SAR.

The specific transfer cask that was used in the criticality safety evaluation in Chapter 6 is not identified. This is required for the staff to assess compliance with 10 CFR 72.124 and 72.236(c).

Response to Question 6-2

The cask used in the criticality analyses is the MP187 transport cask (C of C 71-9255). A comparison of pertinent dimensions for the MP187 cask and the OS-197 cask has been added to Section 6 of the SAR. The differences between the two casks are shown to be minor. A comparative analysis of the 24PT1-DSC in the OS-197 transfer cask for the WE 14 X 14 SC fuel damaged fuel geometry case was performed to confirm that these differences are minor. The result of this analysis reflects a small decrease in reactivity which is approximately equal to the 1 σ uncertainty for both runs, approximately 0.0015.

Question 6-3

Justify that any other NRC licensed transfer cask is acceptable for use with the 24PT1-DSC without any consideration for criticality safety, as inferred in Section 1.2.1.3.1 of the SAR.

Section 1.2.1.3.1 of the SAR infers that any other NRC licensed transfer cask is acceptable for use with the 24PT1-DSC subject to a site specific evaluation which considers only the following cask characteristics; cavity dimensions, payload, heat load capacity, and shielding. The criticality safety analysis in Chapter 6 does not provide justification for use of other transfer casks, which may be constructed of different types and amounts of materials. This is required for the staff to assess compliance with 10 CFR 72.124 and 72.236(c).

Response to Question 6-3

SAR Section 6 has been revised to specify that the OS-197 is the only cask authorized for fuel transfer operations as discussed in the response to RAI Question 1-1. The criticality safety analysis is bounded by the results presented in the SAR for the NUHOMS®-MP187 as documented in the response to RAI Question 6-2.

Question 6-4

Resolve the discrepancy between Tables 6.1-1 and 6.4-3.

Tables 6.1-1 and 6.4-3 report different keff values for what appears to be the same case for the most limiting WE 14x14 SC fuel scenario. This is required for the staff to assess compliance with 10 CFR 72.124 and 72.236(c).

Response to Question 6-4

The discrepancy between SAR Tables 6.1-1 and 6.4-3 is a typographical error. SAR Table 6.4-3 is correct. SAR Table 6.1-1 has been revised to address a new case associated with uncertainty in fuel enrichment for UO2 fuel. This new case is discussed in the response to RAI Question 4-6.

Question 6-5

Provide the fissile material compositions used in the criticality safety analysis in Tables 6.3-2 and 6.3-3.

The fissile material compositions used in the SCALE calculational models were not provided. This is required for the staff to assess compliance with 10 CFR 72.124 and 72.236(c).

Response to Question 6-5

The as modeled fuel pellet material densities have been added to SAR Tables 6.3-2 and 6.3-3.

Question 6-6

Provide SCALE inputs for each of the following cases;

1 - the most limiting normal cases for the intact UO2 fuel, intact MOX fuel, and damaged fuel (either UO2 or MOX), and
2 - the most limiting accident cases for the intact UO2 fuel, intact MOX fuel, and damaged fuel (either UO2 or MOX).

The inputs used in the SCALE calculational models were not provided. This is required for the staff to assess compliance with 10 CFR 72.124 and 72.236(c).

Response to Question 6-6

Section 6.6.2 "KENO Input Files" has been added to the SAR. SCALE inputs are included in this section as requested.

Question 6-7

Describe in greater detail in Section 6 how the Upper Subcritical Limit (USL) was determined.

The SAR does not discuss any bias and uncertainty associated with the USL determination, nor does it discuss any uncertainty due to modeling approximations. Note that only biases that increase keff should be applied. This is required for the staff to assess compliance with 10 CFR 72.124.

Response to Question 6-7

SAR Section 6.5.1 has been revised to incorporate additional discussion of the method used for calculation of the Upper Subcritical Limit (USL). The methodology used is based on NUREG/CR-6361, USL method 1.

Question 6-8

Describe which factors were considered when choosing the experiments used to validate the computer code used for the criticality safety analysis.
The bias and uncertainty should be established using critical experiments that are applicable to the package design. Several of the experiments, such as BW1810A through E, DSN 399-1 through -4 and W3269A through C contain materials such as gadolinium,

hafnium, or cadmium which are not used in the criticality analysis computer models. Therefore, it is not clear why these experiments were used. This is required by the staff to determine the applicability of the critical experiments to the application and to assess compliance with 10 CFR 72.124.

Response to Question 6-8

The benchmark analysis performed included many experiments associated with various parameters. This set of benchmarks is considered generic and is used for application of the computer code to various system designs. Included in this set are 15 benchmarks that contain materials not present in the system analyzed for this application. The benchmarks are:

Case No.	Case designation	Enrich. (wt %)	Pitch (cm)	H2O/fuel volume	Description
31	BW1810A	2.46	1.636	1.841	UO_2-Gd_2O rods, water holes, borated H_2O
32	BW1810B	2.46	1.636	1.841	UO_2-Gd_2O rods, water holes, borated H_2O
33	BW1810C	2.46 & 4.02	1.636	1.841 & 1.532	UO_2-Gd_2O rods, water holes, borated H_2O
34	BW1810D	2.46 & 4.02	1.636	1.841 & 1.532	UO_2-Gd_2O rods, water holes, borated H_2O
35	BW1810E	2.46 & 4.02	1.636	1.841 & 1.532	UO_2-Gd_2O rods, water holes, borated H_2O
39	BW1810I	2.46	1.636	1.841	Water holes, Ag-In-Cd rods, borated H_2O
44	DSN399-1	4.74	1.6	3.807	Hafnium separator plates
45	DSN399-2	4.74	1.6	3.807	Hafnium separator plates
46	DSN399-3	4.74	1.6	3.807	Hafnium separator plates
47	DSN399-4	4.74	1.6	3.807	Hafnium separator plates
166	W3269A	5.7	1.422	1.93	Ag-In-Cd rods
167	W3269B1	3.7	1.105	1.432	Ag-In-Cd rods
168	W3269B2	3.7	1.105	1.432	Ag-In-Cd rods
169	W3269B3	3.7	1.105	1.432	Ag-In-Cd rods
170	W3269C	2.72	1.524	1.494	Ag-In-Cd rods

All other benchmarks used to develop the USL contain materials found in the analyzed system and can be used to determine bias associated with the cross section library. These experiments are presented in a revised SAR Table 6.5-1. Little to no effect was found when these 15 experiments were removed from the USL.

In addition, two parameters were added to investigate the calculational bias associated with the Boral neutron absorbing material. Boron weight percent and B-10 areal density are added to the list of parameters used to determine the calculational bias in the modeling system.

SAR Table 6.5-2 has been revised to document the changes in the USL reflecting the removal of the 15 benchmark experiments noted above and adding the Boron parameters. Correlation coefficients for the 8 parameters listed in Table 6.5-2 are included in the last row of Table 6.5-1. The limiting USLs for all 8 parameters are presented in Table 6.5-4.

Section 6.5 of the SAR has been revised to reflect these changes.

Question 6-9

Provide a table of correlation coefficients for the 6 parameters listed in table 6.5-2 and also for boron areal density.

The correlation coefficients are not given for the SCALE 4.4 validation. This is required for the staff to assess compliance with 10 CFR 72.124.

Response to Question 6-9

A linear regression correlation is calculated for each of the eight parameters listed in revised SAR Table 6.5-2 versus k_{eff}. The correlation coefficient for each parameter is provided in the last row of the revised SAR Table 6.5-1. The best correlation is observed for "separation of assemblies", with a correlation of 0.67. All other parameters show much lower correlations, which indicates that there is no real correlation for these parameters. Since there is no strong correlation for any of the data sets, the lowest possible USL-1 result is used as the USL.

Question 6-10

Discuss in Chapter 6 the failed fuel can screen mesh size and either justify that uneven draining is not credible or provide an analysis considering uneven flooding.

Uneven draining may be possible for screens with a mesh size of 350 or less because the water surface tension may be capable of supporting water. Uneven draining in the canister may be more reactive than a fully flooded cask. This is required for the staff to assess compliance with 10 CFR 72.124 and 72.236(c).

Response to Question 6-10

The screen mesh size specified in the SAR 24PT1-DSC drawing (NUH-05-4010, sheet 1, Bill of Material, Item 43), in SAR Section 1.5.2, is a 6 x 6 mesh with 0.047" wire diameter. This large mesh size will not obstruct uniform draining in the canisters. Additional discussion of this issue has been added to Section 6.3.1 of the SAR.

Question 6-11

Clarify TS 12.2.1 d. which appears to disallow storage of intact MOX assemblies.

It is not clear whether the applicant intends to limit this application to storage of one damaged MOX assembly per cask only. The TS does not clearly address storage of any intact MOX assemblies. This is required by the staff to assess compliance with 10 CFR 72.24(g), 72.26, and 72.44(c).

Response to Question 6-11

The text of SAR Section 12.2.1.d has been revised to clarify the requirements and limitations for storage of intact stainless steel clad fuel, intact mixed oxide fuel, damaged stainless steel clad fuel and damaged mixed oxide fuel.

Question 6-12

Revise TS table 12.2-2 to include the number of guide tubes and/or instrument tubes.

The SAR does not address varying the number of guide tubes and/or instrument tubes. This is required by the staff to assess compliance with 10 CFR 72.24(g), 72.26, and 72.44(c).

Response to Question 6-12

SAR Table 12.2-2 has been revised to include the number of guide tubes and/or instrument tubes per assembly.

Question 6-13

Revise Section 12.4.0 to include the basket B-10 loading and the flux trap size.

The B-10 loading and flux trap size are design parameters important to criticality safety. This is required by the staff to assess compliance with 10 CFR 72.24(g), 72.26, and 72.44(c).

Response to Question 6-13

SAR Section 12.4 has been revised to incorporate a new Section 12.4.2.3, titled "Canister Neutron Poison" which now specifies the minimum B-10 loading of 0.025 grams/cm^2. A new Section 12.4.2.4, titled "Canister Flux Trap Configuration" has also been added to specify the flux trap size by reference to the spacer disc dimensions specified in the canister drawings in SAR Section 1.5.2.

Question 6-14

Justify that the postulated failure scenarios for damaged fuel is bounding.

The criticality safety analysis in Section 6.3 of the SAR does not provide justification that the scenarios considered for failed fuel bound other possible scenarios such as missing fuel pins. This is required for the staff to assess compliance with 10 CFR 72.124 and 72.236(c).

Response to Question 6-14

Additional discussion of the damaged fuel analysis is provided in SAR Section 6.4.2 to further demonstrate that the postulated failure scenarios for damaged fuel are bounding.

Chapter 7 Confinement

Question 7-1

Justify the use of an ultrasonic test (UT) for the inner bottom cover plate to canister shell weld in lieu of a radiographic test (RT), as described in SAR section 7.1.3 and Figure 7.1-1. Provide evidence of the UT performance demonstration that was done to qualify the technique for this application, using full scale qualification samples of the same materials and geometry with imbedded cracks (not machined notches or drilled holes). Demonstrate that the sensitivity of the UT procedure meets or exceeds the sensitivity of an RT or the Code acceptance criteria for this application. Update other sections of the SAR as necessary (e.g. ASME code exceptions, and Chapter 9).

The application does not justify the use of the UT technology in an application where UT techniques are difficult and code requirements stipulate RT technology. The NRC notes that the use of ASME Section XI analytical methods and acceptance criteria has not been justified for this application. This information is needed to assure compliance with 10 CFR 72.236(j).

Response to Question 7-1

The inner bottom cover plate to canister shell is defined as a Type 2 Category C corner weld by subarticle NB-3350 and Figures NB-3351-1 and NB-4243-1 (Detail j). The examination requirements for this weld are specified in NB-5231(b) and (c). NB-5231(b) permits the use of RT or UT as approved methods for examination of the joint. NB-5231(c) adds the requirement that if the joint is RT examined, then an additional UT examination of the "...fusion zone and the parent metal beneath the attachment surface to verify freedom from lack of fusion and laminar defects". Therefore, the weld examination described in the SAR is in accordance with the ASME code requirements for a Class 1 vessel. In addition, this joint has been successfully demonstrated to meet ASME code requirements for 24PT1-DSCs fabricated for the Rancho Seco project.

Alternative joint details have also been added to the canister SAR drawing in Section 1.5.2 to provide additional flexibility in fabrication. As shown on NUH-05-4010, Sheet 4, this will permit substituting a forging for the inner bottom cover plate. This effectively moves the weld joint away from the corner to a Category B circumferential weld seam, which is examined by RT methods in accordance with NB-5221. Both joint details fully comply with ASME Section III requirements for a Class 1 vessel. The selection of the joint to be used in fabrication of a 24PT1-DSC has been left to the fabricator. For either joint, the fabricator is required to meet all ASME Section III Class 1 code requirements for the qualification, welding and examination of the joint.

Chapter 10 Radiation Protection

Question 10-1

Provide the dose contribution associated with the maximum contamination levels stated in Section 12.5.2.4 of the SAR.

This information is required for the staff to assess whether the maximum contamination levels bound, combined with the DSC source term, meet the off-site dose requirements of 10 CFR 72.104 and 10 CFR 72.106.

Response to Question 10-1

The 24PT1 DSC smearable surface contamination limits stated in Section 12.5.2.4.c have been revised to be less than 2200 dpm/100 cm^2 for beta and gamma sources, and less than 220 dpm/100 cm^2 from alpha emitting sources.

See Response to RAI Question 12-5 for the dose contribution associated with the maximum contamination levels specified in Section 12.5.2.4.c of the SAR.

Chapter 11 Accident Analysis

Question 11-1

Provide justification that inadvertently loading spent fuel assemblies, not allowed by Section 12 of the SAR, is not a credible occurrence as stated in Section 11.2.10.3 of the SAR.

NRC staff does not accept that inadvertent loading of spent fuel assemblies is not a credible event. The justification should address both the probability and consequences of loading spent fuel not allowed by Section 12 of the SAR.

This information is required by the staff to assess compliance with 72.94 and 72.236(l).

Response to Question 11-1

A review of Westinghouse 14 x 14 stainless steel clad UO2 assemblies and 14 x 14 zircalloy clad mixed oxide fuel assemblies fabricated to date has confirmed, based on current 24PT1-DSC licensing and fabrication schedules, that the inventory of all fuel assemblies of this type will meet the fuel specification requirements of Section 12 of the SAR. Therefore, inadvertent loading of a fuel assembly exceeding these requirements with respect to enrichment, burnup, decay time and decay heat is not credible.

The consequences of a potential misloading (early loading) of fuel assemblies is discussed below.

The highest burnup fuel assembly in inventory as of January 2001 has a decay heat of approximately 0.7 kW. The actual number of fuel assemblies greater than 0.581 kW in inventory is 13. Assuming these 13 assemblies are 0.7 kW each and the balance of the assemblies are 0.581 kW each and including 24 control components at 0.002 kW each, the maximum canister heat load is less than 16 kW. The analysis at 16 kW provided in Chapter 4 of the SAR indicates that vacuum drying is the only operating condition in which a specified material temperature limit is exceeded (the spacer disc temperature limit is exceeded in this case). Since this is a short term scenario and based on the conservative limits used, the misloading can not impact the 24PT1-DSC confinement boundary integrity. Section 11.2.10.2 of the SAR has been revised to address the consequences of loading spent fuel not allowed by Section 12 of the SAR, based on the above discussion.

Chapter 12 Operating Controls and Limits

The following regulatory requirements are applicable in this chapter: 10 CFR 72.11, 72.24(g), 72.26, 72.44(c), 72.104, 72.106, 72.234(a), 72.236, and Subparts C, E, F, G, H, and I. It should be noted that other regulatory requirements may be applicable to this section.

Question 12-1

Specify which transfer and/or transportation casks may be used to perform on-site transfer of the DSC-24PT and any required design criteria.

Technical Specification 12.4.3.3, does not specify transfer or transportation casks that may be used to perform on-site transfer of the DSC-24PT nor does it provide, or reference, a methodology or design criteria to be used to select casks appropriate to perform on-site transfer of the DSC-24PT.

Response to Question 12-1

SAR Sections 12.2.1.c and 12.4.3.3 have been revised to remove references to casks other than the OS-197.

Question 12-2

Provide the analysis to support the 80 degrees F AHSM limit stated in Section 12.5.2.5 of the SAR.

Section 9.1.6 of the SAR states that the heat removal capability is assured through monitoring of the AHSM concrete temperatures. Section 12.5.2.5 suggests corrective actions should be taken to avoid exceeding the concrete and cladding temperature limits if the temperature rises by more than 80 degrees F. Describe how this temperature rise was chosen. Include an explanation of how the fuel cladding temperatures are related to this rise. This information is required by the staff to assess whether the fuel cladding is protected against degradation that could lead to gross ruptures per 10 CFR 71.122(h)(1).

Response to Question 12-2

The specification of an 80 °F temperature rise in the monitored AHSM concrete temperature was chosen as the criteria for monitoring changes in concrete temperature to ensure that temperatures approaching the blocked vent condition are not reached without investigative action. An increase in concrete temperature of 175 °F is expected at the AHSM roof inner surface for a design basis (24 kW AHSM heat load) during the 40 hours allowed for a blocked vent transient. This translates to a temperature increase of approximately 100 °F at the thermocouple location (7" above the inner surface of the AHSM roof). By choosing a temperature increase that is only 80% of the expected increase; the increase in temperature will be identified as significant requiring further

investigation several hours prior to the maximum design basis temperature being reached for an AHSM design basis payload.

This limit also provides additional conservatism since the likelihood of the occurrence of the design basis ambient temperature (117 °F) at the same time as a blocked vent condition is small. The 80 °F concrete temperature rise limit would typically be measured from a long term average ambient temperature of 70 °F and would therefore provide significant additional margin between the maximum temperature increase specified and the maximum concrete temperature limit.

This limit in conjunction with the 225 °F maximum concrete temperature limit will also ensure that the maximum analyzed fuel clad temperatures for the blocked vent case are not exceeded. By extrapolating from the 24 kW AHSM case to the 14 kW case:

$[T_{14kw} = ((T_{24kw}-T_{amb}) \times (14kW/24kW))+T_{amb}]$

a roof temperature of approximately 230 °F would be expected at an ambient temperature of 117 °F (based on a maximum concrete temperature monitor reading of 314 °F, extrapolated from the 393 °F at the inside surface of the roof, for a 24 kW payload). The upper limit of 225 °F bounds this maximum roof temperature thus ensuring that the 14 kW payload design basis fuel clad temperature of 749 °F is not exceeded. The temperature increase between the long term average concrete monitor temperature, for an AHSM loaded with a 14 kW heat load, and the maximum concrete monitor temperature (230 °F) is approximately 100 °F which is also bounded by the 80 °F temperature increase criteria.

Therefore, the maximum allowed temperature chosen and the maximum allowed temperature rise will ensure that AHSM concrete temperature is limited to the design basis maximum for a 24 kW heat load while also ensuring that the 14 kW payload fuel clad temperature limits are not exceeded.

SAR Section 12.5.2.5 has been revised to incorporate a brief discussion of the above basis.

Question 12-3

Clarify the design criteria for Design Feature 12.4.2.2, Storage Pad.

Design Feature 12.4.2.2, refers to Chapter 2 which provides general information and also makes reference to other portions of the SAR. Design Feature 12.4.2.2, should contain sufficient information regarding the evaluation methods required for a licensee to ensure its site is bounded for the Advanced NUHOMS® System. This information is required by the staff to assess compliance with 10 CFR 72.102(c) and (e), 10 CFR 72.212(b)(2) and (3), and 10 CFR 72.122(b).

Response to Question 12-3

SAR Section 12.4.2.2 has been revised to more clearly specify the analysis to be performed by the licensee to ensure that the effect of amplification of the seismic accelerations due to soil structure interaction are addressed. In addition, the storage pad location shall have no potential for liquefaction at the site-specific Safe Shutdown Earthquake level.

Question 12-4

Revise Design Feature 12.4.3.1, Advanced Horizontal Storage Module to include a statement regarding the minimum number of AHSMs that must be attached and spacing on the pad that must be attached to each other to meet the design requirements for a design basis earthquake.

This information is required by the staff to assess compliance with 10 CFR 72.90.

Response to Question 12-4

SAR Section 12.4.4.1 was revised to specify that AHSMs will be tied together in groups of at least three. The required spacing of 20 ft. between each group of modules, which are tied together, and 10 ft. between any module and the edge of the ISFSI pad was also added. The revision was made to SAR Section 12.4.4.1 since SAR Section 12.4.3.1 is associated with AHSM codes and standards.

Question 12-5

Justify the statement in Section 12.5.2.3.b, of the SAR that the ISFSI will not create any radioactive materials or result in any credible liquid or gaseous effluent release.

The SAR did not provide sufficient information for not implementing effluent monitoring program for the Advanced NUHOMS® design. The justification should include an analyses and a discussion of all assumptions and methodology used, to support the statements made in Sections 12.5.2.3 and 12.5.2.4. The analyses should include the potential off-site dose release from the maximum number of Advanced NUHOMS® systems on site with a residual contamination limit of approximately 22,000 dpm/100 cm2 and 2,200 dpm/100 cm2 . The staff cannot confirm that the Advanced NUHOMS® system with the administrative controls program describing dose rates, surface contamination limits, and radioactive effluents will comply with the off-site dose limits of 10 CFR 72.104 for normal and anticipated occurrences.

In the past, the staff has accepted that surface contamination limits set at the values recommended by Regulatory Guide 1.86 will result in no effluent release from an ISFSI. Therefore, the staff has concluded that an effluent monitoring and reporting system in accordance with 72.44(d) (for site specific licensees) or 50.36a (for general licensees) is

not required. This information is required for the staff to assess compliance with 10 CFR 50.36a in lieu of maintaining the contamination limits of Regulatory Guide 1.86, "Termination of Operating Licenses for Nuclear Reactors."

Response to Question 12-5

The 24PT1 DSC smearable surface contamination limits stated in Section 12.5.2.4.c have been revised to be less than 2200 dpm/100 cm^2 for beta and gamma sources, and less than 220 dpm/100 cm^2 from alpha emitting sources.

The Advanced NUHOMS® System is a self contained passive system that does not produce routine solid, liquid or gaseous effluents.

The contamination limits specified above are based on the allowed removable external radioactive contamination specified in 49 CFR 173.443 (as referenced in 10 CFR 71.87(i)) the system provides significant additional protection for the 24PT1-DSC surface than the transportation configuration. The AHSM will protect the 24PT1-DSC from direct exposure to the elements and will therefore limit potential releases of removable contamination. The probability of any removable contamination being entrapped in the AHSM air flow path released outside the AHSM is considered extremely small.
To demonstrate that the Advanced NUHOMS® System with the 24PT1-DSC surface contamination limits specified in SAR Section 12.5.2.4.c complies with the off site dose limits of 10CFR 72.104, TN West has performed an analysis. This analysis is evaluating a non-mechanistic event and thus many of the parameters used in this evaluation are assumed or postulated. The assumptions which support the analysis are listed below:

- The entire surface of the canister is assumed to have the maximum allowed contamination level. Therefore, the total activity available for release is assumed to be the surface area of the outside of the canister times the contamination limits.

- A single individual ingests all of the contamination on the surface of a single canister.

- All of the contamination is released in one second from the AHSM vent, and that the resultant contamination cloud exists for two hours at the controlled area boundary (100 meters from the facility).

- The downstream (ambient) pressure for all leak calculations is assumed to be one atmosphere. This is representative of the bulk of the atmosphere. Small variations in atmospheric pressure will not significantly affect the results of the calculation.

- The dispersion factor is calculated using Regulatory Guide 1.135 assuming D stability and a wind speed of 5 meters per second with a distance to the controlled area boundary of 328 feet (100 meters). These atmospheric conditions are consistent with the guidance of ISG-5 for normal and off-normal conditions. The distance to the controlled area boundary (100 meters) is the shortest distance permitted by 10CFR72.106. Using the shortest distance maximizes the exposures due to the release.

- The worst-case clearance class is conservatively used for each organ/nuclide combination.

- Based on several representative "crud" data measurements, the radionuclide content of surface contamination from a PWR reactor is provided in Table 12-5.1.

Table 12-5.1
Composition of Typical Surface Contamination

Nuclide	% Activity
β,γ emitters	
C14	0.20
Fe55	12.75
Ni59	0.15
Co60	18.10
Ni63	21.40
Sr90	2.40
Cs134	8.10
Cs137	36.90
Total	100.00
α emitters	
Pu238	4.00
Pu239,240	1.30
Pu241	87.50
Am241	4.70
Cm243,244	2.50
Total	100.00

The methodology used for this evaluation is summarized below.

1. Determine total activity (μCi) on the 24PT1-DSC shell for each radioactive isotope based on the surface area of the canister, the allowed surface contamination limit and the representative radionuclide composition of the surface contamination.

2. Determine the "Committed Dose Equivalent per Unit Intake" from Federal Guidance Report No. 11 [12-5.1]. Multiply the total activity for each nuclide by the Committed Dose Equivalent values to determine the total dose to an individual that ingests all of the contamination.

3. Determine the Atmospheric Dispersion Factors at the controlled area boundary (100 meters from the facility) and a wind speed of 5 meters per second using Regulatory Guide 1.145 [12-5.2]. The Dose Conversion Factors for air submersion are taken from Table III.1 of Federal Guidance Report No. 11 [12-5.1]. The Dose Conversion Factors for inhalation are taken from Table 2.1 of Federal Guidance Report No. 12 [12-5.3].

4. The Deep Dose Equivalent (DDE) due to air submersion for the whole body and

each individual organ is given by:

$$DDE_{i,o} = Q_i\left(\frac{Bq}{sec}\right)\cdot DCF_{i,o}\left(\frac{Sv\cdot m^3}{Bq\cdot sec}\right)\cdot \frac{\chi}{Q}\left(\frac{sec}{m^3}\right)\cdot t(sec) \qquad \textbf{Equation 1}$$

where:

$DDE_{i,o}$ is the deep dose equivalent contribution from nuclide i to organ o, mrem (this is the shallow dose equivalent (SDE) when used for the skin)

Q_i is the isotope specific leak rate, Bq/sec (All assumed to leak in 1 second)

$DCF_{i,o}$ is the dose conversion factor for nuclide i to organ o

χ/Q is the atmospheric dispersion factor, 1.730×10^{-3} sec/m^3 for normal operation

t is the duration of the exposure, 2 hours or 7,200 seconds

5. The Committed Dose Equivalent (CDE) for internal organ doses (Committed Effective Dose Equivalent, CEDE, for the internal whole body dose) due to inhalation is given by:

$$CDE_{i,o} = Q_i\left(\frac{Bq}{sec}\right)\cdot DCF_{i,o}\left(\frac{Sv}{Bq}\right)\cdot \frac{\chi}{Q}\left(\frac{sec}{m^3}\right)\cdot R\left(\frac{m^3}{sec}\right)\cdot t(sec) \qquad \textbf{Equation 2}$$

where:

$CDE_{i,o}$ is the committed dose equivalent contribution from nuclide i to organ o, mrem (this is the committed effective dose equivalent (CEDE) when used for the whole body)

Q_i is the isotope specific leak rate, Bq/sec (All assumed to leak in 1 second)

$DCF_{i,o}$ is the dose conversion factor for nuclide i to organ o

χ/Q is the atmospheric dispersion factor, 1.730×10^{-3} sec/m^3.

R is the respiration rate, 3.3×10^{-4} m^3/sec (Federal Guidance Report 11)

t is the duration of the exposure, 2 hours or 7,200 seconds

6. The Total Effective Dose Equivalent (TEDE) is equal to the sum of the whole body Deep Dose Equivalent (DDE) and the Committed Effective Dose Equivalent (CEDE). The Total Organ Dose Equivalent (TODE) for a given organ is equal to the sum of the DDE for that organ and the CDE for that organ.

7. Compare the calculated TEDE and TODE results to the requirements of 10CFR72.104(a) for normal and anticipated occurrences.

A summary of the calculated exposures is presented in Table 12-5.2. As demonstrated by these results, the calculated doses using extremely conservative assumptions are less than 1.2 % of the 10CFR72.104(a) annual dose limits. Therefore, it is concluded that the maximum contamination levels specified in the revised Section 12.5.2.4.c of the SAR (2,200 dpm/100cm^2 β,γ and 220 dpm/100cm^2 α) are negligible.

SAR Section 12.5.2.4.c has been revised to specify the reduced limits and provide the basis for these limits.

Table 12-5.2

Dose Summary and Comparison to 10CFR72.104(a) Limits

Organ	10CFR72.104(a) Limit (mrem)	Total Ingestion Dose (mrem)	DDE + CDE @ 100 meter (mrem)	Total Ingestion Dose / 72.104 Limit	DDE + CDE @ 100 meter / 72.104 Limit
Whole Body	25	0.0240	0.0072	0.0010	0.0003
Thyroid	75	0.0078	<0.0001	0.0001	<0.0001
Other Critical Organ	25	0.2790	0.1284	0.0112	0.0051

[12-5.1] Federal Guidance Report No. 11, "Limiting Values of Radionuclide Intake and Air Concentration and Dose Conversion Factors for Inhalation, Submersion, and Ingestion," DE89 011 065, 1988.

[12.5-2] Regulatory Guide 1.145, "Atmospheric Dispersion Models for Potential Accident Consequence Assessments at Nuclear Power Plants", Revision1, February 1982.

[12.5-3] Federal Guidance Report No. 12, "External Exposure to Radionuclides in Air, Water, and Soil," EPA 402-R-93-081, September 1983.

TRANSNUCLEAR WEST

ATTACHMENT 3

RAI 3-6 RESPONSE

Attachment 3

RESPONSE TO REQUEST FOR ADDITIONAL INFORMATION
TRANSNUCLEAR WEST INC., TAC NO. L23203

RESPONSE TO RAI 3-6

Question 3-6

Provide a soil-structure interaction analysis that would be typical for a site deploying the Advanced NUHOMS® System.

The design basis response spectra of the Advanced NUHOMS® System design is based on the standard spectrum shape in NRC Regulatory Guide 1.60, "Design Response Spectra for Seismic Design of Nuclear Power Plants," Revision 1, 1973, anchored at 1.5g zero period acceleration for the horizontal direction. The vertical design spectrum is set at 2/3 of the horizontal over the entire frequency range. The horizontal and vertical spectra are specified at the top of the basemat.

Nonlinear analyses were performed in Chapter 11 of the SAR to determine the maximum sliding and rocking/tipping response of the AHSM during a design basis seismic event. These analyses were based on acceleration time histories from the Taiwan earthquake in 1999, the Landers/Lucern earthquake in 1992, and the Tabas earthquake in 1978. However, the staff requires the analysis including the soils and structure interactions, the methodologies and computer model, and the specific acceleration histories that envelope the parameters of a typical site. This is required for the staff to assess compliance with 10 CFR 72.122(b).

Note: The above question was restated in accordance with a communication from Mr. Steve Baggett (NRC) to Mr. U. B. Chopra (TN-West) via e-mail dated 4/18/01, 9:57 am, subject: "Reference RAI 3-6 for the Advanced NUHOMS design".

Response to Question 3-6

A general licensee that deploys the Advanced NUHOMS® Storage System that is the subject of this Safety Analysis Report shall engineer and construct the concrete pad which supports the storage modules. A site-specific soil-structure interaction analysis is required to establish the seismic response at the interface with the base of the storage modules. The site-specific analysis must be documented as part of the evaluations required of the general licensee by 10 CFR 72.212(b)(2) and is subject to NRC review through inspection at the site. All figures and tables referred to in the Response to RAI Question 3-6 are provided at the end of the response.

1. Soil-Structure Interaction Analysis Example

The following is an example of a soil-structure interaction (SSI) analysis for an Independent Spent Fuel Storage Installation (ISFSI) concrete pad that will support the Advanced NUHOMS storage system. The example uses the soil parameters and seismic ground motions at an exemplifying high seismic west coast site. It is not necessarily bounding for all sites. As can be seen from the results, substantial margins remain to the design earthquake response spectra. The soil-structure interaction analysis employs the methods that are typical of an analysis to be performed by the general licensee.

2. Site Seismic Input

The seismic input for the SSI analyses of the ISFSI was defined by the site's safe shutdown earthquake (SSE) as required by 10 CFR 72.102. The SSE response spectra are shown in Figure 2-1 for the horizontal and vertical response spectra (target response spectra) at 5% critical damping ratio.

To perform the SSI analyses, three artificial acceleration time histories (the three components of a single earthquake) were developed to envelop the target response spectra. These time histories were developed following the criteria given by the Standard Review Plan (Reference 1), Section 3.7 for response spectra enveloping, total duration, strong motion duration, statistical correlation, and power spectral density enveloping.

Figures 2-2 to 2-4 show the comparison between the target response spectra and the response spectra calculated from the artificial acceleration time histories. This comparison shows that the artificial time histories meet the response spectra enveloping requirements.

Figures 2-5 to 2-7 are the plots of the three artificial time histories. Their total duration is 40 seconds with a time step of 0.01 seconds. The strong motion duration times are 24.21 seconds and 23.11 seconds for the two horizontal components, and 20.99 seconds for the vertical component. The total duration and strong motion duration times meet the requirements in the Standard Review Plan, Section 3.7.1 and they are consistent with the duration times suggested for the seismic level at the plant (Reference 2).

The strong motion duration was defined as the difference between the time when the energy reaches 90% and the time when the energy reaches 5%. Energy was calculated as the integral of the square of the acceleration ($\int a^2 dt$).

The correlation coefficient between the two horizontal components is 0.0147, and between the two horizontal components and the vertical components are 0.0614 and 0.1013, respectively. These coefficients are lower than the 0.16 value recommended in Reference 4 and the value of 0.30 recommended in Reference 3. Thus, the three components are statistically independent.

3. Soil Model

The site soil profile corresponds to a relatively homogeneous medium with dynamic properties varying with depth. The soil beneath the pad is a very dense well graded sands

with a depth of about 900 feet under the ISFSI. The surface of the soil is at elevation +15.75' and the water table is at elevation +5.0'. The bottom of the concrete slab supporting the AHSMs was assumed to be at the surface of the soil.

3.1 Low Strain Soil Properties

The best estimate soil properties were developed as a function of depth down to elevation -145.0'. Below that elevation, the soil properties were kept constant. Table 3-1 gives the low strain, best estimate soil properties. Note that the P wave velocity for the saturated soil was set equal to the compression wave velocity in water.

To account for the possible variation in soil properties, two bounding cases were defined in accordance with the Standard Review Plan, Section 3.7.2: an upper bound case obtained by scaling the best estimate soil shear modulus by 2, and a lower bound case obtained by scaling the best estimate soil shear modulus by 0.5. The P wave velocity for the saturated layers was kept constant since it corresponds to the velocity in water. Table 3-2 gives the low strain lower and upper bound soil properties.

The shear modulus and shear wave velocity profiles for the three low strain soil cases are shown in Figures 3-1 and 3-2, respectively.

3.2 Strain Compatible Soil Properties

During an earthquake, the soil behaves in a nonlinear manner and its dynamic properties change as a function of the shear strain imposed by the seismic motion. To account for this nonlinear behavior when performing soil-structure interaction analysis, the accepted practice is to develop an equivalent linear soil profile that is consistent with the level of shear strain imposed by the seismic motion.

The equivalent linear soil profile was developed by performing an iterative wave propagation analysis by modifying the dynamic soil properties according to the level of shear strain. The equivalent linear soil profile was developed with computer code SHAKE. The shear modulus-shear strain and soil damping-shear strain relationships are given in Table 3-3 and shown in Figure 3-3. The equivalent linear soil profile is normally referred to as the strain compatible or high strain soil profile.

Reference 1 states that the strain compatible soil properties for the upper bound case should not be lower than the low strain best estimate properties. In this analysis, due to the high seismic level and relatively soft soil properties, the strain compatible upper bound soil properties were lower than the low strain best estimate properties. To comply with Reference 1's requirements, a fourth soil profile was developed corresponding to the low strain best estimate soil profile.
The shear wave velocity profiles for these four cases are given in Table 3-4 and shown in Figure 3-4. The soil material damping ratios are given in Table 3-5 and shown in Figure 3-5. During the soil-structure interaction analysis, the material soil damping for P waves was limited to 10%.

The P wave velocity profile for the lower bound case was modified due to the following. The strain compatible shear wave velocity for the lower bound case at the saturated soil varies from 272 fps to 466 fps, if a constant P wave velocity of 5,000 fps is maintained, then the equivalent Poisson's ratios for several layers become very close to 0.5. This causes numerical instability during the soil-structure interaction analyses. Therefore, a reduced P wave velocity of 3,500 fps was used for the saturated layers of the lower bound soil case. The P wave velocity profiles for the four cases are given in Table 3-6 and shown in Figure 3-6.

4. Structural Model

A structural model was developed for the AHSMs and the supporting concrete slab using three-dimensional finite element techniques. The combined slab-AHSMs model is the input for the SASSI module HOUSE which generates the structural stiffness matrix for the SSI analysis.

Three structural models were developed to assess the effects on the ISFSI responses when the AHSM masses are varied:

a) Total mass of the AHSMs on the slab

b) Half of the AHSMs mass on the slab

c) No AHSM mass (to avoid numerical problems, the masses of the AHSMs were assumed equal to 1 % of the full mass instead of zero mass)

4.1 Basic Data

The ISFSI pad size is about 42'-7" wide by 111 feet long to support ten AHSMs and is 3 foot thick. The pad may be expanded in length for additional AHSMs in the future. The reinforced concrete pad will have a minimum compressive concrete strength of 3000 psi. Although the design basis for the AHSM requires a minimum group of three, this example site will be using a minimum of ten AHSM at its ISFSI.

The geometric and weight data for the slab and the AHSMs consist of ten storage AHSMs (Figure 4-1) supported on a reinforced concrete pad. The ten AHSMs are placed in a single line side-by-side without separation between them. The AHSM units interact together at their interfaces due to shear keys, steel reinforcement connections at the top and bolted connections near the base. The AHSMs are not anchored to the concrete pad. The configuration of the AHSM ensemble will tend to uniformly distribute the weight over the concrete slab in the area under the AHSMs. At the back of each AHSM there is a rear concrete shield wall bolted to the AHSMs. The two end AHSMs also have an end concrete shield wall bolted to their exterior sides. These shield walls were added to properties of their respective AHSMs.

The properties of the pad, shield walls, and the AHSMs are given below for the model and are conservative relative to the final design properties of the AHSMs. The final weights are shown in brackets.

Slab dimensions: Length = 111'

Width = 42' 7" = 42.583'

Thickness = 3'

Slab Young's Modulus: $E_c = 57{,}000\ (3{,}000)^{1/2} = 3.122 \times 10^6$ psi = 450,000 ksf

Slab unit weight = 0.15 k/ft^3

Slab Poisson's ratio = 0.20

Center of gravity of AHSMs (without shield walls) = 110.30" = 9.192' from front
= 50.38" = 4.198' from side
= 119.85" = 9.988' up

Weight of AHSMs (without shield walls) = 404.5 k [400.3 k]*

Weight of shield walls: End Wall = 205.79 k [188.0 k]*
Rear Wall = 76.51 k [69.72 k]*
* [final design weight]

The center of gravity of the AHSMs including the shield walls and their translational and rotational weights are summarized in Table 4-1.

The system of coordinates for the development of the finite element model of the ISFSI is as follows: The origin is located at the center of the concrete pad and at its bottom level. The X axis is along the longitudinal direction of the pad, the Y axis is along the transverse direction of the slab, and the Z axis is upward.

4.2 Finite Element Model of Concrete Pad

The concrete slab was modeled by a single layer of eight node brick elements. To properly capture the bending effects, incompatible deformation modes were included in these elements. The mesh for the slab consists of 360 brick elements with 806 nodes as shown in Figure 4-2

For the dynamic analysis, 7% damping was assumed for the concrete slab.

4.3 Finite Element Model of AHSMs

The AHSMs were modeled using an assembly of rigid elements. The mass of each AHSM was located at its center of gravity. The assembly of rigid elements for each AHSM consisted basically of one vertical element connected to the finite element mesh of the concrete slab by a set of horizontal and short vertical rigid beams. Each assembly of rigid elements was

connected to the pad only at slab nodes in the perimeter of the footprint of the AHSMs. Figures 4-3a, b and c show sketches of the AHSMs models.

To model all AHSMs and the connecting rigid elements, 559 beam elements were used and 248 new nodes were added to the 806 nodes defining the concrete slab.

4.4 Combined Slab-AHSMs Finite Element Model

The slab and AHSMs finite element models were combined. Figure 4-5 shows the combined model of the slab and the AHSMs. In the design, the AHSMs are not anchored to the pad, but for the purposes of the linear SSI analysis the AHSMs were modeled connected to the pad. The main characteristics of this model are:

Total number of brick elements modeling the slab: 360

Total number of beam elements modeling the AHSMs and their connections: 559

Total number of nodes at the slab: 806

Total number of nodes at AHSMs: 248

Table 4-2 gives the numbers, of the nodes at the center of gravity (cg) of the AHSMs and at the slab directly below the cg of the AHSMs. These are the nodes where the acceleration response spectra were calculated. Figure 4-6 shows the location where the acceleration responses were calculated. Three AHSM locations at their cg: nodes 817, 819, and 821; three top of slab locations below the AHSMs cg: nodes 475, 540, and 592; four top of slab locations at the corners of the footprint of the AHSMs: nodes 446, 452, 758, and 764.

5. Description of Analysis

A series of soil-structure interaction analyses were performed with computer code SASSI to generate the acceleration response spectra at the center of gravity of the AHSMs. The seismic input for all the analyses consisted of the acceleration time histories described in Section 2.

The base case of the SSI analysis is defined by the structural model of the ISFSI with the fully loaded AHSM mass and the four soil cases described in Section 3.

For each of the soil cases, the acceleration response spectra at the ten locations shown in Figure 4-6 were calculated for a damping ratio of 4%. 4% damping was used because the AHSM were analyzed and designed using the 4% damping response spectra. For each soil case, the spectra over the ten locations were enveloped. For the horizontal components, only the spectra at the AHSMs' center of gravity were enveloped. For the vertical component the spectra at the AHSMs' center of gravity and at the corners of the AHSMs were enveloped. This was done to include the maximum effect of rocking in the vertical response spectra.

In the next step, the resulting spectra for all soil cases were enveloped. These spectra are considered the final spectra at the AHSMs' center of gravity and are compared with the TN West design spectra for the AHSMs.

To assess the effect that the variation of the AHSMs' mass participating in the dynamic response has on the acceleration response spectra, two additional cases were analyzed. The first case considered only half of the AHSMs' mass and the second, as a bounding case, considered essentially zero mass in the AHSMs. The analyses for these two cases were done only for the best estimate soil case. As in the base case, the final response spectra were the envelope of the spectra at all response locations.

To assess the effect that the slab stiffness has in the response spectra at the AHSMs' center of gravity, a bounding case with the slab infinitely rigid was analyzed. The analysis for this case was done only for the best estimate soil case. As in the base case, the final response spectra were the envelope of the spectra at all response locations.

6. Results and Conclusions

The main results of the analyses performed for the ISFSI were the acceleration response spectra (4% damping) at the center of gravity of the AHSMs. These response spectra are compared to the response spectra used for the seismic design of the AHSMs by TN West. This comparison is done to evaluate if the design of the AHSMs will bound the site specific seismic design criteria.

The acceleration response spectra generated during the various analyses are presented in Figures 6-1 to 6-9.

Response Spectra for Base Case: Figures 6-1 to 6-4 show, for each soil case, the response spectra obtained by enveloping the spectra over all the locations defined in Section 5. Figure 6-5 shows the response spectra obtained by enveloping the spectra over all locations and all soil cases. The spectra in Figure 6-5 are considered as the final spectra to be compared with the AHSM design spectra used by TN West.

Sensitivity Cases: Figure 6-6 shows the envelope of the response spectra (over all locations) generated assuming only half of the AHSMs' mass in the finite element structural model and best estimate soil properties. Figure 6-7 shows the envelope of the response spectra (over all locations) generated assuming essentially no AHSM mass in the finite element structural model and best estimate soil properties. Figure 6-8 shows the envelope of the response spectra (over all locations) generated assuming full AHSM mass in the finite element structural model, a rigid pad, and best estimate soil properties.
The comparison of the design response spectra used by TN West with the final enveloped response spectra generated in the SSI analysis of the ISFSI is shown in Figures 6-9a, 6-9b, and 6-9c, for the horizontal and vertical directions.

Figures 6-1 to 6-4 for the Base Case show that the soil-structure interaction effects will amplify the free-field ground motion, generating spectral peaks at the slab and AHSMs'

CG levels on the order of 20% higher than the spectral peak of the input ground motion. The results of spectra plots at several top-of-pad and CG locations show that rocking has only a minor effect on the AHSMs' responses at their center of gravity for motions in the transverse direction of the pad. The low frequency range of the final response spectra will be controlled by the lower bound soil case, and the medium to high frequency range will be controlled by the upper bound soil cases, especially by the best estimate-low strain soil case.

The comparison of Figures 6-6 and 6-7 with Figure 6-2, shows that the reduction of the AHSM mass will result in a slight reduction of the response spectra at the center of gravity of the AHSMs. Thus the Base Case can be considered as an upper bound with respect to the effects of mass variations.

The comparison of Figure 6-8 with Figure 6-2 shows that an increase in concrete pad stiffness practically does not change the response of the AHSMs. Therefore, potential increase in concrete modulus with aging is of no consequence.
Figures 6-9a, 6-9b, and 6-9c show that the response spectra calculated at the center of gravity of the ISFSI AHSMs with the site specific SSE is lower than the acceleration response spectra used by TN West for the seismic design of the AHSMs.

No changes to the SAR have been made with respect to this RAI Question response.

References

1. NUREG-0800, "Standard Review Plan for the Review of Safety Analysis Reports for Nuclear Power Plants," Sections 3.7.1 and 3.7.2, Rev. 2.

2. Report UCRL-CR-117769, "Strong Motion Duration and Earthquake Magnitude Relationships," M.W. Salmon, S.A. Short, R.P. Kennedy, June 1992, Lawrence Livermore National Laboratory.

3. ASCE Standard: "Seismic Analysis of Safety Related Nuclear Structure and Commentary," ASCE 4-86.

4. Regulatory Guide 1.92, "Combining Modal Responses and Spatial Components in Seismic Response Analysis," Rev. 1, February 1976.

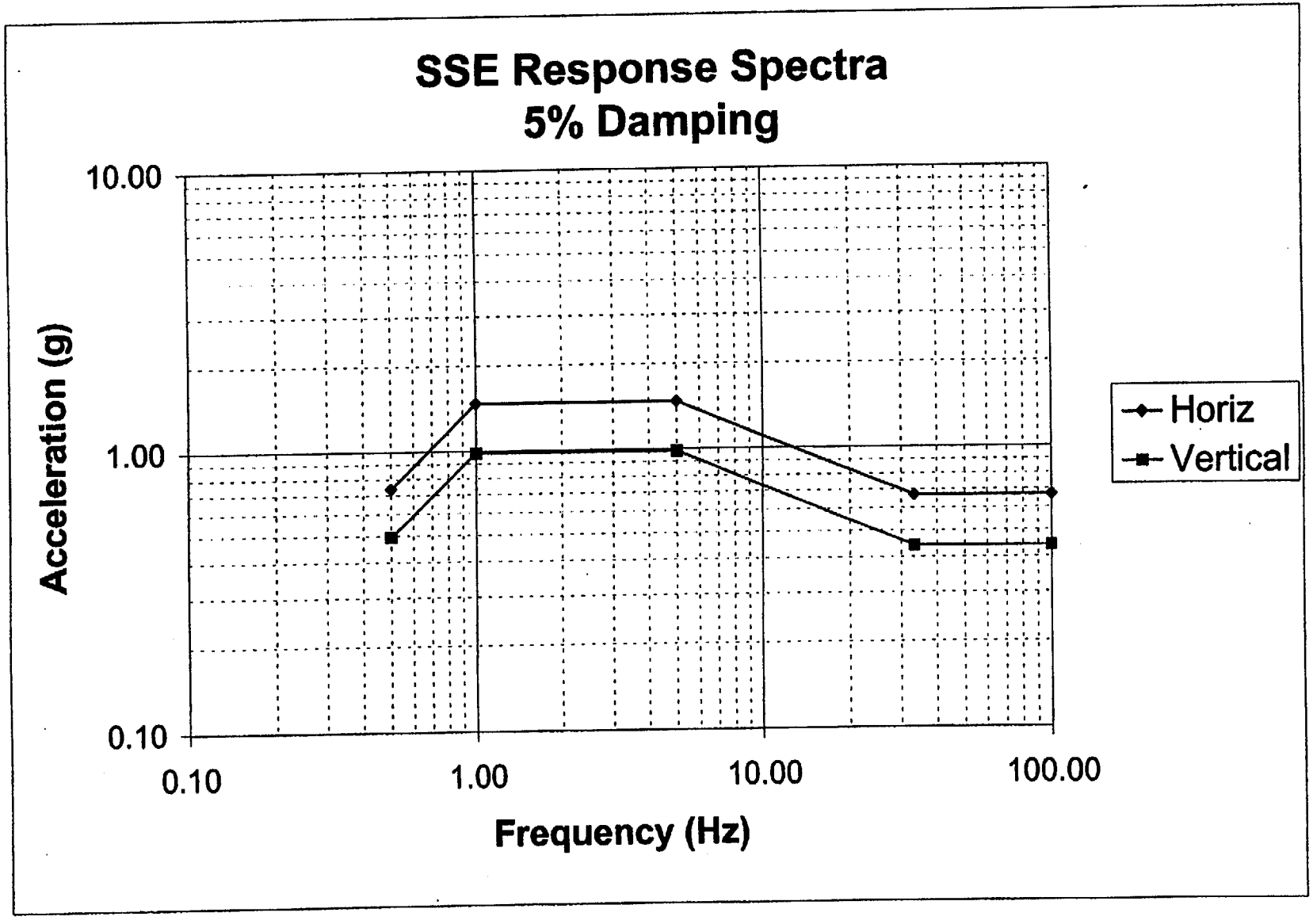

Figure 2-1: SER Response Spectra, 5% Damping

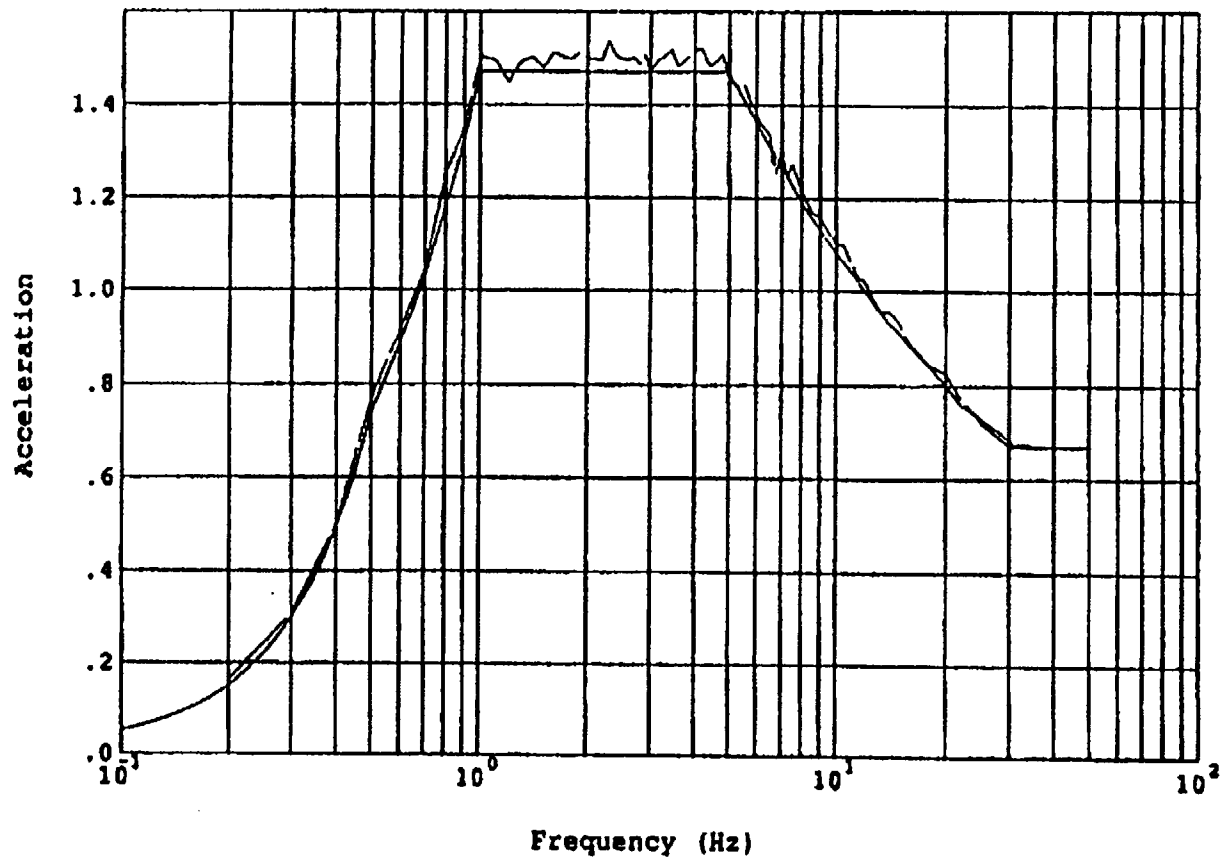

Legend:

Target Spectrum ————————

Actual Spectrum ——— ———

Notes:

At 75 SRP Frequencies

5% Spectral Damping

Acceleration in g's

Figure 2-2: Comparison Horizontal Spectrum to Target Spectrum. Component X

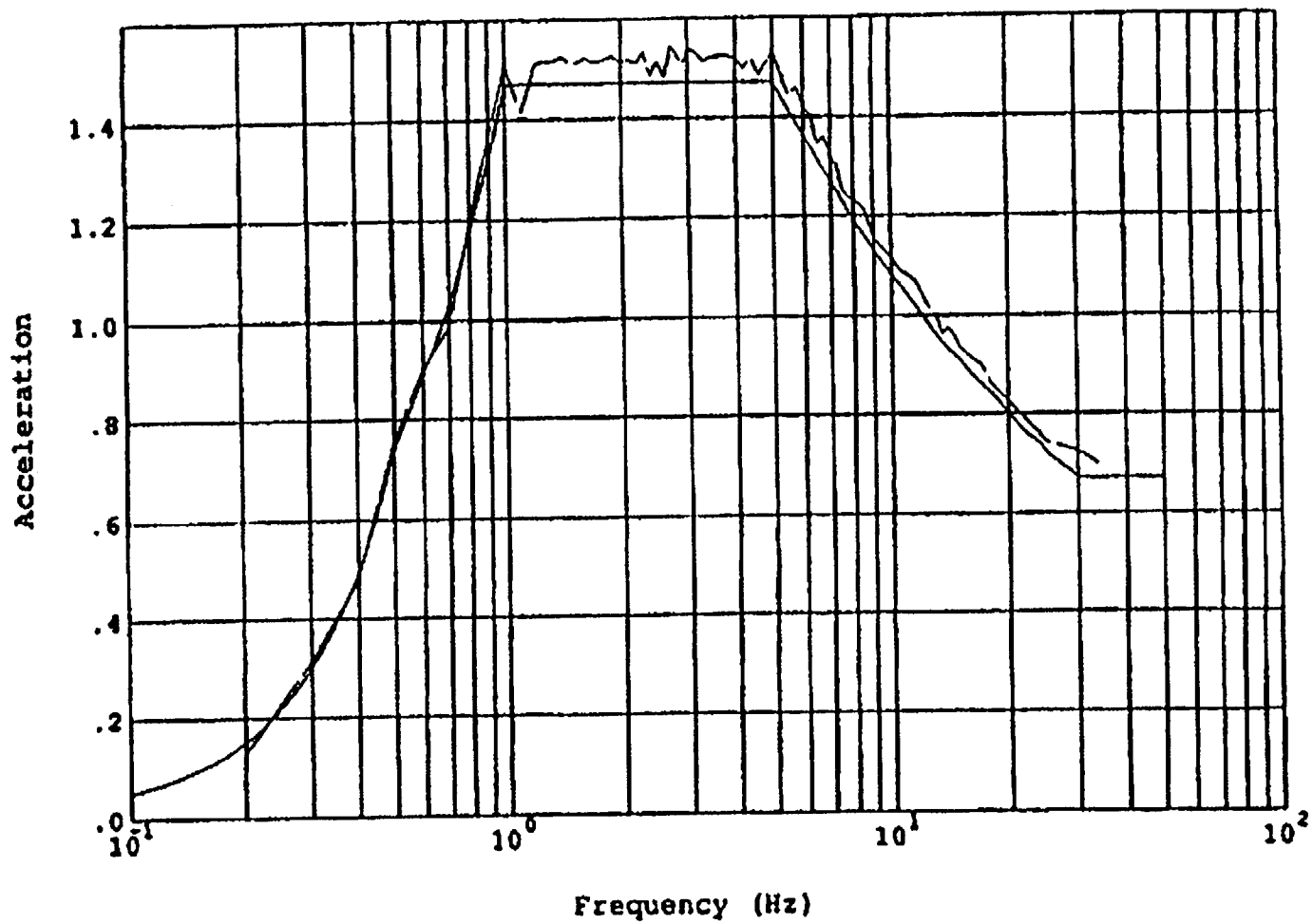

Legend:

Target Spectrum ————————

Actual Spectrum ——— ———

Notes:

At 75 SRP Frequencies

5% Spectral Damping

Acceleration in g's

Figure 2-3: Comparison Horizontal Spectrum to Target Spectrum. Component Y

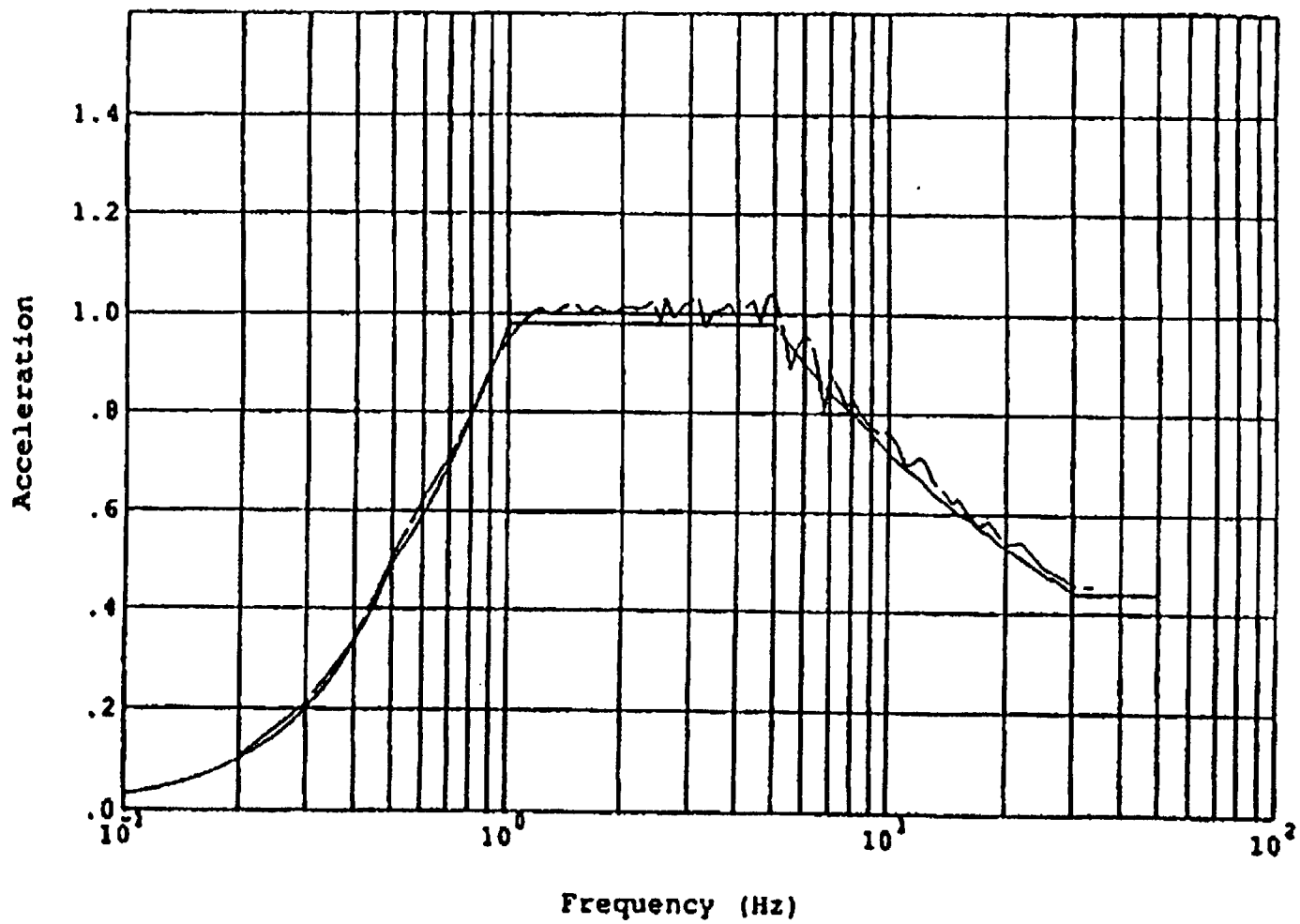

Legend:

Target Spectrum ————————

Actual Spectrum ——— ———

Notes:

At 75 SRP Frequencies

5% Spectral Damping

Acceleration in g's

Figure 2-4: Comparison Vertical Spectrum to Target Spectrum

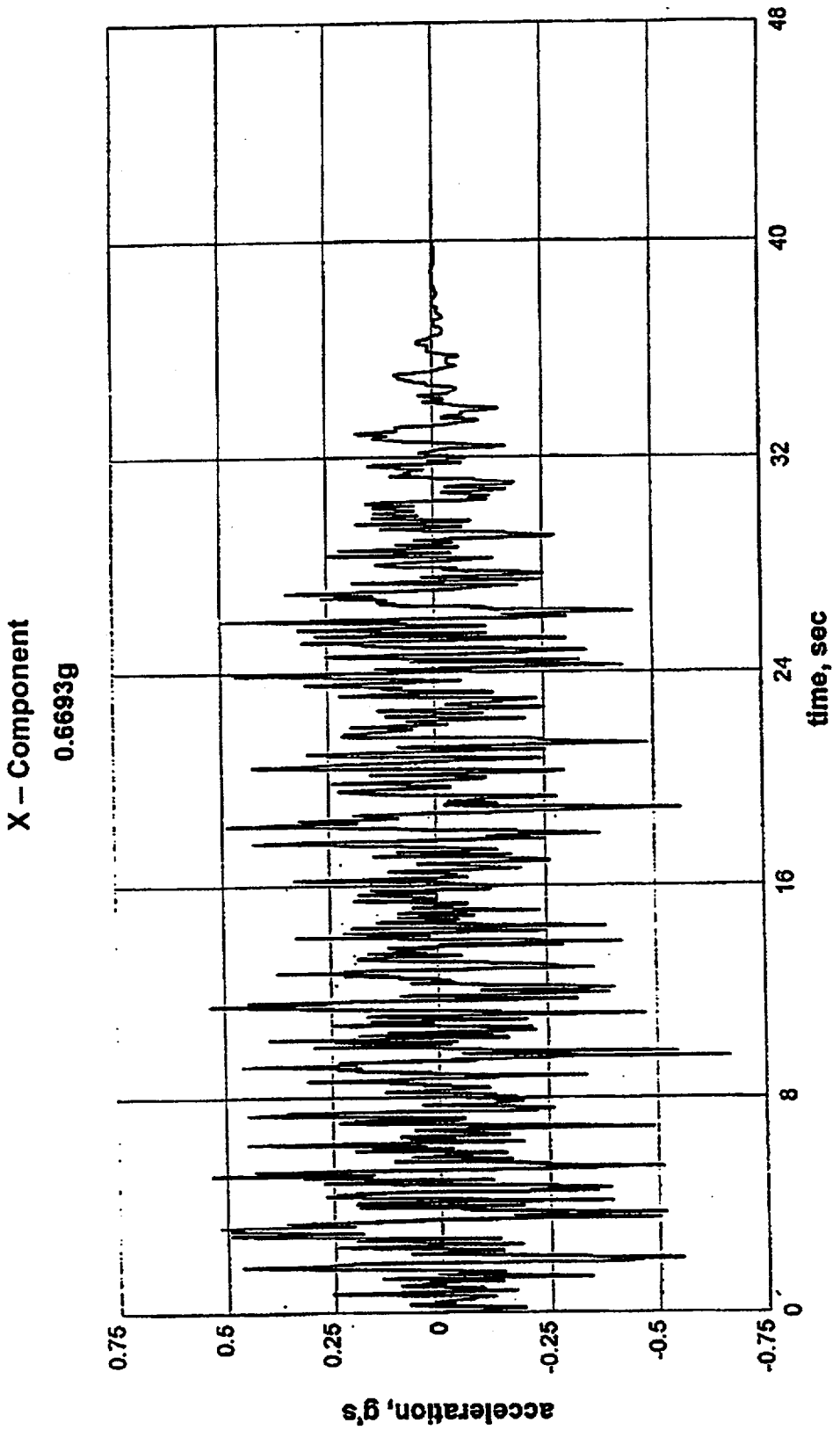

Figure 2-5: Artificial Acceleration Time History

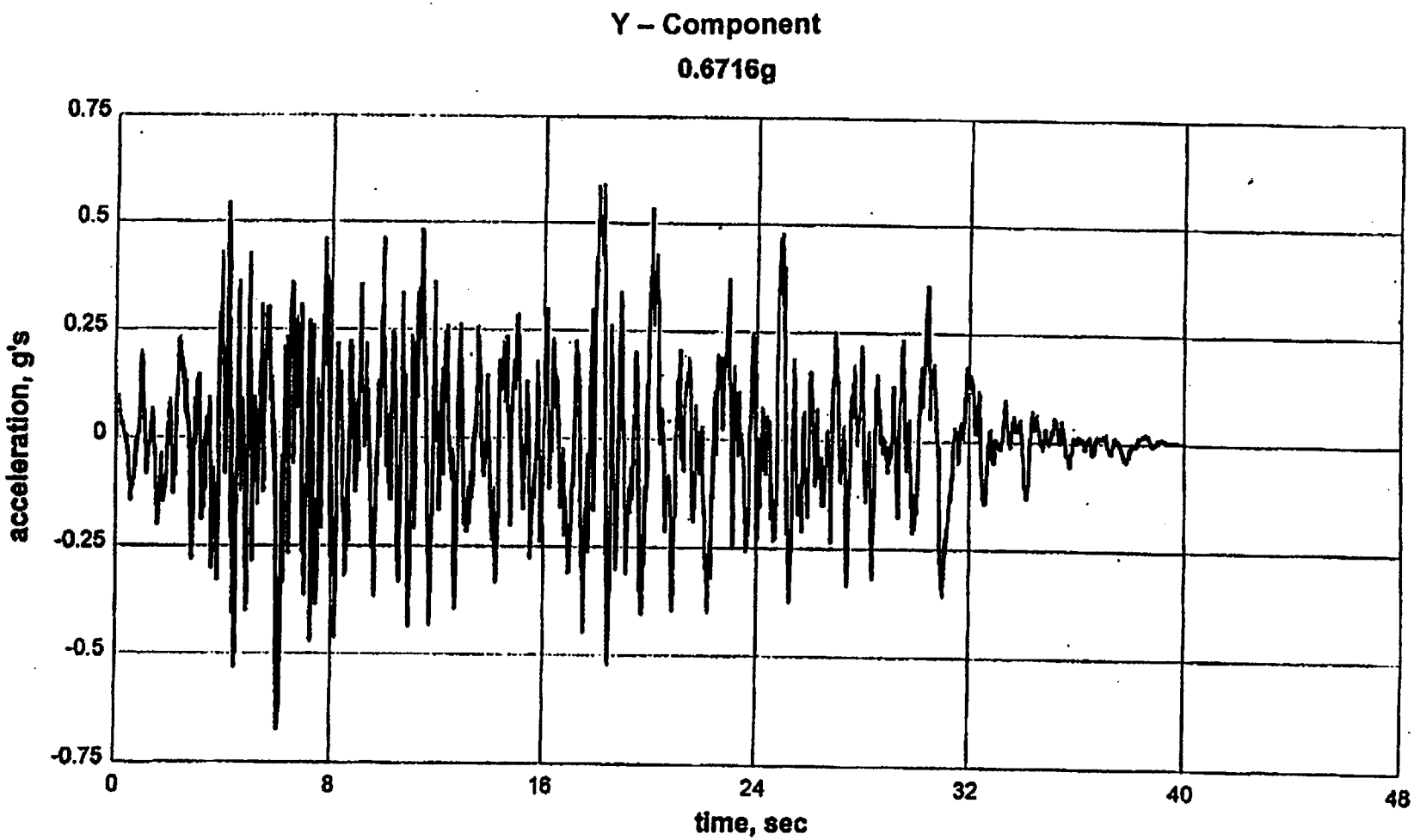

Figure 2-6: Artificial Acceleration Time History

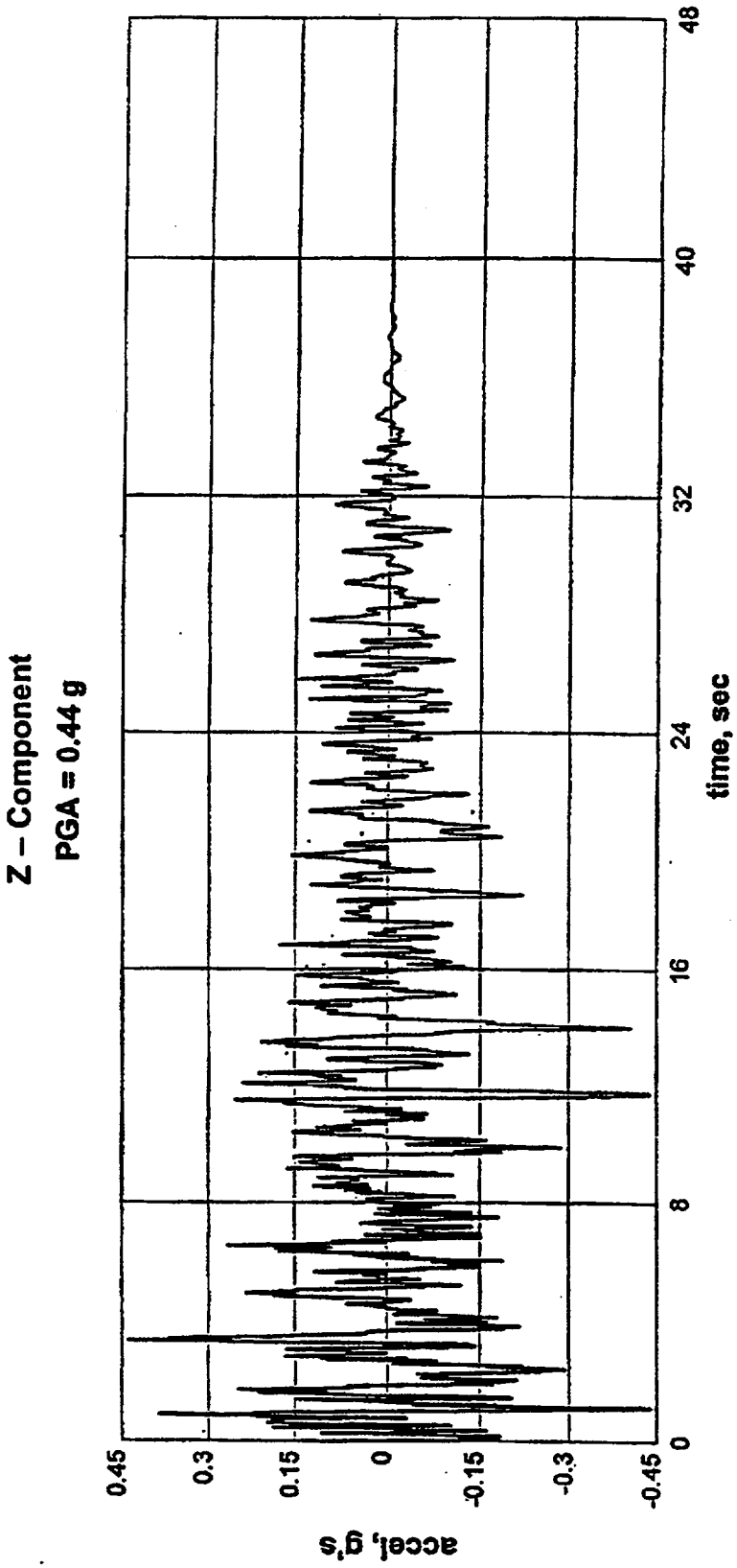

Figure 2-7: Artificial Acceleration Time History

Table 3-1

LOW STRAIN BEST ESTIMATE SOIL PROPERTIES

Layer	Thickness (ft) (Surface at 15.75')	Shear Modulus (ksf)	Vs (1) (fps)	Unit Weight (kcf)	Poisson's ratio	Vp (2) (fps)
1	3.50	3,599.27	930.00	0.134	0.35	1,935.95
2	3.50	3,599.27	930.00	0.134	0.35	1,935.95
3	3.75	3,599.27	930.00	0.134	0.35	1,935.95
4	5.00	4,337.14	1,002.36	0.139	0.48	5,000.00
5	5.00	4,991.60	1,075.33	0.139	0.48	5,000.00
6	5.00	5,605.60	1,139.55	0.139	0.48	5,000.00
7	5.00	6,187.62	1,197.24	0.139	0.48	5,000.00
8	5.00	6,743.43	1,249.86	0.139	0.48	5,000.00
9	5.00	7,277.19	1,298.38	0.139	0.48	5,000.00
10	5.00	7,792.04	1,343.53	0.139	0.48	5,000.00
11	5.00	8,290.41	1,385.83	0.139	0.48	5,000.00
12	5.00	8,774.22	1,425.69	0.139	0.48	5,000.00
13	5.00	9,245.03	1,463.44	0.139	0.48	5,000.00
14	5.00	9,704.15	1,499.34	0.139	0.48	5,000.00
15	5.00	10,152.65	1,533.59	0.139	0.48	5,000.00
16	5.00	10,591.45	1,566.38	0.139	0.48	5,000.00
17	5.00	11,021.34	1,597.86	0.139	0.48	5,000.00
18	5.00	11,443.01	1,628.14	0.139	0.48	5,000.00
19	5.00	11,857.04	1,657.33	0.139	0.48	5,000.00
20	5.00	12,263.96	1,685.53	0.139	0.48	5,000.00
21	10.00	12,862.03	1,726.14	0.139	0.48	5,000.00
22	10.00	13,638.50	1,777.48	0.139	0.48	5,000.00
23	10.00	14,393.46	1,826.01	0.139	0.48	5,000.00
24	10.00	15,129.11	1,872.09	0.139	0.48	5,000.00
25	10.00	15,847.28	1,916.01	0.139	0.48	5,000.00
26	15.00	16,722.77	1,968.22	0.139	0.48	5,000.00
27	H. S. (-160.75' ->)	17,744.05	2,027.43	0.139	0.48	5,000.00

(1) Lower limit for Vs = 930 fps
(2) Layers below water table, Vp = 5,000 fps (P wave velocity in water)

Table 3-2

LOW STRAIN LOWER AND UPPER BOUND SOIL PROPERTIES

Layer	Thickness (ft) (Surface at 15.75')	L.B. Shear Modulus (ksf)	L.B. Vs (fps)	U.B. Shear Modulus (ksf)	U.B. Vs (fps)
1	3.50	1,799.64	657.61	7,198.54	1,315.22
2	3.50	1,799.64	657.61	7,198.54	1,315.22
3	3.75	1,799.64	657.61	7,198.54	1,315.22
4	5.00	2,168.57	708.77	8,674.27	1,417.55
5	5.00	2,495.80	760.37	9,983.20	1,520.74
6	5.00	2,802.80	805.78	11,211.21	1,611.56
7	5.00	3,093.81	846.58	12,375.24	1,693.16
8	5.00	3,371.71	883.78	13,486.85	1,767.57
9	5.00	3,638.60	918.09	14,554.38	1,836.19
10	5.00	3,896.02	950.02	15,584.09	1,900.03
11	5.00	4,145.20	979.93	16,580.82	1,959.85
12	5.00	4,387.11	1,008.11	17,548.44	2,016.23
13	5.00	4,622.52	1,034.81	18,490.07	2,069.62
14	5.00	4,852.07	1,060.19	19,408.30	2,120.38
15	5.00	5,076.32	1,084.41	20,305.30	2,168.83
16	5.00	5,295.72	1,107.60	21,182.90	2,215.20
17	5.00	5,510.67	1,129.86	22,042.68	2,259.71
18	5.00	5,721.50	1,151.27	22,886.01	2,302.53
19	5.00	5,928.52	1,171.91	23,714.08	2,343.82
20	5.00	6,131.98	1,191.85	24,527.93	2,383.70
21	10.00	6,431.01	1,220.56	25,724.05	2,441.13
22	10.00	6,819.25	1,256.87	27,276.99	2,513.73
23	10.00	7,196.73	1,291.18	28,786.91	2,582.37
24	10.00	7,564.55	1,323.77	30,258.21	2,647.54
25	10.00	7,923.64	1,354.82	31,694.57	2,709.65
26	15.00	8,361.39	1,391.75	33,445.55	2,783.49
27	H. S. (-160.75' ->)	8,872.02	1,433.61	35,488.10	2,867.23

Table 3-3

SOIL DEGRADATION CURVES

Shear Strain (%)	G/GMAX	Soil Damping Ratio (%)
0.0001	1.000	2.061
0.0003	0.978	2.691
0.001	0.852	3.568
0.003	0.600	4.621
0.01	0.391	6.067
0.03	0.258	7.496
0.1	0.173	10.158
0.3	0.128	12.930
1.0	0.095	16.442
2.0	0.076	19.031
3.0	0.066	20.900
10.0 (1)	0.063 (1)	20.900 (1)

(1) These values were added to allow for larger deformation.

Table 3-4

STRAIN COMPATIBLE SHEAR WAVE VELOCITY

Layer	Thickness (ft)	Vs lower bound (strain comp.) (fps)	Vs best est. (strain comp.) (fps)	Vs upper bound (strain comp.) (fps)	Vs best est. (low strain) (fps)
1	3.50	376.53	649.40	1096.24	930.00
2	3.50	282.88	468.14	815.56	930.00
3	3.75	258.93	420.26	706.30	930.00
4	5.00	272.27	435.31	711.29	1002.36
5	5.00	282.29	453.55	739.86	1075.33
6	5.00	292.37	468.13	770.84	1139.55
7	5.00	303.64	484.66	802.93	1197.24
8	5.00	315.25	500.19	830.44	1249.86
9	5.00	326.79	515.02	851.11	1298.38
10	5.00	335.88	530.09	870.48	1343.53
11	5.00	344.06	544.96	888.00	1385.83
12	5.00	352.37	559.23	904.67	1425.69
13	5.00	360.50	572.94	920.16	1463.44
14	5.00	368.44	586.32	935.52	1499.34
15	5.00	376.22	599.22	951.48	1533.59
16	5.00	382.93	609.76	967.29	1566.38
17	5.00	389.23	618.62	982.74	1597.86
18	5.00	395.14	627.55	998.87	1628.14
19	5.00	401.25	636.34	1014.40	1657.33
20	5.00	407.83	645.38	1029.59	1685.53
21	10.00	416.82	658.88	1052.18	1726.14
22	10.00	426.44	676.23	1081.71	1777.48
23	10.00	436.11	692.98	1110.03	1826.01
24	10.00	445.82	707.37	1135.51	1872.09
25	10.00	455.34	720.19	1153.43	1916.01
26	15.00	466.15	736.26	1173.24	1968.22
H.S.		480.17	758.40	1208.53	2027.43

Table 3-5

STRAIN COMPATIBLE DAMPING RATIOS

Layer	Thickness (ft)	Damping Ratio Lower bound (strain comp.)	Damping Ratio Best estimate (strain comp.)	Damping Ratio Upper bound (strain comp.)	Damping Ratio Best estimate (low strain)
1	3.50	0.067	0.054	0.042	0.021
2	3.50	0.098	0.076	0.061	0.021
3	3.75	0.113	0.092	0.072	0.021
4	5.00	0.117	0.097	0.077	0.021
5	5.00	0.123	0.100	0.082	0.021
6	5.00	0.127	0.104	0.084	0.021
7	5.00	0.129	0.107	0.085	0.021
8	5.00	0.130	0.110	0.087	0.021
9	5.00	0.130	0.111	0.088	0.021
10	5.00	0.131	0.112	0.090	0.021
11	5.00	0.132	0.113	0.091	0.021
12	5.00	0.133	0.113	0.093	0.021
13	5.00	0.133	0.114	0.094	0.021
14	5.00	0.134	0.114	0.095	0.021
15	5.00	0.134	0.114	0.095	0.021
16	5.00	0.135	0.115	0.096	0.021
17	5.00	0.135	0.116	0.097	0.021
18	5.00	0.136	0.117	0.097	0.021
19	5.00	0.136	0.117	0.097	0.021
20	5.00	0.136	0.118	0.097	0.021
21	10.00	0.136	0.118	0.098	0.021
22	10.00	0.137	0.119	0.098	0.021
23	10.00	0.138	0.119	0.098	0.021
24	10.00	0.138	0.120	0.098	0.021
25	10.00	0.139	0.121	0.099	0.021
26	15.00	0.139	0.122	0.100	0.021
H.S.		0.139	0.122	0.100	0.021

Table 3-6

STRAIN COMPATIBLE P WAVE VELOCITY

Layer	Thickness (ft)	Vp lower bound (strain comp.) (fps)	Vp best est. (strain comp.) (fps)	Vp upper bound (strain comp.) (fps)	Vp best est. (low strain) (fps)
1	3.50	783.81	1351.84	2282.00	1935.95
2	3.50	588.86	974.50	1697.73	1935.95
3	3.75	539.00	874.84	1470.28	1935.95
4	5.00	3500.00	5000.00	5000.00	5000.00
5	5.00	3500.00	5000.00	5000.00	5000.00
6	5.00	3500.00	5000.00	5000.00	5000.00
7	5.00	3500.00	5000.00	5000.00	5000.00
8	5.00	3500.00	5000.00	5000.00	5000.00
9	5.00	3500.00	5000.00	5000.00	5000.00
10	5.00	3500.00	5000.00	5000.00	5000.00
11	5.00	3500.00	5000.00	5000.00	5000.00
12	5.00	3500.00	5000.00	5000.00	5000.00
13	5.00	3500.00	5000.00	5000.00	5000.00
14	5.00	3500.00	5000.00	5000.00	5000.00
15	5.00	3500.00	5000.00	5000.00	5000.00
16	5.00	3500.00	5000.00	5000.00	5000.00
17	5.00	3500.00	5000.00	5000.00	5000.00
18	5.00	3500.00	5000.00	5000.00	5000.00
19	5.00	3500.00	5000.00	5000.00	5000.00
20	5.00	3500.00	5000.00	5000.00	5000.00
21	10.00	3500.00	5000.00	5000.00	5000.00
22	10.00	3500.00	5000.00	5000.00	5000.00
23	10.00	3500.00	5000.00	5000.00	5000.00
24	10.00	3500.00	5000.00	5000.00	5000.00
25	10.00	3500.00	5000.00	5000.00	5000.00
26	15.00	3500.00	5000.00	5000.00	5000.00
H.S.		3500.00	5000.00	5000.00	5000.00

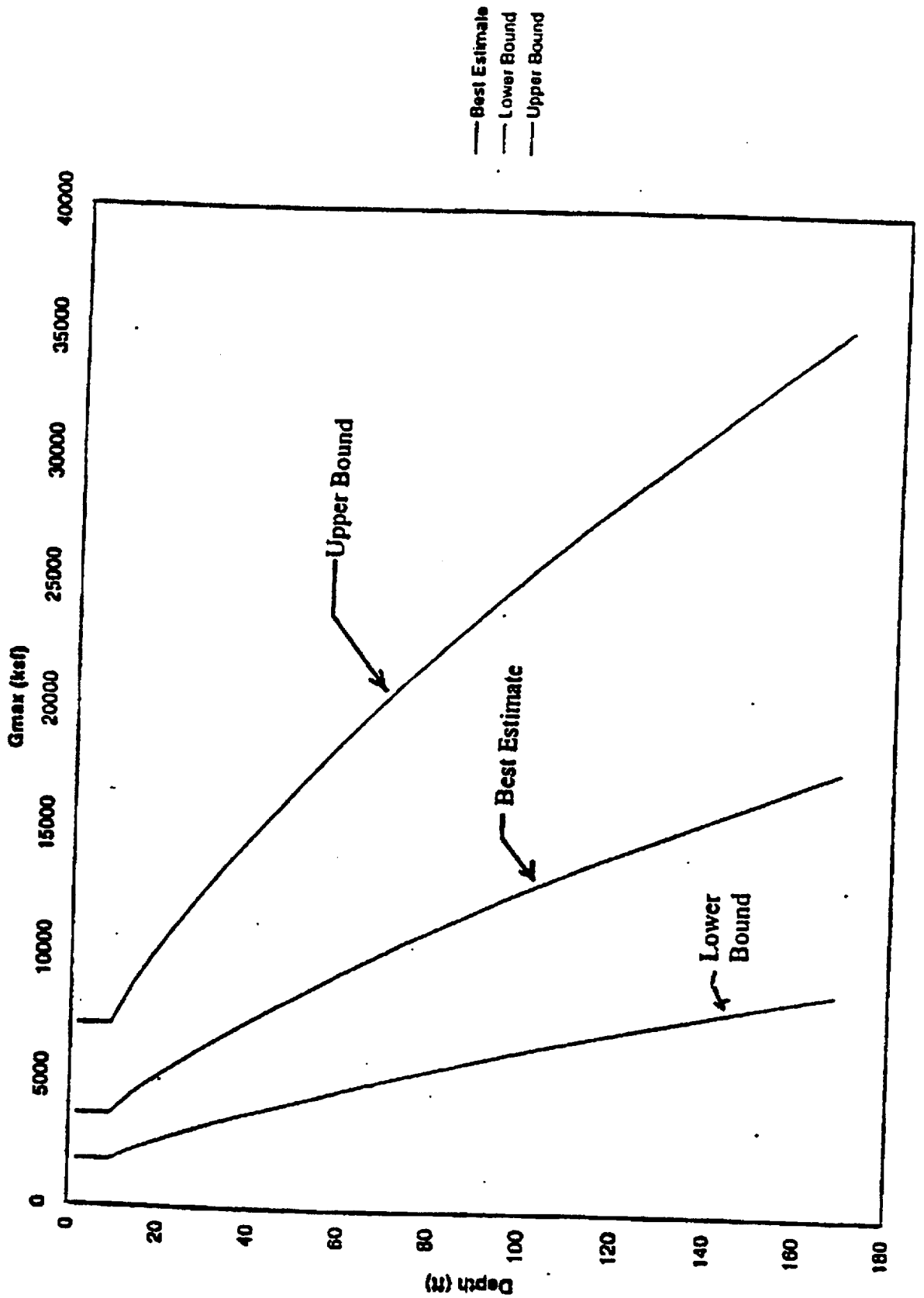

Figure 3-1: Low Strain Shear Modulus

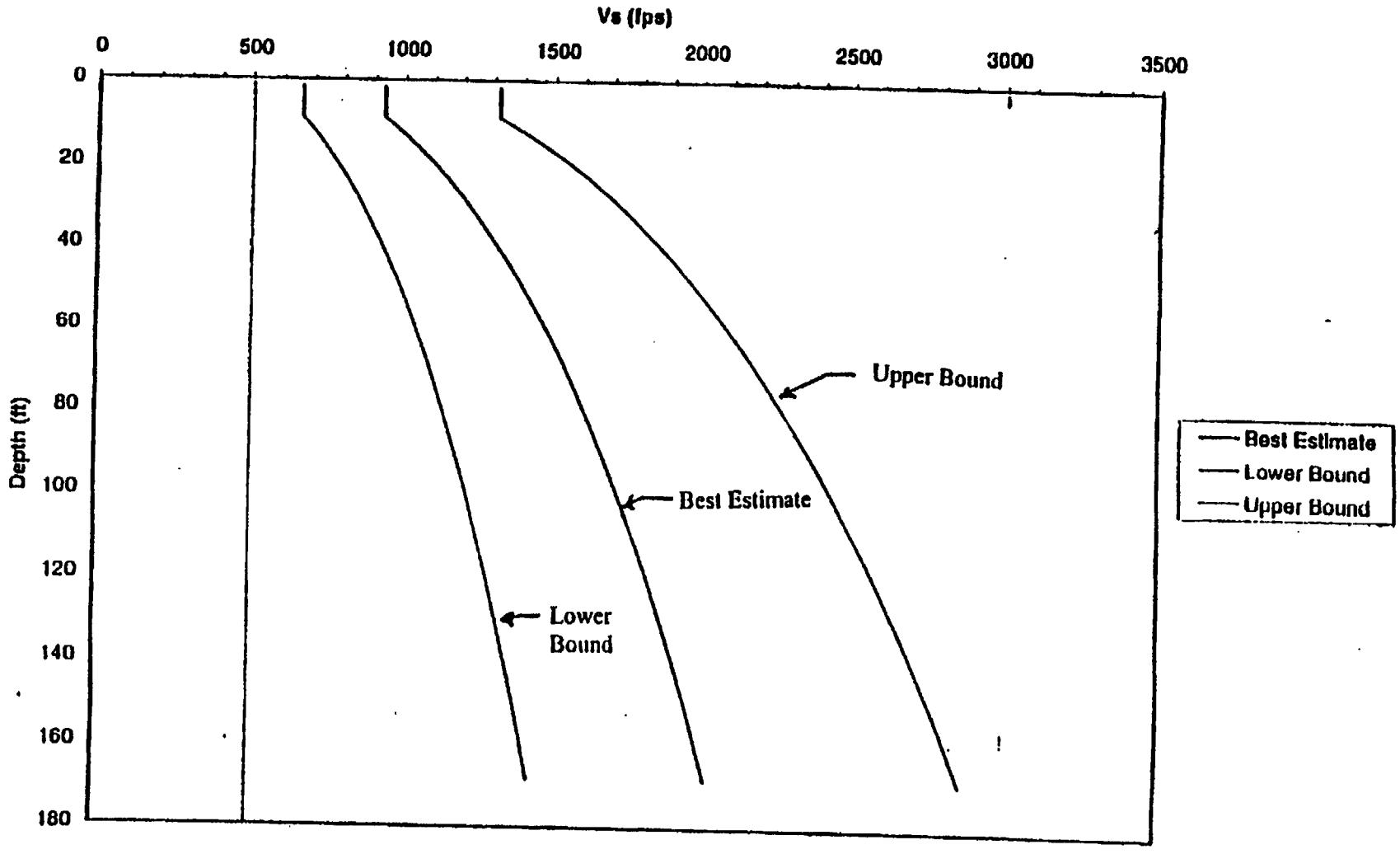

Figure 3-2: Low Strain Shear Wave Velocity

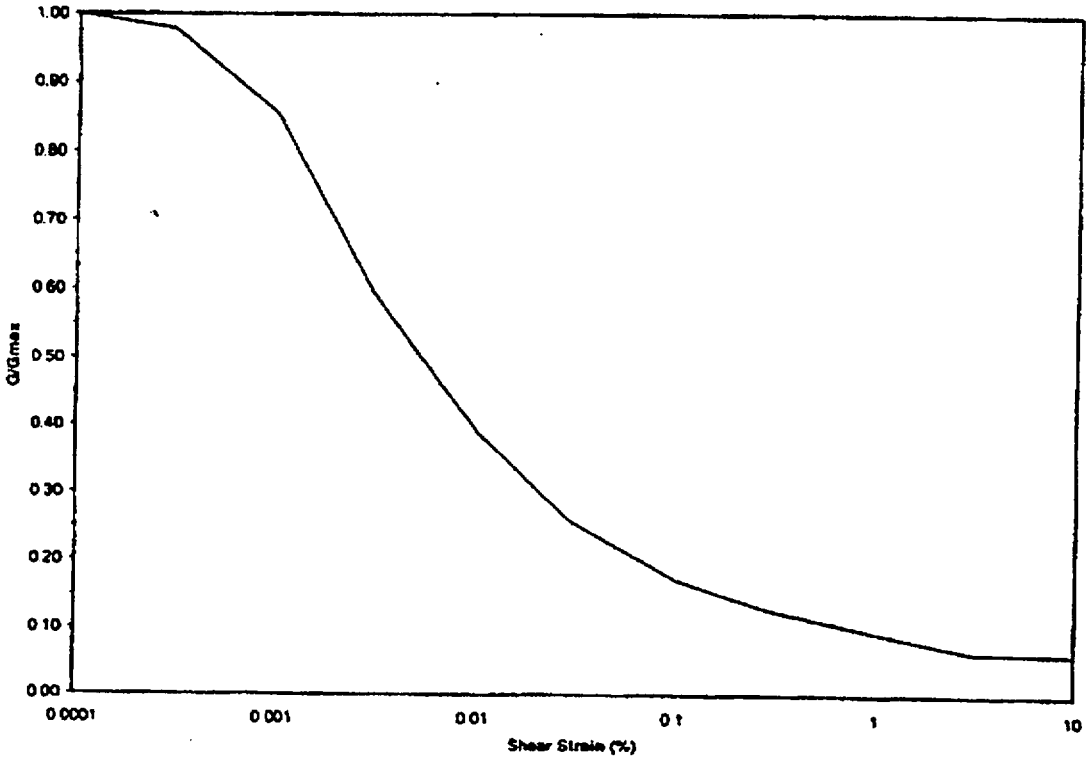

Figure 3-3a: Soil Shear Modulus Degradation Curve

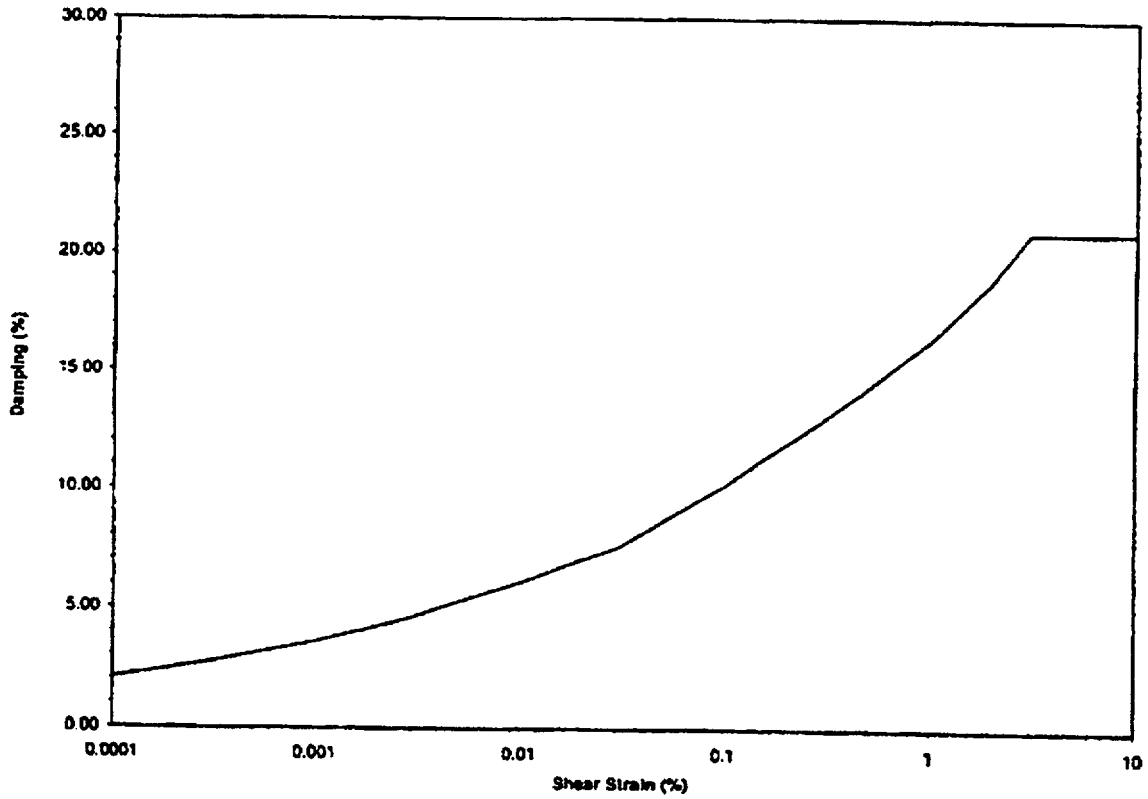

Figure 3-3b: Soil Material Damping Curve

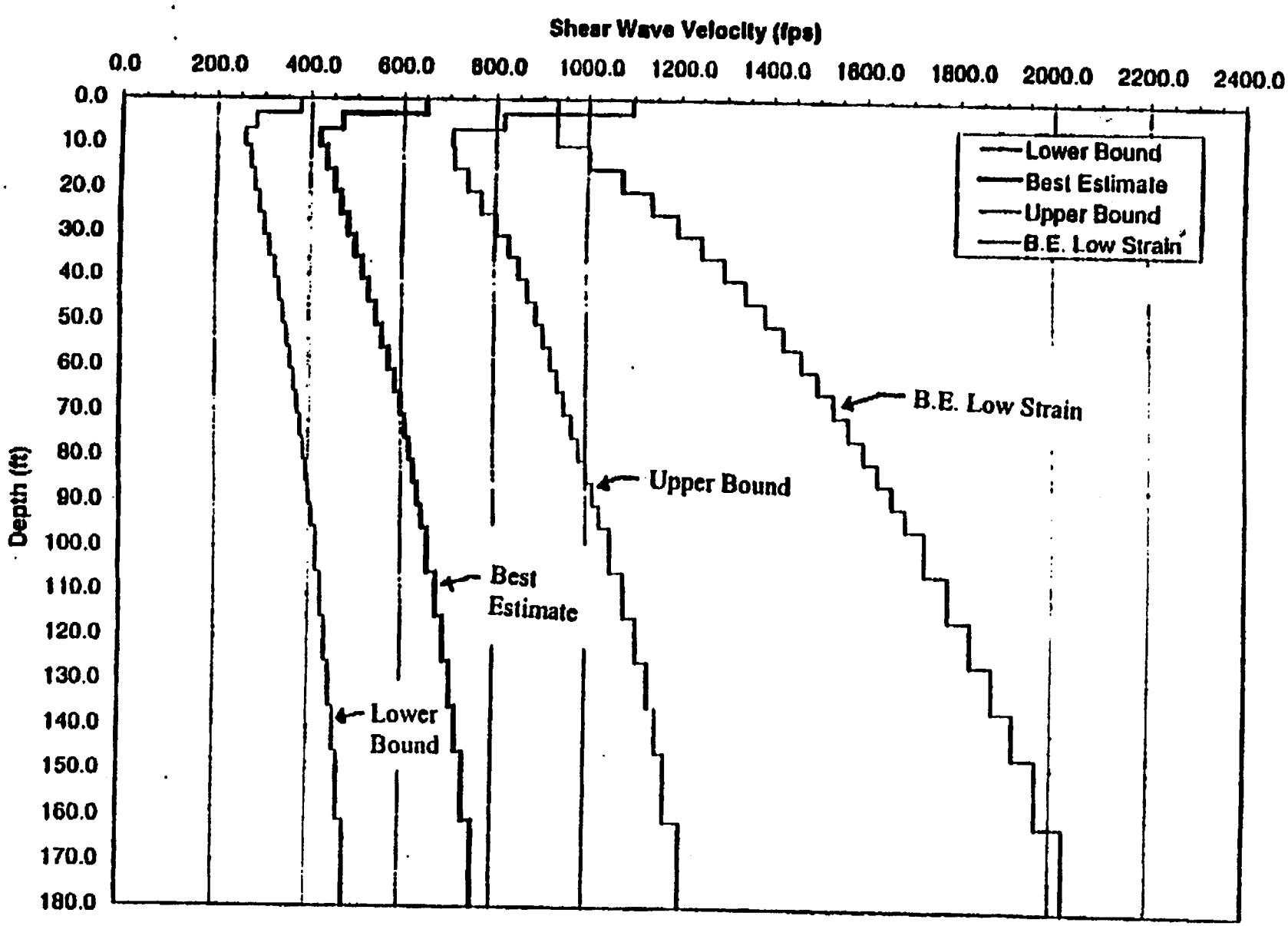

Figure 3-4: Strain Compatible Shear Wave Velocity

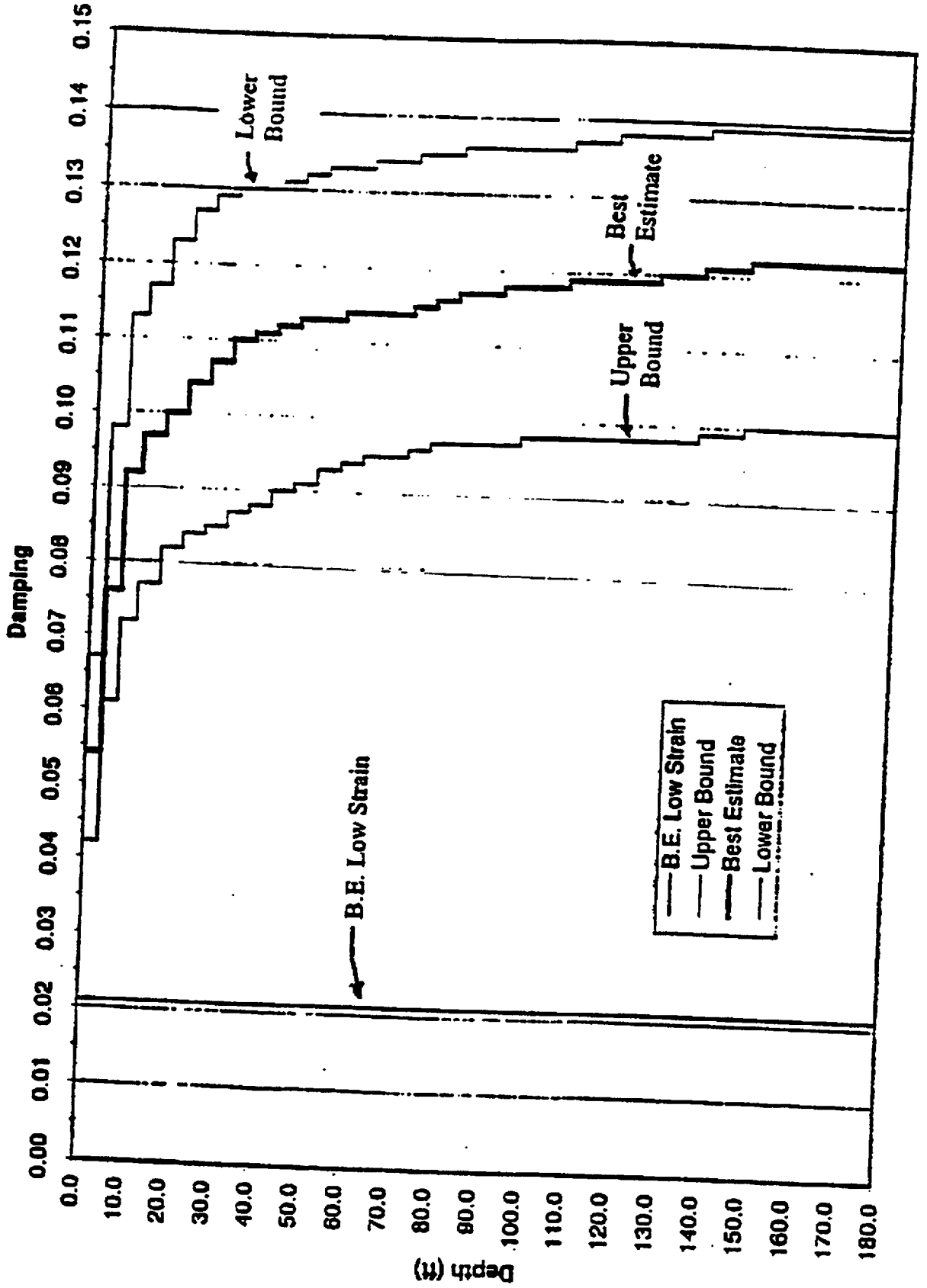

Figure 3-5: Strain Compatible Damping Ratios

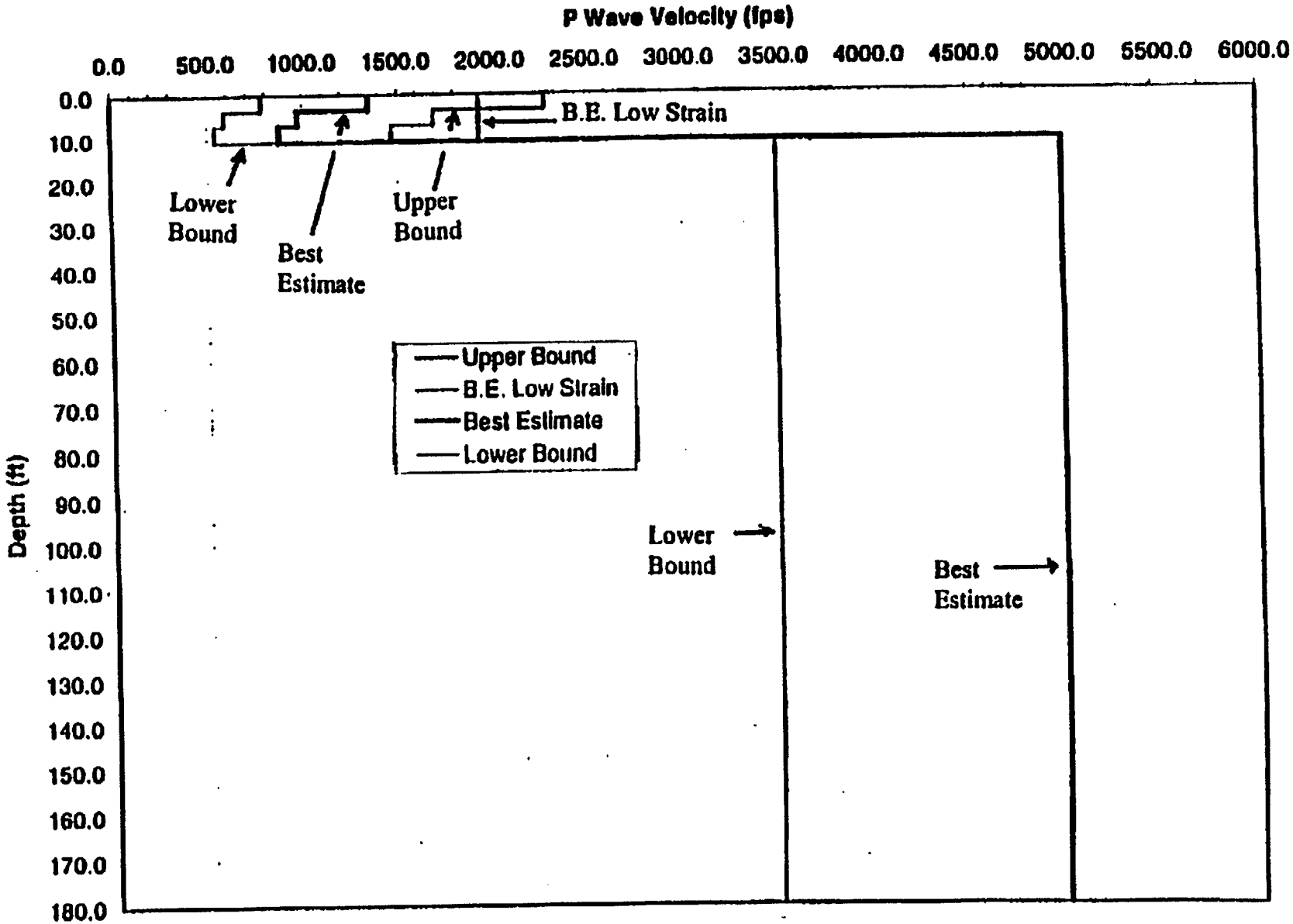

Figure 3-6: Strain Compatible P Wave Velocity

Table 4-1

SUMMARY OF CASKS PROPERTIES (INCLUDING WALLS)

CASK	CG (ft)			Weight (kips)	Wxx ($k\text{-}ft^2$)	Wyy ($k\text{-}ft^2$)	Wzz ($k\text{-}ft^2$)
	X (1)	Y (2)	Z (3)				
1	6.00	11.292	10.0	686.80	52,657.78	31,038.35	36,757.64
2	4.25	11.292	10.0	481.01	36,879.61	19,333.10	23,338.68
3	4.25	11.292	10.0	481.01	36,879.61	19,333.10	23,338.68
4	4.25	11.292	10.0	481.01	36,879.61	19,333.10	23,338.68
5	4.25	11.292	10.0	481.01	36,879.61	19,333.10	23,338.68
6	4.25	11.292	10.0	481.01	36,879.61	19,333.10	23,338.68
7	4.25	11.292	10.0	481.01	36,879.61	19,333.10	23,338.68
8	4.25	11.292	10.0	481.01	36,879.61	19,333.10	23,338.68
9	4.25	11.292	10.0	481.01	36,879.61	19,333.10	23,338.68
10	6.00	11.292	10.0	686.80	52,657.78	31,038.35	36,757.64

(1) From internal side

(2) From front side

(3) From bottom

Table 4-2

NODAL NUMBERS

CASK	At Cask CG	At Slab Below Cask CG
1	817	475
2	818	514
3	819	540
4	820	566
5	821	592
6	822	618
7	823	644
8	824	670
9	825	696
10	826	735

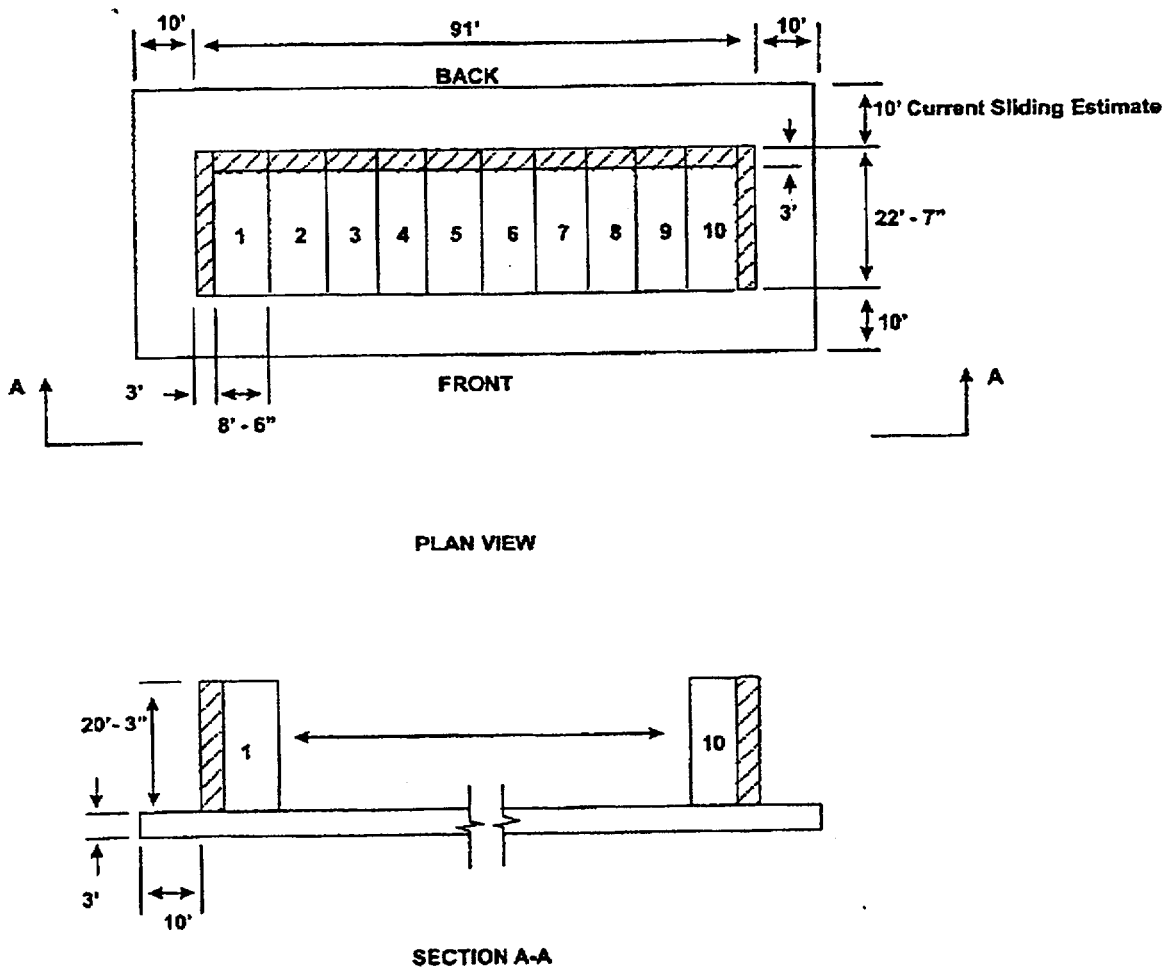

Figure 4-1: ISFSI Dimensions and Configuration

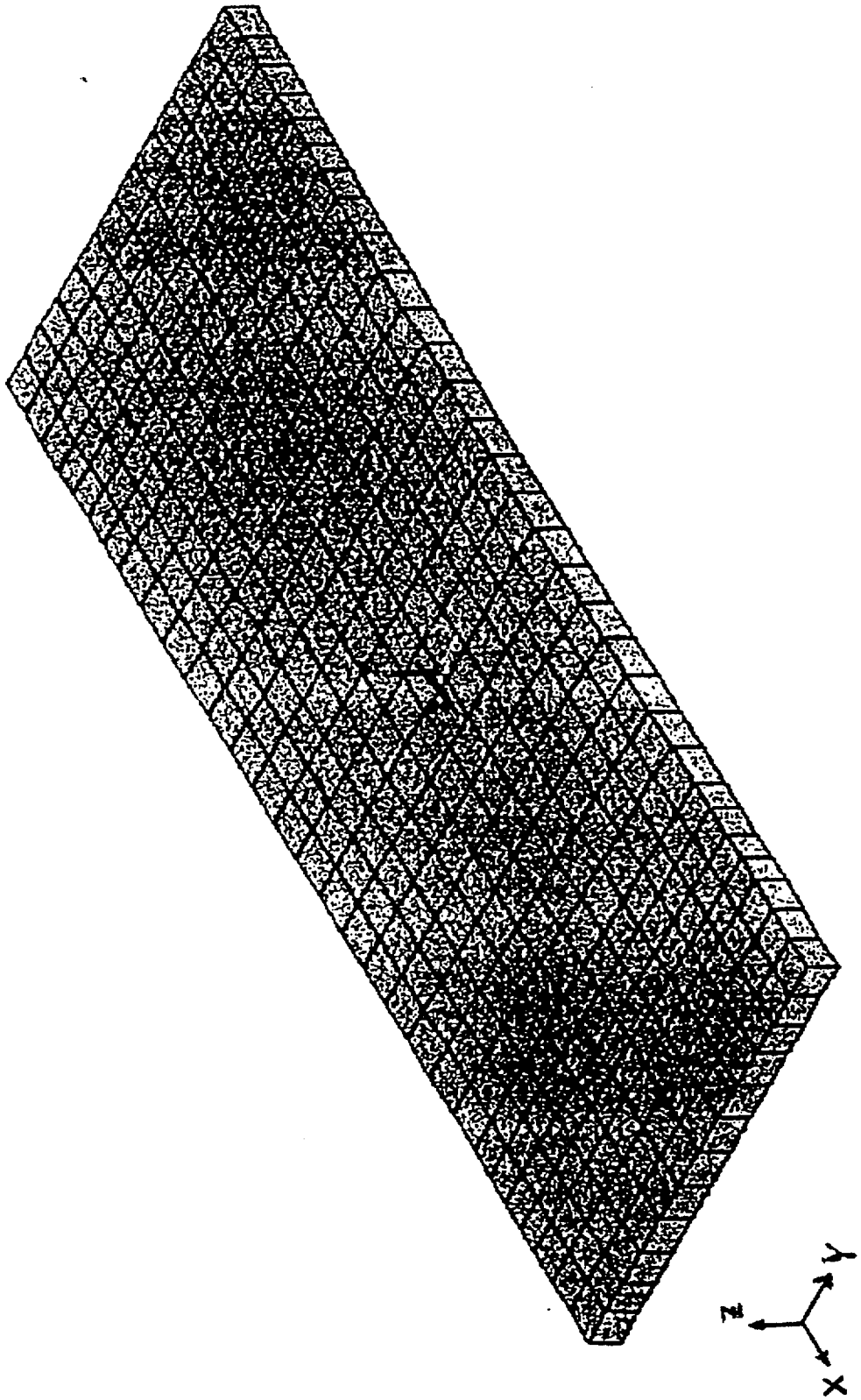

Figure 4-2: Concrete Pad Finite Element Model

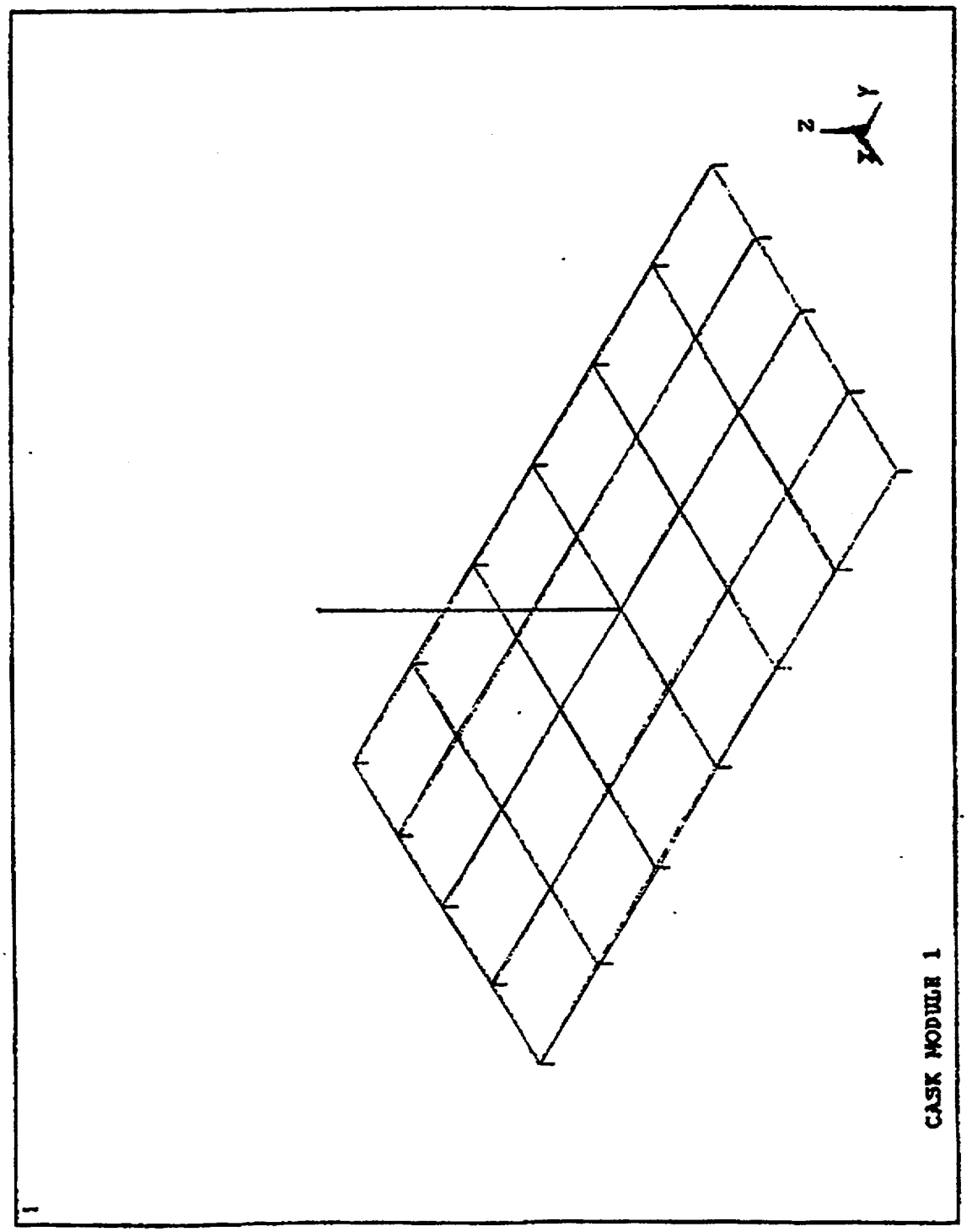

Figure 4-3a: Model Casks 1 and 10 (Footprint includes back and side shield walls)

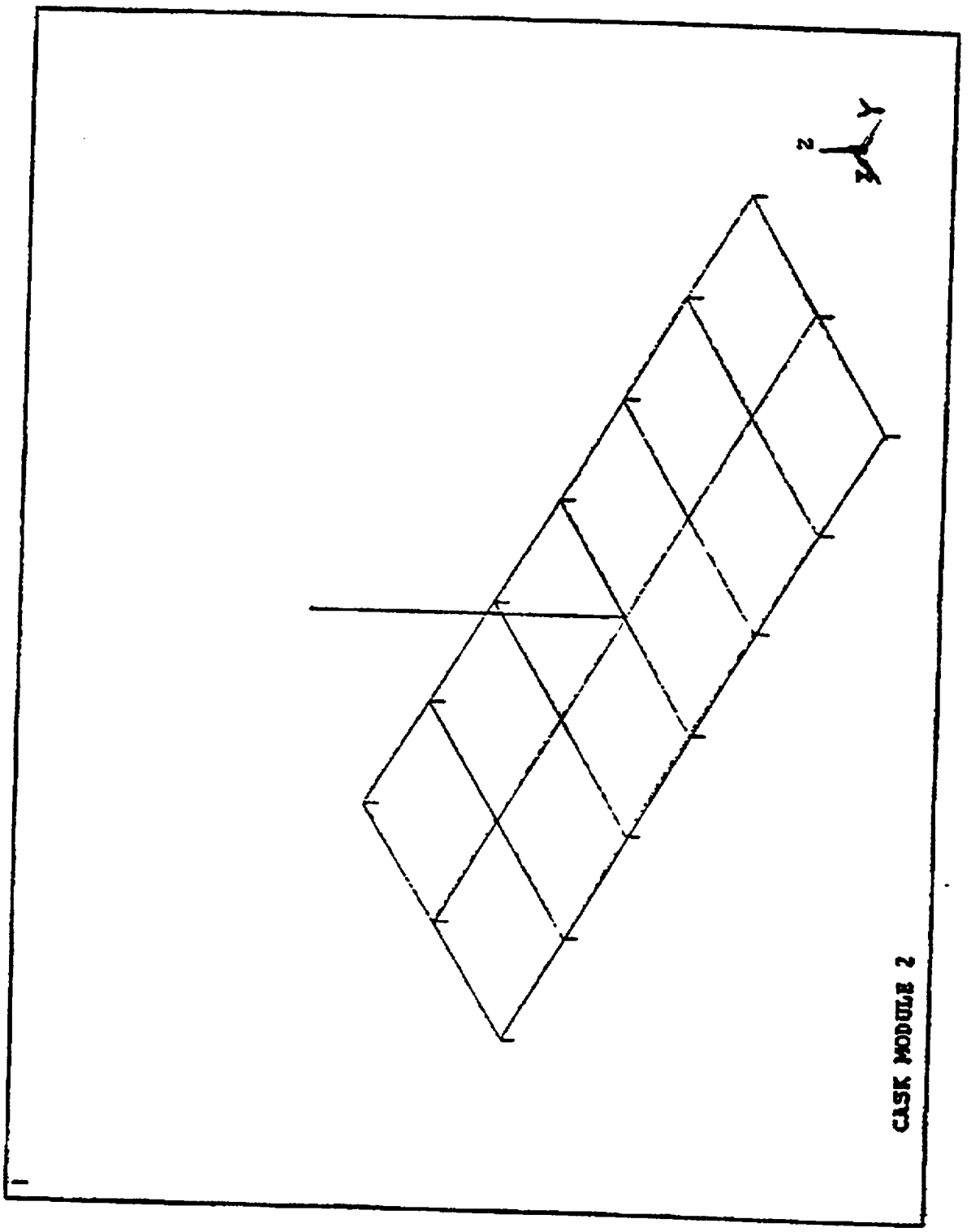

Figure 4-3b: Model Casks 2 to 9 (Footprint includes back shield wall)

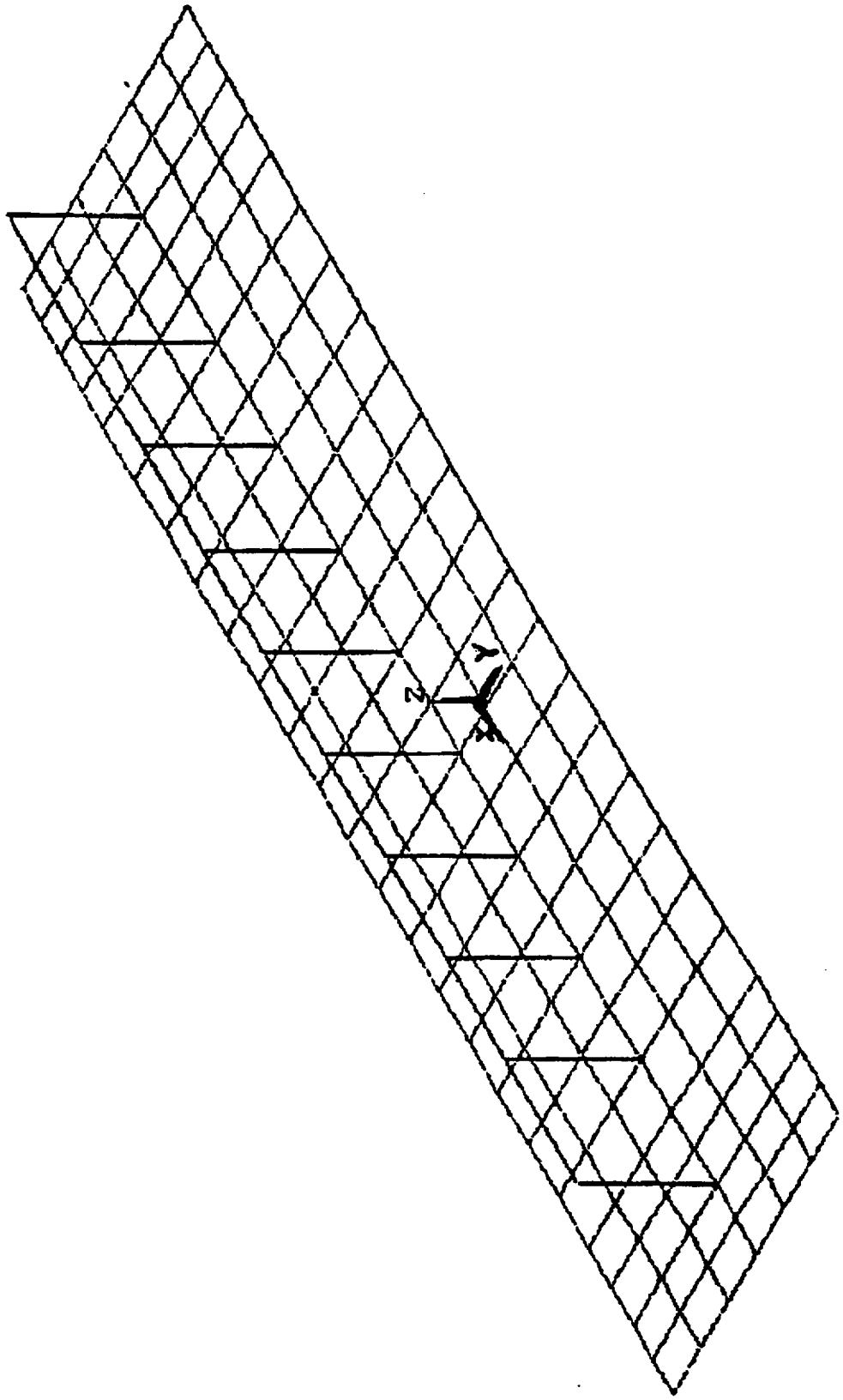

Figure 4-3c: Combined Model for Casks 1 to 10
(Horizontal, very soft axial elements connecting the tops of the vertical beams were included to allow monitoring of potential relative motion between cask CGs)

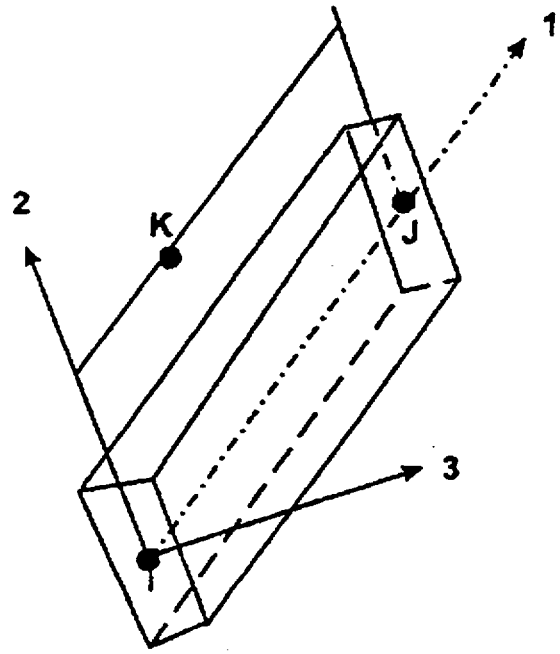

For "Cask" Elements

Local Axis 1 = Global Axis Z

Local Axis 2 = Global Axis X

Local Axis 3 = Global Axis Y

Figure 4-4: Local Coordinate System for Beam Elements. Module HOUSE

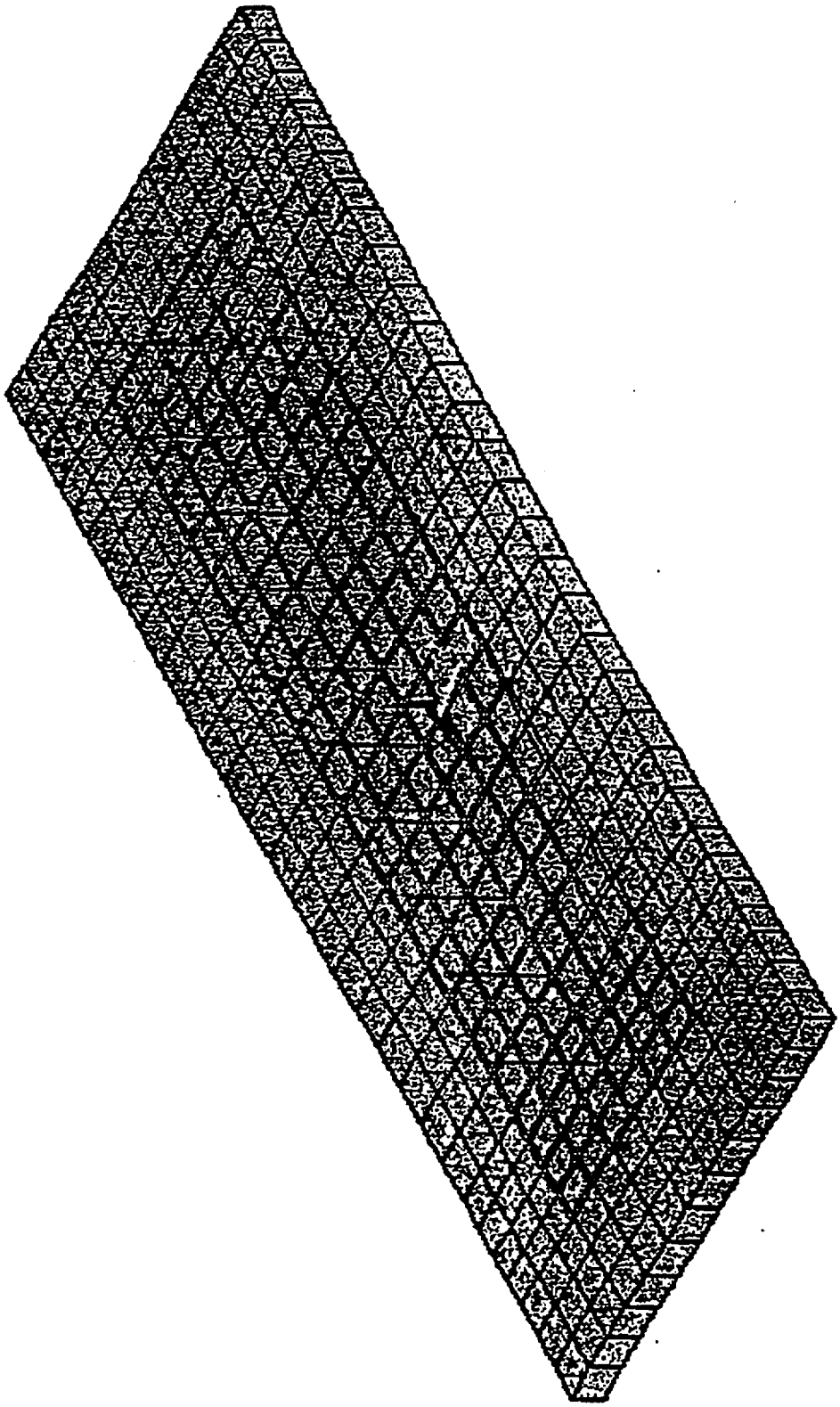

Figure 4-5: Combined Models of Casks and Concrete Pad

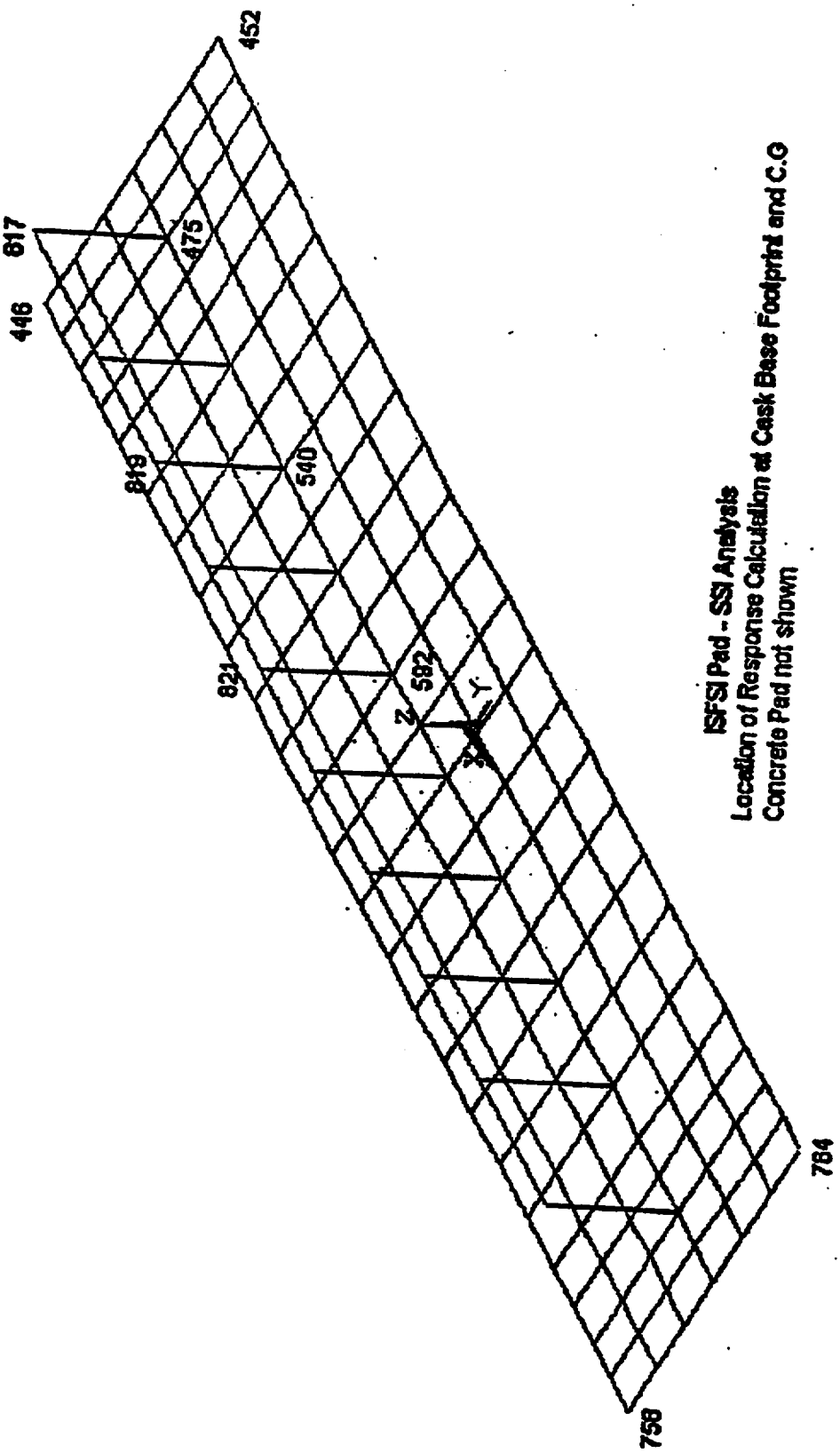

Figure 4-6: Location of Response Calculation

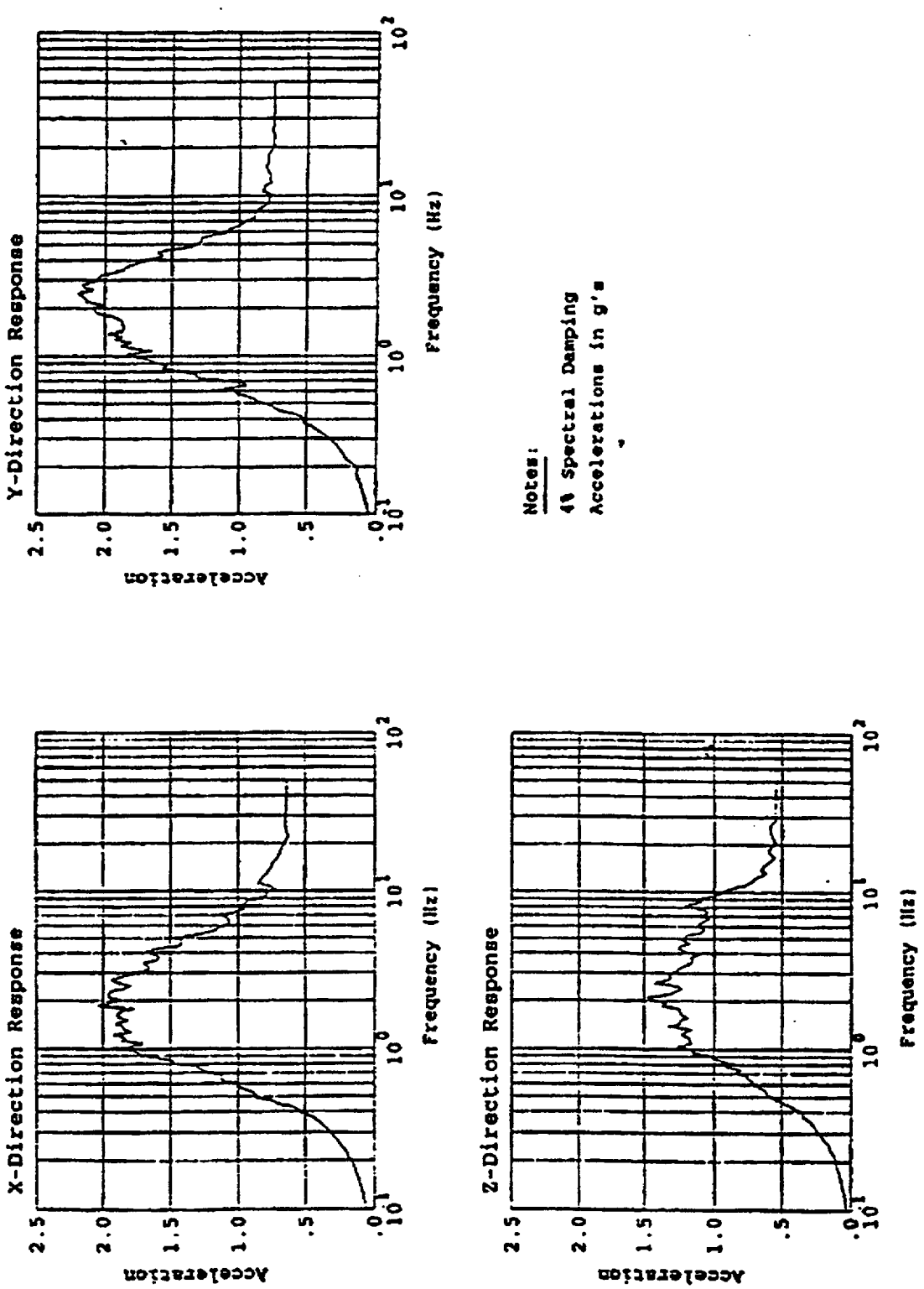

Figure 6-1: ISFSI SSI SASSI Solution: 100% Cask Mass, Lower Bound Soil, X+Y+Z EQ, Envelope All Locations

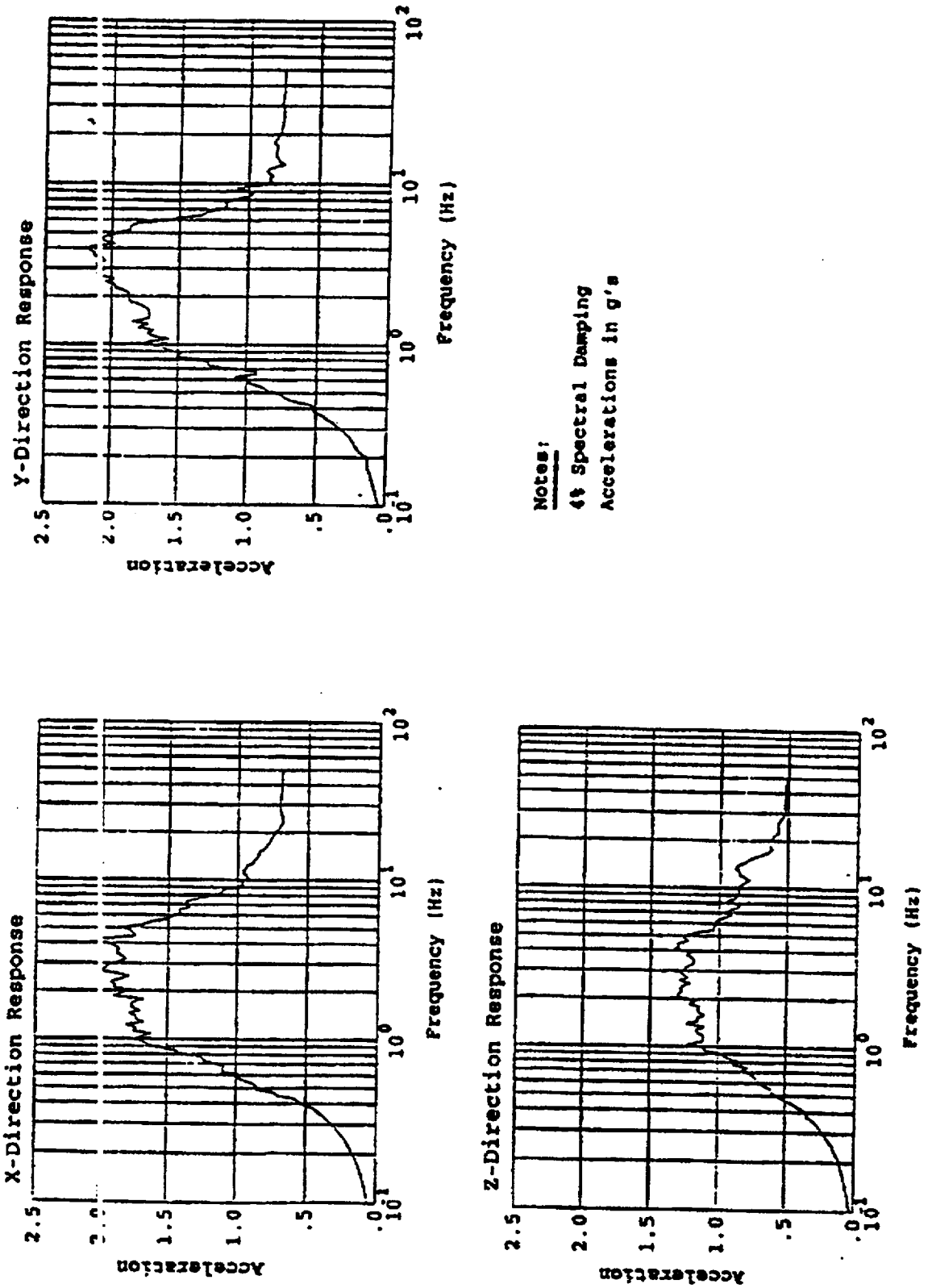

Figure 6-2: ISFSI SSI SASSI Solution: 100% Cask Mass, Best Estimate Soil, X+Y+Z EQ, Envelope All Locations

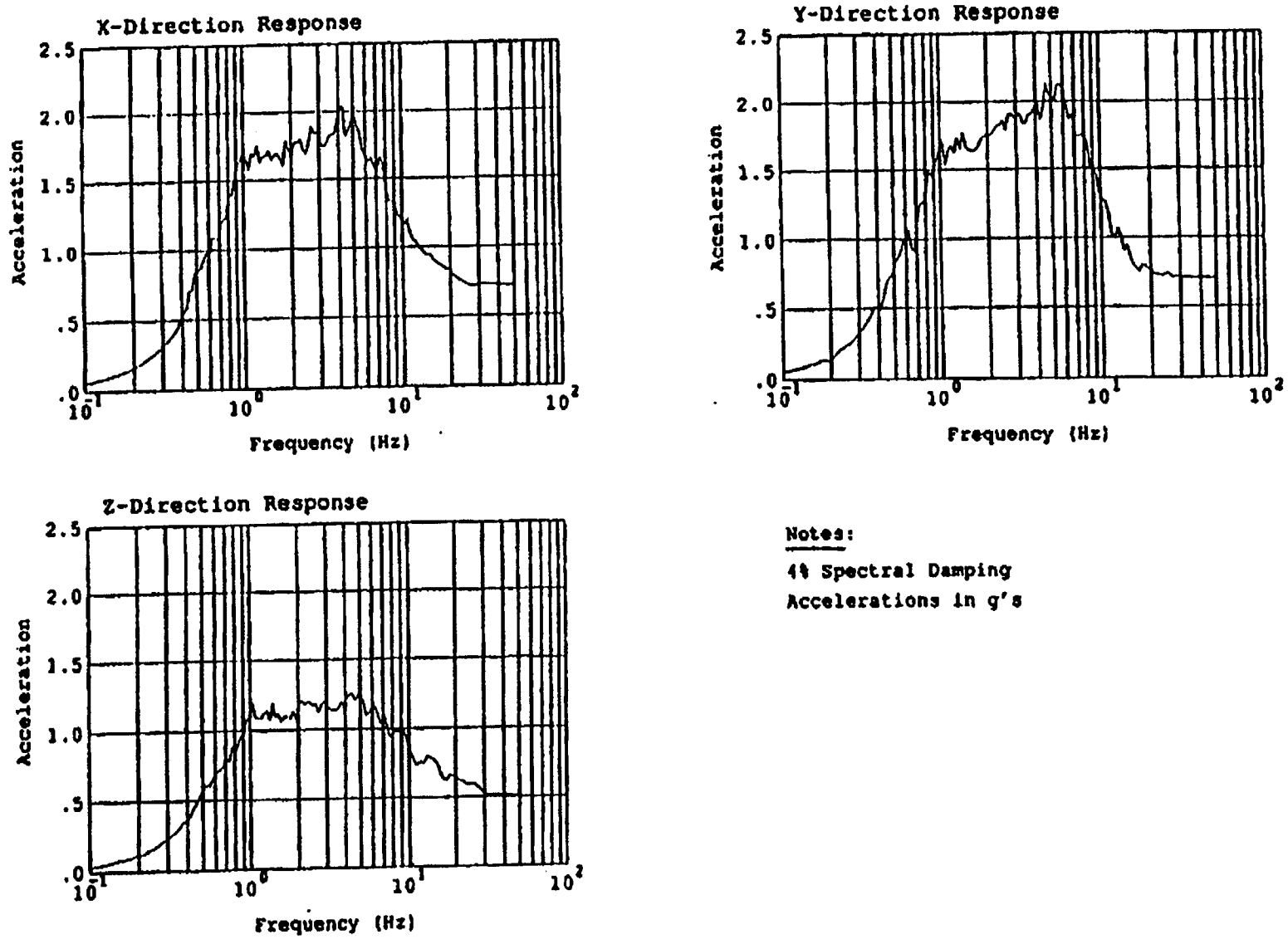

Figure 6-3: ISFSI SSI SASSI Solution: 100% Cask Mass, Upper Bound Soil, X+Y+Z EQ, Envelope All Locations

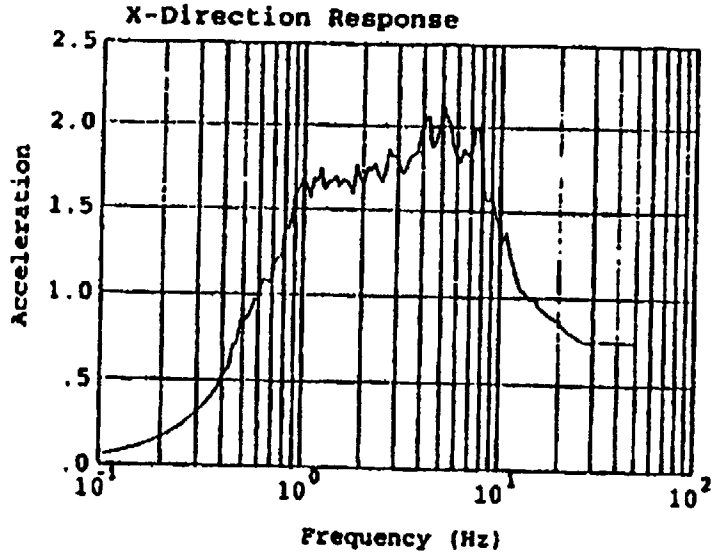

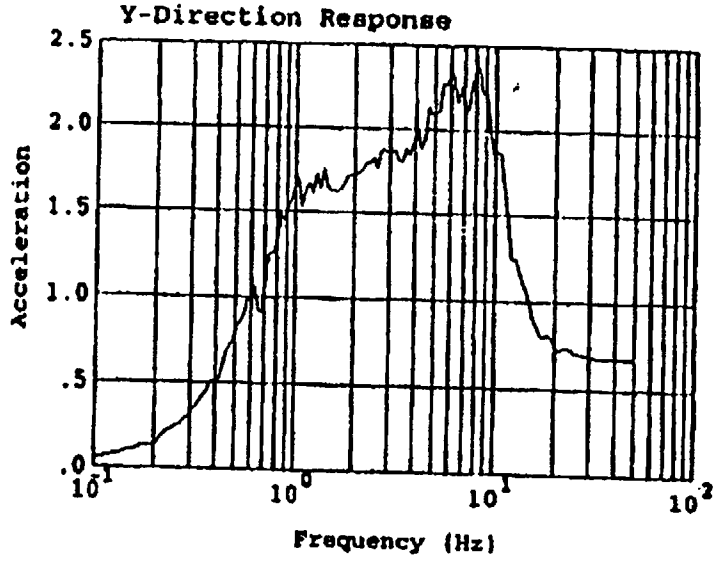

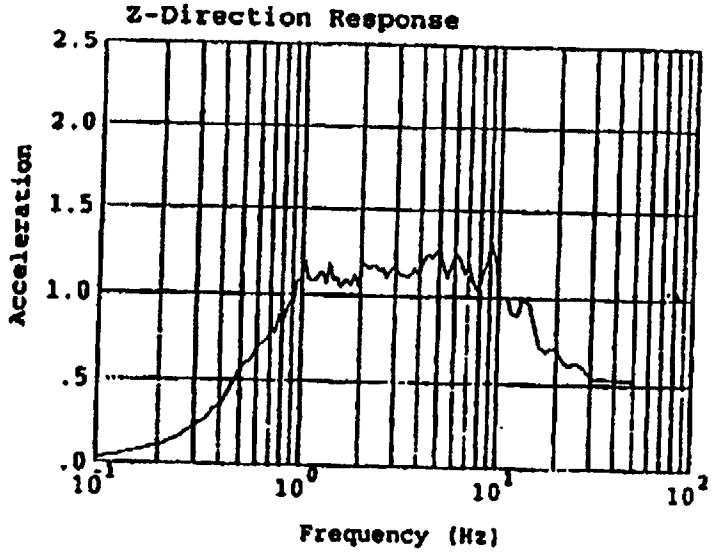

Notes:

4% Spectral Damping

Accelerations in g's

Figure 6-4: ISFSI SSI SASSI Solution: 100% Cask Mass, Low Strain Soil, X+Y+Z EQ, Envelope All Locations

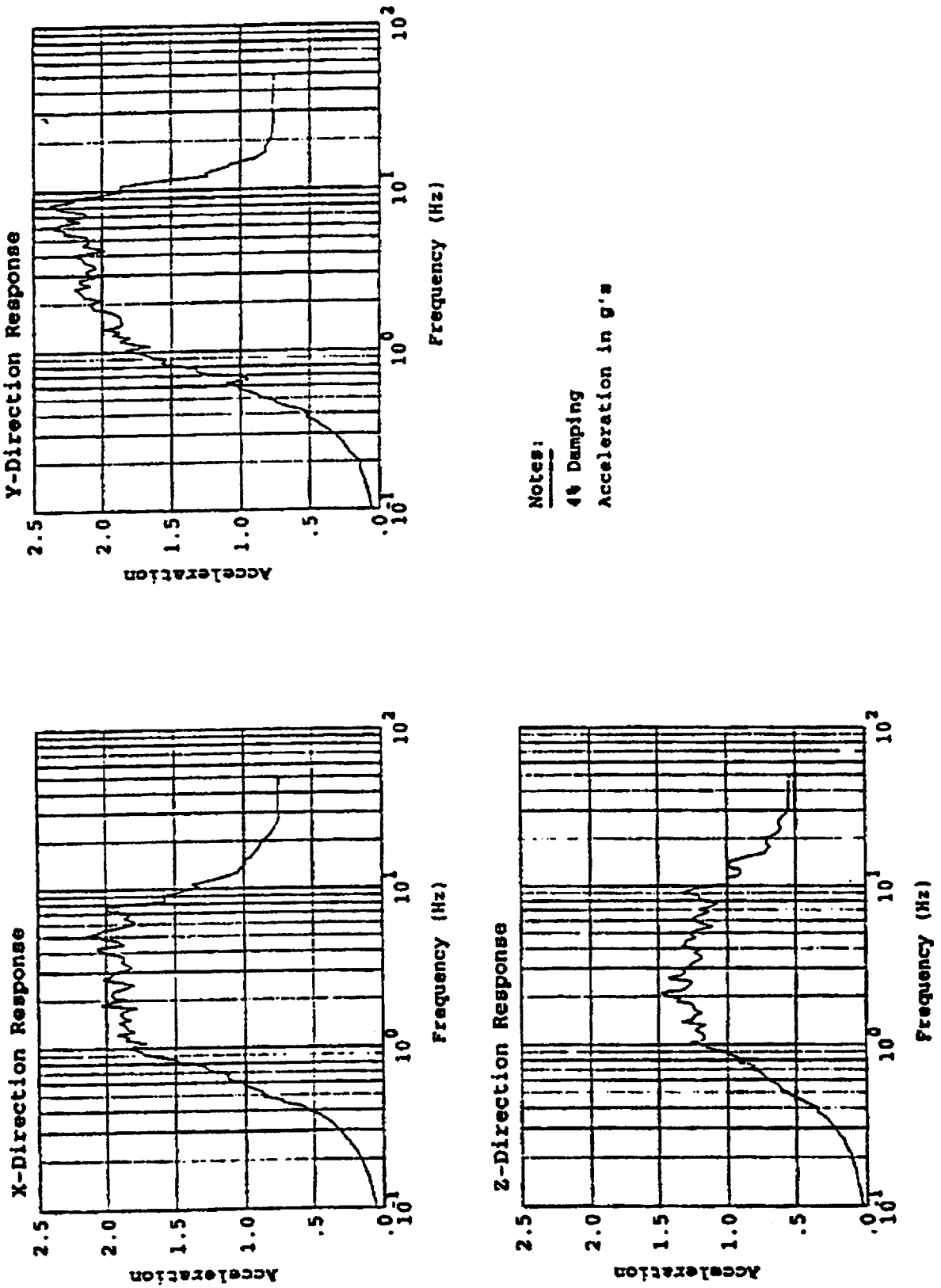

Figure 6-5: ISFSI SSI SASSI Solution: 100% Cask Mass, Envelope LB, BE, UB, LS Soil, X+Y+Z EQ, Envelope All Locations

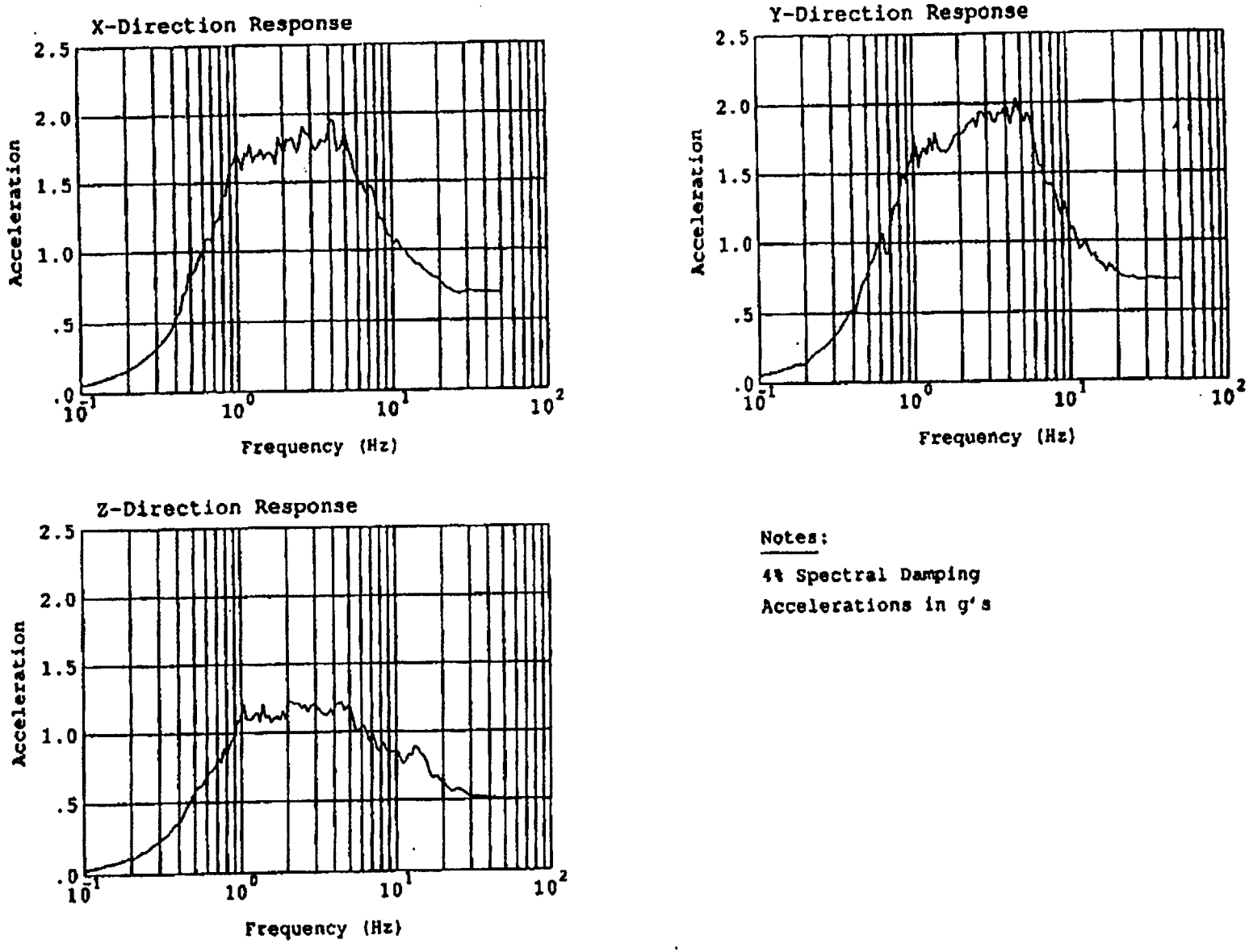

Figure 6-6: ISFSI SSI SASSI Solution: Hall Cask Mass, Best Estimate Soil, X+Y+Z EQ, Envelope All Locations

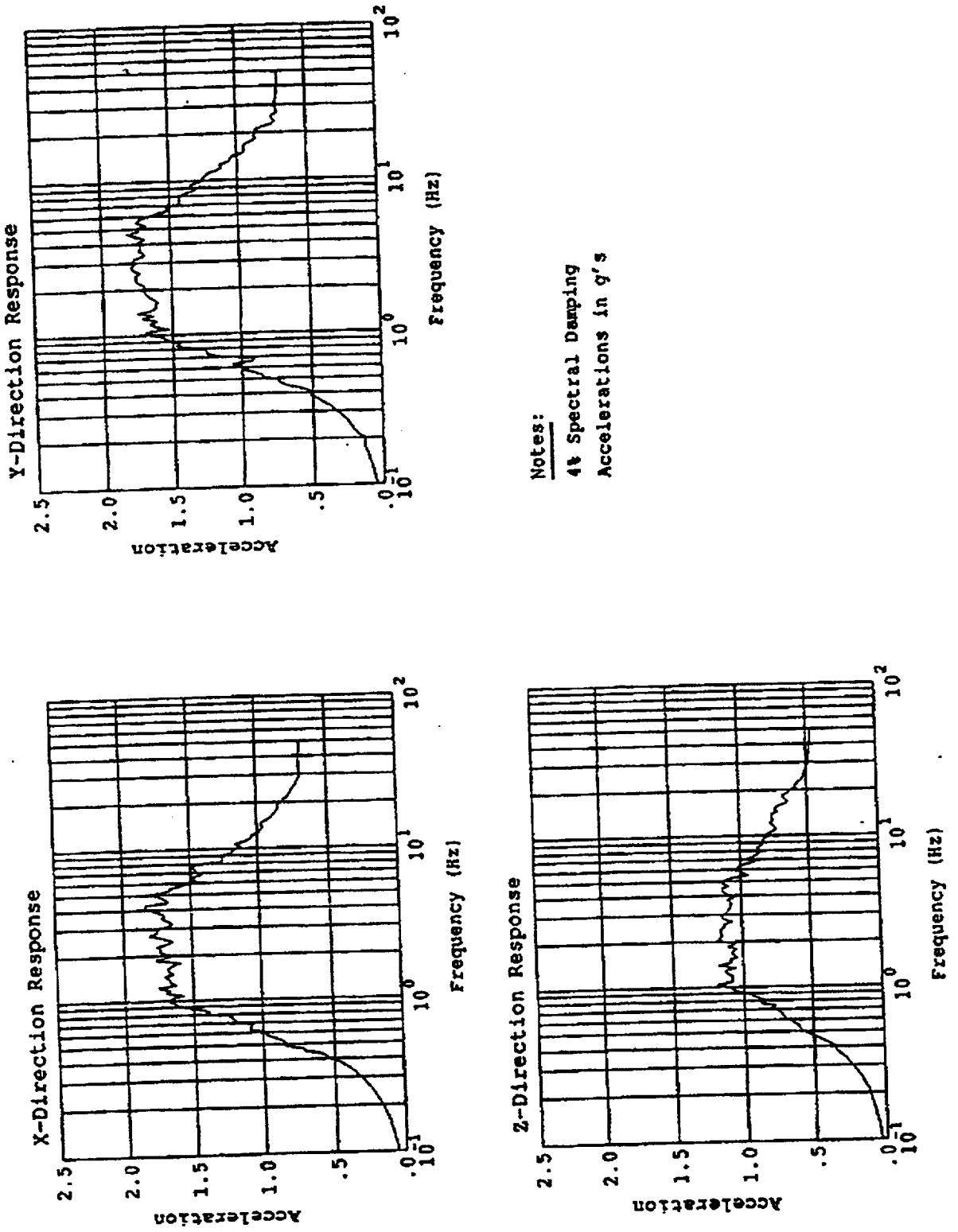

Figure 6-7: ISFSI SSI SASSI Solution: No Cask Mass, Best Estimate Soil, X+Y+Z EQ, Envelope All Locations

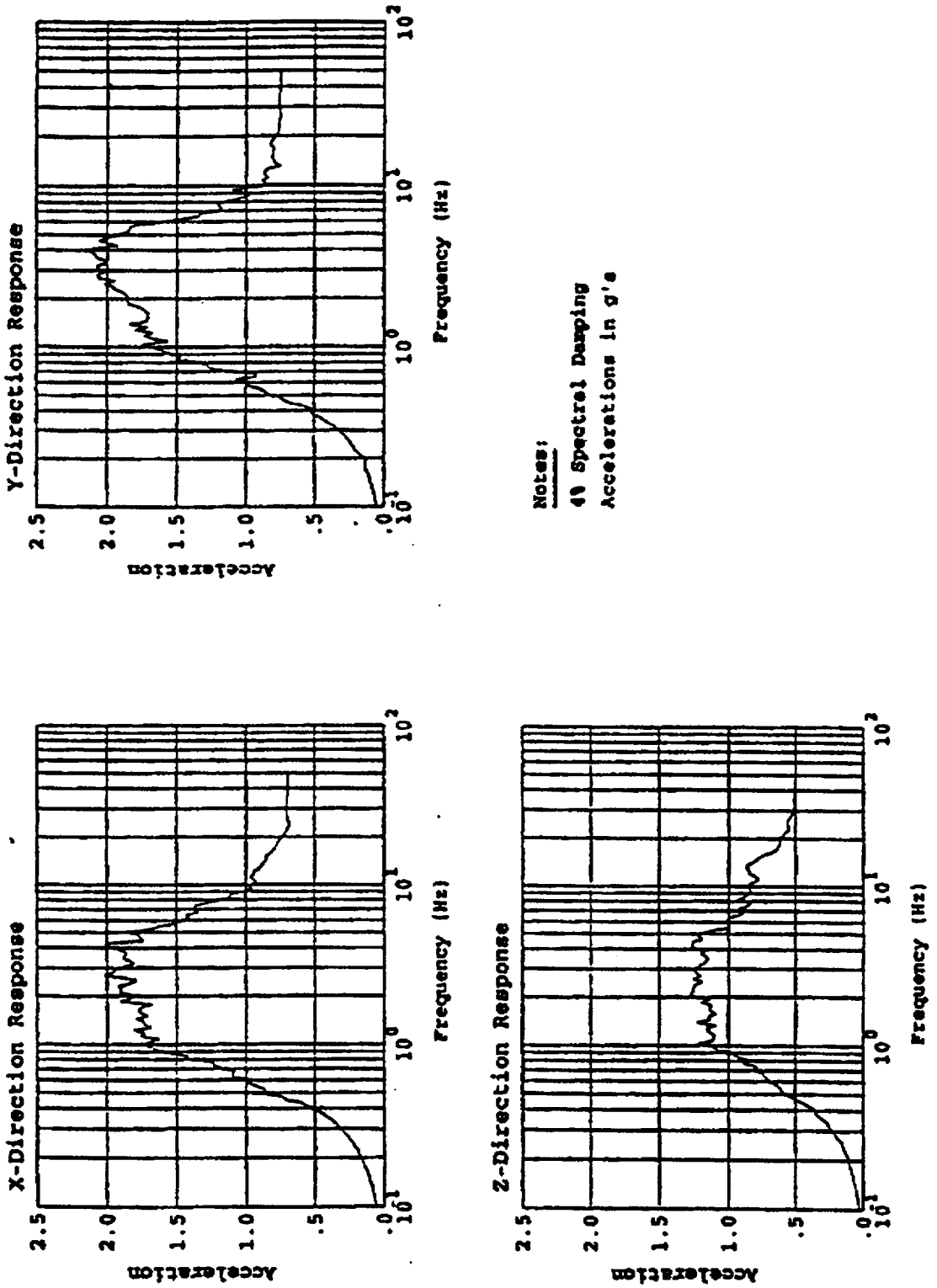

Figure 6-8: ISFSI SSI SASSI Solution: 100% Cask Mass, Rigid Pad, Best Estimate Soil, X+Y+Z EQ, Envelope All Locations

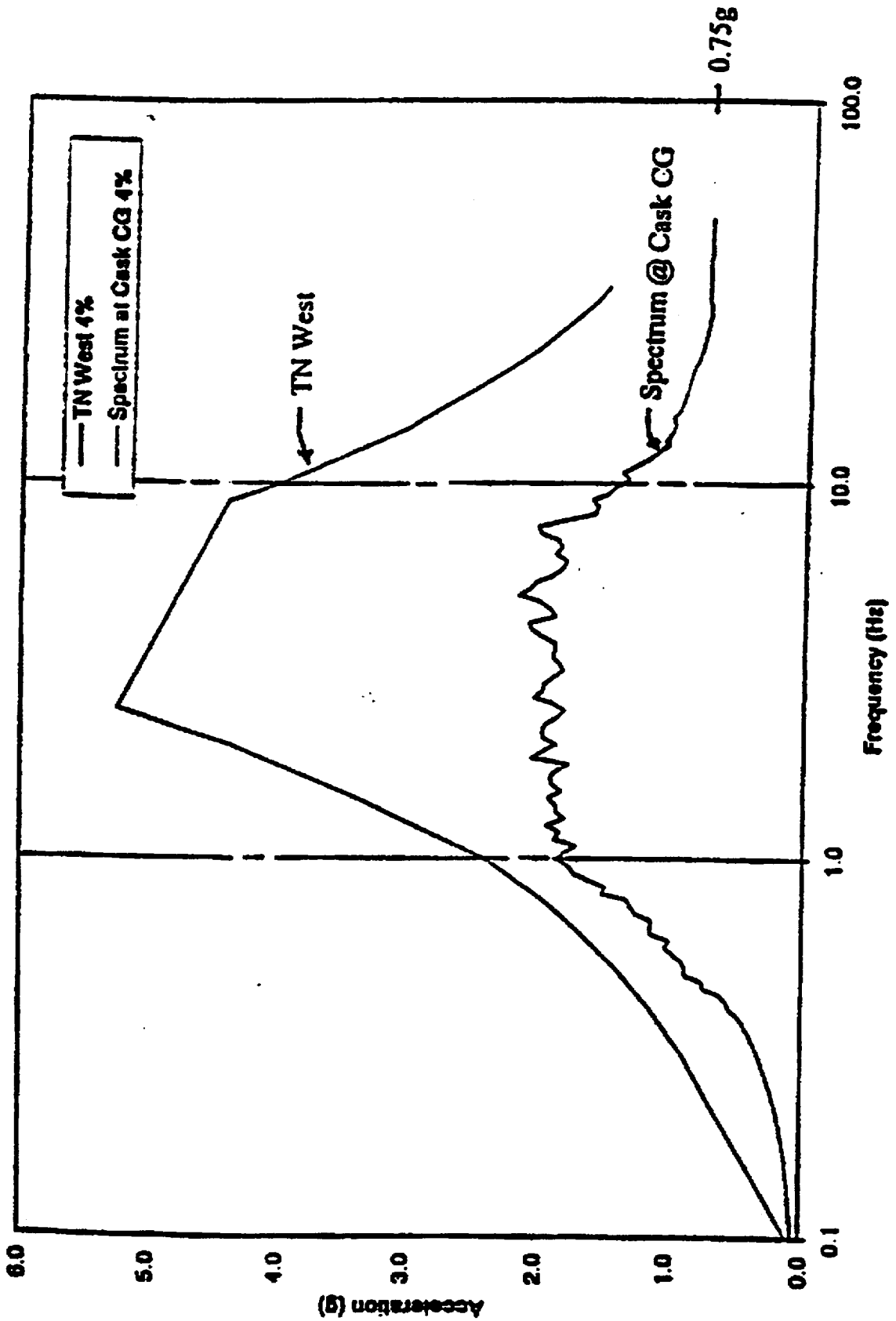

Figure 6-9a: TN West vs. SSE Casks CG Spectra – Horizontal Longitudinal Direction

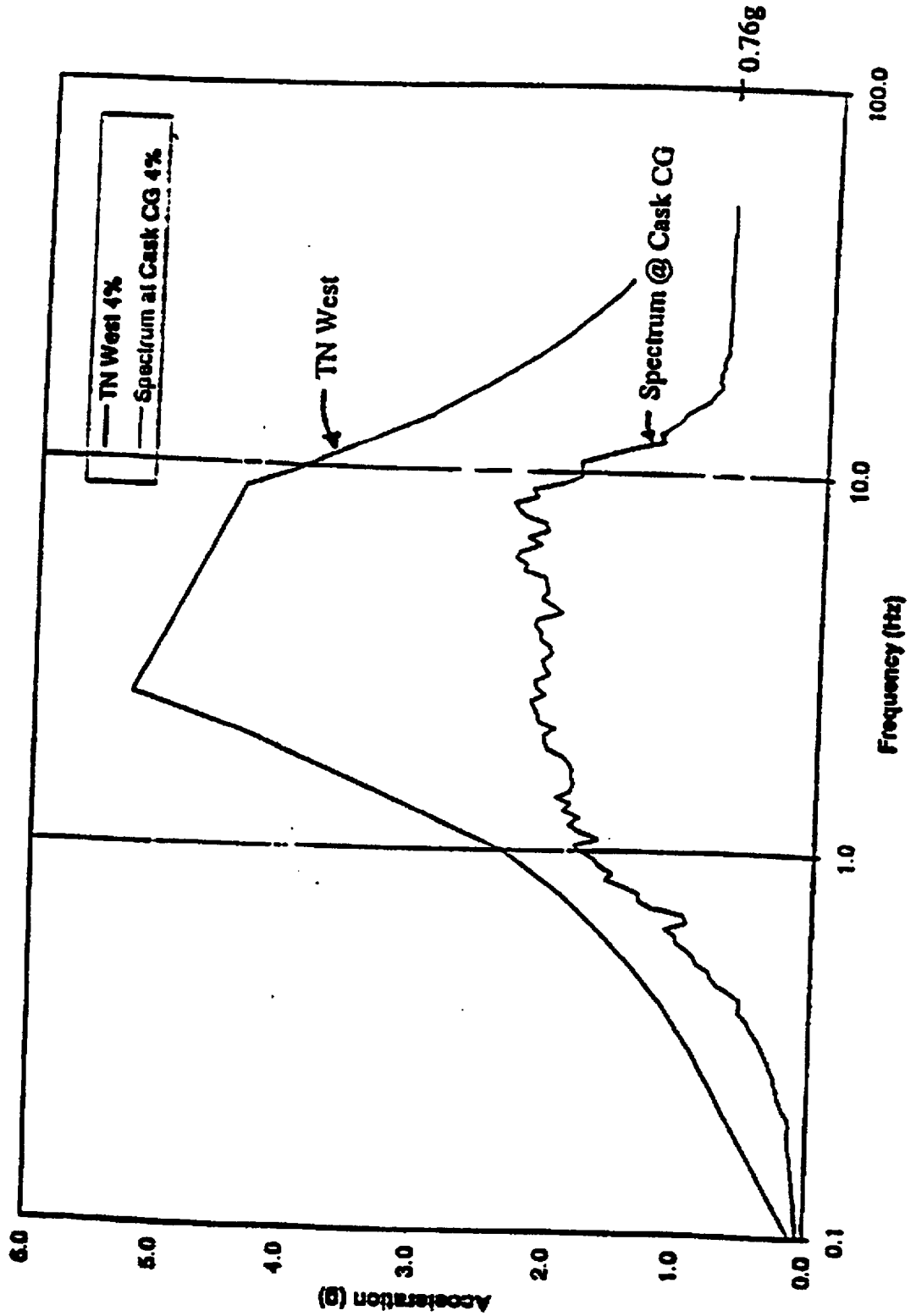

Figure 6-9b: TN West vs. SSE Casks CG Spectra – Horizontal Transverse Direction

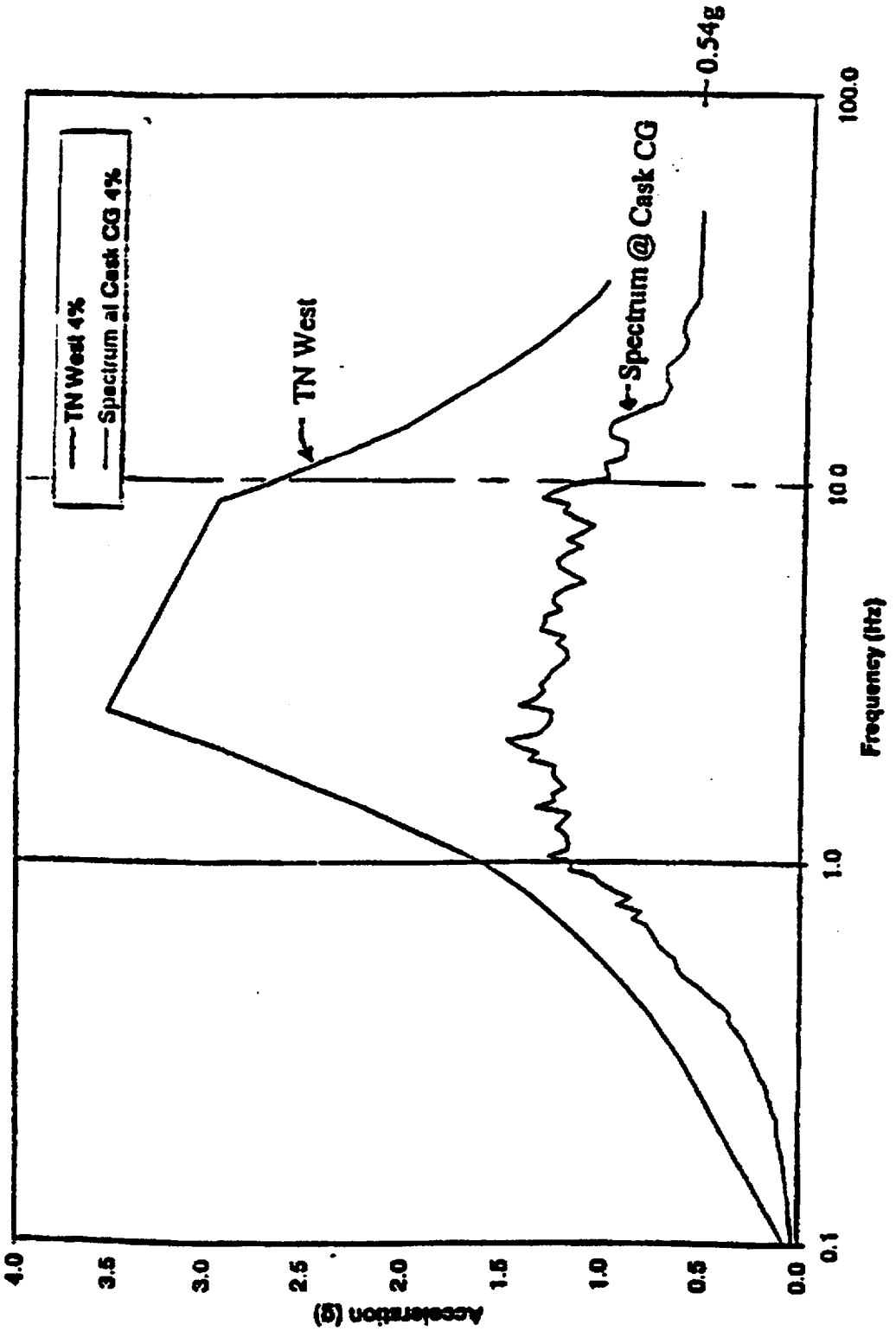

Figure 6-9c: TN West vs. SSE Casks CG Spectra – Vertical Direction

TRANSNUCLEAR WEST

ATTACHMENT 2

RAI RESPONSES

Attachment 2

RESPONSE TO REQUEST FOR ADDITIONAL INFORMATION
TRANSNUCLEAR WEST INC., TAC NO. L23203

Chapter 1 General Information

Question 1-1

Specify which transfer casks will be used to perform on-site transfer of the dry shielded canister (DSC).

Section 1.2.1.3.1 of the Safety Analysis Report (SAR) states that "the OS-197, MP-187, or any other NRC licensed transfer or transportation cask of sufficient size and payload capacity is acceptable for use with the Advanced NUHOMS® System subject to a site specific safety evaluation prior to the first usage." However, the SAR does not provide a methodology used to evaluate that the transfer or transportation cask has the appropriate shielding, heat transfer, structural integrity, and criticality characteristics to be used with the DSC-24PT. The application references previous evaluations of the OS-197 and MP-187 performed for the Standardized NUHOMS® System and the Rancho Seco site-specific application but does not demonstrate that those evaluations bound the DSC-24PT1.

This information is required by the staff to assess compliance with 10 CFR 72.24(c)(3), to assess whether all structures, systems, and components important to safety will satisfy the design bases with an adequate margin of safety.

Response Question 1-1

The SAR has been revised to specify that only the OS-197 transfer cask will be used for onsite transfer of the 24PT1-DSC. SAR Sections 1.1, 1.2 and 1.2.1.3.1 have been revised to delete references to transfer casks other than the OS-197. See responses to RAI Questions 4-1, 5-2, 6-2, 6-3 and 12-1 for specific changes regarding transfer cask configuration for the associated SAR Chapters. In addition, a review of the entire SAR was performed and SAR Sections 3.1, 3.6, 9.1, 9.2 and 12.1.1 were also revised to remove reference to alternate casks.

TN West has revised the AHSM and DSC drawings included in SAR section 1.5.2 to enhance fabricability, correct minor interference errors, and provide clarification to the notes shown on these drawings. A brief description of the changes implemented and a justification for each change is provided herewith. Change number 6 addresses RAI Question 7-1; all other changes were initiated as a result of TN West internal review.

BRIEF DESCRIPTION OF CHANGES IMPLEMENTED TO DSC DRAWINGS NUH-05-4010 and NUH-05-4010NP:

1. Editorial changes to notes to clarify the intent/ meaning of note. Added notes as required by the inclusion of additional details. Permitted the substitution of alternate material specifications and fabrication of grapple ring and grapple plate from a single forging/plate.
2. Revised the Vent and Siphon block configuration and increased siphon tube to 1 1/4" diameter to provide larger passages for better draining and drying of cavity.
3. Reduced size of lifting lug to remove interference with top spacer disc.
4. Revised guide sleeve poison length and location to cover active fuel length under all drop conditions. Added bottom spacer plate for interface with bottom spacer disc.
5. Clarified threaded lengths for support rods
6. Added alternate details for bottom closure to provide options for fabrication. Revised weld detail for inner bottom cover to shell.
7. Revised the minimum thickness of the outer top cover from 1.24" to 1.31".

BRIEF DESCRIPTION OF CHANGES IMPLEMENTED TO AHSM DRAWINGS NUH-03-4011 and NUH-03-4011NP:

8. Editorial changes were made to the notes. Detailed changes are shown on attached sheets.
9. Corrected the material specification for the support rail plate in the DSC Support Structure.
10. Increased width and radius of rear wall recess and extended the length of the heat shields.
11. Clarified primary reinforcement requirements for the door and added flag note to permit a composite door structure using the 1/2" plate (in lieu of reinforcement behind the plate).
12. Added flag note to the DSC Support Structure to permit construction holes in the interior stiffeners.

REASON FOR CHANGE & TECHNICAL JUSTIFICATION:

1. Editorial changes to clarify the meaning of notes. Added Note 9 to specify that the weld contours shown on the drawing are permissive and not required by the design. Removed over specification from notes and added notes 37 through 45 to clarify the added details.
2. Vent and siphon block passages were revised to give additional flow capacity and restore the intent of the dog leg to minimize shine paths.
3. There was a minor interference between the bottom of the lifting lug and the top spacer disc in the worst-case tolerance condition. Removing a small amount from the bottom of the lug resolves this issue.
4. Guide sleeve details were reviewed and revised to provide adequate support for

the ends of the guide sleeve and to locate poison plates where they covered the worst case location for the active fuel to be in compliance with the criticality calculations.

5. Fixed the potential interference between support rods and the threaded portions of the top and bottom spacer sleeves.
6. Added alternate details for the bottom closure to allow flexibility for fabricator to pick a solution that best meets the shop capabilities. Increased the thickness of the inner bottom cover plate to 1.24" min./ 2.0" max. to ensure that the plate will carry the defined ASME loads without assistance from the bottom shield plug. This permits the classification of the shield plug and outer bottom cover plate as ASTM materials. Also, permitted the use of a forging for the inner bottom cover plate to move the Class C tee joint weld to a Class B circumferential weld that is easier to inspect than the existing joint. Because of the increased plate thickness revised the weld callout for the Tee (existing) joint to allow any of the configurations permitted by Figure-NB-4243-1 of the ASME code. This will allow fabricator to minimize the weld volume if this detail is used.
7. The outer top cover plate thickness assumed in the supporting calculations is 1.31".
8. Editorial changes clarify the meaning of notes.
9. The material specification is corrected for the support rail plate to reflect the finish product. Nitronic® 60 is a brand name material that initially complies to ASTM A240, after it is cold rolled to meet the specified hardness it no longer meets all ASTM A240 properties. Therefore, specifying just the brand name and desired hardness is sufficient.
10. The rear wall recess is increased to simplify fabrication and improve clearance to the DSC. The change results in a consistent cross-section along the full length of the AHSM cavity. The heat shield is increased in length through this area. The net affect is an improvement in thermal performance of the AHSM. This change does not affect the reported results in the SAR based on a review of the shielding, thermal and structural calculations.
11. The flag note permits the 1/2" door plate to act as a tension element in a composite design. Such a design eliminates the primary reinforcement on the inner face.
12. The design of the DSC Support Structure requires only one crossbeam (in its installed configuration). Temporary crossbeam bracing at the other three rail stiffener locations is desirable to facilitate fabrication and installation. The bracing permits shop control and accuracy in the alignment of the rails and provides a means of maintaining rail alignment during shipment and installation of the DSC Support Structure. The bracing may be welded or bolted to the stiffeners. Bolted braces would be completely removed just leaving holes in the stiffeners. Welded bracing would be cut and the welds and/or ends of welded bracing could remain in place.

Chapter 2 Principle Design Criteria

Question 2-1

Remove the statement in Sections 2.1.1 and 3.1.1.1, that refer to the storage of 'Greater than Class C' (GTCC) waste inside an advanced NUHOMS® Systems (AHSM).

Approval to store GTCC will not be addressed in a Certificate of Compliance, issued in accordance with 10 CFR Part 72, for the Advanced NUHOMS® Storage System. This changes is required by the staff to confirm compliance with 10 CFR 72.2.

Response to Question 2-1

SAR Sections 2.1.1 and 3.1.1.1 have been revised to delete reference to storage of GTCC waste.

Question 2-2

Discuss design features of the Advanced NUHOMS® system to enhance decontamination and decommissioning.

The SAR did not contain sufficient detail with regard to decontamination and decommissioning of the Advanced NUHOMS® System. Include a discussion of the effect of the contamination limits stated in Section 12.5.2.4.b on potential off-site releases such as through the outlet vent at the top of the AHSM. The discussion should also include a statement on what affect the contamination level will have on the ability to decontaminate and decommission the concrete AHSM, the ISFSI pad, and the surrounding soils. Consideration of decontamination and decommissioning activities is required under 10 CFR 72.130 and 72.236(i).

Response to Question 2-2

The NUHOMS® system incorporates several design features to limit contamination of the NUHOMS® system components. These include:

- The transfer cask and dry shielded canister are designed and fabricated to limit contamination by specification of appropriate surface finishes.
- The dry shielded canister outer surface is also isolated from the spent fuel pool by filling the annular gap between the canister and the cask with clean water and sealing this volume at the top with an inflatable seal. This limits the ingress of pool water and contamination of the canister outer surface.

By limiting contamination of the 24PT1-DSC outer surface, contamination of the horizontal storage module is virtually eliminated. Contamination that may be present on the canister surface will be protected by the AHSM from direct exposure to the elements (wind, rain, etc.) and will therefore limit any potential release of removable

contamination. The probability of any removable contamination being entrapped in the AHSM air flow path and released outside the AHSM is considered extremely small given the low flow velocities characteristic of natural ventilation cooling. The effect of the contamination limits specified in SAR Section 12.5.2.4.c is addressed in the response to RAI Question 12-5.

The effect of these limits on decommissioning of the Advanced NUHOMS® system components is negligible. However, additional decontamination at the time of decommissioning may be required to allow free release of the canister (canister decommissioning is likely to occur offsite at a DOE facility), AHSM, ISFSI pad and surrounding soil. The spread of contamination from the canister surface, if any should occur, to the AHSM, ISFSI pad and surrounding soil is limited to very small areas of the ASHM internal surface. Performance of final decontamination for free release at the time of decommissioning is considered more appropriate since these decontamination activities will be performed under minimal radiation field conditions and would therefore be consistent with ALARA practices.

Chapter 3 Structural

Question 3-1

Justify the 392 degrees F maximum concrete temperature for accident conditions given in Table 4.1-5. This temperature exceeds the allowable range of 0 - 350 degrees F stated in the table.

Note 2 in Table 4.1-5 states testing will be performed to document that concrete compression strength will be greater than that assumed in structural analyses. The tests are to be on the exact concrete mix and are to acceptably demonstrate the level of strength reduction which needs to be applied, and to show that the increased temperatures do not cause deterioration of the concrete either with or without load. However, there is no discussion of what type of testing will be performed and why the testing is sufficient to confirm performance of the AHSM. The test details are required for the staff to assess compliance with 10 CFR 72.146 (b).

Response to Question 3-1

As described in the SAR, the following acceptance criteria apply to the concrete materials used in the construction of the AHSM:

- Satisfy ASTM C 33 requirements and other requirements referenced in ACI 349 for aggregates, and
- Have demonstrated a coefficient of thermal expansion (tangent in temperature range of 70°F to 100°F) no greater than 6x10-6 in/in/°F, or be one, or a mixture of the following minerals: limestone, dolomite, marble, basalt, granite, gabbro, or rhyolite.
- If concrete temperatures of general or local areas in normal conditions do not exceed 200°F and in off-normal conditions do not exceed 225°F, in addition to the above list of acceptable aggregates, quartz sands and sandstone sands are also acceptable as a fine aggregate only.

The calculated temperatures within the concrete AHSM demonstrate that the concrete meets ACI 349 and NUREG 1536 temperature criteria for all normal and off-normal cases. There are three areas of the AHSM predicted to experience temperatures in excess of 350°F during a 40 hour duration blocked vent accident that require evaluation for acceptability to ACI 349-97 criteria, as modified by NUREG 1536. The subject areas are as follows:

1. An area of 101" (along the 24PT1-DSC longitudinal axis) x 36" x 2.2" deep on each of the side walls. These areas are centered about the 24PT1-DSC centroid projected horizontally onto the two side walls.
2. An area of 85" (along the 24PT1-DSC longitudinal axis) x 52" x 4" deep immediately above the heat shield opening into the vent system. This area is centered about the 24PT1-DSC centroid projected onto the roof. This area is the

top part of the base block with vent openings, which is not required for transferring structural loads.

3. An area 6"x 2"x 1.5"deep located on the top surface of the front vent shielding block under the longitudinal axis of the 24PT1-DSC. Other areas of the shield block that are less than 350°F provide support for the 24PT1-DSC support structure steel.

The proposed elevated temperature testing for the AHSM design mix for the storage block will satisfy the following:

- A minimum of two sets of five 6" x 12" cylinders shall be made from a test batch,
- One set of cylinders will be used as the control (room temperature) set; the second set will be heated to 400 °F at a rate similar to that predicted by the thermal analysis for the high temperature areas. The maximum temperature will be held at a steady state for a time of at least 36 hours to exceed the anticipated effects of the blocked vent case,
- The heated cylinders shall be examined for soundness prior to strength tests. The concrete shall not show signs of spalling, cracks and/or loss of cement bond to aggregate due to the elevated temperatures.
- Each set of cylinders will be broken using standard compressive strength test methods,
- The average test results for the high temperature set, reduced by two standard deviations, shall not be less than 4,500 psi. Computation of the standard deviation shall be consistent with applicable methods within ACI 214. If a proposed design mix does not have sufficient test data to compute a standard deviation, then an equivalent standard deviation shall be computed consistent with trial batch requirements specified within ACI 318.

The above tests are for concrete cylinders heated without load. Since the normal condition compressive stress in the volumes of concrete that exceed 350°F during accident conditions is relatively low, testing cylinders under load is not necessary to simulate service conditions. Relevant published test reports [3-1.1] indicate that testing cylinders under load produces higher compressive strength test results than identical cylinders tested without load. Therefore, heating and testing unrestrained cylinders (without load) is adequate and conservative.

This testing will be re-performed if the concrete mix is changed by the concrete fabricator or as a result of a change in concrete fabricators.

As an alternative to the above testing requirements, the AHSM structural analysis may be revised by defining the volume of concrete exceeding 350°F as *non-structural* and excluding these areas from the blocked vent accident structural analyses (or modeling the areas with negligible structural properties). The location of primary reinforcement within these volumes would be adjusted to provide appropriate reinforcement for the reduced thickness *structural* concrete. Standard temperature and shrinkage reinforcement would then be provided for the *non-structural* concrete in order to ensure integrity for shielding.

Implementation of this design alternative would eliminate the need to perform elevated temperature testing of concrete since the *structural* concrete would be at or below 350°F.

SAR Table 4.1-5, Note 2 has been revised to incorporate a summary of the above discussion.

[3-1.1] M. S. Abrams, Compressive Strength of Concrete at Temperatures to 1600°F, ACI Special Publication SP25 (Paper SP 25-2), American Concrete Institute, Detroit, MI (1971).

Question 3-2

Justify the use of the selected friction coefficients between the AHSM and the storage pad.

The friction coefficients determine the AHSM rocking/tipping and sliding responses. The AHSM sliding analyses are performed using a range of friction coefficients between the cask and pad surfaces. The range varies between 0.3 and 0.7. However, it is not clear why these values were selected or if they are conservative. This information is required by the staff to assess compliance with 10 CFR 72.122(b)(2).

Response to Question 3-2

The selected range of friction coefficients is judged to be broad enough to adequately represent concrete sliding behavior considering potential variations in concrete-to-concrete surface conditions. The lower bound is intended to maximize sliding response while the upper bound is intended to maximize rocking response. The basis for the selected range is as follows:

- Available results of tests performed to determine the friction coefficient between concrete and steel surfaces show static friction coefficients of approximately 0.39 to 0.58 [3-2.1]. The data presented in [3-2.1] is for coated steel plates resting on a broom finished concrete pad. The friction coefficient for concrete-to-concrete is expected to be higher than for steel-to-concrete. Based on these considerations a reasonable "best estimate" approximation of the static coefficient of friction for concrete-to-concrete is judged to be 0.6. Also, the range is broadened from 0.6 to 0.7 to cover possible uncertainties.

- A reduction factor of 2/3 of the static value is taken as the dynamic friction coefficient, which yields a 0.4 friction coefficient (2/3x0.6). An additional reduction of 25% is taken to cover other possible uncertainties (e.g. wet conditions [3-2.2]), thus broadening the range to 0.3.

To demonstrate that the sliding displacements do not change significantly, TNW has performed two additional LS-DYNA analyses using 0.2 and 0.8 friction coefficients. These analyses further broaden the range of friction coefficients to 0.2 at the lower end and 0.8 at the upper end. Although the 0.2 friction coefficient is considered unrealistically low for concrete-to-concrete (typically applicable for steel-to-steel

surfaces) it is provided here to represent a bounding result. This lower value is also not supported by available test data of steel-to-concrete friction tests as reported in [3-2.1].

The maximum sliding displacement obtained from the 0.2 analysis case is 47.9 inches. This compares with a maximum of 41.9 inches for the 0.3 case. This comparison indicates that a change in friction coefficient from 0.3 to 0.2 causes only a 14% change in maximum sliding displacement response.

The 0.8 friction coefficient case is reported as an upper bound static coefficient of friction in [3-2.2], validating the use of 0.7 as a reasonable upper bound for dynamic friction value. The analysis for the 0.8 case yields a maximum sliding displacement of 35.1 inches, compared with 39.3 for the 0.7 case. As in the 0.7 friction case, the rocking uplift for the 0.8 friction case remains negligibly small. These two cases are included in revised SAR Table 11.2-2.

The calculated sliding displacement remains substantially less than the 120 inches space allowed in the ISFSI design for sliding of the AHSM.

No changes to the SAR have been made with respect to this RAI Question response.

[3-2.1] Duke Power Co., McGuire Nuclear Station, "Steel on Concrete-Coefficient of Friction Testing for Dry Cask Storage Project," dated January 20, 1999
[3-2.2] PCI Design Handbook, Fifth Edition, Precast/Prestressed Concrete Institute.

Question 3-3

Provide the following clarifications for Table 11.2-2 of the SAR.

For Case 2, evaluate how a group of three AHSMs would respond to a design basis earthquake when only one is loaded with a 24PT1-DSC.

Explain why Cases 3 and 4 are more sensitive to the friction coefficient than Cases 1 and 2. For Cases 3 and 4 when the friction coefficient changes from 0.7 to 0.3 the X-displacement increases from 11.9 inches to 32.4 inches, however, similar friction coefficient changes for Cases 1 and 2 only result in an increase from 39.3 inches to 41.9 inches.

This information is required by the staff to assess compliance with 10 CFR 72.122(b)(2).

Response to Question 3-3

An additional analysis has been performed as requested using the Case 2 analysis model with only one AHSM loaded with a 24PT1-DSC. The resulting maximum sliding displacements are summarized in SAR Table 11.2-2 as Analysis Case 13. As shown in SAR Table 11.2-2, the maximum sliding displacements for the fully loaded (3 AHSMs loaded with 24PT1-DSCs, Case 2) and one AHSM loaded case (Cases 13) are essentially the same.

For completeness, an additional analysis using Case 11 analysis model (AHSMs loaded with one 24PT1-DSC, 0.7 friction coefficient with construction tolerances) was also analyzed with a 0.3 coefficient of friction. The resulting and maximum displacements are summarized in SAR Table 11.2-2 analysis Case 14. As shown in SAR Table 11.2-2, the maximum sliding displacement (ΔX_{max}) for the fully loaded AHSMs is slightly larger than for the one AHSM loaded case (Cases 2 and 14, respectively) and, thus, is controlling.

Based on the analyses performed, it is concluded that the effect of one AHSM loaded versus a fully loaded group of three AHSMs with a 0.3 friction factor does not significantly affect the AHSM sliding displacement response.

In the analyses results reported in Table 11.2-2 of the SAR, Case 1 and Case 2 used time history set 1 (TH1), whereas Case 3 and Case 4 used time history set 2 (TH2). These two time histories sets were developed from different recordings of large magnitude earthquakes using spectral matching techniques that preserve the time domain characteristics of the natural record. Time history set 1, TH1, was developed using the Magnitude 7.6, 1999 Taiwan, Chi-Chi earthquake. Time history set 2, TH2, was developed using the Magnitude 7.4 1978 Tabas earthquake. Since the starting seeds used for the spectral matching are different, the resulting time histories will have different characteristics.

The X-direction component (H1) for time history sets TH1 and TH2 are shown in SAR Figures 11.2-2 and 11.2-5, respectively. It can be observed from SAR Figure 11.2-2 that the TH1 displacement time history is asymmetric or one-sided, e.g., the maximum displacements generally occur on one side of the time history baseline. This characteristic of the record produces a ratcheting effect in the sliding response of the AHSM, e.g., a continuous monotonic increase with time in sliding displacement of the AHSM in a single direction. These responses are shown in SAR Figure 11.2-11 (Case 1, 0.7 friction coefficient) and SAR Figure 11.2-16 (Case 2, 0.3 friction coefficient). As expected, Case 2 (with the lower, 0.3 friction coefficient case) exhibits more back-and-forth sliding and a larger maximum sliding displacement. However, the ratcheting effect is more pronounced for the higher friction coefficient case (Case 1, with 0.7 friction coefficient). The end result is that the maximum sliding displacements are not significantly different between Case 1 and Case 2 (39.3 inches for the 0.7 case versus 41.9 inches for the 0.3 case).

The X-direction component (H1) displacement time history TH2 (used for Case 3 and Case 4) is shown in SAR Figure 11.2-5. Time history set TH2 does not exhibit the same characteristics as TH1, e.g., the positive versus negative direction displacements are about the same magnitude. The resulting sliding displacements for time history TH2 are shown in SAR Figure 11.2-17 (Case 3, 0.7 friction coefficient) and SAR Figure 11.2-18 (Case 4, 0.3 friction coefficient). It can be observed that for this time history the sliding response is primarily a function of the friction coefficient, e. g., a larger sliding displacement is obtained for the 0.3 friction case than for the 0.7 friction case. The lack of a significant ratcheting effect does not mask the effect of the friction coefficient, as is the case for time history TH1.

Question 3-4

Discuss why the three sets of time histories each have a total duration of 40 seconds.

The discussion should include statements on what the affects a longer duration would have on the time histories or a statement stating why 40 seconds is sufficient for the time histories. This information is required by the staff to assess compliance with 10 CFR 72.122(b)(2).

Response to Question 3-4

The design ground motions for the Advanced NUHOMS® System are based on NRC R.G. 1.60 spectrum shape anchored to ZPA accelerations of 1.5g (horizontal) and 1.0g (vertical). These high ZPA acceleration levels and spectral characteristics suggest ground motions representative of large magnitude earthquakes ($M \geq 7.5$) and close epicentral distances (≤ 10 km).

The selected recorded motions used as starting seed for spectral matching generally reflect the magnitude, distance implied by the target spectrum. Given that the spectral matching procedure used for generation of the time histories preserves the time domain characteristics of the recorded motion, the duration of the matched time histories is consistent with the recorded durations.

To assess the reasonableness and adequacy of the duration of the input "design" ground motions, the 5% to 75% Husid durations of Arias Intensities are used as a measure of comparison and benchmarking with durations predicted by empirical models based on Western US recorded motions [3-4.1]. The 5% to 75% Arias Intensity is a measure of the duration of strong shaking of significance to stiff structures. The method for ensuring the time histories have sufficient duration is described in Reference [3-4.2]. Table 3-4.1 shows the 5% to 75% duration for ground motions based on the Western US empirical model, for magnitude 7.5 and above. Table 3-4.2 shows the 5% to 75% Arias Intensity duration for the spectrally matched time histories used for design of the Advanced NUHOMS® System. It can be observed that the strong motion durations are consistent with or conservatively exceed those of the empirical model and thus represent large magnitude earthquakes. Additionally the total duration of 40 seconds provides additional margin of conservatism for non-linear sliding response.

Table 3-4.1: 5% to 75% Husid Durations of Arias Intensity - Empirical Model

Magnitude	Component	Site Condition	Rupture Distance (km)	Strong Motion Duration Median (sec)		
				-1 σ	Median	+1σ
7.5	H	Rock	0 – 10	5.21	9.16	16.12
7.5	V	Rock	0 – 10	5.04	8.13	13.11
7.75	H	Rock	0 – 10	6.47	11.38	20.00
7.75	V	Rock	0 – 10	5.91	9.53	15.38
7.50	H	Soil	0 – 10	5.57	9.98	17.55
7.50	V	Soil	0 – 10	5.73	9.24	14.90
7.75(1)	H	Soil	0 – 10	6.93	12.19	21.45
7.75(1)	V	Soil	0 – 10	6.60	10.65	17.17

Notes :

1. Extrapolated data

Table 3-4.2: 5% to 75% Husid Durations of Arias Intensity – Advanced NUHOMS Time Histories

Time History Set	Component	Strong Motion Duration Based on Arias Intensity (sec)
TH1	H1	16.67
	H2	21.32
	V	19.33
TH2	H1	13.74
	H2	12.88
	V	13.25
TH3	H1	9.82
	H2	12.53
	V	11.16

Notes:

1. TH1 is based on the 1999 Taiwan Chi-Chi earthquake M=7.6
2. TH2 is based on the 1978 Tabas earthquake M=7.4
3. TH3 is based on the 1992 Landers/Lucern M=7.3

As additional information to address an example of a Western US ISFSI site with a seismic time history of 80 seconds total duration, a specific LS-DYNA analysis has been performed.

Consistent with the criteria specified in Section 12.4.2.2 of the Advanced NUHOMS® SAR, the time histories provided correspond to the amplified response spectra obtained at the center of gravity elevation of the AHSM, and include the effects of soil-structure interaction (SSI) of the ISFSI pad. The details of the SSI analysis is provided in the response to RAI Question 3-6. A seismic time history of 80 seconds duration was developed for the response spectra of the AHSM center of gravity (cg) shown in Figures 6-9a to 6-9c provided in the response to RAI Question 3-6 (Attachment 3). Time histories were not directly used from the SSI analysis because the AHSM cg response spectra are the results of an envelope of various soil cases and nodal locations. Also, the SSI analysis used a seismic input of 40 seconds duration due to the limitations of the SASSI program. Development of the time history followed the criteria given by the Standard Review Plan [3-4.3], Section 3.7 for response spectra enveloping, strong motion duration, statistical correlation and power spectral density enveloping. The time history components combined two records from the Taiwan 1999 (Chi-Chi) earthquake as the seeds to obtain a total duration of 80 seconds. The acceleration time history plots are shown in Figure 3-4.1. Amplified peak accelerations are 0.77g on the horizontal directions and 0.55g in the vertical direction.

The LS-DYNA analysis is performed using the same model described in Chapter 11 of Advanced NUHOMS® SAR. A 0.3 value for the static and dynamic coefficient of friction is selected as a reasonable lower bound to maximize sliding displacements.

The results of the analysis indicate that maximum sliding displacements are on the order of 13.7 inches (1.1 ft) in the X-direction and 19.1 inches (1.6 ft) in the Y-direction. The maximum vertical relative displacement is negligible (0.01 inches). These maximum values are significantly less than the maximum sliding displacements obtained from all the analyses cases considered in the SAR (on the order of 48 inches, SAR Table 11.2-2). Furthermore, they are bounded with significant margin by the clear distance of 10 ft. allowed for sliding around the row of AHSMs.

No changes to the SAR have been made with respect to this RAI Question response.

[3-4.1] Silva, W.J., N. Abrahamson, G. Toro, C. Costantino (1997). "Description and validation of the stochastic ground motion model." Submitted to Brookhaven National Laboratory, Associated Universities, Inc. Upton, New York.

[3-4.2] Kennedy, R.P., Short, S.A., Merz, K.L., Tokarz, F.J., Idriss, I.M., Power, M.S., and Sadigh, K. (1984). "Engineering characterization of ground motion, Task I: Effects of characteristics of free-field motion on structural response." Prepared for U.S. Nuclear Regulatory Commission. NUREG/CR-3805, vol.1.

[3-4.3] NUREG-0800, "Standard Review Plan for the Review of Safety Analysis Reports for Nuclear Power Plants," Sections 3.7.1 and 3.7.2, Revision 2.

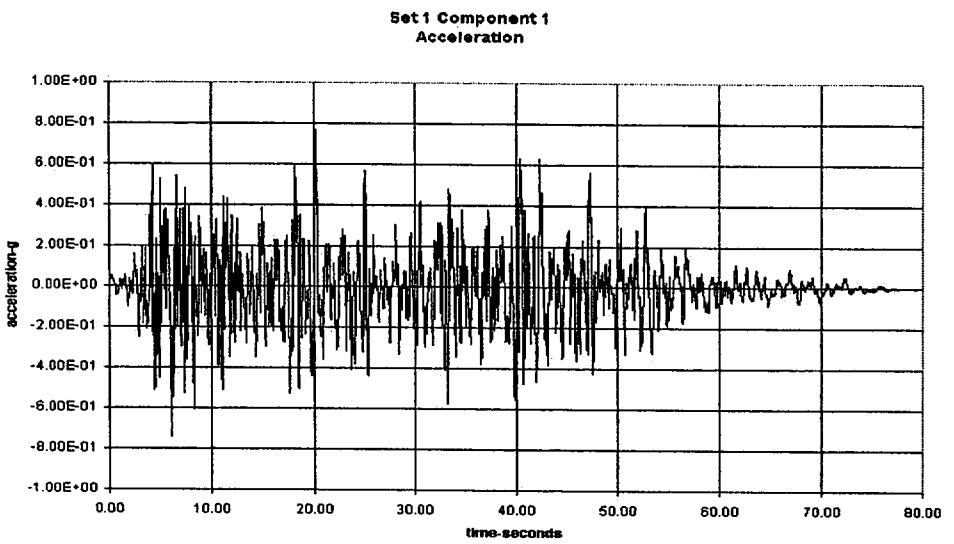

Horizontal Acceleration Time History Component S1H1

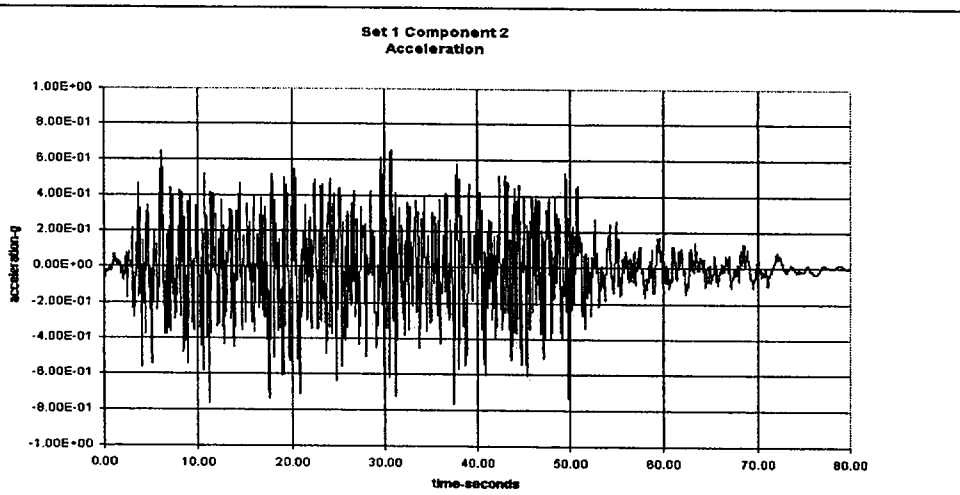

Horizontal Acceleration Time History Component S1H2

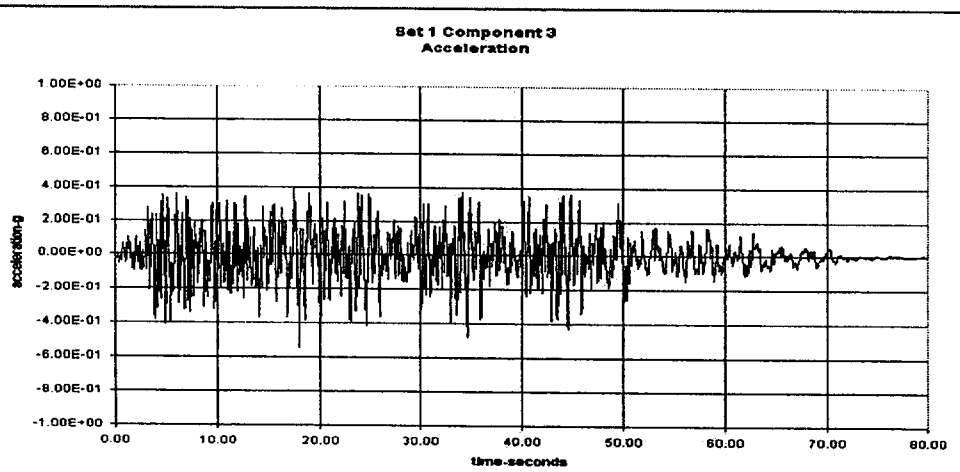

Horizontal Acceleration Time History Component S1V

Figure 3-4.1 - 80 Second Acceleration Time Histories

Question 3-5

Justify the use of a short term fuel cladding temperature limit of 1058 degrees F for stainless steel cladding in lieu of 806 degrees F as previously approved by the staff, or revise the allowable maximum temperature for the stainless steel cladding to 806 degrees F.

Section 3.5.1.2.1 of the SAR references EPRI TR-106440 "Evaluation of Expected Behavior of LWR Stainless Steel Fuel in Long-Term Dry Storage" as the basis of the long term cladding temperature limit. However, this reference also states that dry storage at temperatures above 806°F should be discouraged because of the increased potential to sensitize the stainless steel.

The justification should address the effect of sensitization on the stainless steel cladding integrity and retrievability of the fuel assembly at temperatures above the short term allowable fuel cladding temperature limits for stainless steel cladding of 806 degrees F.

Reference 3.33 of the SAR should also be provided along with a discussion on how the methods and data encompassed can be used to address the conclusions in Reference 3.30 of the SAR, specifically, that stress rupture by the development of a micron-sized pinhole leak is a possible failure mechanism for stainless steel cladding at temperatures above 806 degrees F. Issues that should be addressed include:

The fuel cladding material's microstructural properties and characterization after sensitization.

The material operating environment including maximum fuel rod internal pressure.

Fuel rod cladding susceptibility to the failure mechanism described in Reference 3.30 of the SAR during short term events.

Data and calculational methods, including applicable assumptions and codes, which address this failure mechanism.

This information is required by the staff to assess compliance with 10 CFR 72.236(f).

Response to Question 3-5

The Westinghouse 14x14 Stainless Steel Clad Fuel temperature limit has been revised to reflect a conservative maximum temperature of 806 °F. This temperature limit is based on EPRI TR-106440 for the sensitization of stainless steel at elevated temperatures in a non-inert environment. The 24PT1-DSC is inerted with helium for storage and transfer, so the use of non-inert temperature limit is conservative.

Since the Westinghouse 14x14 Stainless Steel Clad Fuel temperature limit has been revised to 806 °F, therefore the issues identified in this RAI Question related to stainless steel clad fuel temperature effects need not be evaluated further.

SAR Sections 3.5.1.2.2, Table 3.5-2, Table 4.1-4, Table 4.1-5, Table 4.4-7, Section 4.7.1 and Table 4.7-1 have been revised to reflect the 806 °F cladding temperature limit. SAR Reference 3.33 and associated data in Table 3.5-1 have been deleted.

In addition, SAR Table 4.4-7 has been revised to correct the maximum fuel clad temperature reported (for the 14 kW vacuum drying case).

Question 3-6

Provide a soil-structure interaction analysis that would be typical for a site deploying the Advanced NUHOMS® System.

The design basis response spectra of the Advanced NUHOMS® System design is based on the standard spectrum shape in NRC Regulatory Guide 1.60, "Design Response Spectra for Seismic Design of Nuclear Power Plants," Revision 1, 1973, anchored at 1.5g zero period acceleration for the horizontal direction. The vertical design spectrum is set at 2/3 of the horizontal over the entire frequency range. The horizontal and vertical spectra are specified at the top of the basemat.

Nonlinear analyses were performed in Chapter 11 of the SAR to determine the maximum sliding and rocking/tipping response of the AHSM during a design basis seismic event. These analyses were based on acceleration time histories from the Taiwan earthquake in 1999, the Landers/Lucern earthquake in 1992, and the Tabas earthquake in 1978. However, the staff requires the analysis including the soils and structure interactions, the methodologies and computer model, and the specific acceleration histories that envelope the parameters of a typical site. This is required for the staff to assess compliance with 10 CFR 72.122(b).

Note: The above question was restated in accordance with a communication from Mr. Steve Baggett (NRC) to Mr. U. B. Chopra (TN-West) via e-mail dated 4/18/01, 9:57 am, subject: "Reference RAI 3-6 for the Advanced NUHOMS design".

Response to Question 3-6

See Attachment 3 to the RAI Question Response transmittal letter for the response to this RAI.

Question 3-7

Demonstrate that the LS-DYNA computer program has been benchmarked against actual test data using a quality assurance program in accordance with 10 CFR Part 72, Subpart G, or justify the use of this program for non-linear seismic stability analyses.

This is required for the staff to assess compliance with 10 CFR 72.122(b).

Response to Question 3-7

The TN West Report documenting the Verification and Validation of the LS-DYNA program (TNW File No. QA040.0227, Revision 1) is provided as Attachment 4. Proprietary and non-proprietary copies of this report are provided. No revision of the SAR is required due to this RAI Question response.

Chapter 4 Thermal

Question 4-1

Specify which transfer casks will be used to perform on-site transfer of the dry shielded canister (DSC) and provide an analysis for each of the transfer cask designs to be used with the Advanced NUHOMS® System and provide design details or demonstrate why a previous analysis of the transfer casks bound its use with the 24PT1-DSC.

Section 1.2.1.3.1 of the SAR states that any NRC licensed transfer cask of sufficient size and payload capacity is acceptable for use. That statement has not been supported. The maximum heat load specified for the 24PT1-DSC is 14 kW. A previous calculation using a higher heat load for a different system may be bounding to determine the effects of that heat load on a transfer cask. However, the review is also focused on the response of the 24PT1-DSC components important to safety and the fuel cladding when subjected to the heat load and heat transfer characteristics associated with the system and particular transfer cask used. Additionally, Section 4 of the SAR provides an example which demonstrates that the MP 187 is not allowed for the content heat load in excess of 13.5 kW. This information is required by the staff to assess whether the system design can perform its function when subjected to the licensed content heat load under normal and accident conditions per 10 CFR 72.128(a).

Response to Question 4-1

See response to RAI Question 1-1. SAR Sections 4., 4.1.2 and 4.4.3.1 have been revised to remove references to casks other than the OS-197.

Question 4-2

Justify the assumption stated in Section 4.4.2.2 that the side and back surfaces of the AHSM should be modeled as adiabatic in order to simulate adjacent modules.

Applying the heat load generated in adjacent modules may be the more appropriate approach. The results of this calculation based on actual system arrangement will be used to determine compliance to 72.128(a).

Response to Question 4-2

Two adjacent modules with the same design basis heat load back to back or side to side result in no heat transfer between the modules due to symmetry of the heat loads and boundary conditions. Therefore, an adiabatic boundary condition is appropriate.

The thermal analysis of the AHSM and 24PT1-DSC shell is performed by using conservative assumptions. The use of side and back surfaces of the AHSM as adiabatic boundary conditions produces maximum component temperatures. This analysis is used to obtain maximum AHSM and 24PT1-DSC temperatures. To maximize the gradients in the AHSM concrete, for structural analysis of the AHSM, a module containing a design

basis heat load is modeled with adjacent modules empty. The maximum temperature cases are used to qualify materials and establish code allowables while the maximum gradient cases are used to calculate thermal stresses.

No SAR change has been made.

Question 4-3

When reformatting the SAR, ensure proper pagination.

Note that there are two pages identified as 4.1-3.

Response to Question 4-3

The pagination has been corrected in the section specified. Pagination of the remainder of the SAR was verified to be correct.

Question 4-4

Clarify actual Pu enrichments in mixed oxide (MOX) fuel descriptions.

Fissile Pu enrichments listed on Page 5.2-2 (2.78, 3.05, 3.25 w/o) are different from those listed as footnote (1) of Table 2.1-2 (2.81, 3.1, 3.31 fissile Pu w/o), and Table 6.2-2 (2.84, 3.1, 3.31 - fissile Pu w/o = 3.30, 3.65, 3.85 - total Pu w/o). Also, include the minimum fissile Pu enrichments in Table 12.2-1. Information must be presented accurately and in sufficient detail for the staff to assess compliance with 10 CFR 72.24(c)(3).

Response to Question 4-4

The MOX fuel assemblies each contain fuel rods with different plutonium enrichments. Minimum enrichments are used for shielding analyses and maximum enrichments are used for criticality analyses. The corrected Pu enrichments are shown below.

Number of Fuel Rods	Minimum Fissile Pu Weight Percent	Maximum Fissile Pu Weight Percent	Total Pu Weight Percent
64	2.78	2.84	3.30
92	3.05	3.10	3.65
24	3.25	3.31	3.85

Maximum Fissile Pu Weight Percent values presented in Table 2.1-2 of the SAR have been revised. The enrichments specified in SAR Section 5 on page 5.2-2 of the SAR have been clarified by specifying them as minimum enrichments and providing the corresponding maximum enrichments. The minimum Fissile Pu enrichments, specified on page 5.2-2 of the SAR for use in the shielding analyses, as modified to address

enrichment uncertainty (see RAI Question 4-6 response), have also been included in Table 12.2-1. Figure 6.3-6 and Table 12.2-1 of the SAR have been revised to clarify that the Pu weight % specified is Fissile Pu weight %. The Fissile Pu Weight Percent values in SAR Table 6.2-2 are correct as presented.

Question 4-5

Include a discussion of MOX fuel He production effects on maximum nominal operating pressure and cladding failure.

Section 4.4.8 of the SAR refers to Table 4.4-9 and states that based on the information listed, the UO2 assemblies are bounding for the analysis. However, the SAR does not include a discussion of the MOX rod void volume, a plot of gas generation over time, including He, and cladding strength which would provide a complete characterization of the condition of the contents stored. This information is required by the staff to assess whether the fuel cladding is protected against degradation that could lead to gross ruptures in accordance with 10 CFR 71.122(h)(1).

Response to Question 4-5

A comparison of stainless steel clad fuel (SC) and mixed oxide fuel (MOX) parameters affecting the canister pressure analysis (fill pressure, fuel rod void volume, fission gas generation during operation and during fuel decay, and fuel cladding material strength) have been added to SAR Section 4.4.8 to clarify the basis for performance of the pressure analysis based on SC fuel only.

Question 4-6

Clarify that a maximum heat load of 14 kW bounds the allowed contents of the 24PT1-DSC.

Section 1.2.1.1 of the SAR states that the 24PT1-DSC is designed for a maximum heat load of 14 kW. However, the staff found that the maximum heat load, based on allowable contents, is 16 kW. This information is required by the staff to assess compliance with 10 CFR 72.24(d)(1).

Response to Question 4-6

The maximum heat load is specified in SAR Section 12.2.1.c as a specific limitation to be confirmed by a licensee prior to storage of fuel in the 24PT1-DSC. However, to eliminate the need for further analysis to determine the heat load, Table 12.2-4, Fuel Qualification Table, has been added to the SAR to specify burnup/enrichment/cooling time limits to ensure a heat load of $\leq$ 14 kW per 24PT1-DSC.

In conjunction with this fuel qualification table, the fuel enrichment specification in SAR Tables12.2-1, 12.2-2 and 12.2-4 have been revised to accommodate an uncertainty in the

enrichment specified. Revisions to enrichment values specified in SAR Sections 1.2.3, 2.1.1, Tables 2.1-1 and 2.1-2 have been revised. An analysis of the effects of these uncertainties have been added to the SAR in Sections 5.2.3 and 6.4.4. The effect of these uncertainties on criticality analysis results is addressed in SAR Sections 6.1 and 6.4.3.

Question 4-7

Justify the statement in Section 4.4.5 of the SAR that the conservative modeling approach precludes the necessity to perform thermal testing.

Section 4.4.5 of the SAR states that detailed, conservative evaluations were performed for heat transfer from the AHSM, OS 197 transfer cask and the 24PT1-DSC. However, as noted in RAI question 4-6 those evaluations could not be confirmed by the staff. In addition, the SAR did not provide design details for all transfer casks intended to be used with the 24PT1-DSC. This information is required by the staff to assess compliance with 10 CFR 72.128(a)(4).

Response to Question 4-7

Additional constraints have been imposed in new SAR Table 12.2-4 to ensure that the maximum heat load is maintained $\leq$ 14 kW, see RAI Question 4-6 response. The response to RAI Question 4-1 addresses the use of a single transfer cask (OS-197).

Question 4-8

Separately tabulate and provide all assumptions, including initial and boundary conditions, when describing component temperatures under normal, off-normal, and accident conditions.

Tables 4.1-3, 4, and 5, of the SAR assume different heat load assumptions that vary between 14 kW and 24 kW. As discussed in RAI question 4-6, it is not clear that assuming a 14 kW heat load is conservative. This information is required by the staff to assess compliance with 10 CFR 72.24(d)(1).

Response to Question 4-8

SAR Table 4.1-1 provides the ambient temperature and solar insolation values used for Normal, Off-Normal, Long Term Average, Accident and Fuel Building conditions. In accordance with Section 1.2.1.1, the maximum total decay heat load authorized for the 24PT1-DSC is 14.0 kW. Analyses at higher heat loads demonstrate the robustness of the system and may be utilized in future amendments to qualify higher heat load fuel.

SAR Table 4.1-6 is added to provide a summary of the limiting 24PT1-DSC heat loads and the corresponding ambient temperatures and insolation values assumed in the analysis of each major system component. Heat loads specified in SAR Tables 4.1-3, 4.1-4, 4.1-5 and 4.4-6 are deleted and a reference is provided to SAR Table 4.1-6.

Question 4-9

Explain why direct engulfment of the AHSM is unlikely and justify why any fire while the DSC is loaded in the AHSM is bounded by an engulfing fire around the transfer cask.

Section 11.2.4.1 of the SAR includes a discussion of the fire accident. A fire at the inlet of the AHSM may have a greater impact on the 24PT1-DSC than a fire engulfing the transfer cask and, therefore, should be addressed to determine reasonable assurance of adequate safety under normal and accident conditions. This information is required by the staff to assess compliance with 10 CFR 72.128(a).

Response to Question 4-9

Direct engulfment of the AHSM is unlikely because the source of combustible materials near the AHSM is limited to the quantity of fuel and hydraulic fluid associated with vehicles and equipment supporting Advanced NUHOMS® system operation and expansion. The most likely ignition sources would be associated with operation of manned equipment. Plant personnel are likely to be present should a fire occur and will ensure prompt detection and extinguishment of any fire. Therefore, the likelihood of an ignition source being present in the vicinity of the combustibles with the combustibles in an ignitable configuration (fuel/fluid leak) without plant personnel in the vicinity is extremely small. The AHSM inlet is 24" above the ground, precluding the flow of combustible liquid into the AHSM. Any flames or products of combustion would tend to rise rapidly and would have to pass through more than 8 feet of concrete ducting before reaching the canister. The high thermal mass of the concrete would absorb most of the associate heat. Therefore, the smaller, lower thermal mass, more accessible transfer cask represents the bounding fire case.

SAR Section 4.6.4 has been revised to provide additional discussion of the effects of a fire on the 24PT1-DSC stored in an AHSM.

Chapter 5 Shielding

Question 5-1

Describe how ^{59}Co impurities in the fuel assembly structural material and cladding were modeled in determining bounding source terms. Section 5.2 "Source Specification" does not detail how this material was accounted for in the design basis bounding source term for the stainless steel fuel cladding, fuel hardware, and Inconel materials described in Tables 5.2-2 through 5.2-6.

Independent NRC staff calculations using ^{59}Co impurity levels described in EPRI TR-104329 "Evaluation of Shielding Analysis Methods in Spent Fuel Cask Environments" show that this impurity may be important and could lead to significant non - conservatism in both the shielding and thermal source terms.

Alternatively, provide references which characterize the ^{59}Co impurity levels of the materials used to generate the design basis source term and compare those to the impurity levels described in EPRI TR 104329. This information is required under 10 CFR 72.236(d) and (f).

Response to Question 5-1

Additional text has been added to SAR Section 5.2 "Source Specification" to describe how all of the light elements, including ^{59}Co, are modeled in determining bounding source terms. Table 5.2-18 has also been added to provide the required elemental composition, including ^{59}Co.

Question 5-2

Provide shielding analyses for all loading and unloading configurations that will exist during operations involving the Advanced NUHOMS® System. Include descriptions and shielding analyses of each transfer cask that will be qualified to transfer or transport the 24PT1-DSC during the four "Loading Stages" described in Section 5.3.1.2.

Alternatively, provide a table describing and comparing the characteristics of each transfer cask qualified to transfer or transport the 24PT1-DSC. Include a discussion which contrasts each cask characteristic and describes how the analysis in Section 5.3.1.3 (shown by Table 5.1-1, Figure 5.1-4, and Figures 5.4-4 through 5.4-7) is conservative or bounding. Provide reference for the OS197 transfer cask (as stated in Section 5.3) as the analyzed condition and compare any applicable characteristics such as material types, shielding thickness, streaming paths, neutron absorbing materials and other applicable characteristics described in NUREG 1536 for any requested alternative transfer casks.

Update the remaining sections of the SAR (including providing specific reference to allowable transfer cask designs) which detail the allowable transfer casks used in the Advanced NUHOMS® System (including Section 12.4.3.3) as appropriate. Figures which

describe allowable transfer casks should reference specific casks (either submitted in response to this question or already documented at the NRC) and not general designs such as Figure 5.1-4.

Section 5 of the SAR does not describe all of the transfer casks that will be used in the operation of the Advanced NUHOMS® System. Further, the analysis does not explicitly state that the OS197 transfer cask is the basis for the transfer condition model or provide references to the applicable documents which contain OS197 specifications. The staff does not accept the use of transfer casks which are not analyzed and qualified for the Advanced NUHOMS® System. This information is required to show compliance with 72.236(d).

Response to Question 5-2

As discussed in the response to RAI Question 1-1, the SAR has been revised to limit the transfer casks for use with the Advanced NUHOMS® system to the OS-197 transfer cask. The shielding analysis presented in Chapter 5 of the SAR is based on the OS-197 transfer cask. Revisions to SAR Sections 5., 5.1, 5.3.1, 5.5, Table 5.1-1 and Figure 5.1-4 have been made to clearly specify the OS-197 cask configuration in the shielding analysis.

Question 5-3

Clarify the particle transport model discussed in Section 5.4.1. Further describe the discrete ordinates method and limitations and how the DORT-PC computer code used addresses these limitations. Provide an in depth discussion and documentation (including benchmarking, verification, and validation) of reference 5.2 and how the analysis in Sections 5.3 and 5.4 addresses the limitations of the discrete ordinates method including:

1. *The ability to solve mixed problem geometries such as mixed rectangular and cylindrical geometry systems encountered in the cylindrical DSC and the rectangular AHSM.*

2. *Problems with irregular boundaries and material distributions.*

3. *Production of spurious oscillations in the spatial distribution of the calculated flux density (also known as the ray effect) as an inherent consequence of the angular discretization. Discuss whether penetration through large non-scattering regions are encountered (where this effect may be particularly important).*

4. *How the code in reference 5.2 addresses multidimensional situations in which the flux density is anisotropic and in which the medium is many mean-free paths in size.*

5. *Numerical truncation errors introduced through the discretization of the spatial and angular variables and the required mesh fineness of the angular and spatial meshes which are required to obtain flux densities that are independent of the mesh size, particularly for large system models.*

6. *How modeling of streaming effects may be effected by the problems discussed in (a) - (e).*

How the three models described in Sections 5.3 and 5.4 adequately address (a) - (f).

The staff notes that although reference 5.2 is distributed by ORNL/RSIC, no documentation is provided with respect to benchmarking, verification, and validation; and that similar code packages (e.g. CCC-650) may have more applicability as "industry standards." This information is required by the staff to assess compliance with 72.24 and 72.236(d).

Response to Question 5-3

The DORT computer code has been benchmarked, verified and validated in accordance with TN West's QA program requirements for use of computer software in support of safety related analyses. This included a verification of the operation of the code on the software/hardware platform used by replicating the results of sample problems provided in the user's manual. Benchmarking and validation was performed by comparison of results with a previously benchmarked/validated ANISN model. Figures 5.4-8 though 5.4-12 have been added to the SAR to provide a simplified depiction of the shielding analysis models used. A non-proprietary version of these figures is also included in these RAI responses (5-3, 5-5) to facilitate the review of these responses.

1. Limitations of the DORT computer code preclude explicit modeling of combinations of rectangular and cylindrical geometry systems encountered in the cylindrical 24PT1-DSC and the rectangular AHSM in a single DORT model. Nevertheless, DORT allows the description of cylindrical shapes in "R-Z" mode and rectangular shapes in "X-Z" mode. It is possible to conservatively model this rectangular problem by breaking the AHSM geometry into smaller parts and then modeling these parts using "R-Z" or "X-Z" geometry.

For the doses at the top and bottom of the AHSM, the AHSM geometry is split into two parts, an upper half and a lower half, by a horizontal plane through the 24PT1-DSC longitudinal axis, shown in Figure 5-3.1 along line A-A'. These two halves are rectangular in shape, however an "R-Z" model of the rectangular shape is developed by setting the AHSM outer surface radius equal to the distance between the 24PT1-DSC centerline and the AHSM outer surface along line C-C' in Figure 5-3.1. This ensures that the DORT model AHSM surface represents the nearest point on the roof and the floor, as appropriate for the respective model (See Figure 5-3.2).

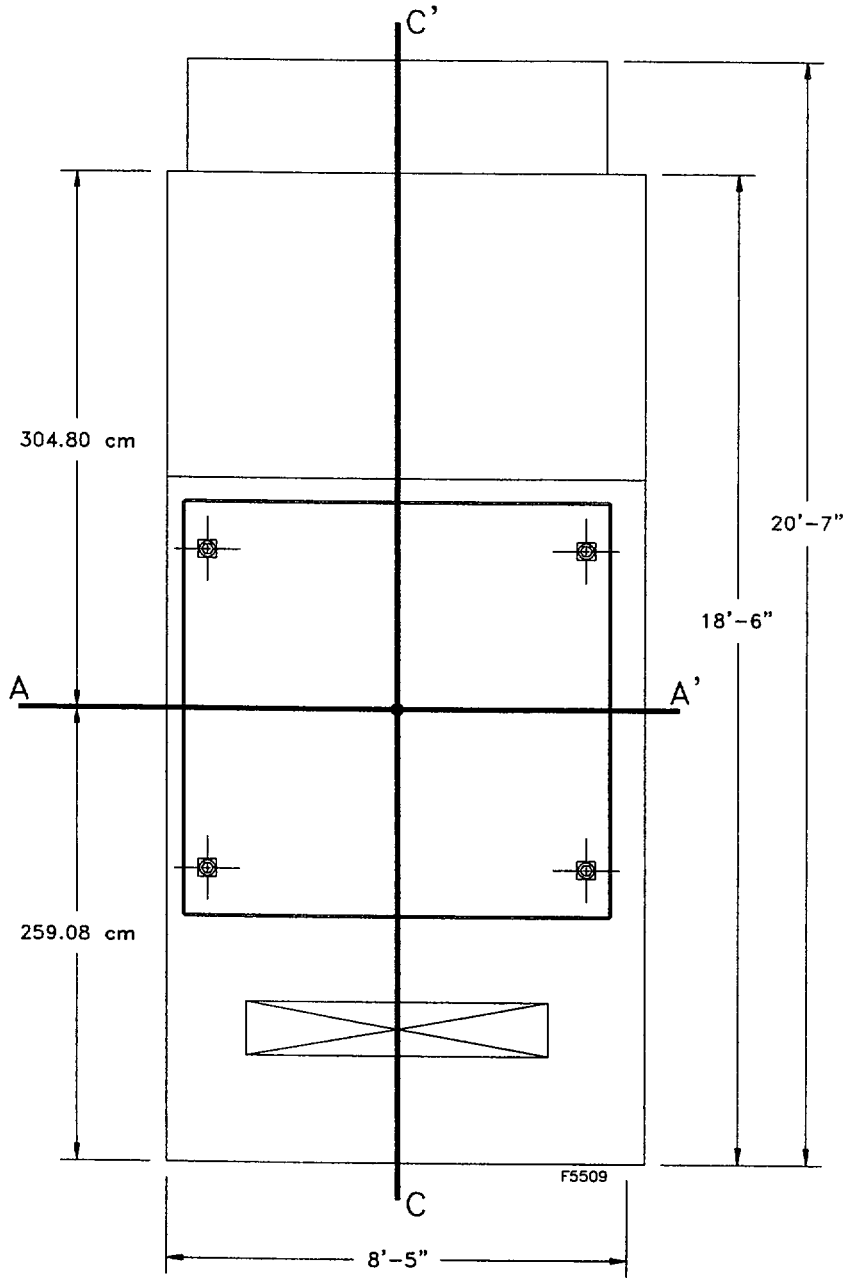

Figure 5-3.1 - AHSM Front View

The rectangle shown in Figure 5-3.2 represents the outer edge of the AHSM halves described above. The radial dimensions are determined from the center of the ASHM door to the roof and floor surface along line C-C' in Figure 5-3.1. Two models are created, one for each half of the AHSM. These models are identified as the "roof" and "floor" models and represent the AHSM geometry above and below the horizontal plane through the 24PT1-DSC longitudinal axis. These models are conservative because they model the thinnest roof and floor shielding. These models are used to estimate dose rates along lines AA', CC' and EE' shown in Figures 5-3.1

and 5-3.3. The DORT models are shown in Figures 5-3.3, 5-3.4, 5-3.5 and 5-3.6. The results calculated with these two models match at the 24PT1-DSC longitudinal centerline.

Assuming that dose rates obtained along lines AA', CC' and EE ' from the models described above are constant over the corresponding surfaces would be too conservative since these lines are aligned with the 24PT1-DSC centerline which results in the peak doses for the entire surface.

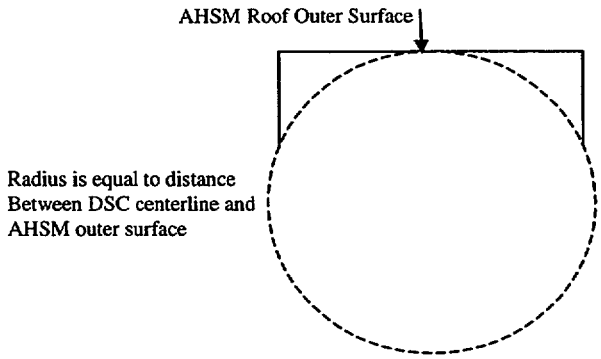

Figure 5.3-2 - Approximation of AHSM Rectangular Geometry in DORT Roof models

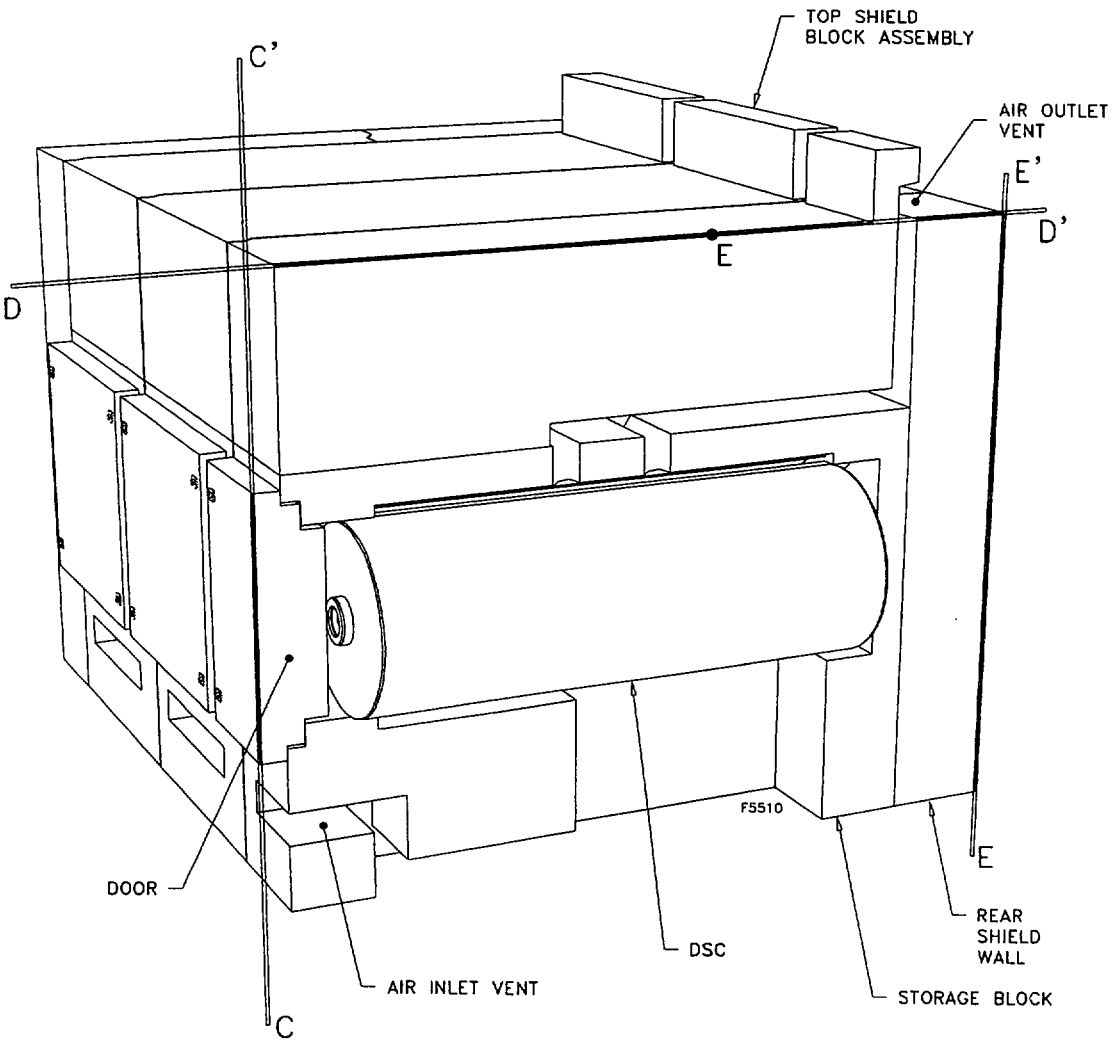

Figure 5-3.3 – AHSM Side View Cross Section

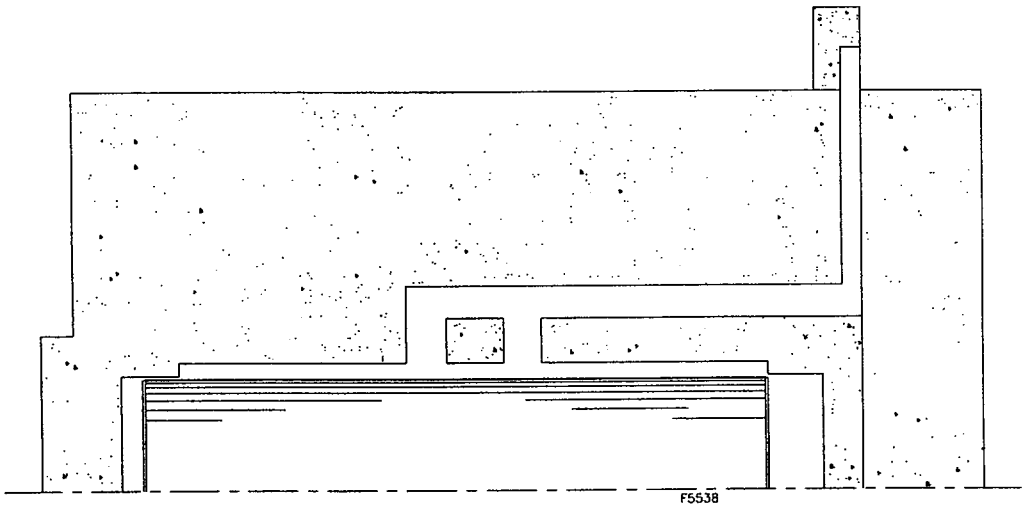

Figure 5-3.4 - AHSM "Roof" Model

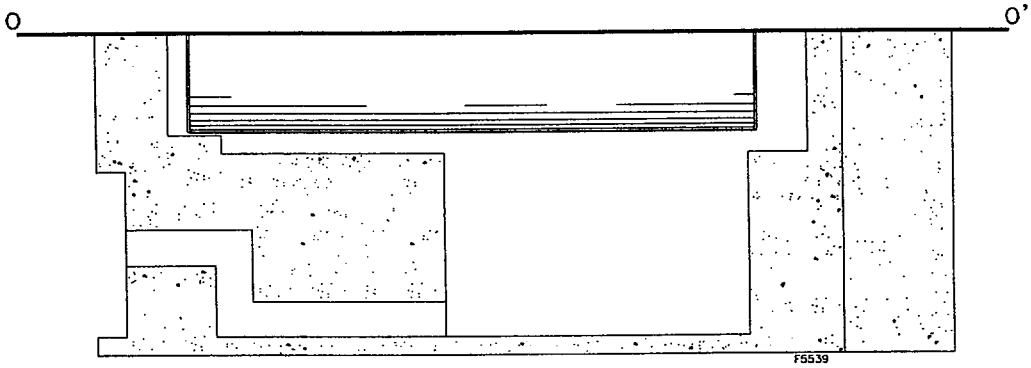

Figure 5-3.5 - AHSM "Floor" Model

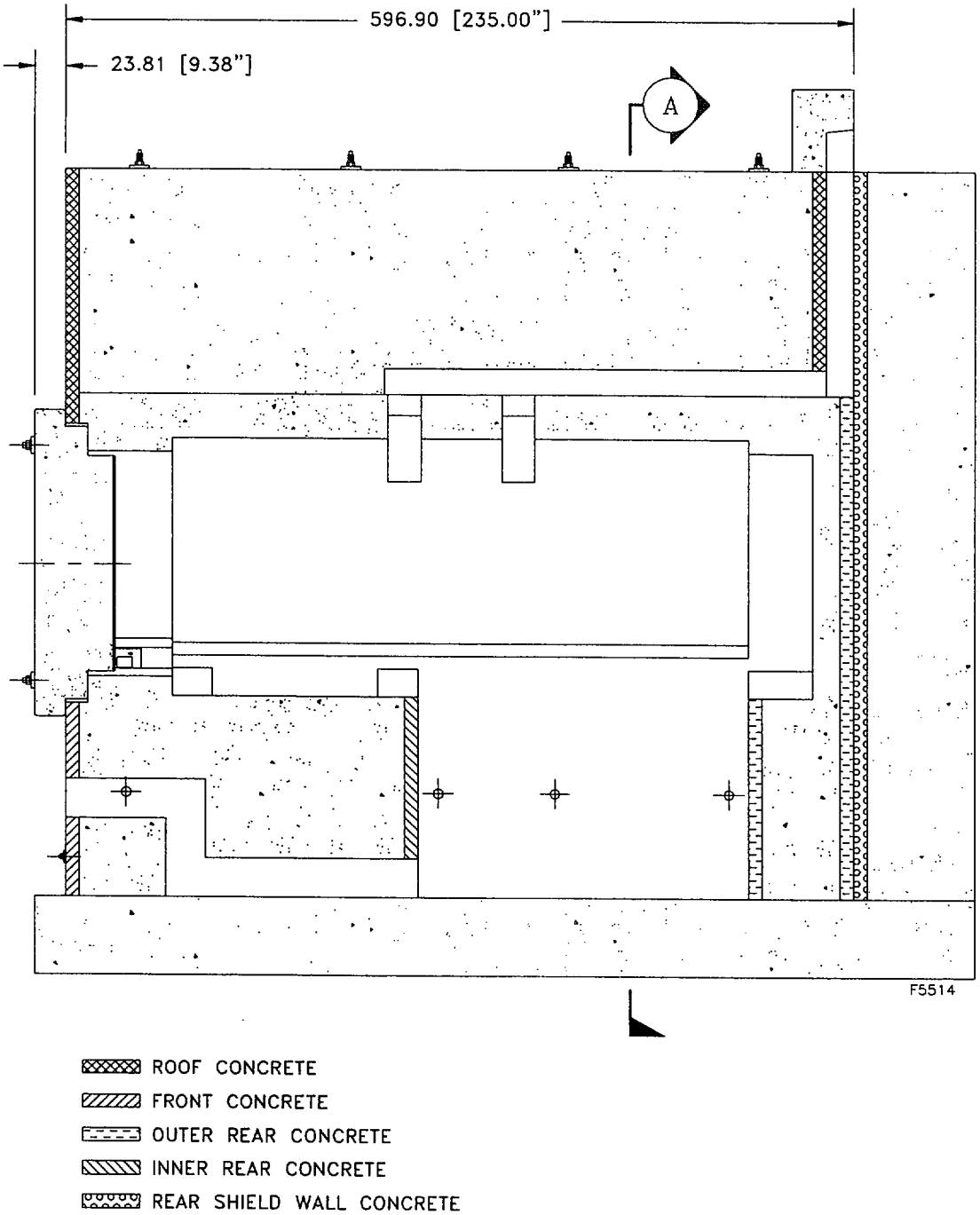

Figure 5-3.6 - AHSM "X-Z" Model

To reduce conservatism and to estimate the shape of the dose rate distribution functions along the AHSM side and front an "X-Z" model is created. This model is shown in Figure 5-3.6. The variation of dose rate along these surfaces is approximated by a Gaussian distribution. As can be seen from Figure 5-3.6, the thickest layer of concrete a particle encounters is in the direction from the 24PT1-

DSC towards the AHSM roof. The shape of the dose rate distribution function on the AHSM roof is determined using an "X-Z" model. This model is used to reshape dose rate distributions on the AHSM front and roof calculated with the two "R-Z" models. This approach appropriately models the geometry of the AHSM.

2. DORT computer code limitations also preclude detailed modeling of irregular boundaries and material distributions. However these irregularities do not affect the overall dose rates. They have only small impact on the dose rates at the surface in localized areas. For example the four cask trunnions are not modeled at all (see response to RAI Question 5-8). Not modeling the trunnions is conservative because they would provide additional shielding in the area adjacent to the trunnions but their presence would have a negligible effect on dose rate distribution at 1 or 3 feet away. Irregularities as described above in this example are neglected in such a way that the model underestimates the actual shielding available. Some irregularities like relief valves may create local 'hot' spots, but these potential hot spots are very localized and do not change the radiation field around the 24PT1-DSC and Transfer Cask as a whole.

3. Schematically the ray effect can be illustrated as shown in Figure 5-3.7, below.

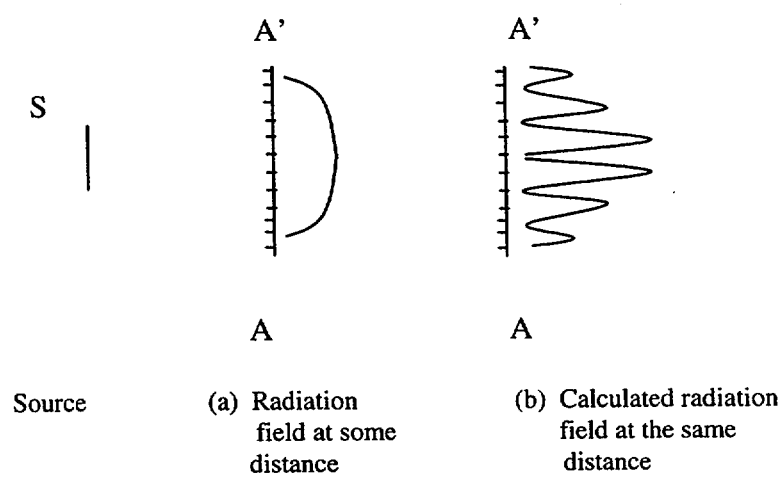

Figure 5-3.7 - Discrete Ray Effect

Figure 5-3.7 depicts the case where the radiation field from source *S* is considered along line AA' at some arbitrary distance. At (a) a real radiation field is depicted. Due to angular discretization the calculated distribution might look like (b). This effect is especially pronounced if the only separation between a source and the area of interest is media with large mean free paths (e.g., air). Even though there are cavities inside of the AHSM (see Figure 5-3.3) most of the points on the AHSM surfaces are separated from the source by very thick layers of concrete. The only place to expect the ray effect is in areas near the air inlet or outlet. As can be seen from Figure 5-3.3 particles streaming through the air vents must experience at least

three collisions before reaching the surface. This leaves little, if any, room for the ray effect. In addition, upward and downward biased quadratures with 420 and 400 directions are used to reduce the possibility of this effect when calculating dose rates on the front and rear surfaces of the AHSM (or Transfer Cask).

Finally, applying small size meshes as along AA' and plotting dose rates would reveal any ray effects. Two examples of dose rate plots are shown in Figures 5-3.8 and 5-3.9 below. The dose rates in these figures show very smooth behavior; no erratic changes, spikes or jumps are observed even in front of the air vents. Any changes are strongly correlated with material type change, geometry change or both.

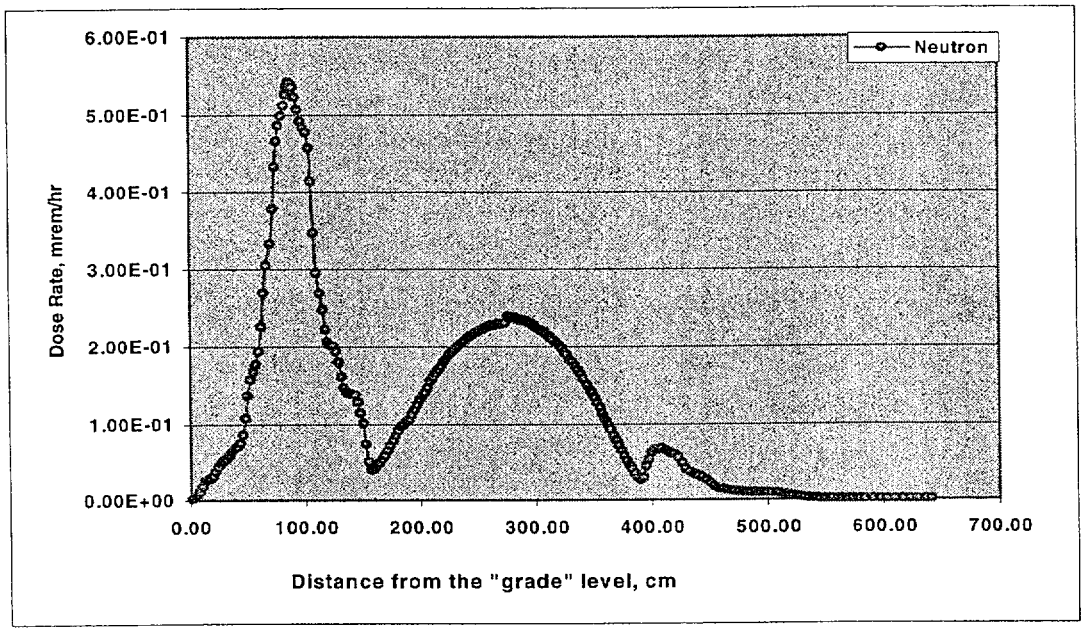

Figure 5-3.8 - Neutron Dose Rates on AHSM Front Surface

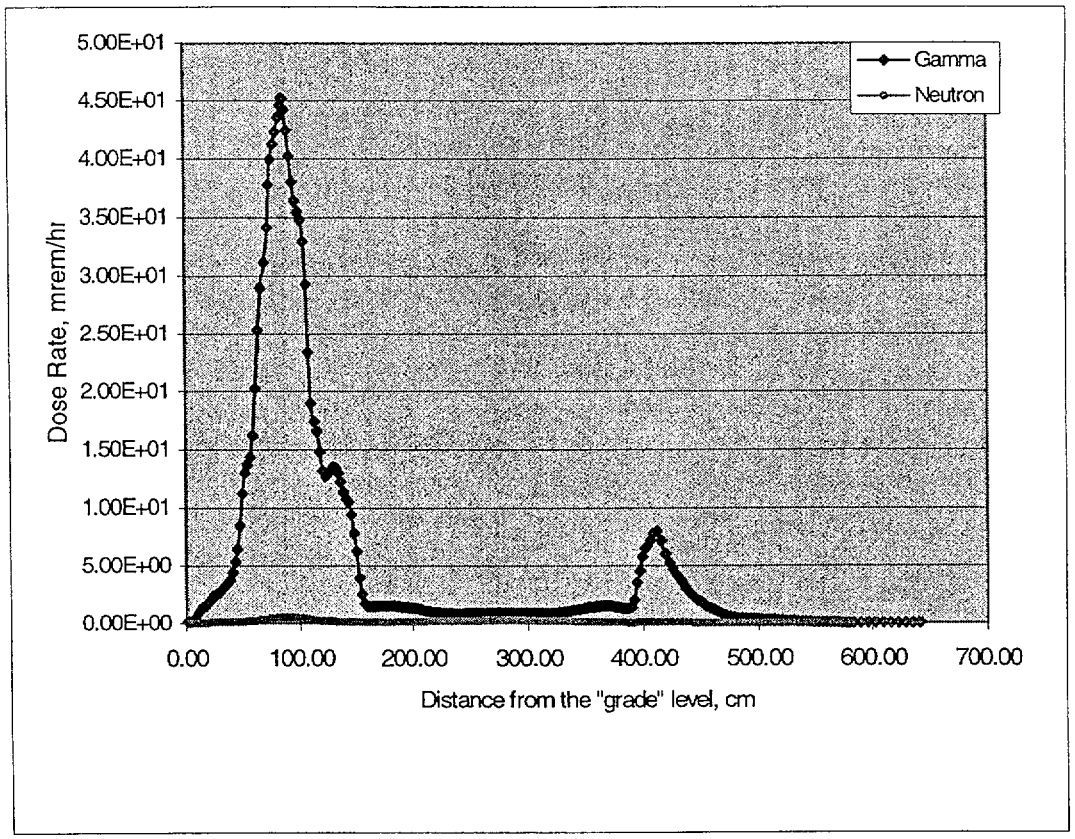

Figure 5-3.9 - Neutron and Gamma Dose Rates on AHSM Front Surface

The 276 cm distance on the above Figures corresponds to the AHSM door center. Dose rates below this point are calculated with the "floor" model, dose rates above this point are obtained with the "roof" model. As can be seen in the figures above, the models are in a very good agreement at the center of the door.

4&5. Some aspects of the theoretical foundation of the discrete-ordinate method are provided in SAR Reference 5.2. Mathematical and physical considerations for simplifications used to solve the transport equation written in the finite difference form are also provided in this reference. The version of DORT provided in the CCC 650 code package is a simple replica of that in Reference 5.2. DORT distributed with the CCC 650 code package has enhanced capabilities related to data storage and manipulation (for example DORT in Reference 5.2 limits fast memory objective to 1Mb but the parameter used to describe this variable is present in both CCC packages).

Table 5-3.1 and Table 5-3.2 are macroscopic cross sections of neutron and gamma interactions in some materials used. The tables provide guidance for choosing the size of finite meshes. Because most of the intensity of a gamma source is concentrated between 1 and 2 MeV the mesh size of 3.0 cm (approximately half a mean free path) in the fuel region is appropriate.

Table 5-3.1. Neutron Macroscopic Cross Sections in Different Materials

Energy		Concrete		Air		SS-304		Lead Plug		In-core Region	
Mev	Gr. #	x-sect., cm^{-1}	mfp., cm	x-sect., cm^{-1}	mfp., cm	x-sect., cm^{-1}	mfp., cm	x-sect., cm^{-1}	mfp., cm	x-sect., cm^{-1}	mfp., cm
4.17E-07	22	0.554621	1.80303	0.000453	2206.31	1.11696	0.895287	0.367537	2.72081	2.7526	0.3633
1.12E-06	21	0.374645	2.66919	0.000406	2462.17	0.955357	1.04673	0.367669	2.71984	1.2114	0.8255
3.06E-06	20	0.37275	2.68276	0.000401	2494.44	0.936653	1.06763	0.371987	2.68827	1.1405	0.8768
1.07E-05	19	0.371236	2.6937	0.000397	2517.07	0.924401	1.08178	0.369317	2.7077	1.2288	0.8138
2.90E-05	18	0.370142	2.70167	0.000394	2537.76	0.917098	1.0904	0.369152	2.70891	1.2133	0.8242
1.01E-04	17	0.369124	2.70912	0.000391	2560.14	0.912799	1.09553	0.369152	2.70891	1.2554	0.7965
5.83E-04	16	0.367333	2.72233	0.000375	2669.28	0.888237	1.12583	0.368789	2.71158	1.1403	0.8770
3.33E-03	15	0.397722	2.51432	0.000345	2902.66	0.770032	1.29865	0.365856	2.73332	1.0483	0.9539
0.111	14	0.340036	2.94087	0.000264	3785.89	0.791259	1.26381	0.353529	2.82862	0.9198	1.0871
0.55	13	0.351613	2.84404	0.000163	6146.13	0.317619	3.14843	0.246023	4.06466	0.5449	1.8352
1.11	12	0.273412	3.65748	0.000101	9913.16	0.240246	4.1624	0.190304	5.25475	0.3539	2.8257
1.83	11	0.202515	4.93791	9.78E-05	10224.4	0.247636	4.03819	0.176293	5.67237	0.2661	3.7575
2.35	10	0.161852	6.17848	7.20E-05	13889.1	0.278292	3.59335	0.192806	5.18656	0.2139	4.6744
2.46	9	0.104616	9.55877	5.57E-05	17962.5	0.290527	3.44202	0.214556	4.66079	0.1754	5.7005
3.01	8	0.129925	7.69675	6.22E-05	16085.4	0.297668	3.35945	0.23338	4.28486	0.1875	5.3321
4.06	7	0.180413	5.54284	8.53E-05	11723.6	0.302938	3.30101	0.249623	4.00604	0.2155	4.6411
4.96	6	0.13817	7.23746	7.31E-05	13686	0.318535	3.13937	0.248245	4.02828	0.1755	5.6992
6.36	5	0.117598	8.50355	6.23E-05	16047.4	0.315963	3.16493	0.230852	4.33178	0.1541	6.4902
8.18	4	0.102732	9.73407	5.80E-05	17245.5	0.304386	3.2853	0.191827	5.21303	0.1351	7.4004
10	3	0.106341	9.40371	5.71E-05	17516.6	0.278948	3.5849	0.164368	6.08391	0.1261	7.9324
12.2	2	0.112431	8.89434	6.44E-05	15516.5	0.252216	3.96486	0.162463	6.15525	0.1228	8.1440
15	1	0.117272	8.52718	7.14E-05	13997.2	0.225212	4.44026	0.170746	5.85665	0.1177	8.4942

The neutron cross section sets shown here are for the case of DSC filled with water. The values will decrease (mfp increases) in dry cask.

Table 5-3.2. Gamma Macroscopic Cross Sections in Different Materials

Energy		Concrete		Air		SS-304		Lead Plug		In-core Region	
Mev	Gr. #	x-sect., cm^{-1}	mfp., cm	x-sect., cm^{-1}	mfp., cm	x-sect., cm^{-1}	mfp., cm	x-sect., cm^{-1}	mfp., cm	x-sect., cm^{-1}	mfp., cm
0.05	40	7.56069	0.132263	0.000637	1569.81	178.309	0.005608	545.092	0.001835	89.5280	0.0112
0.1	39	0.515942	1.9382	0.000179	5587.09	5.90219	0.169429	46.968	0.021291	7.4643	0.1340
0.2	38	0.325435	3.07281	0.000147	6821.75	1.56637	0.638419	25.7286	0.038867	3.8832	0.2575
0.3	37	0.26439	3.78229	0.000124	8072.07	0.948611	1.05417	6.71593	0.1489	1.3835	0.7228
0.4	36	0.2319	4.3122	0.000109	9142.61	0.781874	1.27898	3.21073	0.311456	0.7235	1.3821
0.6	35	0.200828	4.97939	9.50E-05	10530.2	0.659843	1.51551	1.76231	0.567437	0.4370	2.2881
0.8	34	0.173034	5.77921	8.19E-05	12208.3	0.562068	1.77914	1.11088	0.900187	0.2987	3.3474
1	33	0.153789	6.50242	7.28E-05	13730.8	0.49753	2.00993	0.851357	1.1746	0.2388	4.1882
1.33	32	0.135542	7.37779	6.42E-05	15576.3	0.437638	2.28499	0.68247	1.46527	0.1964	5.0913
1.66	31	0.119206	8.38884	5.64E-05	17725.3	0.385695	2.59272	0.573669	1.74317	0.1666	6.0034
2	30	0.107384	9.31237	5.07E-05	19725.7	0.35026	2.85502	0.521922	1.916	0.1500	6.6652
2.5	29	0.096597	10.3523	4.54E-05	22021	0.319466	3.13022	0.487841	2.04985	0.1375	7.2750
3	28	0.087238	11.463	4.07E-05	24540.8	0.294475	3.39587	0.470141	2.12702	0.1286	7.7753
4	27	0.077705	12.8692	3.59E-05	27860.8	0.271149	3.68801	0.46612	2.14537	0.1218	8.2082
5	26	0.06926	14.4384	3.15E-05	31769.5	0.253002	3.95254	0.471822	2.11944	0.1173	8.5239
6.5	25	0.06256	15.9846	2.79E-05	35861.8	0.240896	4.15117	0.482897	2.07083	0.1147	8.7147
8	24	0.057344	17.4387	2.50E-05	40002.7	0.233465	4.2833	0.50142	1.99434	0.1142	8.7602
10	23	0.05402	18.5116	2.29E-05	43573.6	0.233505	4.28256	0.532238	1.87886	0.1166	8.5770

The gamma and cross section sets shown here are for the case of DSC filled with water. The values will decrease (mfp increases) in dry cask.

A 1D ANISN run was prepared to evaluate the transport of gamma radiation through a concrete cylinder to assess spectral distribution of the dose rate. The thickness of the shell is equal to the thickness of the AHSM roof slab. Spectral distributions of gamma and neutron dose rate within and on the outer surface of the shell are shown in Figures 5.3-10 and 5.3-11 below.

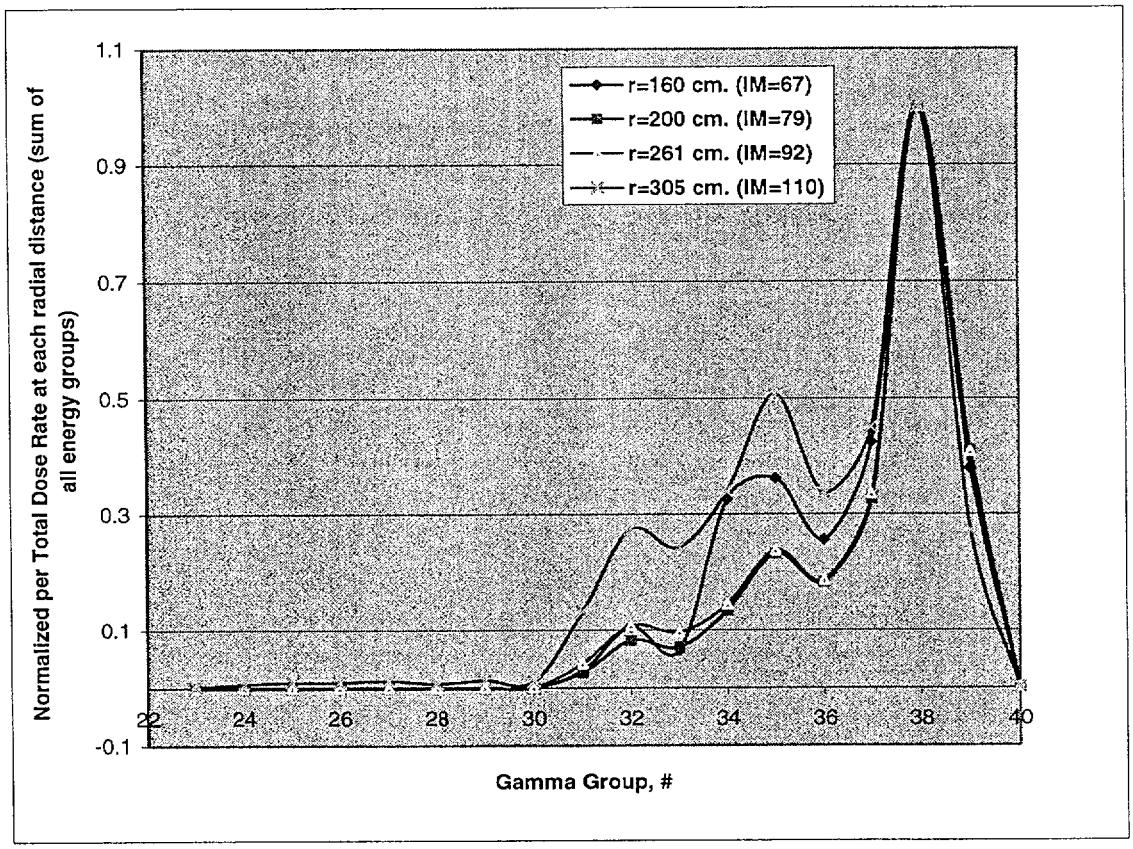

Figure 5-3.10 - Normalized Gamma Dose Rates at Different "IM" Layers in ANISN AHSM Model (Roof Block Starts at r=98 cm and ends at r~300 cm)

As can be seen from Figure 5-3.10, most of the gamma dose rate on the AHSM roof is distributed between groups 32-39. The photon mean free path in concrete is between ~7.4 and 1.9 cm. for these energy groups.

There are two inputs for the "roof" and "floor" AHSM models to calculate the dose rate on the front and rear AHSM surfaces. To calculate dose rates on the front, finer meshes are used in the regions where the front door and 24PT1-DSC bottom shield plugs and plates are located while a mesh size on the order of one mfp is used within an AHSM rear wall. The axial mesh size in the 24PT1-DSC shield plugs and plates is 0.25-0.7 cm. (a few nodes have mesh sizes of between 0.7 and 1.0 cm.). The AHSM door axial mesh is 0.3-1.0 cm. (a few nodes have mesh sizes of 1.16 cm.). A similar approach is used when the dose rate is calculated in the rear parts of the AHSM. Finer meshes are used within rear regions of the AHSM and coarser meshes are used in regions near the front of the AHSM . The mesh size in the radial direction is about 2.33 cm. in both cases.

Special runs are performed to calculate dose rates on the roof. A mesh size between 1.00 and 2.33 cm. is employed in the radial direction in these runs.
The ANISN run shows that spectral distribution of neutron dose on the roof of the AHSM is mostly concentrated within the last, 22-nd, group. The spectral distribution of neutron dose rates on the AHSM roof is shown in Figure 5-3.11 below.

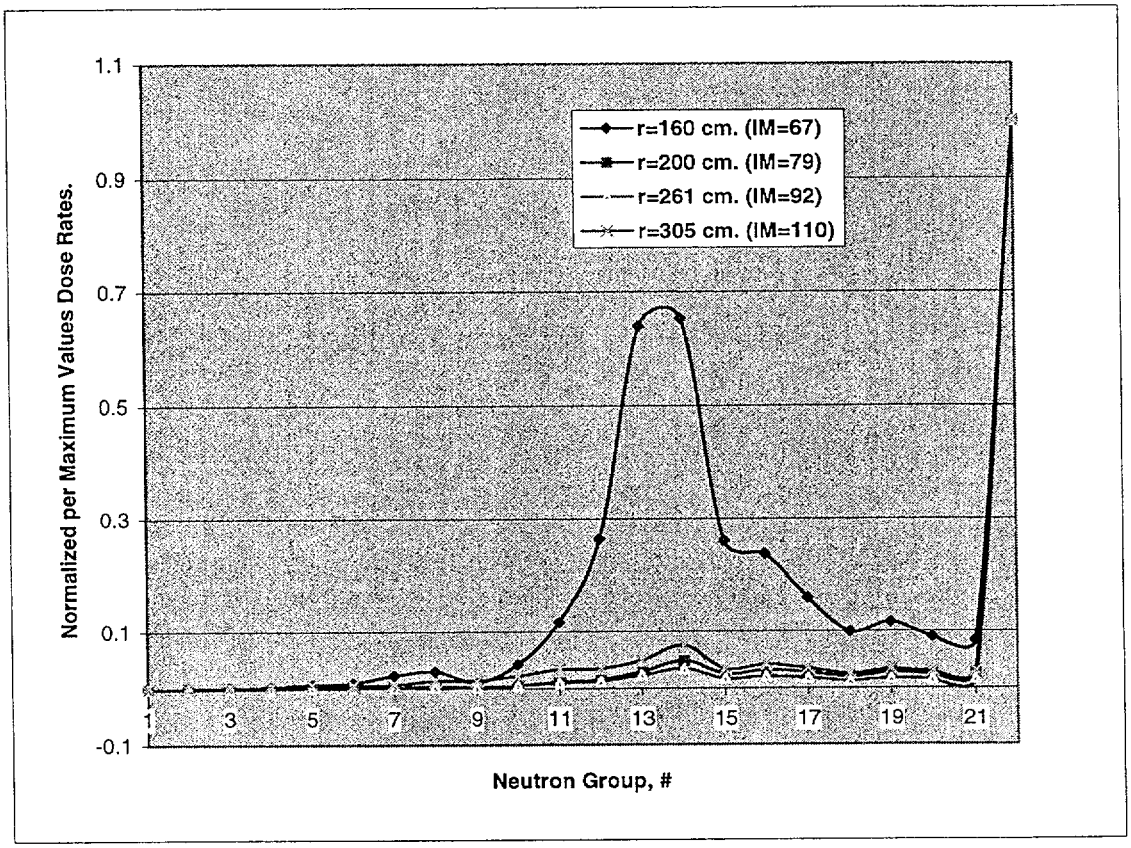

Note: The peak for r = 160 cm is associated with the source term spectrum which is attenuated as neutrons are thermalized for larger distance r into the roof

Figure 5-3.11 - Normalized Neutron Dose Rates at Different "IM" Layers in ANISN AHSM Model (Roof Block Starts at r=98 cm. and ends at ~300 cm.)

As can be seen from the discussion and analysis of Figures 5-3.10 and 5-3.11 and Tables 5-3.1 and 5-3.2; one mean free path or less finite mesh size is used in the DORT models. In most cases such spatial discretization along with fine angular discretization is sufficient. Upward and downward biased quadrature sets with 420 and 400 directions are used to calculate dose rates on the front and rear surfaces of the AHSM. Symmetric quadrature with mm=320 is used to calculate dose rates on the roof. The directional dependence of scattering cross sections is approximated with Legandre polynomials of the third order.

Finally, even finer spatial mesh sizes were used in several trial runs. No change in calculated dose rate values were observed. To keep the duration of computer runs within a manageable time frame the discretization scheme described earlier is used.

6&7. See responses to 1 through 5 above.

Question 5-4

Submit reference 5.7, which is used to describe the "Normalized Conservative Burn-up Shape on WE 14 x 14 Fuel Assembly" shown in Table 5.4-1. This information is required by the staff to assess compliance with 72.236(d).

Response to Question 5-4

Attachment 5 provides a copy of Reference 5.7 of the SAR, as requested. Reference 5.7 in SAR Section 5.5.1 has been revised to identify the associated ORNL document number.

Question 5-5

Provide concise figures which describe the DORT shielding model used. The figures should show clear descriptions of materials and thicknesses including boundaries and should contain dimensions and thickness that relate the model Figures (5.4-1 through 5.4-7) to the drawings shown in Section 1. The figures should also clarify what the letters and numbers (including bold or not bold fonts) shown in the model figures (5.4-1 through 5.4-7) physically mean. Further, the figures should show where dose rate measurements are taken and where and how the material "fluxdosium" is located. The figures should also address generic statements made in the SAR when addressing questions 5-2, 5-3, and 5-6 through 5-10 and should provide clear and concise comparison capabilities between the design basis drawings in Section 1 and the model figures 5.4-1 through 5.4-7.

The staff cannot determine the adequacy of the model based on Figures 5.4-1 through 5.4-7 alone. This information is required by the staff to assess compliance with 72.24, 72.236(b) and 72.236(d).

Response to Question 5-5

Figures 5-3.4 through 5-3.6, of the RAI Question 5-3 response above, provide detailed descriptions of the DORT AHSM models used. A Proprietary version of these figures along with Figures 5-5.1 and 5-5.2 have been incorporated into the SAR as Figures 5.4-8 through 5.4-12 to provide a simplified depiction of the shielding analysis models.

Figure 5-5.1 provides a description of the DORT OS-197 transfer cask model used.

SAR Figures 5.4-1 through 5.4-7 are the DORT printouts of the geometry models used. The number of lines and the number of symbols in a line correspond to the number of fine meshes in axial and radial directions. Each symbol is assigned a number which

represents the material comprising a finite cell. The materials associated with the symbols used in SAR Figures 5.4-1 through 5.4-7 are provided below:

SAR Figures 5.4-1 through 5.4-3 (AHSM models):

Fluxdosium – 1
Stainless Steel 304 – 2
Carbon Steel – 3
Concrete – 4
Air – .
Front Concrete – 6
Roof Concrete – 7
Inside Concrete – 8
Rear Concrete – 9
Inner Rear Concrete – a
Outer Rear Concrete – b
Bottom Nozzle – c
In-core – d
Plenum – e
Top Nozzle – f
Rear shield wall concrete – g

The SAR has been revised to add the appropriate note to Figures 5.4-1 through 5.4-3.

SAR Figures 5.4-4 through 5.4-7 (OS-197 transfer cask):

Fluxodium – 1
Stainless Steel 304 – 2
Carbon Steel – 3
Lead – 4
Air - .
Water - ,
Bottom Nozzle – 7
In-Core – 8
Plenum – 9
Top Nozzle – a
BISCO NS-3 - b

The above notes are included in Figure 5.4-4 for the cask models.

Notes explaining the meaning of bold face symbols and figures are provided at the bottom of SAR Figure 5.4-1 through Figure 5.4-4.

Table 5-5.1 lists details and associated materials used in the shielding analysis. Since the radiation shielding property of different types of steel are identical we assumed that there are two types of steel: carbon and stainless steel (SS).

Table 5-5.1 - DCS/TC Hardware Parts and Materials Nomenclature

Item #	Item Name	Material
1	1" THK. TC Bottom Cover Plate	Carbon Steel
2	Inner and Outer Shell Assembly	SS
3	¾" THK. Neutron Shield Plate	SS
4	0.59" THK. Carbon Steel Shield Plate	Carbon Steel
5	1.88" THK. NS3 Shield Plate	NS3
6	2" THK. TC Bottom End Plate	Carbon Steel
7	TC Bottom Support Ring	SS
8	DSC 1.38" THK. Grapple Ring	Carbon Steel
9	DSC Grapple Support Ring	Carbon Steel
10	½" THK Neutron Shield Panel Support Ring	SS
11	3/16" THK. Neutron Shield Panel	SS
12	Neutron Shielding Material	Water
13	Structural TC Shell, 1 ½" THK. Thickened to 2" after 341.25 cm.	Carbon Steel
14	3.54" THK. Lead Gamma Shield	Lead
15	½" THK. Inner Liner Plate	Carbon Steel
16	¼" THK. Plate for Top Cover	SS
17	2" THK. Neutron Shield Plate (Part of TC Top Cover Plate)	NS3
18	¼" THK. Plate for TC Top Cover	SS
19	3" THK. TC Top Cover Plate	Carbon Steel
20	TC Top Support Ring	SS
21	1.85" THK. Outer Bottom Cover Plate	Carbon Steel
22	6.12" THK. Bottom Shield Plug	SS
23	¾" THK. Inner Bottom Cover Plate	Carbon Steel
24	1.38" THK. Outer Top Cover Plate	Carbon Steel
25	1.14" THK. Inner Top Cover Plate	SS
26	7.62" THK. Top Shield Plug	SS
27	Support Ring	Carbon Steel
28	DSC Spacer Disk #25 and #26	Carbon Steel
29	DSC Spacer Disk # 24	Carbon Steel

The AHSM concrete sections contain various layers of rebar within surface layers of the AHSM. The densities of concrete elements in the 4" thick layer, where the rebar is smeared, are recalculated. The mean free path difference for photons is between ~0.01-0.1 cm. in the different types of concrete. The concrete layers with different densities are shown in Figure 5-5.2.

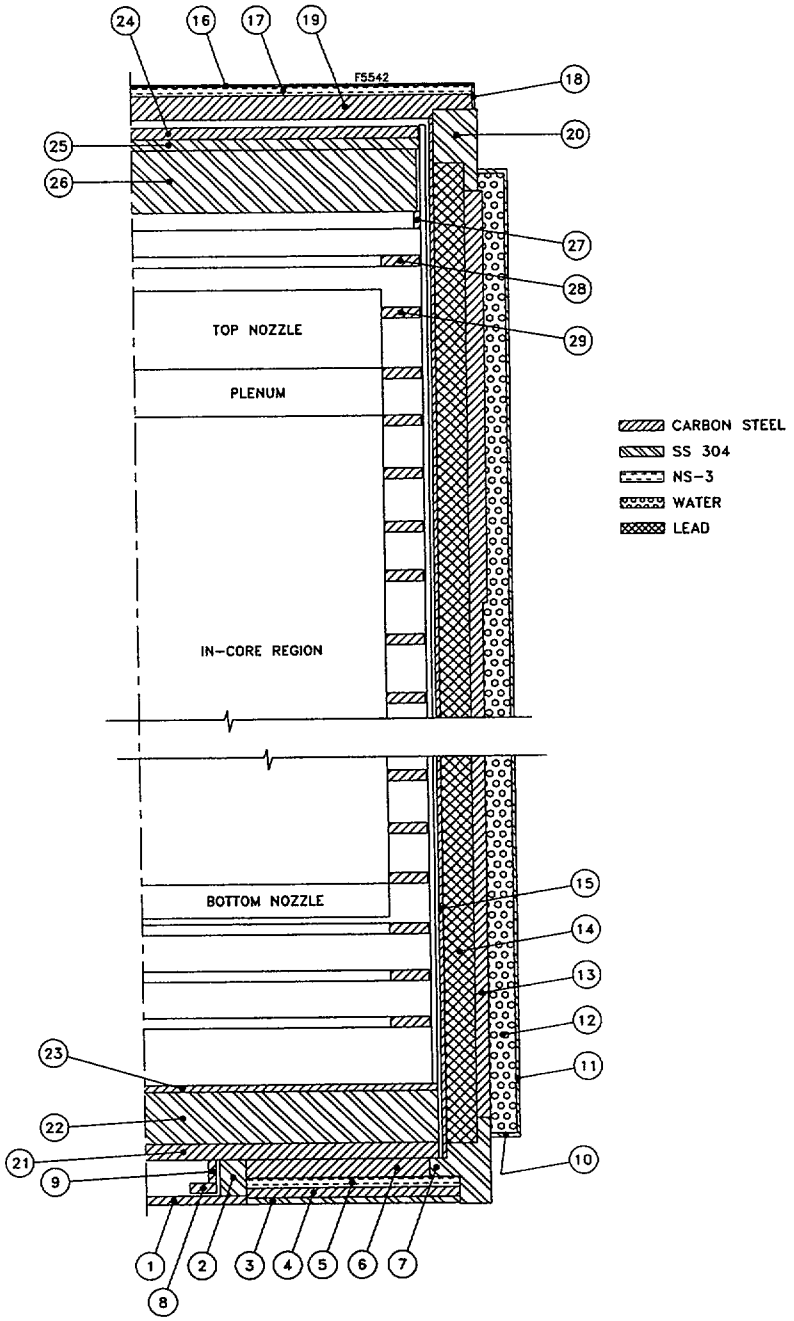

Figure 5-5.1 - 24PT1-DSC inside of Transfer Cask at Transfer Storage Stage
(See Table 5-5.1 for a Description of the item numbers identified above)

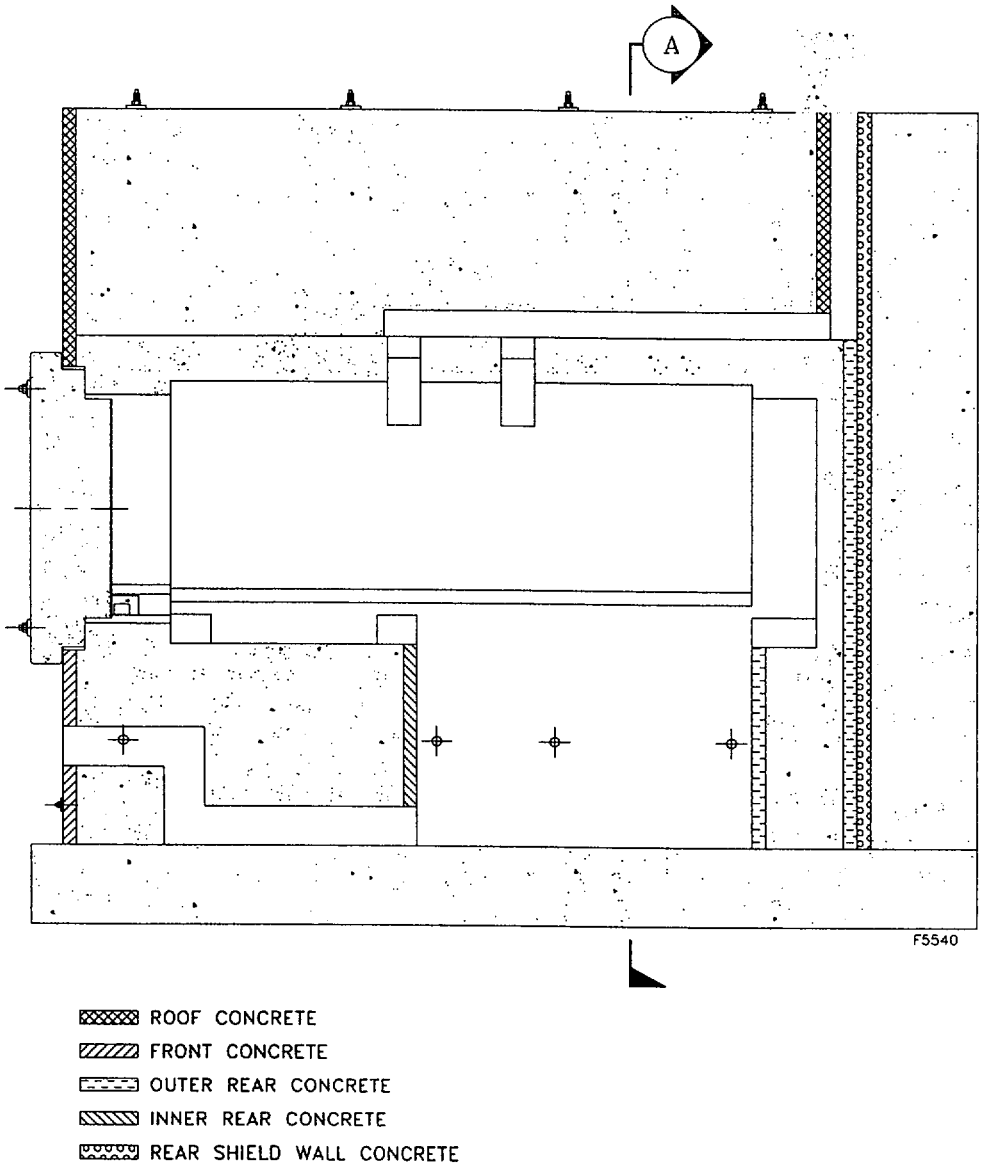

Figure 5-5.2 - AHSM Cross Section View in Vertical Elevation

The material "fluxdosium", used in the calculation of dose rates, is a fictitious material. DORT provides a general formula for the calculation of energy dependent reaction rates. This formula is:

$$A_{i,j} = t \times d_{i,j} \times C_{i,j}^{r,s} \times \sum_{g} \Phi_{i,j}^{g} \times \sigma_{r,s}^{g} \qquad \text{Equation (1)}$$

where:

i,j	- mesh cell index
g	-energy group number
r	-material number
s	-cross section table position number
t	-arbitrary multiplier
d	-density factor if used, if not used it is set equal to 1
σ	-cross section
Φ	-Flux
C	-the number density of the material |r| in cell *i,j*

The parameters for the equation above are described in a so called "activity table". Arrays 25$$, 26$$ and 27** are used to specify the table as following

Array	25$$	26$$	27**
Parameter name	ICMAT	ICPOS	ACMUL
Corresponding Factor in Equation (1)	*r*	*s*	*t*

ICMAT	-material to be used in activity calculation
ICPOS	-cross section table position for activity
ACMUL	-activity multiplier

If we are interested in dose rates we need to replace σ in the equation above with flux-to-dose conversion factors and set *t, d* and *C* to 1. If we use r = -1, per the DORT manual if $r<0$ then $C=1$. Then equation (1) can be written as

$$A_{i,j} = \sum_{g} \Phi_{i,j}^{g} \times \sigma_{r,s}^{g} \qquad \text{Equation (2)}$$

DORT calculates fluxes in each space cell. As can be seen from Equation (2), in order to calculate (or more correctly speaking to output) a reaction rate for material |r| in a space cell i,j one needs to know group flux $\Phi_{i,j}^{g}$. In order to calculate the group flux the materials filling each cell and their groupwise macroscopic cross sections are required. If one is interested in a reaction rate of material |r| knowledge of that material's cross sections is required but material |r| itself need not to be physically present in the cell i,j..

In order to obtain an activity value equal to the dose rate, the cross section in Equation (2) should be replaced with flux-to-dose conversion factors. To accomplish this with GIP, a fictitious material "Fx77" is created. It has a "density" equal to one as can be found from array 12** of the GIP inputs. "Microscopic cross sections" of "Fx77" are equal to ANSI

Standard 6.1.1 flux-to dose conversion factors. These factors for 22 neutron and 18 gamma energy groups are input in array 14** of the GIP inputs. Array 11$$ of the GIP input files indicates that "Fluxdosium" consists of "Fx77". GIP prepares "macroscopic cross section" table for "Fluxdosium" which in fact are groupwise flux to dose conversion factors for that particular "element". So if dose rate is needed in any spatial location one should use " Fluxdosium" for the activity calculation. Setting array 25$$ in a DORT input as

```
25$$ f-1
```

means that material 1 (which in our case is "fluxdosium") will be used in activity calculations in every spatial cell i,j.

Question 5-6

Justify the statement in Section 5.3.1.1 that overestimating the cross-sectional area of the air vents always leads to conservative streaming estimates. Include discussion of how overestimation of these areas is balanced by the limitations of the discrete ordinates method described in question 5-3.

This information is required by the staff to assess compliance with 72.24, 72.236(b) and 72.236(d).

Response to Question 5-6

The AHSM inlet is a square with dimensions of 5.5'×1'. It is not possible to model such a shape in the "floor" model. To account for the streaming effect through the vent, the air inlet is modeled as shown with dotted concentric circles in Figure 5-6.1, below. The difference between radii is equal to 1', the height of the inlet. Because of the huge amount of concrete in the front of the AHSM the dose rate will have its maximum at the center of the inlet and is substantially lower outside the inlet.

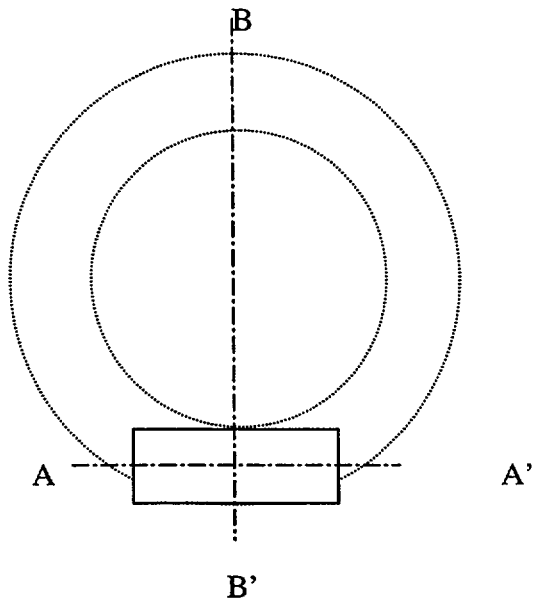

Figure 5-6.1 - Portion of AHSM Geometry Containing Air Vent Inlet.

The width of the inlet is significantly larger than its height. Therefore, the dose rate values in front of the vent along line BB' can be estimated with the "roof" model. The deficiency of the model is that it does not provide a distribution along the horizontal dimension, along line AA'. It inherently assumes that the distribution is not dependent on the horizontal coordinate of the point within the inlet or on the front of the module. Looking at Figures 5-3.8 and 5-3.9 of the response to RAI Question 5-3, it is clear that the dose rate in front of the inlet is caused largely by streaming through the vent. Therefore, based on the geometry of the model discussed above, the streaming would be overestimated. This is the basis for the statement in Section 5.3.1.1 that prompted this question. The assumption that the dose rate is not dependent on the horizontal coordinate is extremely conservative. To reduce this conservatism, a Gaussian function is used to reshape the dose rate distribution on the front and roof of the AHSM in the horizontal dimension. Parameters of the Gaussian function are extracted with a regression analysis of the dose rate distribution function on the AHSM roof. This distribution passes through the same point E in Figure 5-3.3 of the response to RAI Question 5-3. It is obtained from the "X-Z" model and approximated with a Gaussian function. The shape function preserves dose rate values along CC' shown on Figure 5-3.3 but still gives conservative values in the directions perpendicular to CC'. This conservatism is transferred to the final estimate of the average dose rate.

No changes to the SAR have been made with respect to this RAI Question response.

Question 5-7

Clarify the statement in Section 5.3.1.1 that "since the AHSM possesses limited azimuthal cylidrical symmetries, all approximations result in an overestimate of the dose rates on the AHSM surfaces." Justify this statement in relation to question 5-3.

This information is required by the staff to assess compliance with 72.24, 72.236(b) and 72.236(d).

Response to Question 5-7

See response to RAI Question 5-3, part 1, above.

Question 5-8

Clarify the statement in Section 5.3.1.3 of the SAR that "The non-symmetric regions such as the 24 Neutron Shield Panel support angles, the 4 trunnions, relief valves, clevises, eyebolts, etc are modeled such that the dose rate on the surfaces of the cask is overestimated." Describe how these devices are modeled and why resultant dose rates are overestimated.

This information is required by the staff to assess compliance with 72.24, 72.236(b) and 72.236(d).

Response to Question 5-8

Additional discussion has been added to Section 5.3.1.3 of the SAR to describe how the non-symmetric features of the OS-197 cask are modeled and why the resultant dose rates are overestimated.

With the exception of the 24 neutron shield support angles and the trunnions the balance of the items listed as non-symmetric regions are local features that increase the amount of shielding in a small area without replacing any of the shielding material which is included in the model.

The 24 neutron shield support angles provide support for the skin, which contains the water for the neutron shield. The steel that forms these angles is not smeared with the water in the neutron shield; rather it is modeled as water. This is conservative for gamma radiation because water is less than one-seventh the density of steel. The density of the neutron shield water used in the cask DORT models is 0.96 g/cm^3. The resultant reduction in the hydrogen density as compared to full density water results in the water attenuating the neutron dose rate at about the same rate as that for full density steel.
The trunnions penetrate the neutron shield, which locally changes the shielding configuration of the neutron shield. The trunnions are thick steel structures filled with

NS-3 neutron shielding material. These structures provide much more gamma and neutron shielding than the water that they replace

Question 5-9

Clarify the statement in Section 5.3.2 that "...when the source is smeared into a cylinder, the source is moved closer to the surface of the source region. This results in less self-shielding of the source in the model as compared to the actual geometry, which results in an overestimate of the surface dose rates."

Provide a sensitivity analysis that compares the tradeoff between moving the source out closer to the surface of the DSC and the increased material density of the smeared source, which provides more self-shielding compared to helium. This information is required by the staff to assess compliance with 72.24, 72.236(b) and 72.236(d).

Response to Question 5-9

As mentioned in the answer to RAI Question 5-3, item 2 an equivalent cylinder is used to model the non-uniform material distributions associated with fuel assembly components and 24PT1-DSC spacer discs and guide sleeves. The size of the equivalent cylinder is calculated by determining the volume occupied and enclosed by the 24 fuel assemblies, including the guide sleeves, absorber sheets, and oversleeves, in the loaded 24PT1-DSC. The cross sectional area considered for this calculation is shown in Figure 5-9.1 in the lower left quadrant bounded by the outer boundary of the fuel assemblies.

The cylinder with the equivalent radius (r_{eq}), when compared to Figure 5-9.1 indicates that the equivalent cylinder would encompass substantial void regions. Smearing all encompassed elements inside of the entire volume of the cylinder would reduce the density of any element.

As for source points, they are localized within the squares representing the fuel assemblies shown on Figure 5-9.1. When the source points are smeared throughout the cylinder, most of them will move closer to the surface of the cylindrical region.

Reduced material densities and more source points closer to the surface of the equivalent cylinder will result in less self shielding and an overestimate of the surface dose rates. Therefore, a sensitivity analysis comparing the tradeoff between the source location and the shielding material density is not considered necessary.

No changes to the SAR have been made with respect to this RAI Question response.

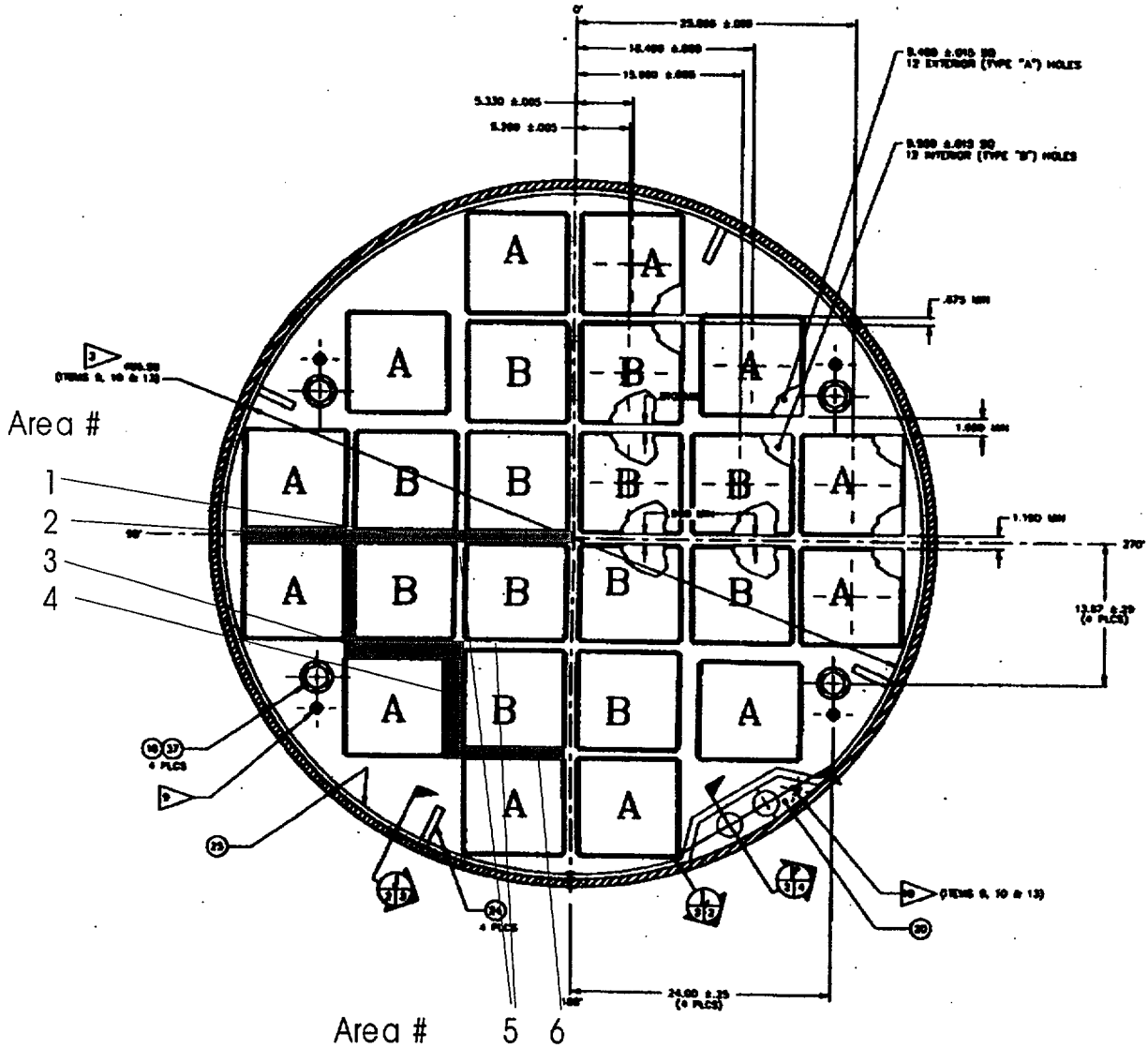

Figure 5-9.1 - Cross section view of 24PT1-DSC loaded with 24 FAs.

Question 5-10

Clarify the statement made in Section 5.3.2 that "For dose rate evaluations made on surfaces that are perpendicular to the spacer disks, credit is taken for the presence of the carbon steel spacer discs..." The staff assumes that the words parallel and perpendicular should be switched. In addition, clarify the statement "For the AHSM evaluation, no credit for the shielding properties of the spacer discs, fuel grid spacers and hold-down springs."

Provide a table which lists the various configurations of the Advanced NUHOMS® System (wet loading, dry transfer, AHSM evaluation) and the type of dose rate evaluation (axial or radial) and the amount of credit taken for the presence of the carbon steel spacer discs, fuel grid spacers, and hold down springs. Relate this table to the figures submitted in response to question 5-5.

This information is required by the staff to assess compliance with 72.24, 72.236(b) and 72.236(d).

Response to Question 5-10

The statement in SAR Section 5.3-2 is incorrect and TN West concurs that the words "parallel" and "perpendicular" should be switched as noted in RAI Question 5-10.

The shielding analysis is performed for two configurations. One configuration consists of the 24PT1-DSC inside the OS-197 Transfer Cask (TC).

There are four stages associated with handling while the 24PT1-DSC is located in the transfer cask. These stages are: Decontamination, Wet Welding, Dry Welding and Transfer/Storage. The definition of these stages is:

1) Cask decontamination. The 24PT1-DSC and the TC are assumed to be completely filled with water, including the region between them referred to as the "cask/DSC annulus." The 24PT1-DSC inner cover plate is assumed to be in place and the temporary shielding has not yet been installed.
2) Wet welding and 24PT1-DSC draining. The water level in the 24PT1-DSC cavity is assumed to be lowered four inches below the bottom of the top shield plug. Temporary shielding consisting of three inches of NS3 and one inch of steel is assumed to cover the 24PT1-DSC top shield plug. The annulus is assumed to remain completely filled with water.
3) Dry welding. The 24PT1-DSC cavity is assumed to be completely dry, the 24PT1-DSC top cover plate has been installed, and temporary shielding consisting of three inches of NS3 and one inch of steel covers the 24PT1-DSC. The annulus is assumed to remain completely filled with water.
4) Transfer-Storage. The 24PT1-DSC cavity and the cask/DSC are completely dry. The 24PT1-DSC inner and outer top cover plates are installed. The top end of the TC is sealed by a 3" thick carbon steel cover plate and a 2" thick NS3 shield. A ¼" thick stainless steel plate covers the NS3 shield.

Two sets of material densities are used at the four stages defined above. These are designated as "dry radial" and "wet axial" densities. For dose rate evaluations made for surfaces that are parallel to the spacer disks (surfaces that are perpendicular to the 24PT1-DSC axial centerline), it is permissible to take credit for the presence of the carbon steel spacer disks and the fuel grid spacers and hold down springs by smearing them in the 24PT1-DSC material regions. Only a part of the spacer disks inside of the equivalent cylinder, defined in the answer to RAI Question 5-9, is smeared. For the purpose of this evaluation these number densities are identified as "axial." For dose rate evaluations made for surfaces that are perpendicular to the spacer disks (parallel to the 24PT1-DSC axial centerline), a considerable fraction of the radiation will travel between the spacer disks, without being attenuated by the spacer disks. Therefore, the spacer disks and fuel grid spacers and hold down springs are not included in these number densities. For the purpose of this evaluation these number densities are identified as "radial." Because the 24PT1-DSC is filled with water at Decontamination and Wet Welding and drained at Dry Welding and Transfer Storage, material densities for these stages are classified as "wet" and "dry", respectively.

The second configuration analyzed is the 24PT1-DSC inside of the AHSM. Dry radial densities are employed in this configuration. Spacer disks are not included in this configuration at all, neither inside nor outside of the "equivalent" cylinder. This provides additional conservatism.

A summary of the configurations analyzed and the credit taken for carbon steel spacer discs is provided below:

Configuration	**Dose Rate Evaluation**	
	Radial	**Axial**
24PT1-DSC in Cask[1]	Cask Side[2]	Cask Top and Bottom Ends[3]
24PT1-DSC in AHSM	AHSM Top, Bottom and Sides[2]	AHSM Front and Back[2]

1 – Cask decontamination, Wet welding and 24PT1-DSC draining, Dry welding and Transfer-Storage configurations
2 – No credit taken for carbon steel spacer discs
3 – Credit taken for carbon steel spacer discs

A revision to SAR Section 5.3.2 to clarify the discussion regarding orientations in which the spacer discs are included in the material densities has been provided.

Chapter 6 Criticality

Question 6-1

Describe the calculational model used for the infinite array of casks which is found on page 6.3-2 of the SAR. Also justify in the SAR that this model is bounding for all actual storage, loading/unloading, and transfer configurations.

The model used for this scenario was not described in sufficient detail. It is not clear whether the casks are an infinite array of canisters in transfer casks or if the array consists of canisters in their typical storage configurations out of the transfer casks. This information is required for the staff to assess compliance with the nuclear criticality safety requirements specified in 10 CFR 72.124 and 72.236(c).

Response to Question 6-1

Additional discussion has been added to SAR Section 6 to demonstrate that the analyses performed are representative of an infinite array of flooded 24PT1-DSCs in flooded MP187 transfer casks. The AHSM storage configuration is bounded by this transfer cask configuration since the canister in the storage configuration is not flooded. The reactivity of the system is highly dependent on the internal moderator density, with the maximum reactivity occurring at maximum internal moderator density.

Question 6-2

Provide a reference for the transfer cask used in the criticality safety analysis in Chapter 6 of the SAR.

The specific transfer cask that was used in the criticality safety evaluation in Chapter 6 is not identified. This is required for the staff to assess compliance with 10 CFR 72.124 and 72.236(c).

Response to Question 6-2

The cask used in the criticality analyses is the MP187 transport cask (C of C 71-9255). A comparison of pertinent dimensions for the MP187 cask and the OS-197 cask has been added to Section 6 of the SAR. The differences between the two casks are shown to be minor. A comparative analysis of the 24PT1-DSC in the OS-197 transfer cask for the WE 14 X 14 SC fuel damaged fuel geometry case was performed to confirm that these differences are minor. The result of this analysis reflects a small decrease in reactivity which is approximately equal to the 1 σ uncertainty for both runs, approximately 0.0015.

Question 6-3

Justify that any other NRC licensed transfer cask is acceptable for use with the 24PT1-DSC without any consideration for criticality safety, as inferred in Section 1.2.1.3.1 of the SAR.

Section 1.2.1.3.1 of the SAR infers that any other NRC licensed transfer cask is acceptable for use with the 24PT1-DSC subject to a site specific evaluation which considers only the following cask characteristics; cavity dimensions, payload, heat load capacity, and shielding. The criticality safety analysis in Chapter 6 does not provide justification for use of other transfer casks, which may be constructed of different types and amounts of materials. This is required for the staff to assess compliance with 10 CFR 72.124 and 72.236(c).

Response to Question 6-3

SAR Section 6 has been revised to specify that the OS-197 is the only cask authorized for fuel transfer operations as discussed in the response to RAI Question 1-1. The criticality safety analysis is bounded by the results presented in the SAR for the NUHOMS®-MP187 as documented in the response to RAI Question 6-2.

Question 6-4

Resolve the discrepancy between Tables 6.1-1 and 6.4-3.

Tables 6.1-1 and 6.4-3 report different keff values for what appears to be the same case for the most limiting WE 14x14 SC fuel scenario. This is required for the staff to assess compliance with 10 CFR 72.124 and 72.236(c).

Response to Question 6-4

The discrepancy between SAR Tables 6.1-1 and 6.4-3 is a typographical error. SAR Table 6.4-3 is correct. SAR Table 6.1-1 has been revised to address a new case associated with uncertainty in fuel enrichment for UO2 fuel. This new case is discussed in the response to RAI Question 4-6.

Question 6-5

Provide the fissile material compositions used in the criticality safety analysis in Tables 6.3-2 and 6.3-3.

The fissile material compositions used in the SCALE calculational models were not provided. This is required for the staff to assess compliance with 10 CFR 72.124 and 72.236(c).

Response to Question 6-5

The as modeled fuel pellet material densities have been added to SAR Tables 6.3-2 and 6.3-3.

Question 6-6

Provide SCALE inputs for each of the following cases;

1 - the most limiting normal cases for the intact UO2 fuel, intact MOX fuel, and damaged fuel (either UO2 or MOX), and
2 - the most limiting accident cases for the intact UO2 fuel, intact MOX fuel, and damaged fuel (either UO2 or MOX).

The inputs used in the SCALE calculational models were not provided. This is required for the staff to assess compliance with 10 CFR 72.124 and 72.236(c).

Response to Question 6-6

Section 6.6.2 "KENO Input Files" has been added to the SAR. SCALE inputs are included in this section as requested.

Question 6-7

Describe in greater detail in Section 6 how the Upper Subcritical Limit (USL) was determined.

The SAR does not discuss any bias and uncertainty associated with the USL determination, nor does it discuss any uncertainty due to modeling approximations. Note that only biases that increase keff should be applied. This is required for the staff to assess compliance with 10 CFR 72.124.

Response to Question 6-7

SAR Section 6.5.1 has been revised to incorporate additional discussion of the method used for calculation of the Upper Subcritical Limit (USL). The methodology used is based on NUREG/CR-6361, USL method 1.

Question 6-8

Describe which factors were considered when choosing the experiments used to validate the computer code used for the criticality safety analysis.
The bias and uncertainty should be established using critical experiments that are applicable to the package design. Several of the experiments, such as BW1810A through E, DSN 399-1 through -4 and W3269A through C contain materials such as gadolinium,

hafnium, or cadmium which are not used in the criticality analysis computer models. Therefore, it is not clear why these experiments were used. This is required by the staff to determine the applicability of the critical experiments to the application and to assess compliance with 10 CFR 72.124.

Response to Question 6-8

The benchmark analysis performed included many experiments associated with various parameters. This set of benchmarks is considered generic and is used for application of the computer code to various system designs. Included in this set are 15 benchmarks that contain materials not present in the system analyzed for this application. The benchmarks are:

Case No.	Case designation	Enrich. (wt %)	Pitch (cm)	H2O/fuel volume	Description
31	BW1810A	2.46	1.636	1.841	UO_2-Gd_2O rods, water holes, borated H_2O
32	BW1810B	2.46	1.636	1.841	UO_2-Gd_2O rods, water holes, borated H_2O
33	BW1810C	2.46 & 4.02	1.636	1.841 & 1.532	UO_2-Gd_2O rods, water holes, borated H_2O
34	BW1810D	2.46 & 4.02	1.636	1.841 & 1.532	UO_2-Gd_2O rods, water holes, borated H_2O
35	BW1810E	2.46 & 4.02	1.636	1.841 & 1.532	UO_2-Gd_2O rods, water holes, borated H_2O
39	BW1810I	2.46	1.636	1.841	Water holes, Ag-In-Cd rods, borated H_2O
44	DSN399-1	4.74	1.6	3.807	Hafnium separator plates
45	DSN399-2	4.74	1.6	3.807	Hafnium separator plates
46	DSN399-3	4.74	1.6	3.807	Hafnium separator plates
47	DSN399-4	4.74	1.6	3.807	Hafnium separator plates
166	W3269A	5.7	1.422	1.93	Ag-In-Cd rods
167	W3269B1	3.7	1.105	1.432	Ag-In-Cd rods
168	W3269B2	3.7	1.105	1.432	Ag-In-Cd rods
169	W3269B3	3.7	1.105	1.432	Ag-In-Cd rods
170	W3269C	2.72	1.524	1.494	Ag-In-Cd rods

All other benchmarks used to develop the USL contain materials found in the analyzed system and can be used to determine bias associated with the cross section library. These experiments are presented in a revised SAR Table 6.5-1. Little to no effect was found when these 15 experiments were removed from the USL.

In addition, two parameters were added to investigate the calculational bias associated with the Boral neutron absorbing material. Boron weight percent and B-10 areal density are added to the list of parameters used to determine the calculational bias in the modeling system.

SAR Table 6.5-2 has been revised to document the changes in the USL reflecting the removal of the 15 benchmark experiments noted above and adding the Boron parameters. Correlation coefficients for the 8 parameters listed in Table 6.5-2 are included in the last row of Table 6.5-1. The limiting USLs for all 8 parameters are presented in Table 6.5-4.

Section 6.5 of the SAR has been revised to reflect these changes.

Question 6-9

Provide a table of correlation coefficients for the 6 parameters listed in table 6.5-2 and also for boron areal density.

The correlation coefficients are not given for the SCALE 4.4 validation. This is required for the staff to assess compliance with 10 CFR 72.124.

Response to Question 6-9

A linear regression correlation is calculated for each of the eight parameters listed in revised SAR Table 6.5-2 versus k_{eff}. The correlation coefficient for each parameter is provided in the last row of the revised SAR Table 6.5-1. The best correlation is observed for "separation of assemblies", with a correlation of 0.67. All other parameters show much lower correlations, which indicates that there is no real correlation for these parameters. Since there is no strong correlation for any of the data sets, the lowest possible USL-1 result is used as the USL.

Question 6-10

Discuss in Chapter 6 the failed fuel can screen mesh size and either justify that uneven draining is not credible or provide an analysis considering uneven flooding.

Uneven draining may be possible for screens with a mesh size of 350 or less because the water surface tension may be capable of supporting water. Uneven draining in the canister may be more reactive than a fully flooded cask. This is required for the staff to assess compliance with 10 CFR 72.124 and 72.236(c).

Response to Question 6-10

The screen mesh size specified in the SAR 24PT1-DSC drawing (NUH-05-4010, sheet 1, Bill of Material, Item 43), in SAR Section 1.5.2, is a 6 x 6 mesh with 0.047" wire diameter. This large mesh size will not obstruct uniform draining in the canisters. Additional discussion of this issue has been added to Section 6.3.1 of the SAR.

Question 6-11

Clarify TS 12.2.1 d. which appears to disallow storage of intact MOX assemblies.

It is not clear whether the applicant intends to limit this application to storage of one damaged MOX assembly per cask only. The TS does not clearly address storage of any intact MOX assemblies. This is required by the staff to assess compliance with 10 CFR 72.24(g), 72.26, and 72.44(c).

Response to Question 6-11

The text of SAR Section 12.2.1.d has been revised to clarify the requirements and limitations for storage of intact stainless steel clad fuel, intact mixed oxide fuel, damaged stainless steel clad fuel and damaged mixed oxide fuel.

Question 6-12

Revise TS table 12.2-2 to include the number of guide tubes and/or instrument tubes.

The SAR does not address varying the number of guide tubes and/or instrument tubes. This is required by the staff to assess compliance with 10 CFR 72.24(g), 72.26, and 72.44(c).

Response to Question 6-12

SAR Table 12.2-2 has been revised to include the number of guide tubes and/or instrument tubes per assembly.

Question 6-13

Revise Section 12.4.0 to include the basket B-10 loading and the flux trap size.

The B-10 loading and flux trap size are design parameters important to criticality safety. This is required by the staff to assess compliance with 10 CFR 72.24(g), 72.26, and 72.44(c).

Response to Question 6-13

SAR Section 12.4 has been revised to incorporate a new Section 12.4.2.3, titled "Canister Neutron Poison" which now specifies the minimum B-10 loading of 0.025 grams/cm^2. A new Section 12.4.2.4, titled "Canister Flux Trap Configuration" has also been added to specify the flux trap size by reference to the spacer disc dimensions specified in the canister drawings in SAR Section 1.5.2.

Question 6-14

Justify that the postulated failure scenarios for damaged fuel is bounding.

The criticality safety analysis in Section 6.3 of the SAR does not provide justification that the scenarios considered for failed fuel bound other possible scenarios such as missing fuel pins. This is required for the staff to assess compliance with 10 CFR 72.124 and 72.236(c).

Response to Question 6-14

Additional discussion of the damaged fuel analysis is provided in SAR Section 6.4.2 to further demonstrate that the postulated failure scenarios for damaged fuel are bounding.

Chapter 7 Confinement

Question 7-1

Justify the use of an ultrasonic test (UT) for the inner bottom cover plate to canister shell weld in lieu of a radiographic test (RT), as described in SAR section 7.1.3 and Figure 7.1-1. Provide evidence of the UT performance demonstration that was done to qualify the technique for this application, using full scale qualification samples of the same materials and geometry with imbedded cracks (not machined notches or drilled holes). Demonstrate that the sensitivity of the UT procedure meets or exceeds the sensitivity of an RT or the Code acceptance criteria for this application. Update other sections of the SAR as necessary (e.g. ASME code exceptions, and Chapter 9).

The application does not justify the use of the UT technology in an application where UT techniques are difficult and code requirements stipulate RT technology. The NRC notes that the use of ASME Section XI analytical methods and acceptance criteria has not been justified for this application. This information is needed to assure compliance with 10 CFR 72.236(j).

Response to Question 7-1

The inner bottom cover plate to canister shell is defined as a Type 2 Category C corner weld by subarticle NB-3350 and Figures NB-3351-1 and NB-4243-1 (Detail j). The examination requirements for this weld are specified in NB-5231(b) and (c). NB-5231(b) permits the use of RT or UT as approved methods for examination of the joint. NB-5231(c) adds the requirement that if the joint is RT examined, then an additional UT examination of the "...fusion zone and the parent metal beneath the attachment surface to verify freedom from lack of fusion and laminar defects". Therefore, the weld examination described in the SAR is in accordance with the ASME code requirements for a Class 1 vessel. In addition, this joint has been successfully demonstrated to meet ASME code requirements for 24PT1-DSCs fabricated for the Rancho Seco project.

Alternative joint details have also been added to the canister SAR drawing in Section 1.5.2 to provide additional flexibility in fabrication. As shown on NUH-05-4010, Sheet 4, this will permit substituting a forging for the inner bottom cover plate. This effectively moves the weld joint away from the corner to a Category B circumferential weld seam, which is examined by RT methods in accordance with NB-5221. Both joint details fully comply with ASME Section III requirements for a Class 1 vessel. The selection of the joint to be used in fabrication of a 24PT1-DSC has been left to the fabricator. For either joint, the fabricator is required to meet all ASME Section III Class 1 code requirements for the qualification, welding and examination of the joint.

Chapter 10 Radiation Protection

Question 10-1

Provide the dose contribution associated with the maximum contamination levels stated in Section 12.5.2.4 of the SAR.

This information is required for the staff to assess whether the maximum contamination levels bound, combined with the DSC source term, meet the off-site dose requirements of 10 CFR 72.104 and 10 CFR 72.106.

Response to Question 10-1

The 24PT1 DSC smearable surface contamination limits stated in Section 12.5.2.4.c have been revised to be less than 2200 dpm/100 cm^2 for beta and gamma sources, and less than 220 dpm/100 cm^2 from alpha emitting sources.

See Response to RAI Question 12-5 for the dose contribution associated with the maximum contamination levels specified in Section 12.5.2.4.c of the SAR.

Chapter 11 Accident Analysis

Question 11-1

Provide justification that inadvertently loading spent fuel assemblies, not allowed by Section 12 of the SAR, is not a credible occurrence as stated in Section 11.2.10.3 of the SAR.

NRC staff does not accept that inadvertent loading of spent fuel assemblies is not a credible event. The justification should address both the probability and consequences of loading spent fuel not allowed by Section 12 of the SAR.

This information is required by the staff to assess compliance with 72.94 and 72.236(l).

Response to Question 11-1

A review of Westinghouse 14 x 14 stainless steel clad UO2 assemblies and 14 x 14 zircalloy clad mixed oxide fuel assemblies fabricated to date has confirmed, based on current 24PT1-DSC licensing and fabrication schedules, that the inventory of all fuel assemblies of this type will meet the fuel specification requirements of Section 12 of the SAR. Therefore, inadvertent loading of a fuel assembly exceeding these requirements with respect to enrichment, burnup, decay time and decay heat is not credible.

The consequences of a potential misloading (early loading) of fuel assemblies is discussed below.

The highest burnup fuel assembly in inventory as of January 2001 has a decay heat of approximately 0.7 kW. The actual number of fuel assemblies greater than 0.581 kW in inventory is 13. Assuming these 13 assemblies are 0.7 kW each and the balance of the assemblies are 0.581 kW each and including 24 control components at 0.002 kW each, the maximum canister heat load is less than 16 kW. The analysis at 16 kW provided in Chapter 4 of the SAR indicates that vacuum drying is the only operating condition in which a specified material temperature limit is exceeded (the spacer disc temperature limit is exceeded in this case). Since this is a short term scenario and based on the conservative limits used, the misloading can not impact the 24PT1-DSC confinement boundary integrity. Section 11.2.10.2 of the SAR has been revised to address the consequences of loading spent fuel not allowed by Section 12 of the SAR, based on the above discussion.

Chapter 12 Operating Controls and Limits

The following regulatory requirements are applicable in this chapter: 10 CFR 72.11, 72.24(g), 72.26, 72.44(c), 72.104, 72.106, 72.234(a), 72.236, and Subparts C, E, F, G, H, and I. It should be noted that other regulatory requirements may be applicable to this section.

Question 12-1

Specify which transfer and/or transportation casks may be used to perform on-site transfer of the DSC-24PT and any required design criteria.

Technical Specification 12.4.3.3, does not specify transfer or transportation casks that may be used to perform on-site transfer of the DSC-24PT nor does it provide, or reference, a methodology or design criteria to be used to select casks appropriate to perform on-site transfer of the DSC-24PT.

Response to Question 12-1

SAR Sections 12.2.1.c and 12.4.3.3 have been revised to remove references to casks other than the OS-197.

Question 12-2

Provide the analysis to support the 80 degrees F AHSM limit stated in Section 12.5.2.5 of the SAR.

Section 9.1.6 of the SAR states that the heat removal capability is assured through monitoring of the AHSM concrete temperatures. Section 12.5.2.5 suggests corrective actions should be taken to avoid exceeding the concrete and cladding temperature limits if the temperature rises by more than 80 degrees F. Describe how this temperature rise was chosen. Include an explanation of how the fuel cladding temperatures are related to this rise. This information is required by the staff to assess whether the fuel cladding is protected against degradation that could lead to gross ruptures per 10 CFR 71.122(h)(1).

Response to Question 12-2

The specification of an 80 °F temperature rise in the monitored AHSM concrete temperature was chosen as the criteria for monitoring changes in concrete temperature to ensure that temperatures approaching the blocked vent condition are not reached without investigative action. An increase in concrete temperature of 175 °F is expected at the AHSM roof inner surface for a design basis (24 kW AHSM heat load) during the 40 hours allowed for a blocked vent transient. This translates to a temperature increase of approximately 100 °F at the thermocouple location (7" above the inner surface of the AHSM roof). By choosing a temperature increase that is only 80% of the expected increase; the increase in temperature will be identified as significant requiring further

investigation several hours prior to the maximum design basis temperature being reached for an AHSM design basis payload.

This limit also provides additional conservatism since the likelihood of the occurrence of the design basis ambient temperature (117 °F) at the same time as a blocked vent condition is small. The 80 °F concrete temperature rise limit would typically be measured from a long term average ambient temperature of 70 °F and would therefore provide significant additional margin between the maximum temperature increase specified and the maximum concrete temperature limit.

This limit in conjunction with the 225 °F maximum concrete temperature limit will also ensure that the maximum analyzed fuel clad temperatures for the blocked vent case are not exceeded. By extrapolating from the 24 kW AHSM case to the 14 kW case:

$[T_{14kw} = ((T_{24kw}-T_{amb}) \times (14kW/24kW))+T_{amb}]$

a roof temperature of approximately 230 °F would be expected at an ambient temperature of 117 °F (based on a maximum concrete temperature monitor reading of 314 °F, extrapolated from the 393 °F at the inside surface of the roof, for a 24 kW payload). The upper limit of 225 °F bounds this maximum roof temperature thus ensuring that the 14 kW payload design basis fuel clad temperature of 749 °F is not exceeded. The temperature increase between the long term average concrete monitor temperature, for an AHSM loaded with a 14 kW heat load, and the maximum concrete monitor temperature (230 °F) is approximately 100 °F which is also bounded by the 80 °F temperature increase criteria.

Therefore, the maximum allowed temperature chosen and the maximum allowed temperature rise will ensure that AHSM concrete temperature is limited to the design basis maximum for a 24 kW heat load while also ensuring that the 14 kW payload fuel clad temperature limits are not exceeded.

SAR Section 12.5.2.5 has been revised to incorporate a brief discussion of the above basis.

Question 12-3

Clarify the design criteria for Design Feature 12.4.2.2, Storage Pad.

Design Feature 12.4.2.2, refers to Chapter 2 which provides general information and also makes reference to other portions of the SAR. Design Feature 12.4.2.2, should contain sufficient information regarding the evaluation methods required for a licensee to ensure its site is bounded for the Advanced NUHOMS® System. This information is required by the staff to assess compliance with 10 CFR 72.102(c) and (e), 10 CFR 72.212(b)(2) and (3), and 10 CFR 72.122(b).

Response to Question 12-3

SAR Section 12.4.2.2 has been revised to more clearly specify the analysis to be performed by the licensee to ensure that the effect of amplification of the seismic accelerations due to soil structure interaction are addressed. In addition, the storage pad location shall have no potential for liquefaction at the site-specific Safe Shutdown Earthquake level.

Question 12-4

Revise Design Feature 12.4.3.1, Advanced Horizontal Storage Module to include a statement regarding the minimum number of AHSMs that must be attached and spacing on the pad that must be attached to each other to meet the design requirements for a design basis earthquake.

This information is required by the staff to assess compliance with 10 CFR 72.90.

Response to Question 12-4

SAR Section 12.4.4.1 was revised to specify that AHSMs will be tied together in groups of at least three. The required spacing of 20 ft. between each group of modules, which are tied together, and 10 ft. between any module and the edge of the ISFSI pad was also added. The revision was made to SAR Section 12.4.4.1 since SAR Section 12.4.3.1 is associated with AHSM codes and standards.

Question 12-5

Justify the statement in Section 12.5.2.3.b, of the SAR that the ISFSI will not create any radioactive materials or result in any credible liquid or gaseous effluent release.

The SAR did not provide sufficient information for not implementing effluent monitoring program for the Advanced NUHOMS® design. The justification should include an analyses and a discussion of all assumptions and methodology used, to support the statements made in Sections 12.5.2.3 and 12.5.2.4. The analyses should include the potential off-site dose release from the maximum number of Advanced NUHOMS® systems on site with a residual contamination limit of approximately 22,000 dpm/100 cm2 and 2,200 dpm/100 cm2 . The staff cannot confirm that the Advanced NUHOMS® system with the administrative controls program describing dose rates, surface contamination limits, and radioactive effluents will comply with the off-site dose limits of 10 CFR 72.104 for normal and anticipated occurrences.

In the past, the staff has accepted that surface contamination limits set at the values recommended by Regulatory Guide 1.86 will result in no effluent release from an ISFSI. Therefore, the staff has concluded that an effluent monitoring and reporting system in accordance with 72.44(d) (for site specific licensees) or 50.36a (for general licensees) is

not required. This information is required for the staff to assess compliance with 10 CFR 50.36a in lieu of maintaining the contamination limits of Regulatory Guide 1.86, "Termination of Operating Licenses for Nuclear Reactors."

Response to Question 12-5

The 24PT1 DSC smearable surface contamination limits stated in Section 12.5.2.4.c have been revised to be less than 2200 dpm/100 cm^2 for beta and gamma sources, and less than 220 dpm/100 cm^2 from alpha emitting sources.

The Advanced NUHOMS® System is a self contained passive system that does not produce routine solid, liquid or gaseous effluents.

The contamination limits specified above are based on the allowed removable external radioactive contamination specified in 49 CFR 173.443 (as referenced in 10 CFR 71.87(i)) the system provides significant additional protection for the 24PT1-DSC surface than the transportation configuration. The AHSM will protect the 24PT1-DSC from direct exposure to the elements and will therefore limit potential releases of removable contamination. The probability of any removable contamination being entrapped in the AHSM air flow path released outside the AHSM is considered extremely small.
To demonstrate that the Advanced NUHOMS® System with the 24PT1-DSC surface contamination limits specified in SAR Section 12.5.2.4.c complies with the off site dose limits of 10CFR 72.104, TN West has performed an analysis. This analysis is evaluating a non-mechanistic event and thus many of the parameters used in this evaluation are assumed or postulated. The assumptions which support the analysis are listed below:

- The entire surface of the canister is assumed to have the maximum allowed contamination level. Therefore, the total activity available for release is assumed to be the surface area of the outside of the canister times the contamination limits.

- A single individual ingests all of the contamination on the surface of a single canister.

- All of the contamination is released in one second from the AHSM vent, and that the resultant contamination cloud exists for two hours at the controlled area boundary (100 meters from the facility).

- The downstream (ambient) pressure for all leak calculations is assumed to be one atmosphere. This is representative of the bulk of the atmosphere. Small variations in atmospheric pressure will not significantly affect the results of the calculation.

- The dispersion factor is calculated using Regulatory Guide 1.135 assuming D stability and a wind speed of 5 meters per second with a distance to the controlled area boundary of 328 feet (100 meters). These atmospheric conditions are consistent with the guidance of ISG-5 for normal and off-normal conditions. The distance to the controlled area boundary (100 meters) is the shortest distance permitted by 10CFR72.106. Using the shortest distance maximizes the exposures due to the release.

- The worst-case clearance class is conservatively used for each organ/nuclide combination.

- Based on several representative "crud" data measurements, the radionuclide content of surface contamination from a PWR reactor is provided in Table 12-5.1.

Table 12-5.1
Composition of Typical Surface Contamination

Nuclide	% Activity
β,γ emitters	
C14	0.20
Fe55	12.75
Ni59	0.15
Co60	18.10
Ni63	21.40
Sr90	2.40
Cs134	8.10
Cs137	36.90
Total	100.00
α emitters	
Pu238	4.00
Pu239,240	1.30
Pu241	87.50
Am241	4.70
Cm243,244	2.50
Total	100.00

The methodology used for this evaluation is summarized below.

1. Determine total activity (μCi) on the 24PT1-DSC shell for each radioactive isotope based on the surface area of the canister, the allowed surface contamination limit and the representative radionuclide composition of the surface contamination.

2. Determine the "Committed Dose Equivalent per Unit Intake" from Federal Guidance Report No. 11 [12-5.1]. Multiply the total activity for each nuclide by the Committed Dose Equivalent values to determine the total dose to an individual that ingests all of the contamination.

3. Determine the Atmospheric Dispersion Factors at the controlled area boundary (100 meters from the facility) and a wind speed of 5 meters per second using Regulatory Guide 1.145 [12-5.2]. The Dose Conversion Factors for air submersion are taken from Table III.1 of Federal Guidance Report No. 11 [12-5.1]. The Dose Conversion Factors for inhalation are taken from Table 2.1 of Federal Guidance Report No. 12 [12-5.3].

4. The Deep Dose Equivalent (DDE) due to air submersion for the whole body and

each individual organ is given by:

$$DDE_{i,o} = Q_i\left(\frac{Bq}{sec}\right)\cdot DCF_{i,o}\left(\frac{Sv\cdot m^3}{Bq\cdot sec}\right)\cdot \frac{\chi}{Q}\left(\frac{sec}{m^3}\right)\cdot t(sec) \qquad \textbf{Equation 1}$$

where:

$DDE_{i,o}$ is the deep dose equivalent contribution from nuclide i to organ o, mrem (this is the shallow dose equivalent (SDE) when used for the skin)

Q_i is the isotope specific leak rate, Bq/sec (All assumed to leak in 1 second)

$DCF_{i,o}$ is the dose conversion factor for nuclide i to organ o

χ/Q is the atmospheric dispersion factor, 1.730×10^{-3} sec/m^3 for normal operation

t is the duration of the exposure, 2 hours or 7,200 seconds

5. The Committed Dose Equivalent (CDE) for internal organ doses (Committed Effective Dose Equivalent, CEDE, for the internal whole body dose) due to inhalation is given by:

$$CDE_{i,o} = Q_i\left(\frac{Bq}{sec}\right)\cdot DCF_{i,o}\left(\frac{Sv}{Bq}\right)\cdot \frac{\chi}{Q}\left(\frac{sec}{m^3}\right)\cdot R\left(\frac{m^3}{sec}\right)\cdot t(sec) \qquad \textbf{Equation 2}$$

where:

$CDE_{i,o}$ is the committed dose equivalent contribution from nuclide i to organ o, mrem (this is the committed effective dose equivalent (CEDE) when used for the whole body)

Q_i is the isotope specific leak rate, Bq/sec (All assumed to leak in 1 second)

$DCF_{i,o}$ is the dose conversion factor for nuclide i to organ o

χ/Q is the atmospheric dispersion factor, 1.730×10^{-3} sec/m^3.

R is the respiration rate, 3.3×10^{-4} m^3/sec (Federal Guidance Report 11)

t is the duration of the exposure, 2 hours or 7,200 seconds

6. The Total Effective Dose Equivalent (TEDE) is equal to the sum of the whole body Deep Dose Equivalent (DDE) and the Committed Effective Dose Equivalent (CEDE). The Total Organ Dose Equivalent (TODE) for a given organ is equal to the sum of the DDE for that organ and the CDE for that organ.

7. Compare the calculated TEDE and TODE results to the requirements of 10CFR72.104(a) for normal and anticipated occurrences.

A summary of the calculated exposures is presented in Table 12-5.2. As demonstrated by these results, the calculated doses using extremely conservative assumptions are less than 1.2 % of the 10CFR72.104(a) annual dose limits. Therefore, it is concluded that the maximum contamination levels specified in the revised Section 12.5.2.4.c of the SAR (2,200 dpm/100cm^2 β,γ and 220 dpm/100cm^2 α) are negligible.

SAR Section 12.5.2.4.c has been revised to specify the reduced limits and provide the basis for these limits.

Table 12-5.2

Dose Summary and Comparison to 10CFR72.104(a) Limits

Organ	10CFR72.104(a) Limit (mrem)	Total Ingestion Dose (mrem)	DDE + CDE @ 100 meter (mrem)	Total Ingestion Dose / 72.104 Limit	DDE + CDE @ 100 meter / 72.104 Limit
Whole Body	25	0.0240	0.0072	0.0010	0.0003
Thyroid	75	0.0078	<0.0001	0.0001	<0.0001
Other Critical Organ	25	0.2790	0.1284	0.0112	0.0051

[12-5.1] Federal Guidance Report No. 11, "Limiting Values of Radionuclide Intake and Air Concentration and Dose Conversion Factors for Inhalation, Submersion, and Ingestion," DE89 011 065, 1988.

[12.5-2] Regulatory Guide 1.145, "Atmospheric Dispersion Models for Potential Accident Consequence Assessments at Nuclear Power Plants", Revision1, February 1982.

[12.5-3] Federal Guidance Report No. 12, "External Exposure to Radionuclides in Air, Water, and Soil," EPA 402-R-93-081, September 1983.

TRANSNUCLEAR WEST

ATTACHMENT 3

RAI 3-6 RESPONSE

Attachment 3

RESPONSE TO REQUEST FOR ADDITIONAL INFORMATION
TRANSNUCLEAR WEST INC., TAC NO. L23203

RESPONSE TO RAI 3-6

Question 3-6

Provide a soil-structure interaction analysis that would be typical for a site deploying the Advanced NUHOMS® System.

The design basis response spectra of the Advanced NUHOMS® System design is based on the standard spectrum shape in NRC Regulatory Guide 1.60, "Design Response Spectra for Seismic Design of Nuclear Power Plants," Revision 1, 1973, anchored at 1.5g zero period acceleration for the horizontal direction. The vertical design spectrum is set at 2/3 of the horizontal over the entire frequency range. The horizontal and vertical spectra are specified at the top of the basemat.

Nonlinear analyses were performed in Chapter 11 of the SAR to determine the maximum sliding and rocking/tipping response of the AHSM during a design basis seismic event. These analyses were based on acceleration time histories from the Taiwan earthquake in 1999, the Landers/Lucern earthquake in 1992, and the Tabas earthquake in 1978. However, the staff requires the analysis including the soils and structure interactions, the methodologies and computer model, and the specific acceleration histories that envelope the parameters of a typical site. This is required for the staff to assess compliance with 10 CFR 72.122(b).

Note: The above question was restated in accordance with a communication from Mr. Steve Baggett (NRC) to Mr. U. B. Chopra (TN-West) via e-mail dated 4/18/01, 9:57 am, subject: "Reference RAI 3-6 for the Advanced NUHOMS design".

Response to Question 3-6

A general licensee that deploys the Advanced NUHOMS® Storage System that is the subject of this Safety Analysis Report shall engineer and construct the concrete pad which supports the storage modules. A site-specific soil-structure interaction analysis is required to establish the seismic response at the interface with the base of the storage modules. The site-specific analysis must be documented as part of the evaluations required of the general licensee by 10 CFR 72.212(b)(2) and is subject to NRC review through inspection at the site. All figures and tables referred to in the Response to RAI Question 3-6 are provided at the end of the response.

1. Soil-Structure Interaction Analysis Example

The following is an example of a soil-structure interaction (SSI) analysis for an Independent Spent Fuel Storage Installation (ISFSI) concrete pad that will support the Advanced NUHOMS storage system. The example uses the soil parameters and seismic ground motions at an exemplifying high seismic west coast site. It is not necessarily bounding for all sites. As can be seen from the results, substantial margins remain to the design earthquake response spectra. The soil-structure interaction analysis employs the methods that are typical of an analysis to be performed by the general licensee.

2. Site Seismic Input

The seismic input for the SSI analyses of the ISFSI was defined by the site's safe shutdown earthquake (SSE) as required by 10 CFR 72.102. The SSE response spectra are shown in Figure 2-1 for the horizontal and vertical response spectra (target response spectra) at 5% critical damping ratio.

To perform the SSI analyses, three artificial acceleration time histories (the three components of a single earthquake) were developed to envelop the target response spectra. These time histories were developed following the criteria given by the Standard Review Plan (Reference 1), Section 3.7 for response spectra enveloping, total duration, strong motion duration, statistical correlation, and power spectral density enveloping.

Figures 2-2 to 2-4 show the comparison between the target response spectra and the response spectra calculated from the artificial acceleration time histories. This comparison shows that the artificial time histories meet the response spectra enveloping requirements.

Figures 2-5 to 2-7 are the plots of the three artificial time histories. Their total duration is 40 seconds with a time step of 0.01 seconds. The strong motion duration times are 24.21 seconds and 23.11 seconds for the two horizontal components, and 20.99 seconds for the vertical component. The total duration and strong motion duration times meet the requirements in the Standard Review Plan, Section 3.7.1 and they are consistent with the duration times suggested for the seismic level at the plant (Reference 2).

The strong motion duration was defined as the difference between the time when the energy reaches 90% and the time when the energy reaches 5%. Energy was calculated as the integral of the square of the acceleration ($\int a^2 dt$).

The correlation coefficient between the two horizontal components is 0.0147, and between the two horizontal components and the vertical components are 0.0614 and 0.1013, respectively. These coefficients are lower than the 0.16 value recommended in Reference 4 and the value of 0.30 recommended in Reference 3. Thus, the three components are statistically independent.

3. Soil Model

The site soil profile corresponds to a relatively homogeneous medium with dynamic properties varying with depth. The soil beneath the pad is a very dense well graded sands

with a depth of about 900 feet under the ISFSI. The surface of the soil is at elevation +15.75' and the water table is at elevation +5.0'. The bottom of the concrete slab supporting the AHSMs was assumed to be at the surface of the soil.

3.1 Low Strain Soil Properties

The best estimate soil properties were developed as a function of depth down to elevation -145.0'. Below that elevation, the soil properties were kept constant. Table 3-1 gives the low strain, best estimate soil properties. Note that the P wave velocity for the saturated soil was set equal to the compression wave velocity in water.

To account for the possible variation in soil properties, two bounding cases were defined in accordance with the Standard Review Plan, Section 3.7.2: an upper bound case obtained by scaling the best estimate soil shear modulus by 2, and a lower bound case obtained by scaling the best estimate soil shear modulus by 0.5. The P wave velocity for the saturated layers was kept constant since it corresponds to the velocity in water. Table 3-2 gives the low strain lower and upper bound soil properties.

The shear modulus and shear wave velocity profiles for the three low strain soil cases are shown in Figures 3-1 and 3-2, respectively.

3.2 Strain Compatible Soil Properties

During an earthquake, the soil behaves in a nonlinear manner and its dynamic properties change as a function of the shear strain imposed by the seismic motion. To account for this nonlinear behavior when performing soil-structure interaction analysis, the accepted practice is to develop an equivalent linear soil profile that is consistent with the level of shear strain imposed by the seismic motion.

The equivalent linear soil profile was developed by performing an iterative wave propagation analysis by modifying the dynamic soil properties according to the level of shear strain. The equivalent linear soil profile was developed with computer code SHAKE. The shear modulus-shear strain and soil damping-shear strain relationships are given in Table 3-3 and shown in Figure 3-3. The equivalent linear soil profile is normally referred to as the strain compatible or high strain soil profile.

Reference 1 states that the strain compatible soil properties for the upper bound case should not be lower than the low strain best estimate properties. In this analysis, due to the high seismic level and relatively soft soil properties, the strain compatible upper bound soil properties were lower than the low strain best estimate properties. To comply with Reference 1's requirements, a fourth soil profile was developed corresponding to the low strain best estimate soil profile.
The shear wave velocity profiles for these four cases are given in Table 3-4 and shown in Figure 3-4. The soil material damping ratios are given in Table 3-5 and shown in Figure 3-5. During the soil-structure interaction analysis, the material soil damping for P waves was limited to 10%.

The P wave velocity profile for the lower bound case was modified due to the following. The strain compatible shear wave velocity for the lower bound case at the saturated soil varies from 272 fps to 466 fps, if a constant P wave velocity of 5,000 fps is maintained, then the equivalent Poisson's ratios for several layers become very close to 0.5. This causes numerical instability during the soil-structure interaction analyses. Therefore, a reduced P wave velocity of 3,500 fps was used for the saturated layers of the lower bound soil case. The P wave velocity profiles for the four cases are given in Table 3-6 and shown in Figure 3-6.

4. Structural Model

A structural model was developed for the AHSMs and the supporting concrete slab using three-dimensional finite element techniques. The combined slab-AHSMs model is the input for the SASSI module HOUSE which generates the structural stiffness matrix for the SSI analysis.

Three structural models were developed to assess the effects on the ISFSI responses when the AHSM masses are varied:

a) Total mass of the AHSMs on the slab

b) Half of the AHSMs mass on the slab

c) No AHSM mass (to avoid numerical problems, the masses of the AHSMs were assumed equal to 1 % of the full mass instead of zero mass)

4.1 Basic Data

The ISFSI pad size is about 42'-7" wide by 111 feet long to support ten AHSMs and is 3 foot thick. The pad may be expanded in length for additional AHSMs in the future. The reinforced concrete pad will have a minimum compressive concrete strength of 3000 psi. Although the design basis for the AHSM requires a minimum group of three, this example site will be using a minimum of ten AHSM at its ISFSI.

The geometric and weight data for the slab and the AHSMs consist of ten storage AHSMs (Figure 4-1) supported on a reinforced concrete pad. The ten AHSMs are placed in a single line side-by-side without separation between them. The AHSM units interact together at their interfaces due to shear keys, steel reinforcement connections at the top and bolted connections near the base. The AHSMs are not anchored to the concrete pad. The configuration of the AHSM ensemble will tend to uniformly distribute the weight over the concrete slab in the area under the AHSMs. At the back of each AHSM there is a rear concrete shield wall bolted to the AHSMs. The two end AHSMs also have an end concrete shield wall bolted to their exterior sides. These shield walls were added to properties of their respective AHSMs.

The properties of the pad, shield walls, and the AHSMs are given below for the model and are conservative relative to the final design properties of the AHSMs. The final weights are shown in brackets.

Slab dimensions: Length = 111'

Width = 42' 7" = 42.583'

Thickness = 3'

Slab Young's Modulus: $E_c = 57{,}000\ (3{,}000)^{1/2} = 3.122 \times 10^6$ psi = 450,000 ksf

Slab unit weight = 0.15 k/ft^3

Slab Poisson's ratio = 0.20

Center of gravity of AHSMs (without shield walls) = 110.30" = 9.192' from front
= 50.38" = 4.198' from side
= 119.85" = 9.988' up

Weight of AHSMs (without shield walls) = 404.5 k [400.3 k]*

Weight of shield walls: End Wall = 205.79 k [188.0 k]*
Rear Wall = 76.51 k [69.72 k]*
* [final design weight]

The center of gravity of the AHSMs including the shield walls and their translational and rotational weights are summarized in Table 4-1.

The system of coordinates for the development of the finite element model of the ISFSI is as follows: The origin is located at the center of the concrete pad and at its bottom level. The X axis is along the longitudinal direction of the pad, the Y axis is along the transverse direction of the slab, and the Z axis is upward.

4.2 Finite Element Model of Concrete Pad

The concrete slab was modeled by a single layer of eight node brick elements. To properly capture the bending effects, incompatible deformation modes were included in these elements. The mesh for the slab consists of 360 brick elements with 806 nodes as shown in Figure 4-2

For the dynamic analysis, 7% damping was assumed for the concrete slab.

4.3 Finite Element Model of AHSMs

The AHSMs were modeled using an assembly of rigid elements. The mass of each AHSM was located at its center of gravity. The assembly of rigid elements for each AHSM consisted basically of one vertical element connected to the finite element mesh of the concrete slab by a set of horizontal and short vertical rigid beams. Each assembly of rigid elements was

connected to the pad only at slab nodes in the perimeter of the footprint of the AHSMs. Figures 4-3a, b and c show sketches of the AHSMs models.

To model all AHSMs and the connecting rigid elements, 559 beam elements were used and 248 new nodes were added to the 806 nodes defining the concrete slab.

4.4 Combined Slab-AHSMs Finite Element Model

The slab and AHSMs finite element models were combined. Figure 4-5 shows the combined model of the slab and the AHSMs. In the design, the AHSMs are not anchored to the pad, but for the purposes of the linear SSI analysis the AHSMs were modeled connected to the pad. The main characteristics of this model are:

Total number of brick elements modeling the slab: 360

Total number of beam elements modeling the AHSMs and their connections: 559

Total number of nodes at the slab: 806

Total number of nodes at AHSMs: 248

Table 4-2 gives the numbers, of the nodes at the center of gravity (cg) of the AHSMs and at the slab directly below the cg of the AHSMs. These are the nodes where the acceleration response spectra were calculated. Figure 4-6 shows the location where the acceleration responses were calculated. Three AHSM locations at their cg: nodes 817, 819, and 821; three top of slab locations below the AHSMs cg: nodes 475, 540, and 592; four top of slab locations at the corners of the footprint of the AHSMs: nodes 446, 452, 758, and 764.

5. Description of Analysis

A series of soil-structure interaction analyses were performed with computer code SASSI to generate the acceleration response spectra at the center of gravity of the AHSMs. The seismic input for all the analyses consisted of the acceleration time histories described in Section 2.

The base case of the SSI analysis is defined by the structural model of the ISFSI with the fully loaded AHSM mass and the four soil cases described in Section 3.

For each of the soil cases, the acceleration response spectra at the ten locations shown in Figure 4-6 were calculated for a damping ratio of 4%. 4% damping was used because the AHSM were analyzed and designed using the 4% damping response spectra. For each soil case, the spectra over the ten locations were enveloped. For the horizontal components, only the spectra at the AHSMs' center of gravity were enveloped. For the vertical component the spectra at the AHSMs' center of gravity and at the corners of the AHSMs were enveloped. This was done to include the maximum effect of rocking in the vertical response spectra.

In the next step, the resulting spectra for all soil cases were enveloped. These spectra are considered the final spectra at the AHSMs' center of gravity and are compared with the TN West design spectra for the AHSMs.

To assess the effect that the variation of the AHSMs' mass participating in the dynamic response has on the acceleration response spectra, two additional cases were analyzed. The first case considered only half of the AHSMs' mass and the second, as a bounding case, considered essentially zero mass in the AHSMs. The analyses for these two cases were done only for the best estimate soil case. As in the base case, the final response spectra were the envelope of the spectra at all response locations.

To assess the effect that the slab stiffness has in the response spectra at the AHSMs' center of gravity, a bounding case with the slab infinitely rigid was analyzed. The analysis for this case was done only for the best estimate soil case. As in the base case, the final response spectra were the envelope of the spectra at all response locations.

6. Results and Conclusions

The main results of the analyses performed for the ISFSI were the acceleration response spectra (4% damping) at the center of gravity of the AHSMs. These response spectra are compared to the response spectra used for the seismic design of the AHSMs by TN West. This comparison is done to evaluate if the design of the AHSMs will bound the site specific seismic design criteria.

The acceleration response spectra generated during the various analyses are presented in Figures 6-1 to 6-9.

Response Spectra for Base Case: Figures 6-1 to 6-4 show, for each soil case, the response spectra obtained by enveloping the spectra over all the locations defined in Section 5. Figure 6-5 shows the response spectra obtained by enveloping the spectra over all locations and all soil cases. The spectra in Figure 6-5 are considered as the final spectra to be compared with the AHSM design spectra used by TN West.

Sensitivity Cases: Figure 6-6 shows the envelope of the response spectra (over all locations) generated assuming only half of the AHSMs' mass in the finite element structural model and best estimate soil properties. Figure 6-7 shows the envelope of the response spectra (over all locations) generated assuming essentially no AHSM mass in the finite element structural model and best estimate soil properties. Figure 6-8 shows the envelope of the response spectra (over all locations) generated assuming full AHSM mass in the finite element structural model, a rigid pad, and best estimate soil properties.
The comparison of the design response spectra used by TN West with the final enveloped response spectra generated in the SSI analysis of the ISFSI is shown in Figures 6-9a, 6-9b, and 6-9c, for the horizontal and vertical directions.

Figures 6-1 to 6-4 for the Base Case show that the soil-structure interaction effects will amplify the free-field ground motion, generating spectral peaks at the slab and AHSMs'

CG levels on the order of 20% higher than the spectral peak of the input ground motion. The results of spectra plots at several top-of-pad and CG locations show that rocking has only a minor effect on the AHSMs' responses at their center of gravity for motions in the transverse direction of the pad. The low frequency range of the final response spectra will be controlled by the lower bound soil case, and the medium to high frequency range will be controlled by the upper bound soil cases, especially by the best estimate-low strain soil case.

The comparison of Figures 6-6 and 6-7 with Figure 6-2, shows that the reduction of the AHSM mass will result in a slight reduction of the response spectra at the center of gravity of the AHSMs. Thus the Base Case can be considered as an upper bound with respect to the effects of mass variations.

The comparison of Figure 6-8 with Figure 6-2 shows that an increase in concrete pad stiffness practically does not change the response of the AHSMs. Therefore, potential increase in concrete modulus with aging is of no consequence.
Figures 6-9a, 6-9b, and 6-9c show that the response spectra calculated at the center of gravity of the ISFSI AHSMs with the site specific SSE is lower than the acceleration response spectra used by TN West for the seismic design of the AHSMs.

No changes to the SAR have been made with respect to this RAI Question response.

References

1. NUREG-0800, "Standard Review Plan for the Review of Safety Analysis Reports for Nuclear Power Plants," Sections 3.7.1 and 3.7.2, Rev. 2.

2. Report UCRL-CR-117769, "Strong Motion Duration and Earthquake Magnitude Relationships," M.W. Salmon, S.A. Short, R.P. Kennedy, June 1992, Lawrence Livermore National Laboratory.

3. ASCE Standard: "Seismic Analysis of Safety Related Nuclear Structure and Commentary," ASCE 4-86.

4. Regulatory Guide 1.92, "Combining Modal Responses and Spatial Components in Seismic Response Analysis," Rev. 1, February 1976.

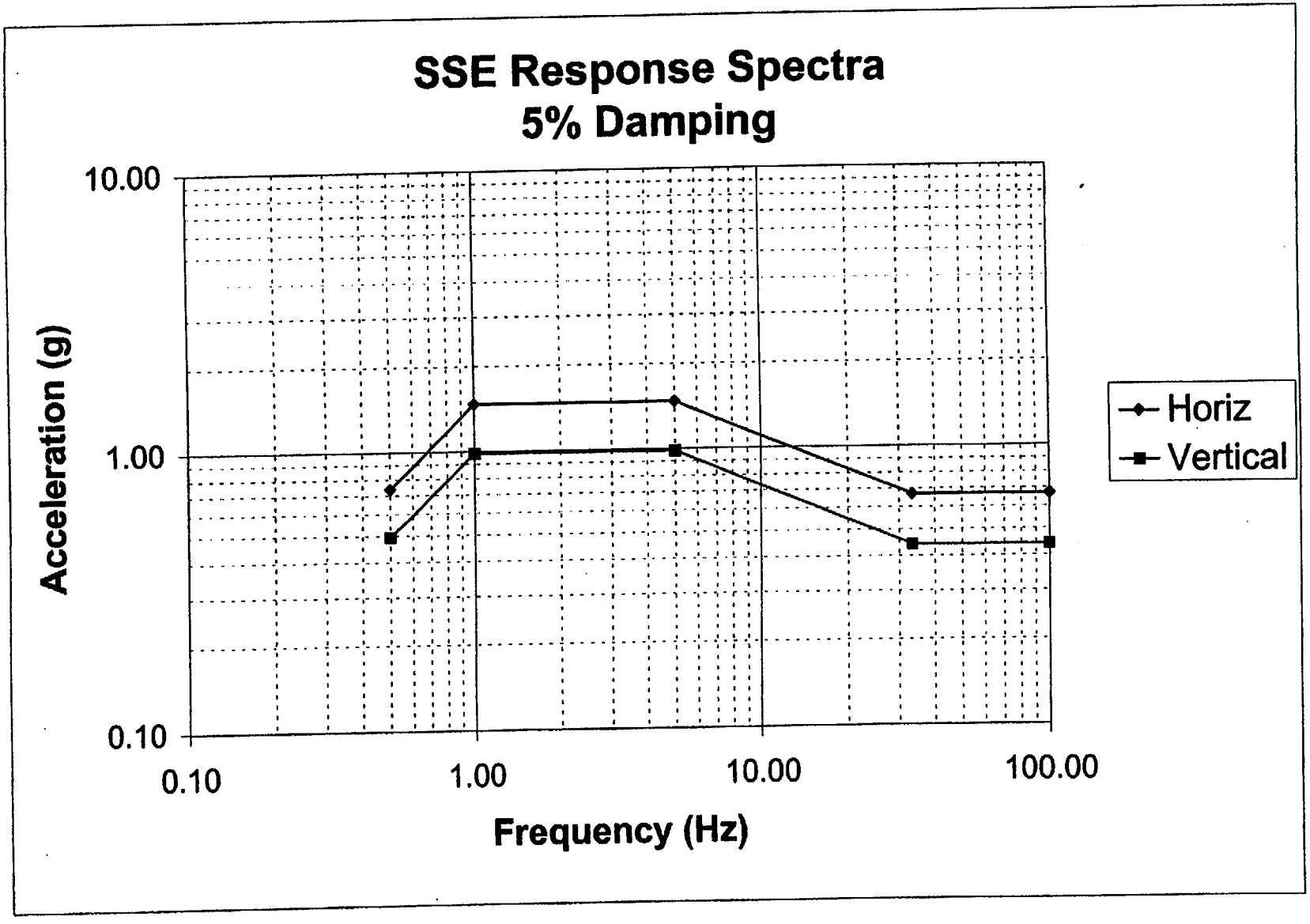

Figure 2-1: SER Response Spectra, 5% Damping

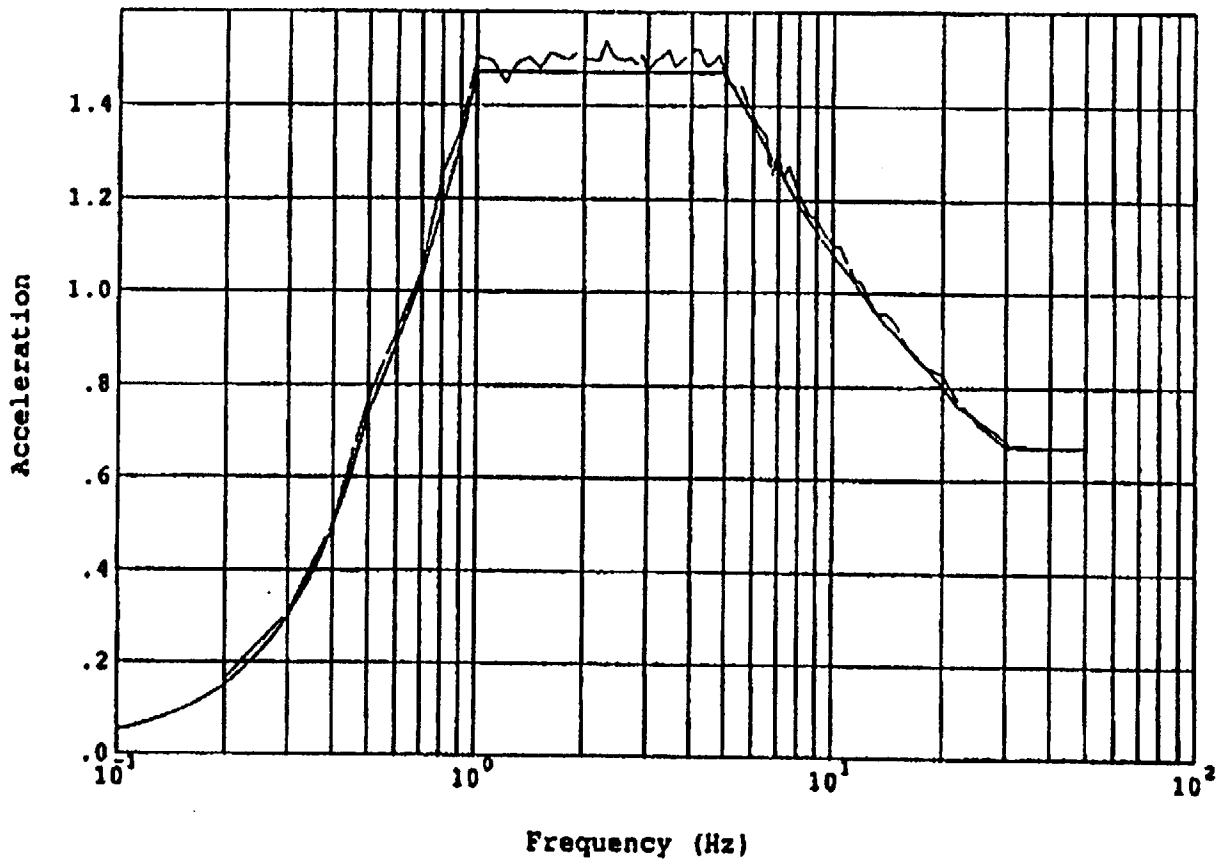

Legend:

Target Spectrum ————————

Actual Spectrum ——— ———

Notes:

At 75 SRP Frequencies

5% Spectral Damping

Acceleration in g's

Figure 2-2: Comparison Horizontal Spectrum to Target Spectrum. Component X

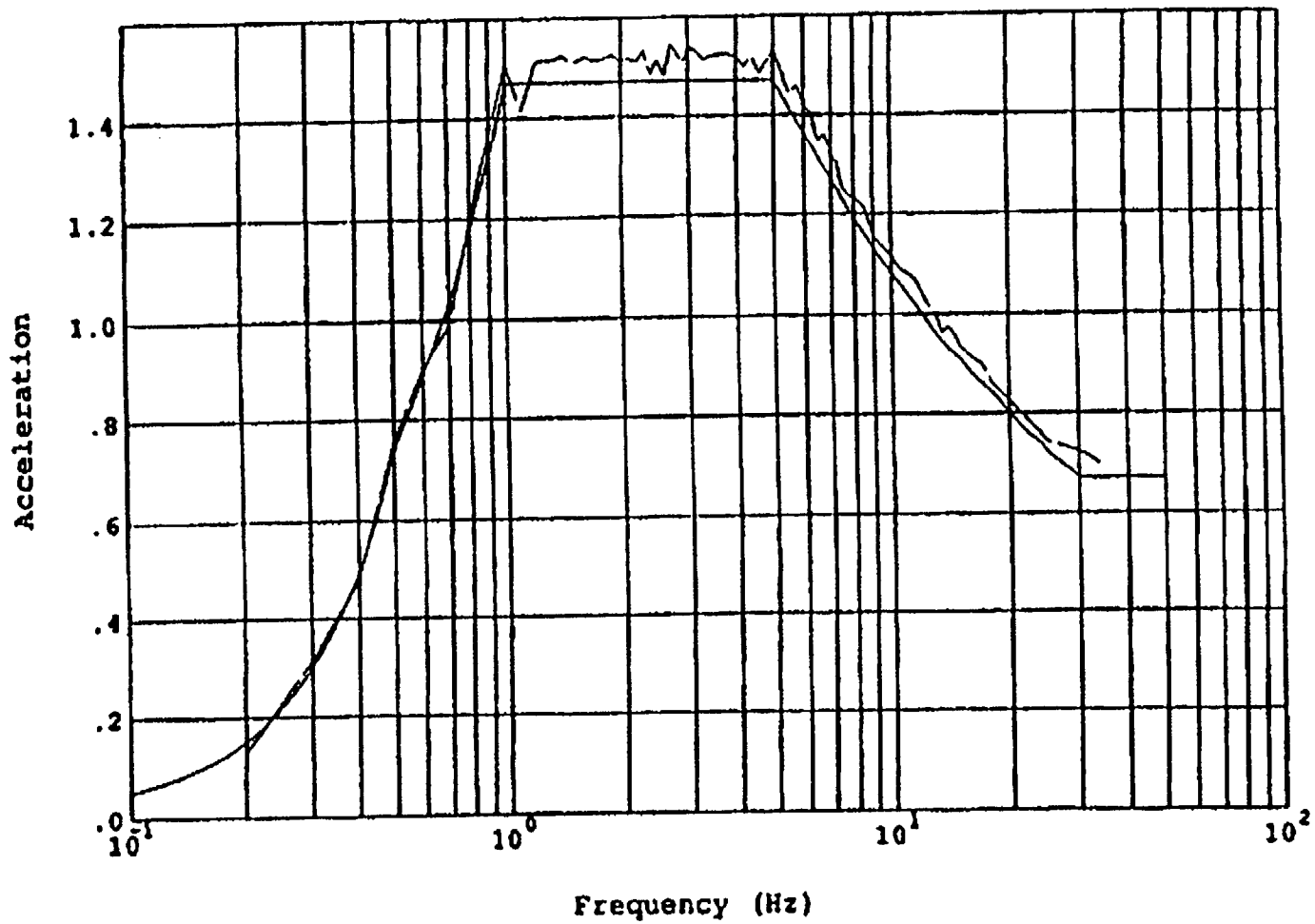

Legend:

Target Spectrum ————————

Actual Spectrum ——— ———

Notes:

At 75 SRP Frequencies

5% Spectral Damping

Acceleration in g's

Figure 2-3: Comparison Horizontal Spectrum to Target Spectrum. Component Y

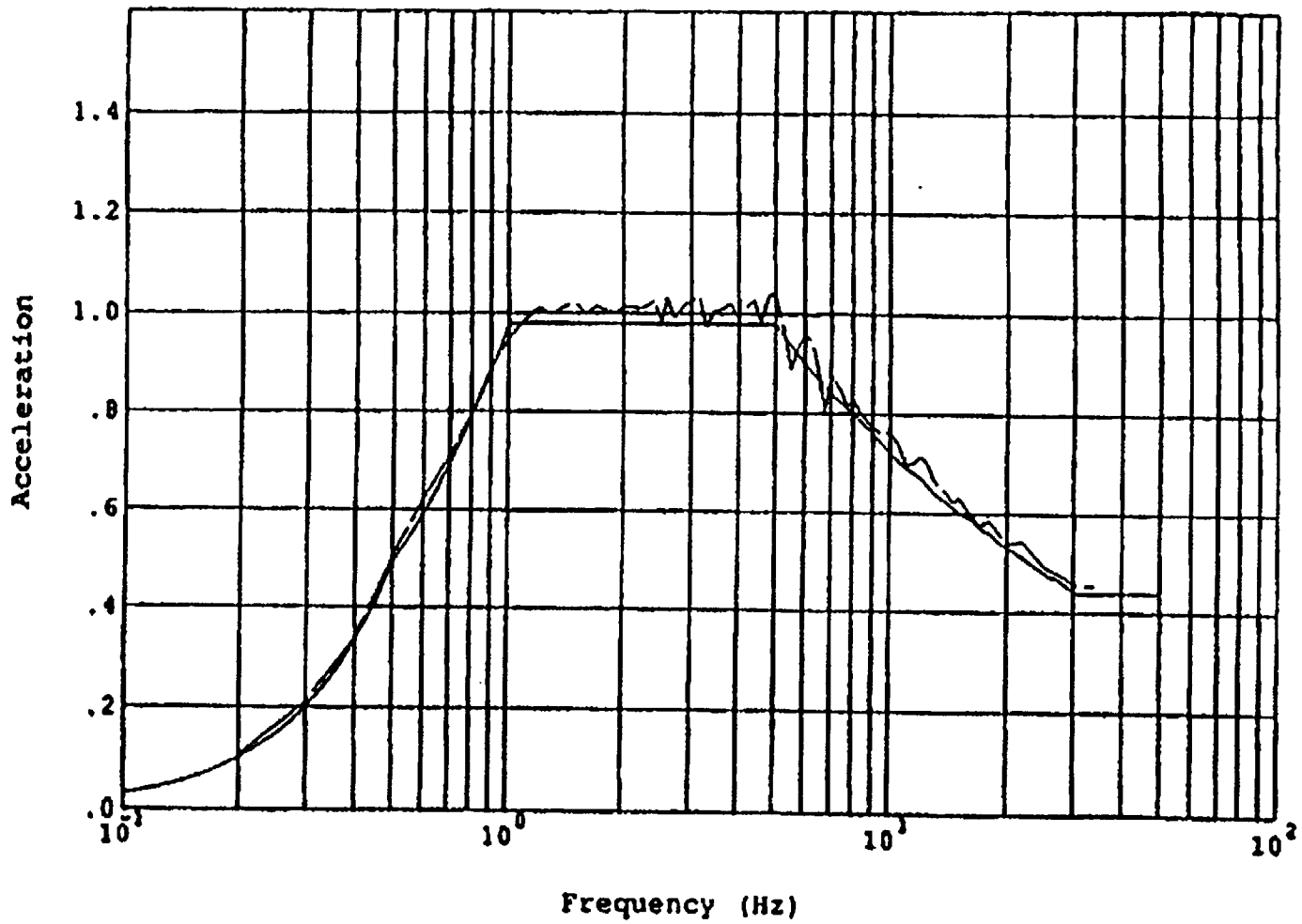

Legend:

Target Spectrum ————————

Actual Spectrum ——— ———

Notes:

At 75 SRP Frequencies

5% Spectral Damping

Acceleration in g's

Figure 2-4: Comparison Vertical Spectrum to Target Spectrum

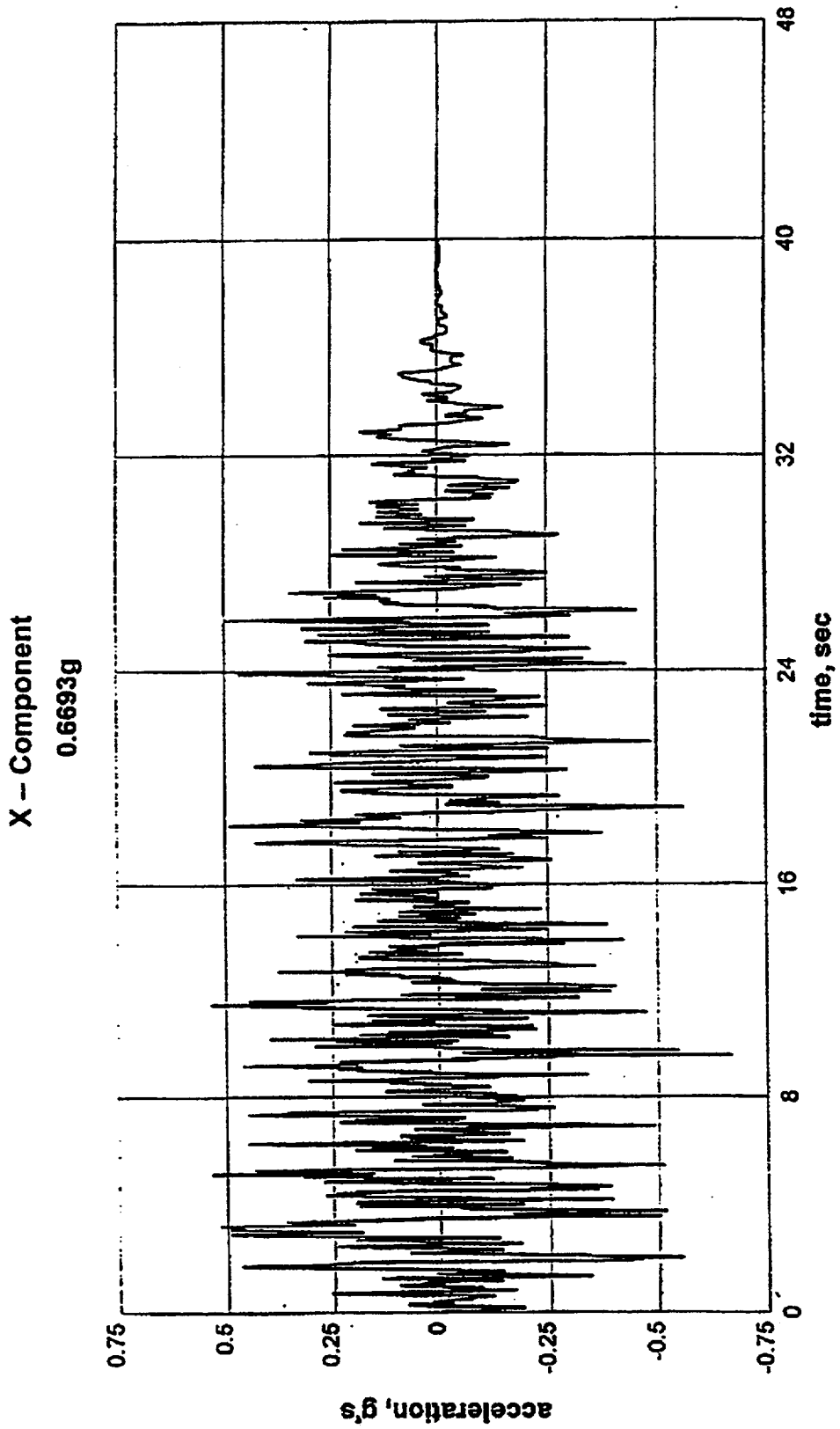

Figure 2-5: Artificial Acceleration Time History

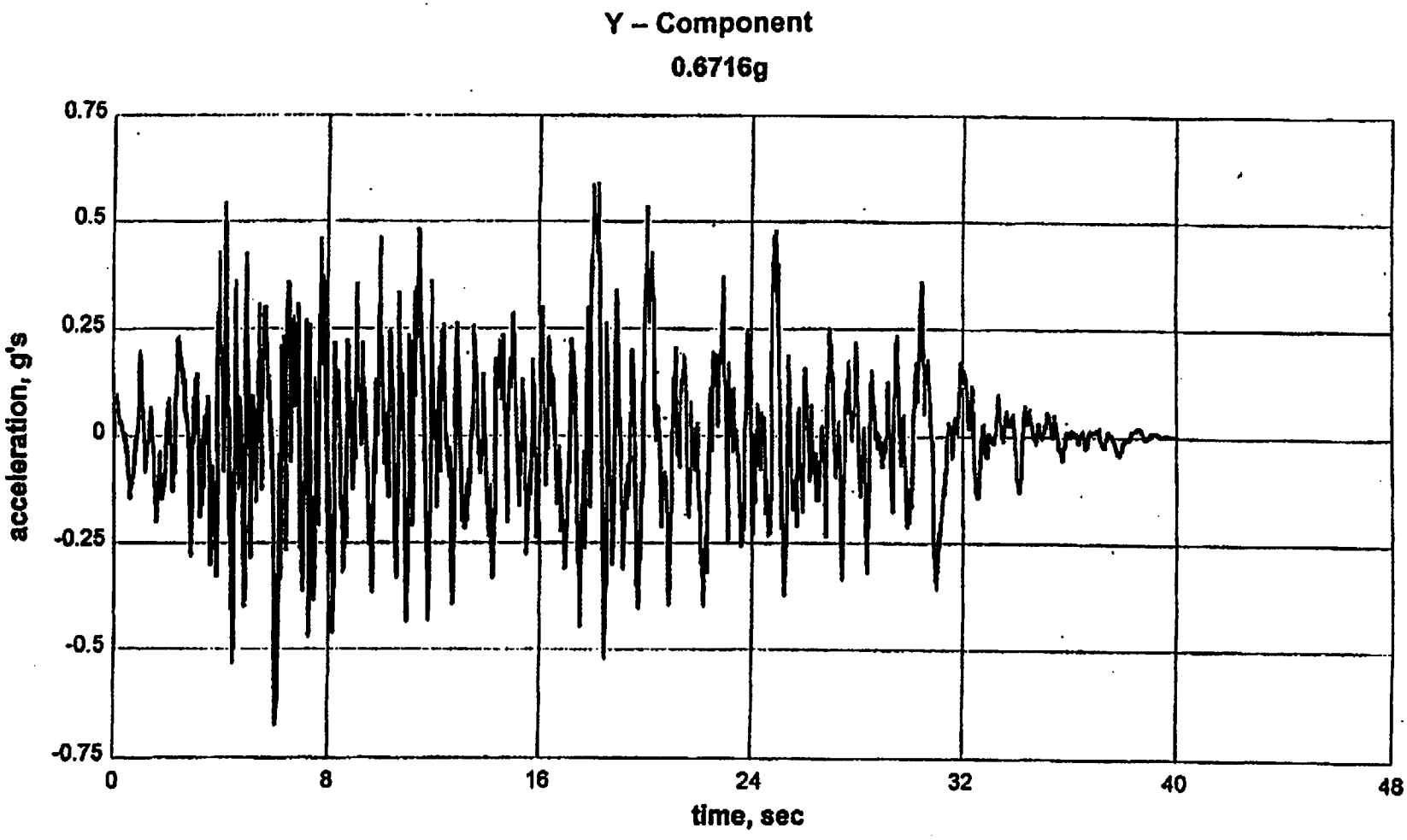

Figure 2-6: Artificial Acceleration Time History

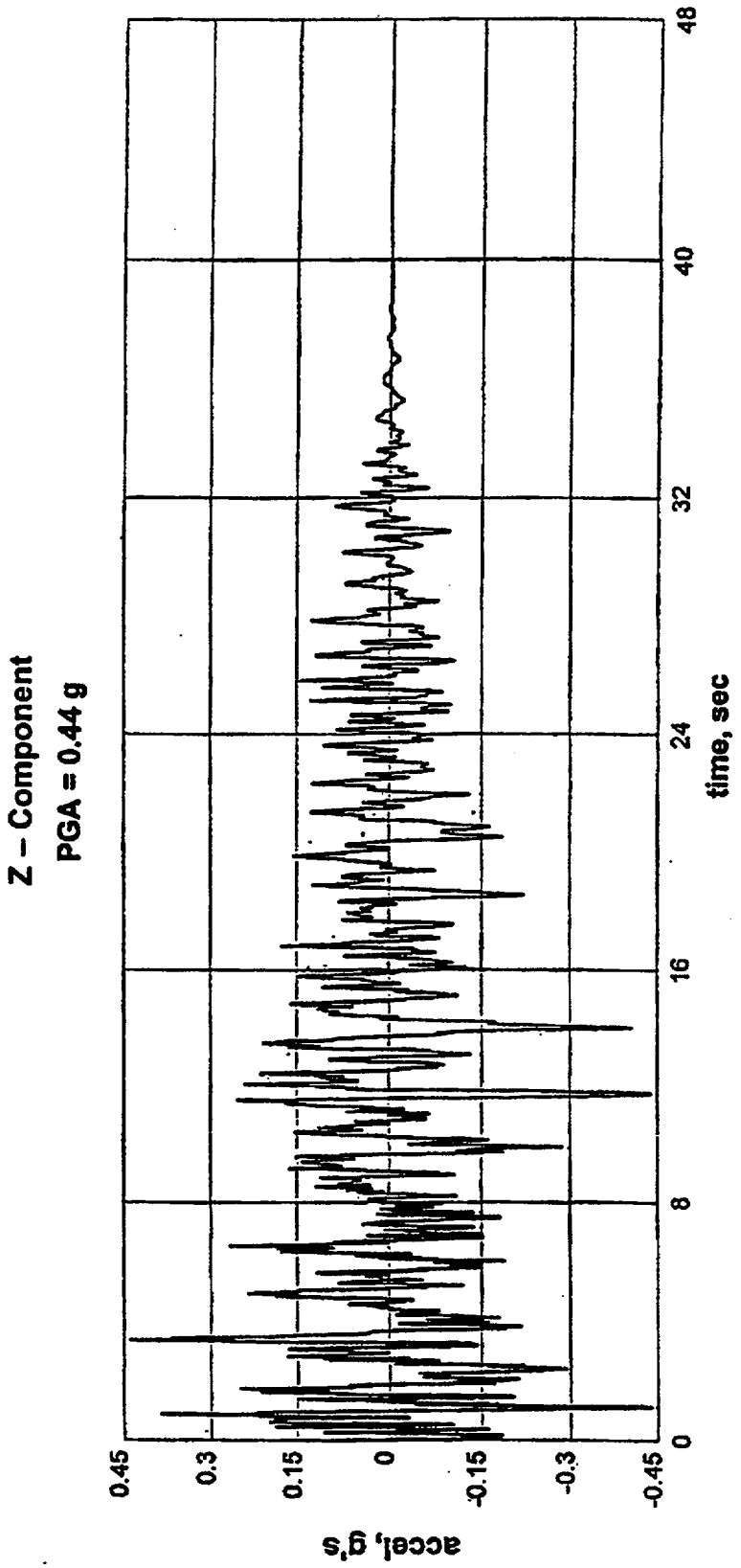

Figure 2-7: Artificial Acceleration Time History

Table 3-1

LOW STRAIN BEST ESTIMATE SOIL PROPERTIES

Layer	Thickness (ft) (Surface at 15.75')	Shear Modulus (ksf)	Vs (1) (fps)	Unit Weight (kcf)	Poisson's ratio	Vp (2) (fps)
1	3.50	3,599.27	930.00	0.134	0.35	1,935.95
2	3.50	3,599.27	930.00	0.134	0.35	1,935.95
3	3.75	3,599.27	930.00	0.134	0.35	1,935.95
4	5.00	4,337.14	1,002.36	0.139	0.48	5,000.00
5	5.00	4,991.60	1,075.33	0.139	0.48	5,000.00
6	5.00	5,605.60	1,139.55	0.139	0.48	5,000.00
7	5.00	6,187.62	1,197.24	0.139	0.48	5,000.00
8	5.00	6,743.43	1,249.86	0.139	0.48	5,000.00
9	5.00	7,277.19	1,298.38	0.139	0.48	5,000.00
10	5.00	7,792.04	1,343.53	0.139	0.48	5,000.00
11	5.00	8,290.41	1,385.83	0.139	0.48	5,000.00
12	5.00	8,774.22	1,425.69	0.139	0.48	5,000.00
13	5.00	9,245.03	1,463.44	0.139	0.48	5,000.00
14	5.00	9,704.15	1,499.34	0.139	0.48	5,000.00
15	5.00	10,152.65	1,533.59	0.139	0.48	5,000.00
16	5.00	10,591.45	1,566.38	0.139	0.48	5,000.00
17	5.00	11,021.34	1,597.86	0.139	0.48	5,000.00
18	5.00	11,443.01	1,628.14	0.139	0.48	5,000.00
19	5.00	11,857.04	1,657.33	0.139	0.48	5,000.00
20	5.00	12,263.96	1,685.53	0.139	0.48	5,000.00
21	10.00	12,862.03	1,726.14	0.139	0.48	5,000.00
22	10.00	13,638.50	1,777.48	0.139	0.48	5,000.00
23	10.00	14,393.46	1,826.01	0.139	0.48	5,000.00
24	10.00	15,129.11	1,872.09	0.139	0.48	5,000.00
25	10.00	15,847.28	1,916.01	0.139	0.48	5,000.00
26	15.00	16,722.77	1,968.22	0.139	0.48	5,000.00
27	H. S. (-160.75' ->)	17,744.05	2,027.43	0.139	0.48	5,000.00

(1) Lower limit for Vs = 930 fps
(2) Layers below water table, Vp = 5,000 fps (P wave velocity in water)

Table 3-2

LOW STRAIN LOWER AND UPPER BOUND SOIL PROPERTIES

Layer	Thickness (ft) (Surface at 15.75')	L.B. Shear Modulus (ksf)	L.B. Vs (fps)	U.B. Shear Modulus (ksf)	U.B. Vs (fps)
1	3.50	1,799.64	657.61	7,198.54	1,315.22
2	3.50	1,799.64	657.61	7,198.54	1,315.22
3	3.75	1,799.64	657.61	7,198.54	1,315.22
4	5.00	2,168.57	708.77	8,674.27	1,417.55
5	5.00	2,495.80	760.37	9,983.20	1,520.74
6	5.00	2,802.80	805.78	11,211.21	1,611.56
7	5.00	3,093.81	846.58	12,375.24	1,693.16
8	5.00	3,371.71	883.78	13,486.85	1,767.57
9	5.00	3,638.60	918.09	14,554.38	1,836.19
10	5.00	3,896.02	950.02	15,584.09	1,900.03
11	5.00	4,145.20	979.93	16,580.82	1,959.85
12	5.00	4,387.11	1,008.11	17,548.44	2,016.23
13	5.00	4,622.52	1,034.81	18,490.07	2,069.62
14	5.00	4,852.07	1,060.19	19,408.30	2,120.38
15	5.00	5,076.32	1,084.41	20,305.30	2,168.83
16	5.00	5,295.72	1,107.60	21,182.90	2,215.20
17	5.00	5,510.67	1,129.86	22,042.68	2,259.71
18	5.00	5,721.50	1,151.27	22,886.01	2,302.53
19	5.00	5,928.52	1,171.91	23,714.08	2,343.82
20	5.00	6,131.98	1,191.85	24,527.93	2,383.70
21	10.00	6,431.01	1,220.56	25,724.05	2,441.13
22	10.00	6,819.25	1,256.87	27,276.99	2,513.73
23	10.00	7,196.73	1,291.18	28,786.91	2,582.37
24	10.00	7,564.55	1,323.77	30,258.21	2,647.54
25	10.00	7,923.64	1,354.82	31,694.57	2,709.65
26	15.00	8,361.39	1,391.75	33,445.55	2,783.49
27	H. S. (-160.75' ->)	8,872.02	1,433.61	35,488.10	2,867.23

Table 3-3

SOIL DEGRADATION CURVES

Shear Strain (%)	G/GMAX	Soil Damping Ratio (%)
0.0001	1.000	2.061
0.0003	0.978	2.691
0.001	0.852	3.568
0.003	0.600	4.621
0.01	0.391	6.067
0.03	0.258	7.496
0.1	0.173	10.158
0.3	0.128	12.930
1.0	0.095	16.442
2.0	0.076	19.031
3.0	0.066	20.900
10.0 (1)	0.063 (1)	20.900 (1)

(1) These values were added to allow for larger deformation.

Table 3-4

STRAIN COMPATIBLE SHEAR WAVE VELOCITY

Layer	Thickness (ft)	Vs lower bound (strain comp.) (fps)	Vs best est. (strain comp.) (fps)	Vs upper bound (strain comp.) (fps)	Vs best est. (low strain) (fps)
1	3.50	376.53	649.40	1096.24	930.00
2	3.50	282.88	468.14	815.56	930.00
3	3.75	258.93	420.26	706.30	930.00
4	5.00	272.27	435.31	711.29	1002.36
5	5.00	282.29	453.55	739.86	1075.33
6	5.00	292.37	468.13	770.84	1139.55
7	5.00	303.64	484.66	802.93	1197.24
8	5.00	315.25	500.19	830.44	1249.86
9	5.00	326.79	515.02	851.11	1298.38
10	5.00	335.88	530.09	870.48	1343.53
11	5.00	344.06	544.96	888.00	1385.83
12	5.00	352.37	559.23	904.67	1425.69
13	5.00	360.50	572.94	920.16	1463.44
14	5.00	368.44	586.32	935.52	1499.34
15	5.00	376.22	599.22	951.48	1533.59
16	5.00	382.93	609.76	967.29	1566.38
17	5.00	389.23	618.62	982.74	1597.86
18	5.00	395.14	627.55	998.87	1628.14
19	5.00	401.25	636.34	1014.40	1657.33
20	5.00	407.83	645.38	1029.59	1685.53
21	10.00	416.82	658.88	1052.18	1726.14
22	10.00	426.44	676.23	1081.71	1777.48
23	10.00	436.11	692.98	1110.03	1826.01
24	10.00	445.82	707.37	1135.51	1872.09
25	10.00	455.34	720.19	1153.43	1916.01
26	15.00	466.15	736.26	1173.24	1968.22
H.S.		480.17	758.40	1208.53	2027.43

Table 3-5

STRAIN COMPATIBLE DAMPING RATIOS

Layer	Thickness (ft)	Damping Ratio Lower bound (strain comp.)	Damping Ratio Best estimate (strain comp.)	Damping Ratio Upper bound (strain comp.)	Damping Ratio Best estimate (low strain)
1	3.50	0.067	0.054	0.042	0.021
2	3.50	0.098	0.076	0.061	0.021
3	3.75	0.113	0.092	0.072	0.021
4	5.00	0.117	0.097	0.077	0.021
5	5.00	0.123	0.100	0.082	0.021
6	5.00	0.127	0.104	0.084	0.021
7	5.00	0.129	0.107	0.085	0.021
8	5.00	0.130	0.110	0.087	0.021
9	5.00	0.130	0.111	0.088	0.021
10	5.00	0.131	0.112	0.090	0.021
11	5.00	0.132	0.113	0.091	0.021
12	5.00	0.133	0.113	0.093	0.021
13	5.00	0.133	0.114	0.094	0.021
14	5.00	0.134	0.114	0.095	0.021
15	5.00	0.134	0.114	0.095	0.021
16	5.00	0.135	0.115	0.096	0.021
17	5.00	0.135	0.116	0.097	0.021
18	5.00	0.136	0.117	0.097	0.021
19	5.00	0.136	0.117	0.097	0.021
20	5.00	0.136	0.118	0.097	0.021
21	10.00	0.136	0.118	0.098	0.021
22	10.00	0.137	0.119	0.098	0.021
23	10.00	0.138	0.119	0.098	0.021
24	10.00	0.138	0.120	0.098	0.021
25	10.00	0.139	0.121	0.099	0.021
26	15.00	0.139	0.122	0.100	0.021
H.S.		0.139	0.122	0.100	0.021

Table 3-6

STRAIN COMPATIBLE P WAVE VELOCITY

Layer	Thickness (ft)	Vp lower bound (strain comp.) (fps)	Vp best est. (strain comp.) (fps)	Vp upper bound (strain comp.) (fps)	Vp best est. (low strain) (fps)
1	3.50	783.81	1351.84	2282.00	1935.95
2	3.50	588.86	974.50	1697.73	1935.95
3	3.75	539.00	874.84	1470.28	1935.95
4	5.00	3500.00	5000.00	5000.00	5000.00
5	5.00	3500.00	5000.00	5000.00	5000.00
6	5.00	3500.00	5000.00	5000.00	5000.00
7	5.00	3500.00	5000.00	5000.00	5000.00
8	5.00	3500.00	5000.00	5000.00	5000.00
9	5.00	3500.00	5000.00	5000.00	5000.00
10	5.00	3500.00	5000.00	5000.00	5000.00
11	5.00	3500.00	5000.00	5000.00	5000.00
12	5.00	3500.00	5000.00	5000.00	5000.00
13	5.00	3500.00	5000.00	5000.00	5000.00
14	5.00	3500.00	5000.00	5000.00	5000.00
15	5.00	3500.00	5000.00	5000.00	5000.00
16	5.00	3500.00	5000.00	5000.00	5000.00
17	5.00	3500.00	5000.00	5000.00	5000.00
18	5.00	3500.00	5000.00	5000.00	5000.00
19	5.00	3500.00	5000.00	5000.00	5000.00
20	5.00	3500.00	5000.00	5000.00	5000.00
21	10.00	3500.00	5000.00	5000.00	5000.00
22	10.00	3500.00	5000.00	5000.00	5000.00
23	10.00	3500.00	5000.00	5000.00	5000.00
24	10.00	3500.00	5000.00	5000.00	5000.00
25	10.00	3500.00	5000.00	5000.00	5000.00
26	15.00	3500.00	5000.00	5000.00	5000.00
H.S.		3500.00	5000.00	5000.00	5000.00

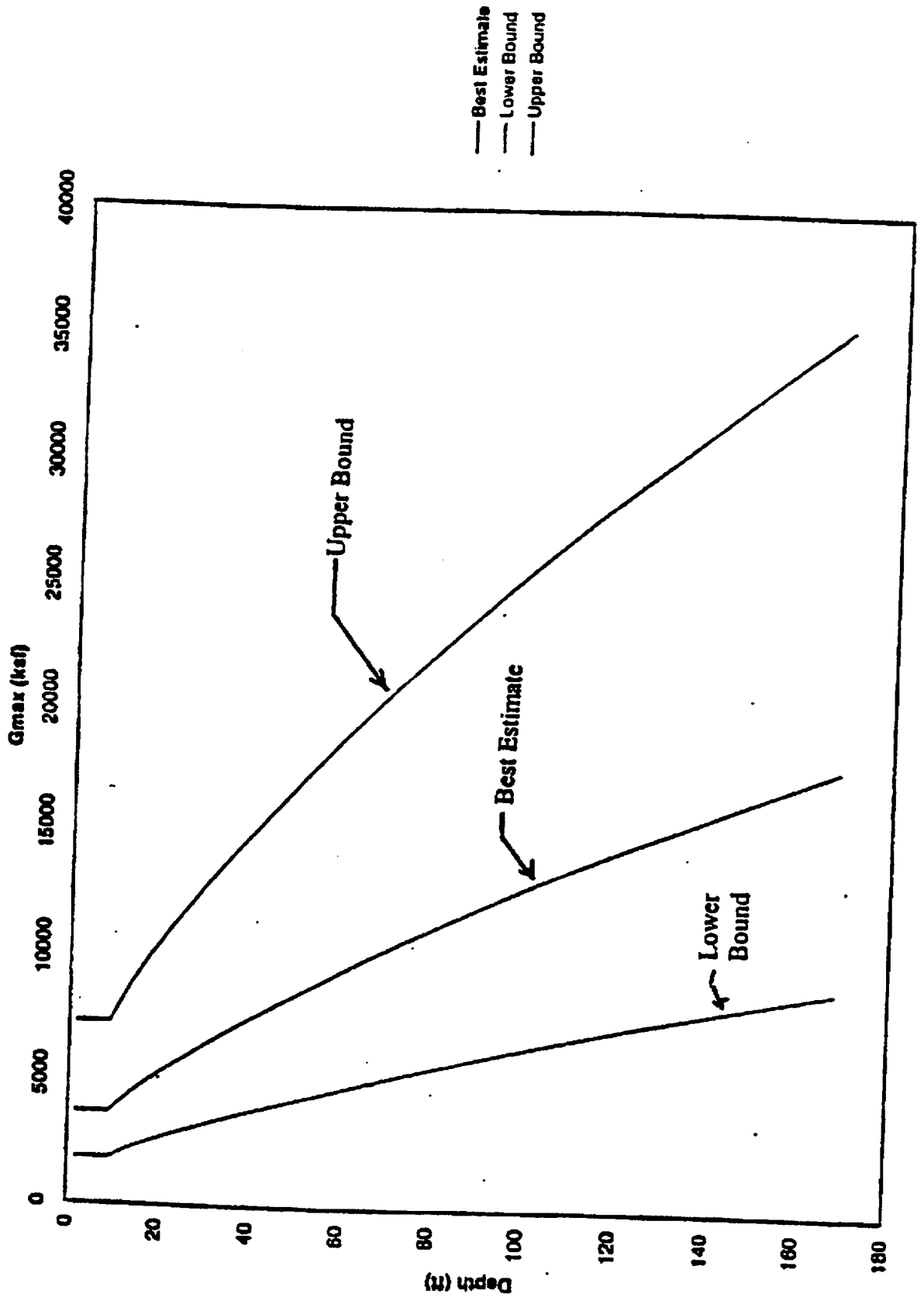

Figure 3-1: Low Strain Shear Modulus

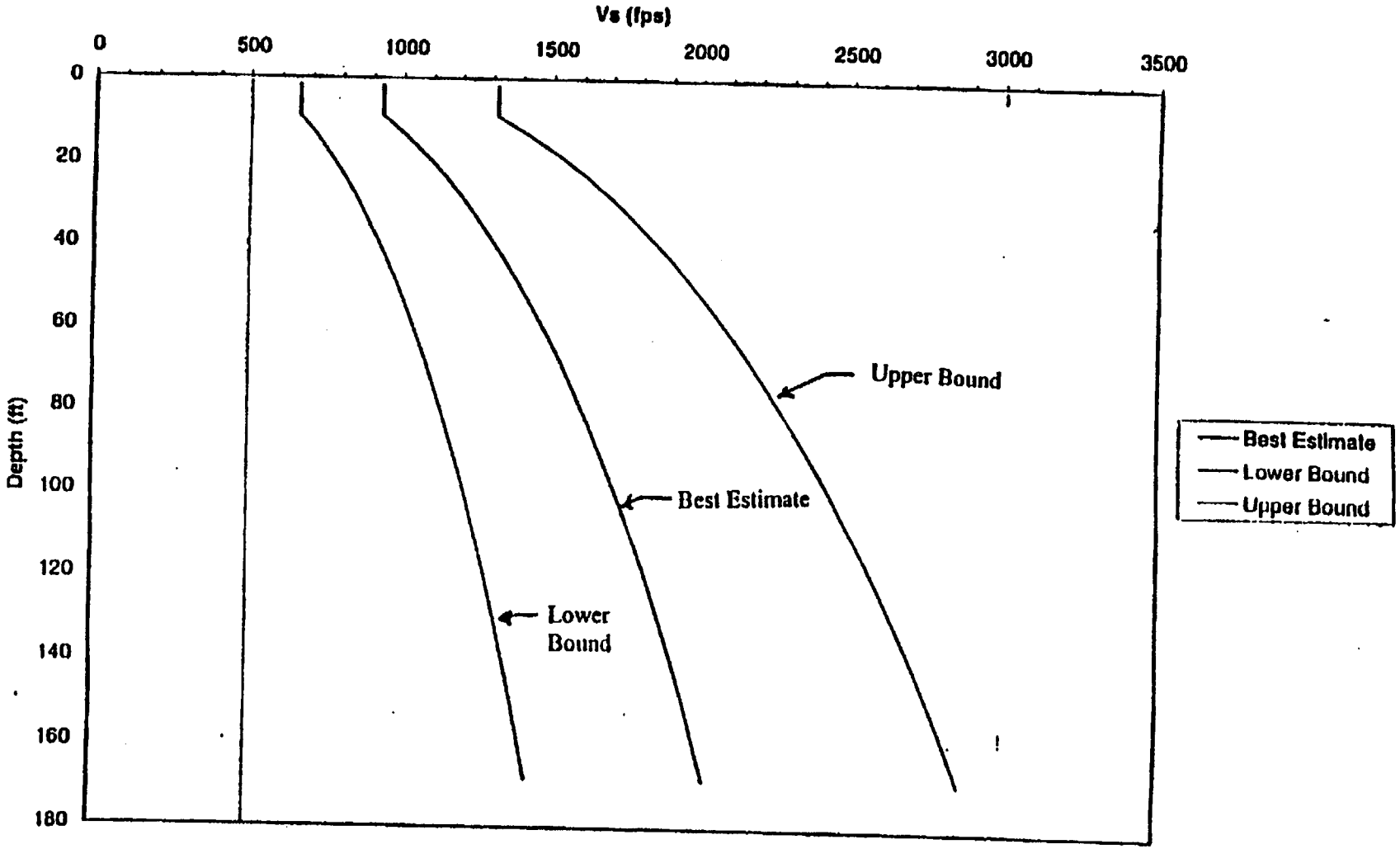

Figure 3-2: Low Strain Shear Wave Velocity

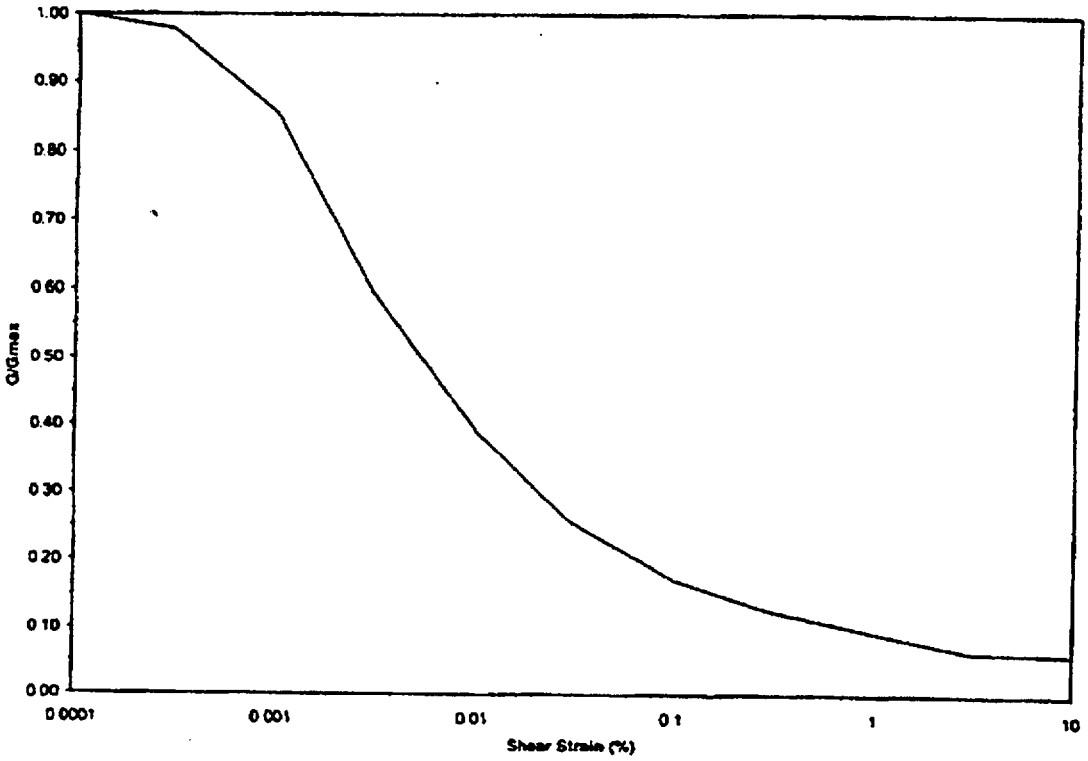

Figure 3-3a: Soil Shear Modulus Degradation Curve

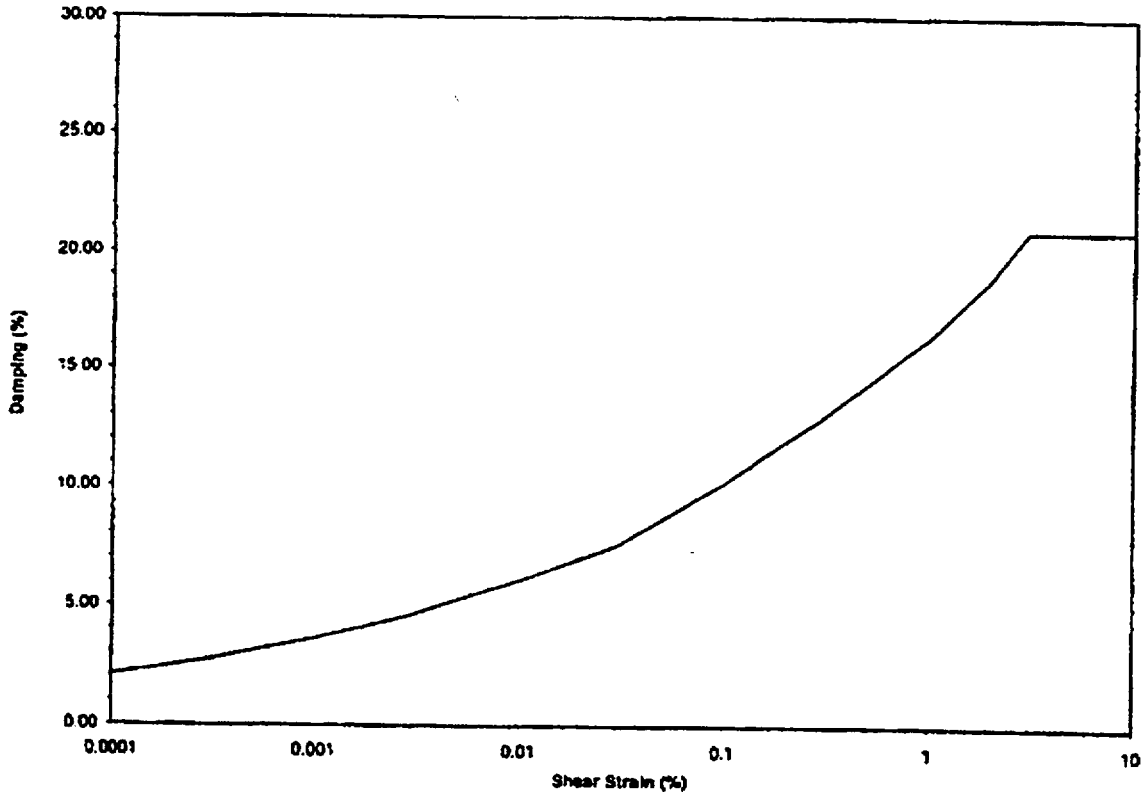

Figure 3-3b: Soil Material Damping Curve

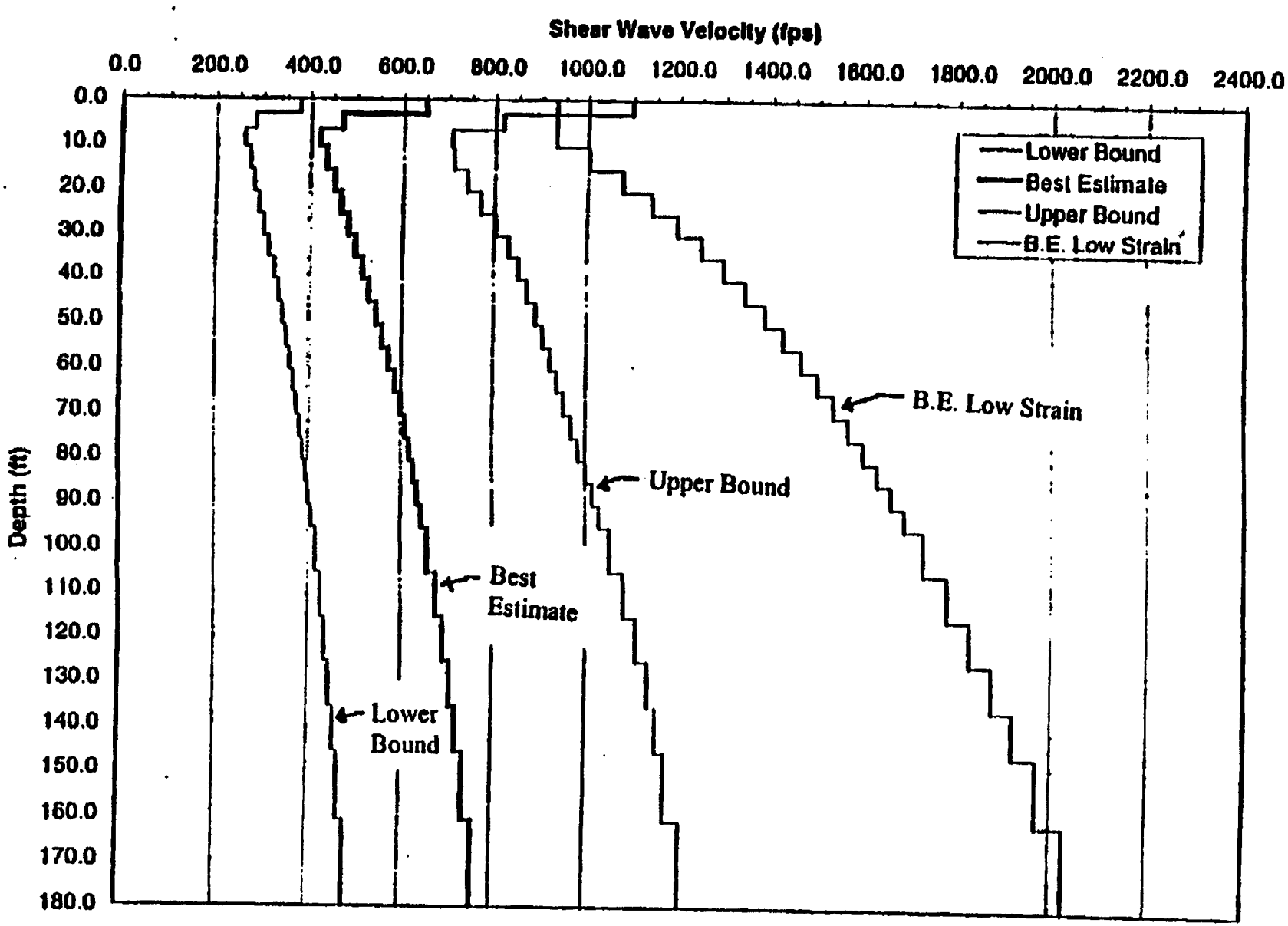

Figure 3-4: Strain Compatible Shear Wave Velocity

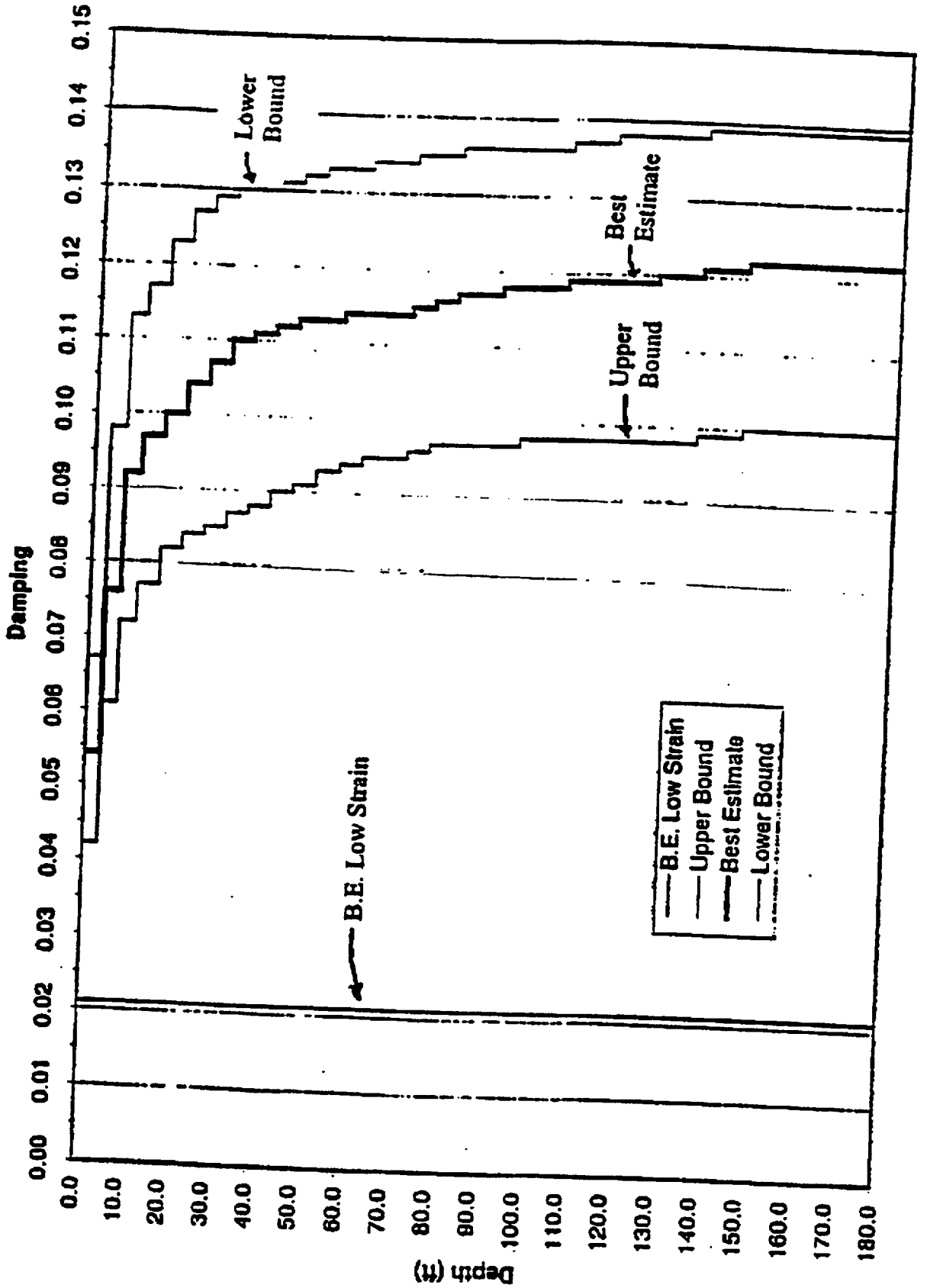

Figure 3-5: Strain Compatible Damping Ratios

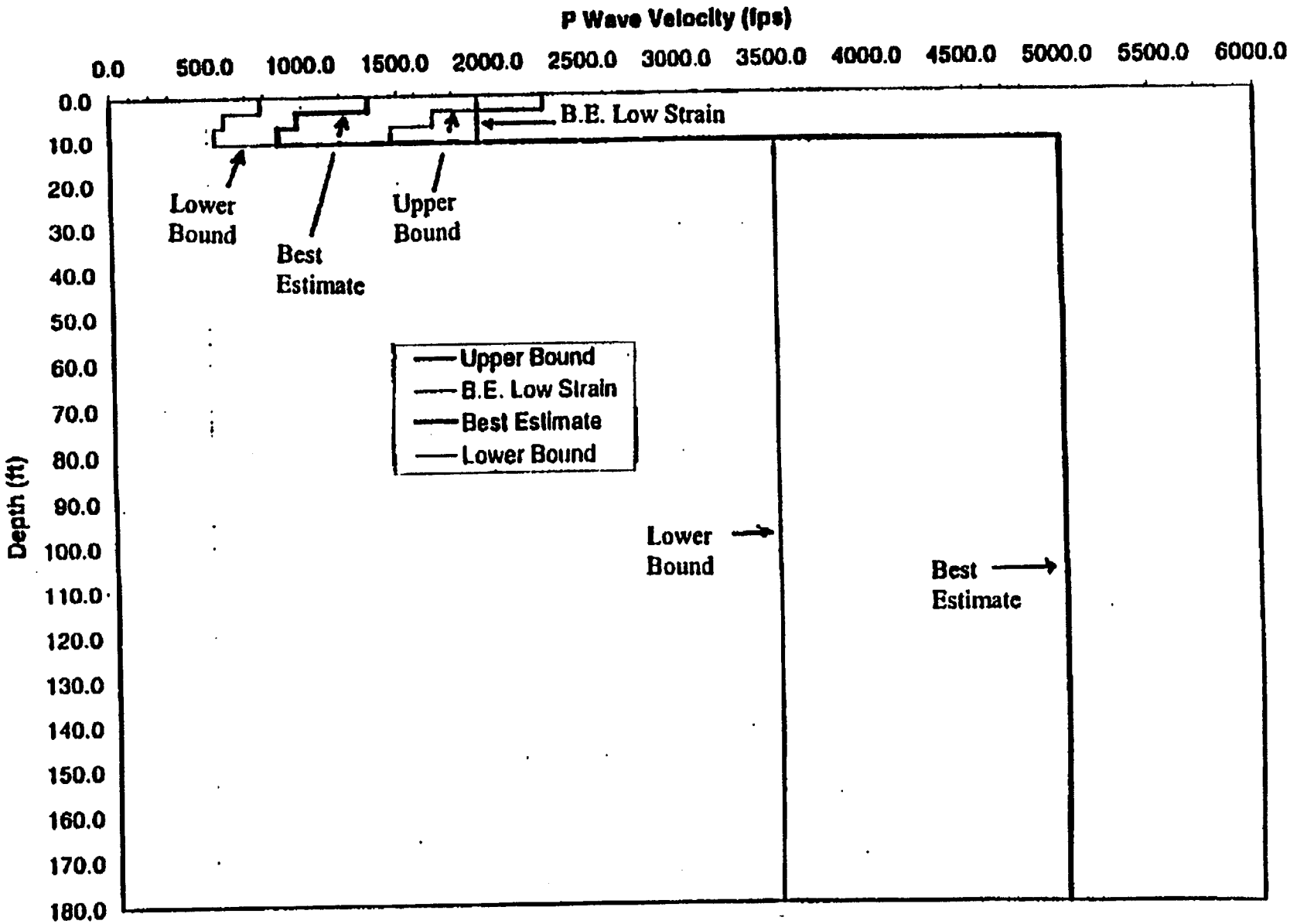

Figure 3-6: Strain Compatible P Wave Velocity

Table 4-1

SUMMARY OF CASKS PROPERTIES (INCLUDING WALLS)

CASK	CG (ft)			Weight (kips)	Wxx ($k\text{-}ft^2$)	Wyy ($k\text{-}ft^2$)	Wzz ($k\text{-}ft^2$)
	X (1)	Y (2)	Z (3)				
1	6.00	11.292	10.0	686.80	52,657.78	31,038.35	36,757.64
2	4.25	11.292	10.0	481.01	36,879.61	19,333.10	23,338.68
3	4.25	11.292	10.0	481.01	36,879.61	19,333.10	23,338.68
4	4.25	11.292	10.0	481.01	36,879.61	19,333.10	23,338.68
5	4.25	11.292	10.0	481.01	36,879.61	19,333.10	23,338.68
6	4.25	11.292	10.0	481.01	36,879.61	19,333.10	23,338.68
7	4.25	11.292	10.0	481.01	36,879.61	19,333.10	23,338.68
8	4.25	11.292	10.0	481.01	36,879.61	19,333.10	23,338.68
9	4.25	11.292	10.0	481.01	36,879.61	19,333.10	23,338.68
10	6.00	11.292	10.0	686.80	52,657.78	31,038.35	36,757.64

(1) From internal side

(2) From front side

(3) From bottom

Table 4-2

NODAL NUMBERS

CASK	At Cask CG	At Slab Below Cask CG
1	817	475
2	818	514
3	819	540
4	820	566
5	821	592
6	822	618
7	823	644
8	824	670
9	825	696
10	826	735

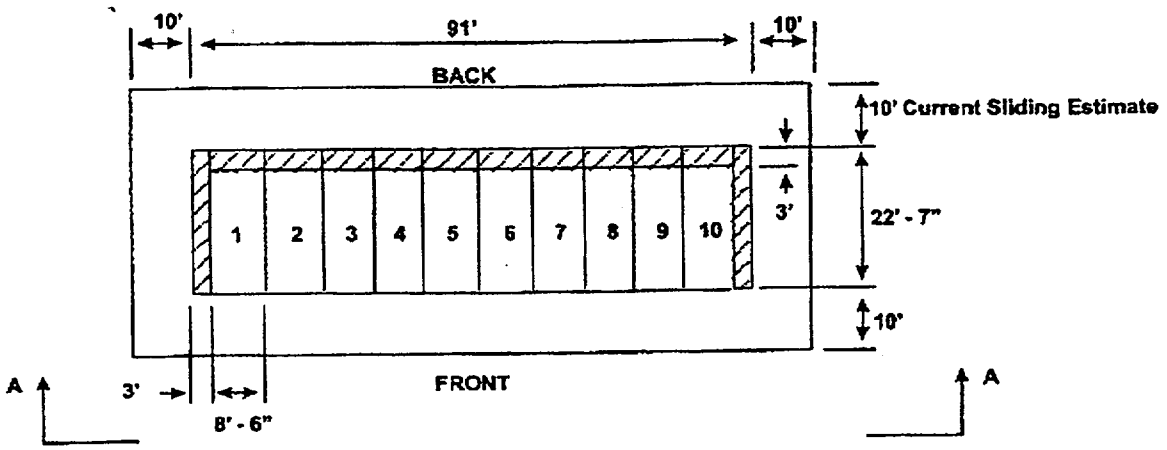

PLAN VIEW

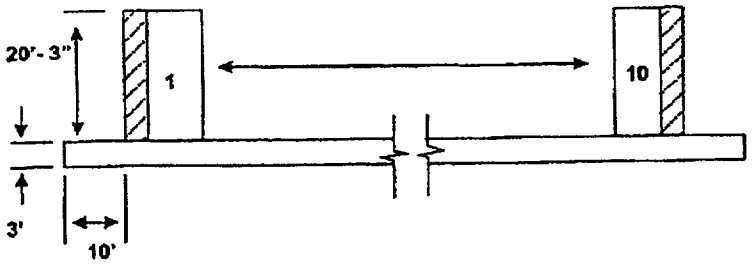

SECTION A-A

Figure 4-1: ISFSI Dimensions and Configuration

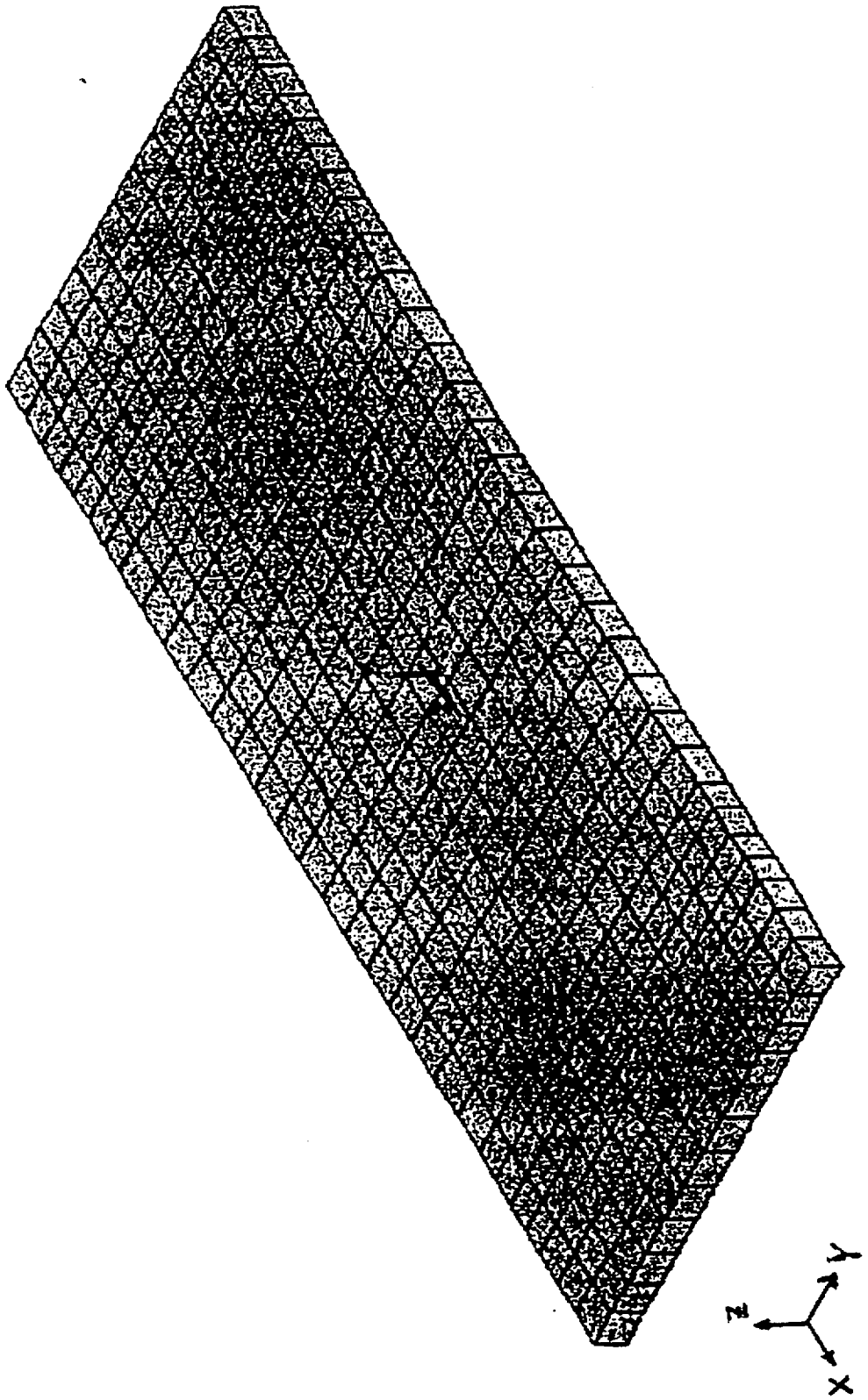

Figure 4-2: Concrete Pad Finite Element Model

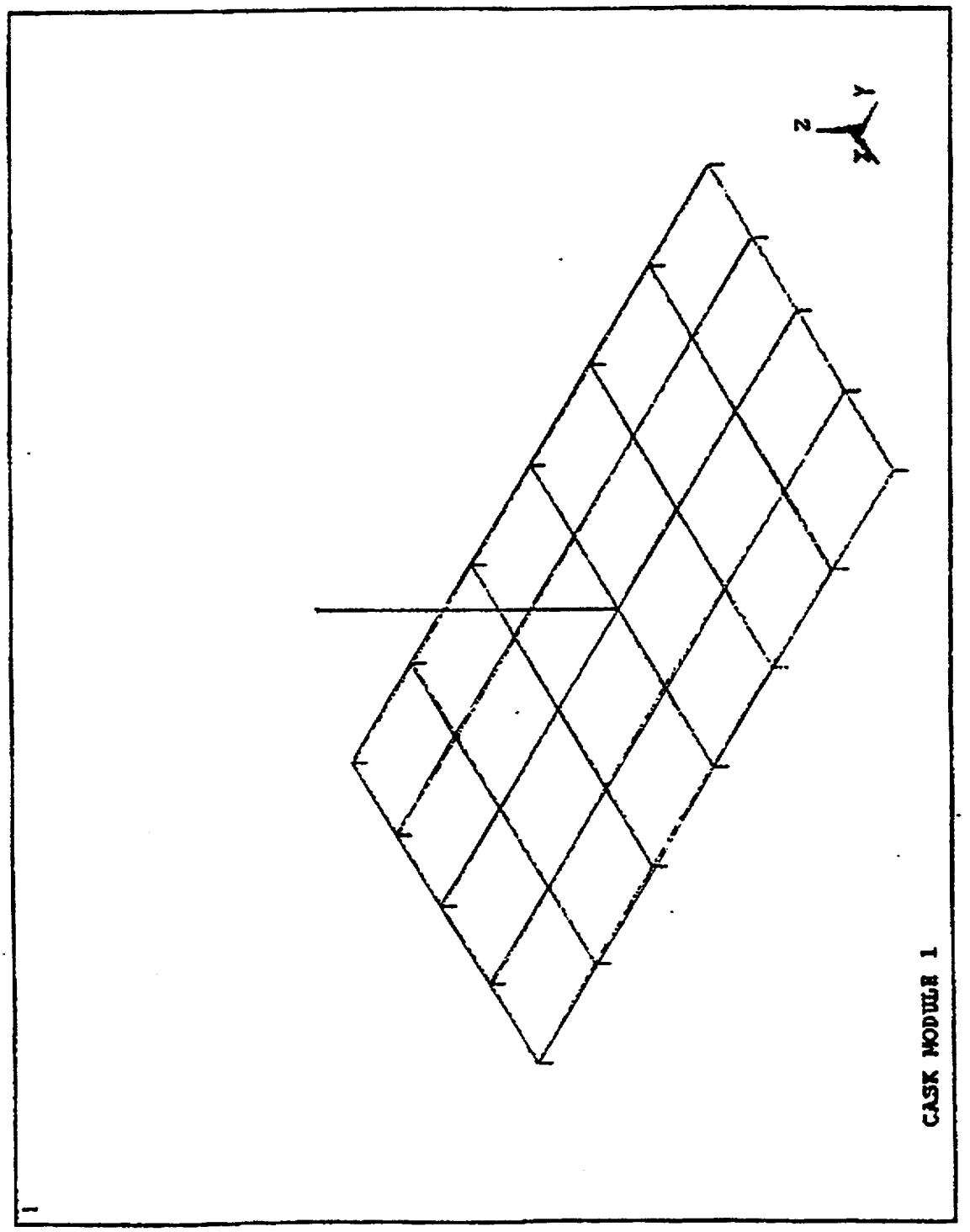

Figure 4-3a: Model Casks 1 and 10 (Footprint includes back and side shield walls)

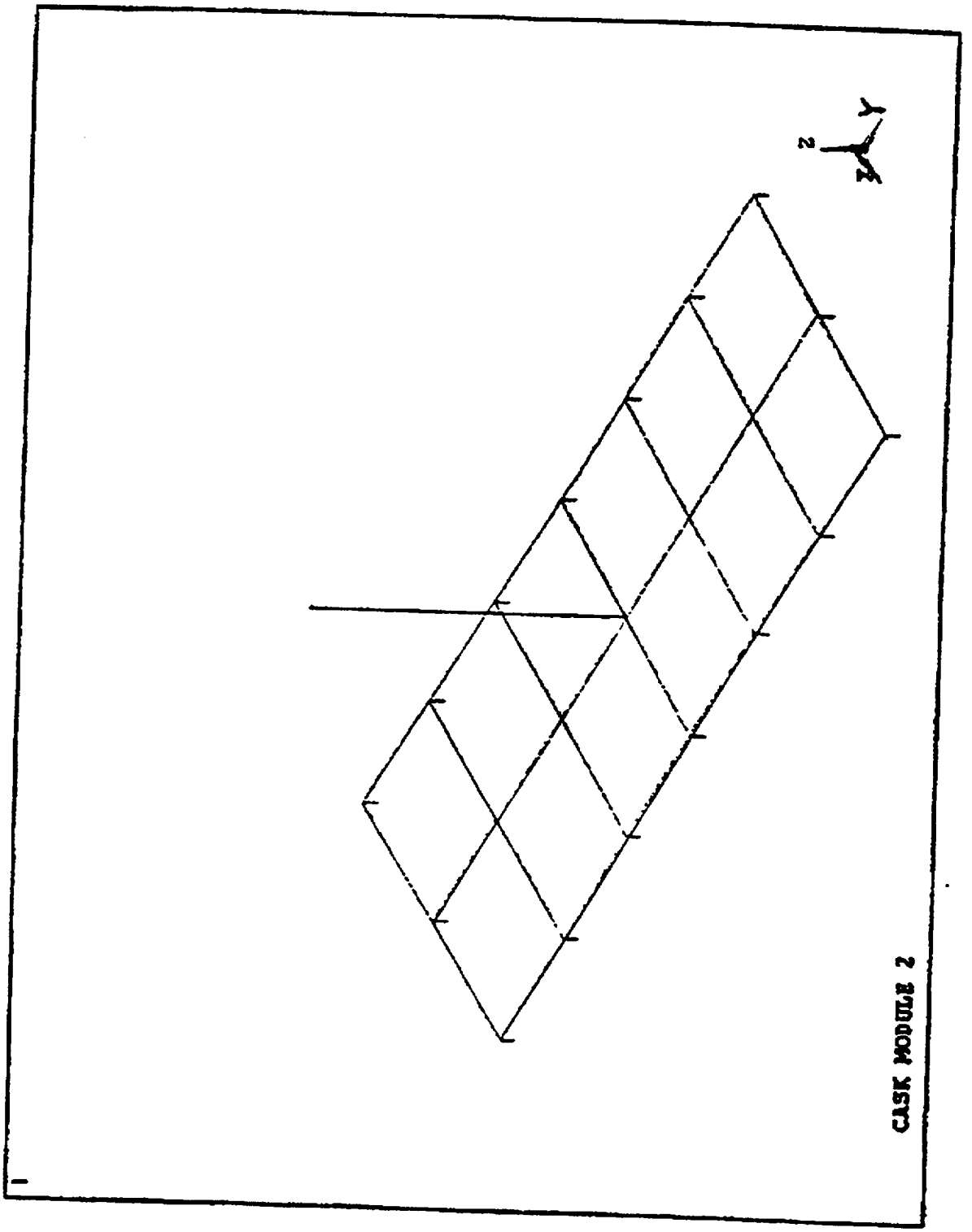

Figure 4-3b: Model Casks 2 to 9 (Footprint includes back shield wall)

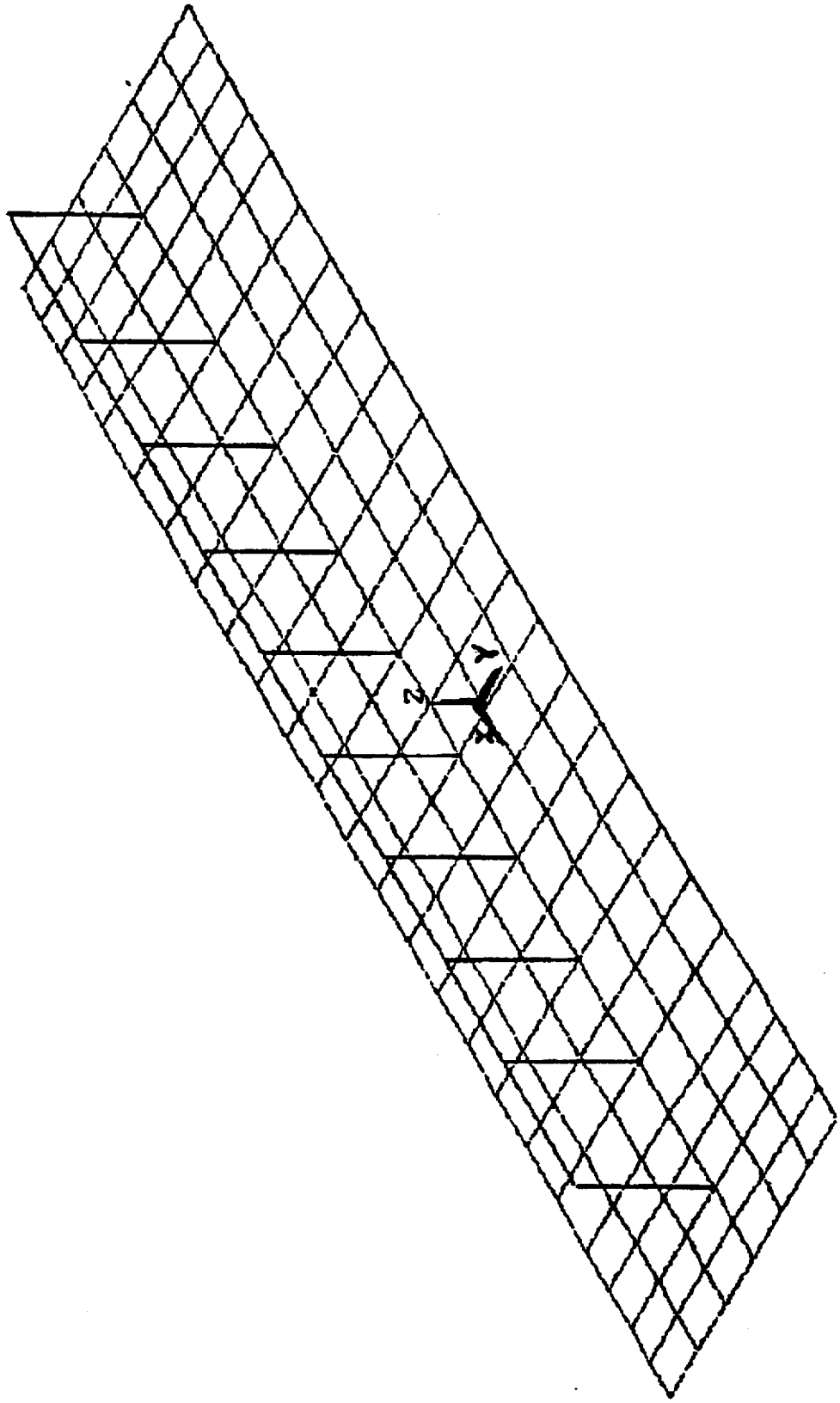

Figure 4-3c: Combined Model for Casks 1 to 10
(Horizontal, very soft axial elements connecting the tops of the vertical beams were included to allow monitoring of potential relative motion between cask CGs)

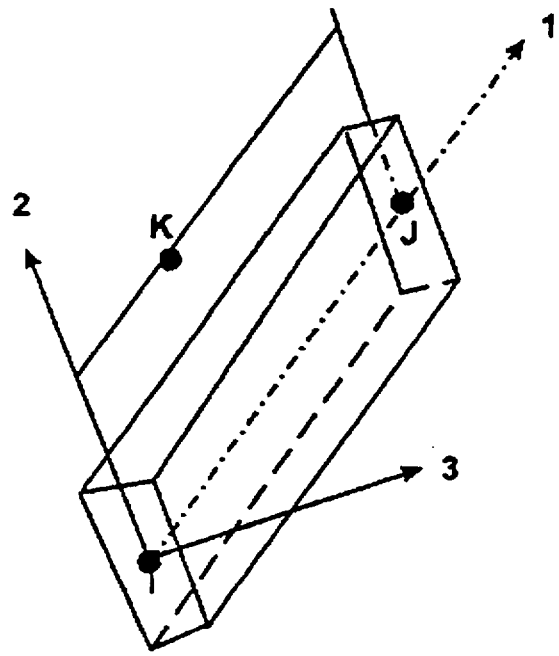

For "Cask" Elements

Local Axis 1 = Global Axis Z

Local Axis 2 = Global Axis X

Local Axis 3 = Global Axis Y

Figure 4-4: Local Coordinate System for Beam Elements. Module HOUSE

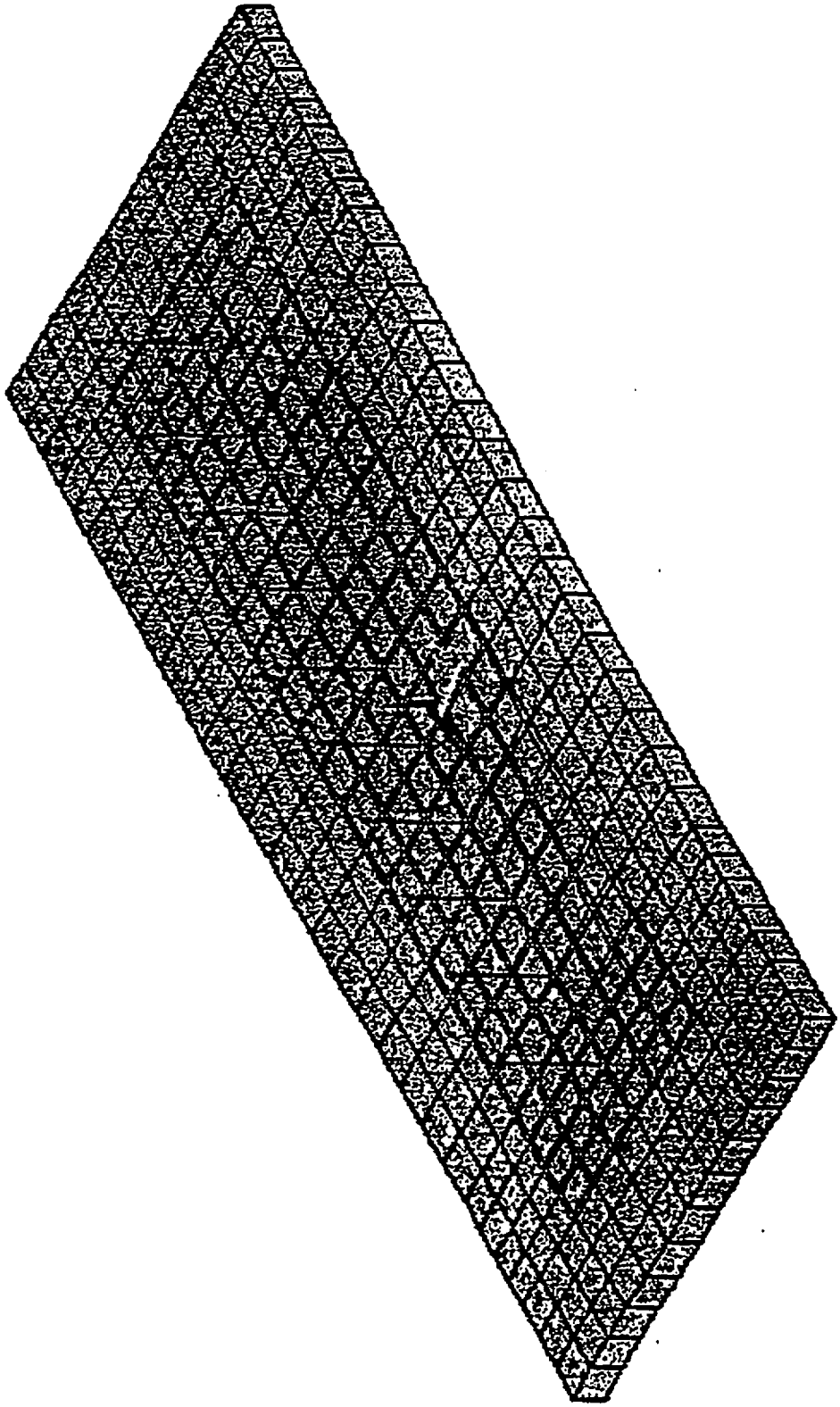

Figure 4-5: Combined Models of Casks and Concrete Pad

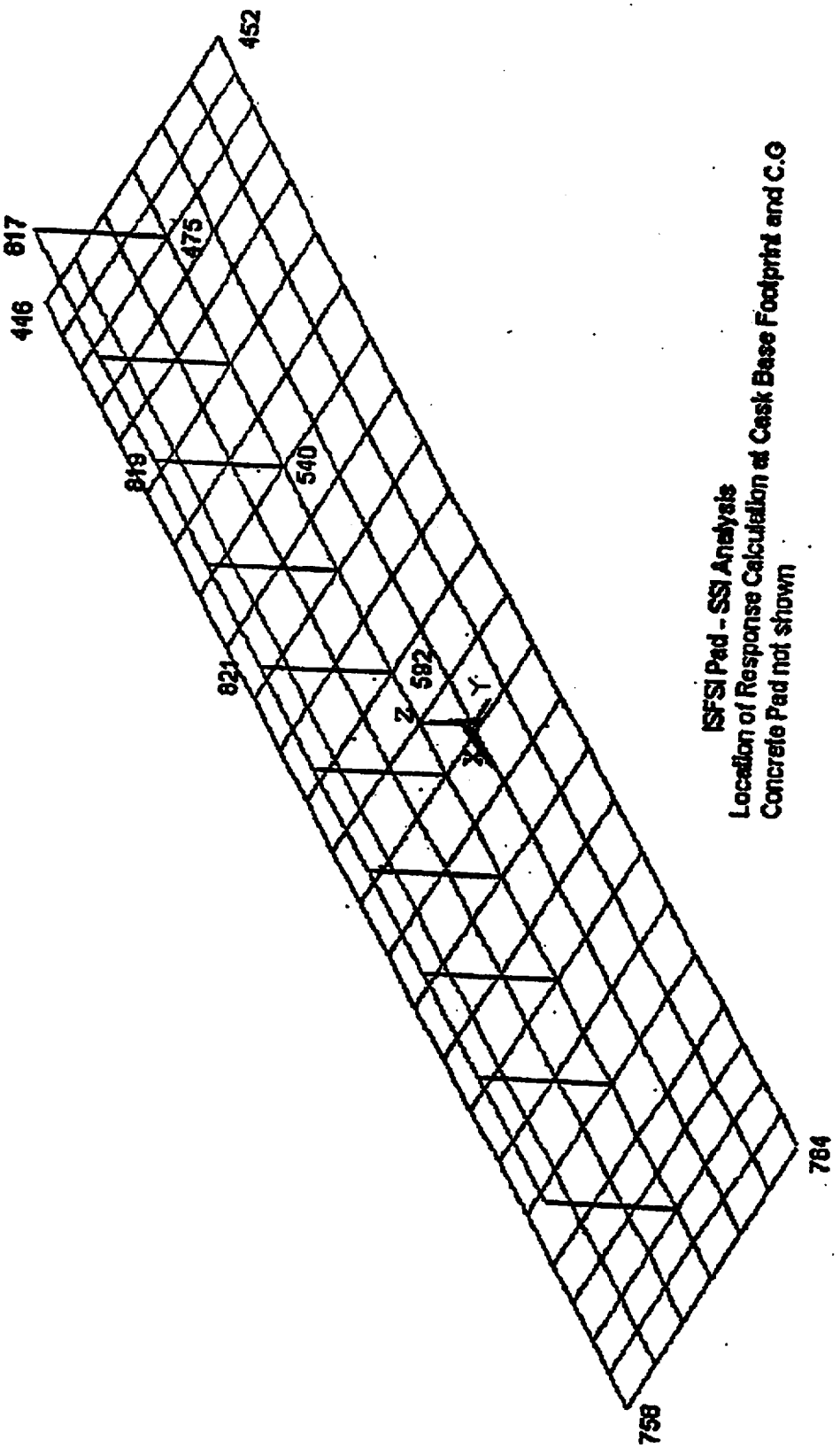

Figure 4-6: Location of Response Calculation

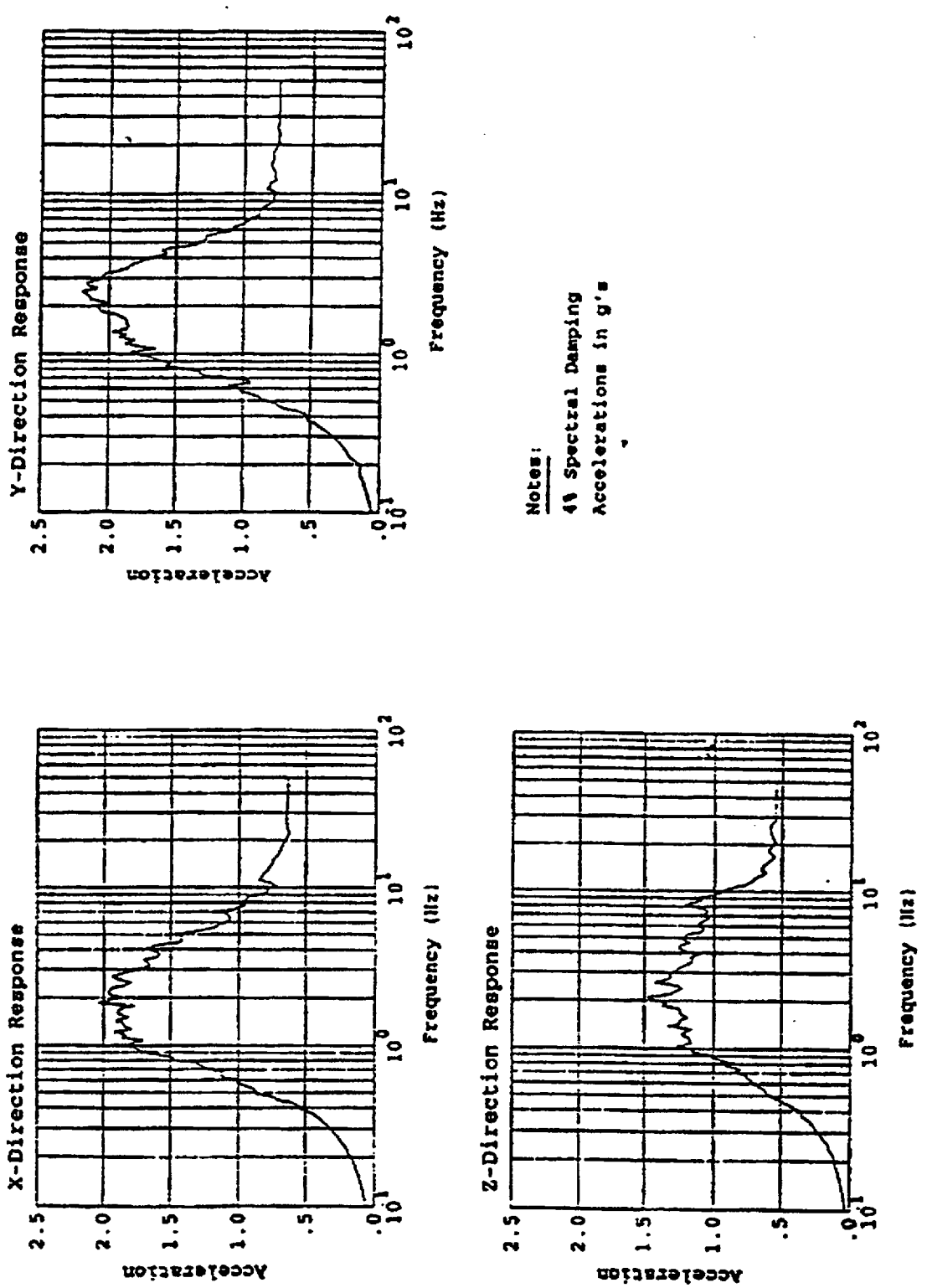

Figure 6-1: ISFSI SSI SASSI Solution: 100% Cask Mass, Lower Bound Soil, X+Y+Z EQ, Envelope All Locations

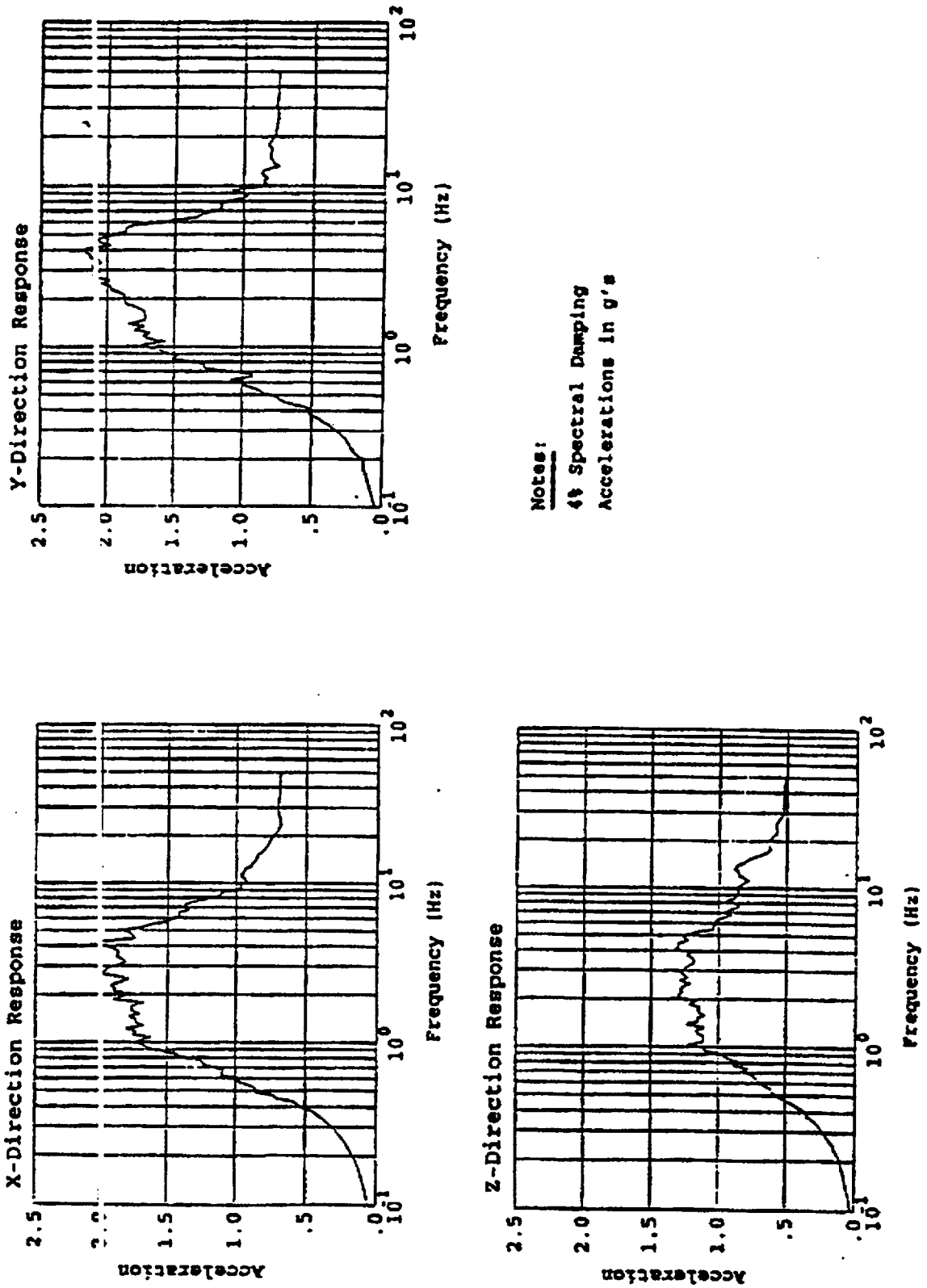

Figure 6-2: ISFSI SSI SASSI Solution: 100% Cask Mass, Best Estimate Soil, X+Y+Z EQ, Envelope All Locations

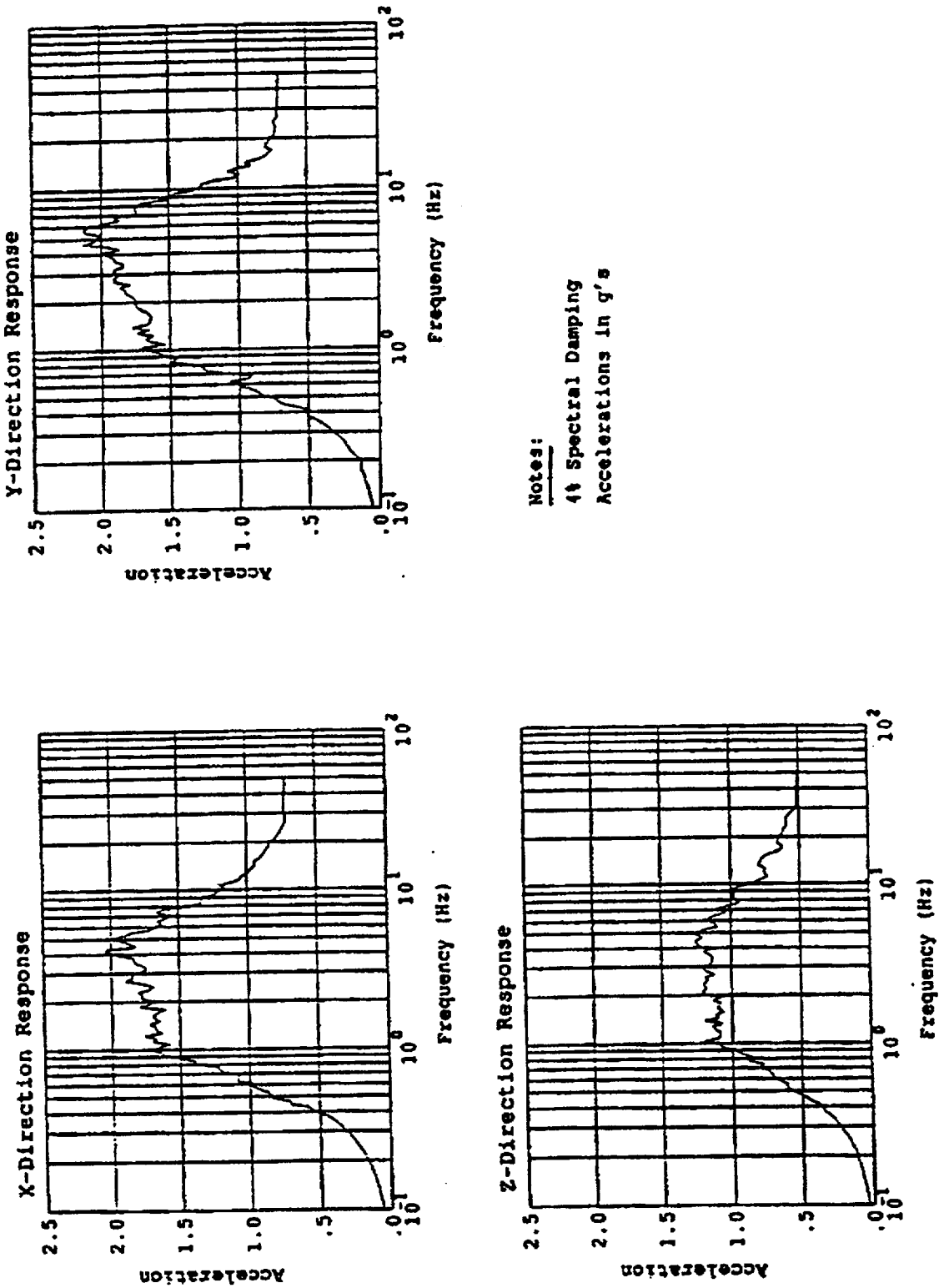

Figure 6-3: ISFSI SSI SASSI Solution: 100% Cask Mass, Upper Bound Soil, X+Y+Z EQ, Envelope All Locations

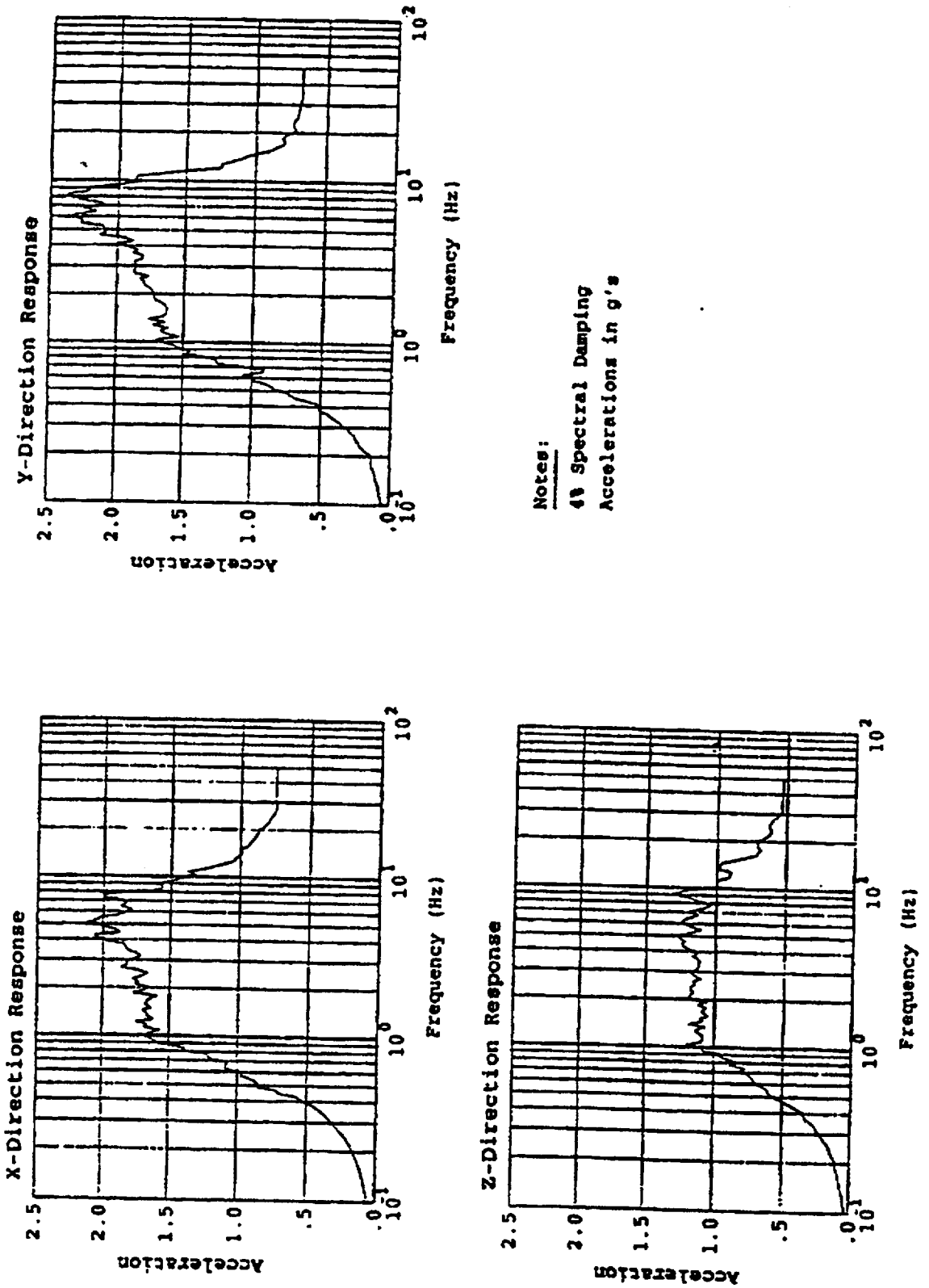

Figure 6-4: ISFSI SSI SASSI Solution: 100% Cask Mass, Low Strain Soil, X+Y+Z EQ, Envelope All Locations

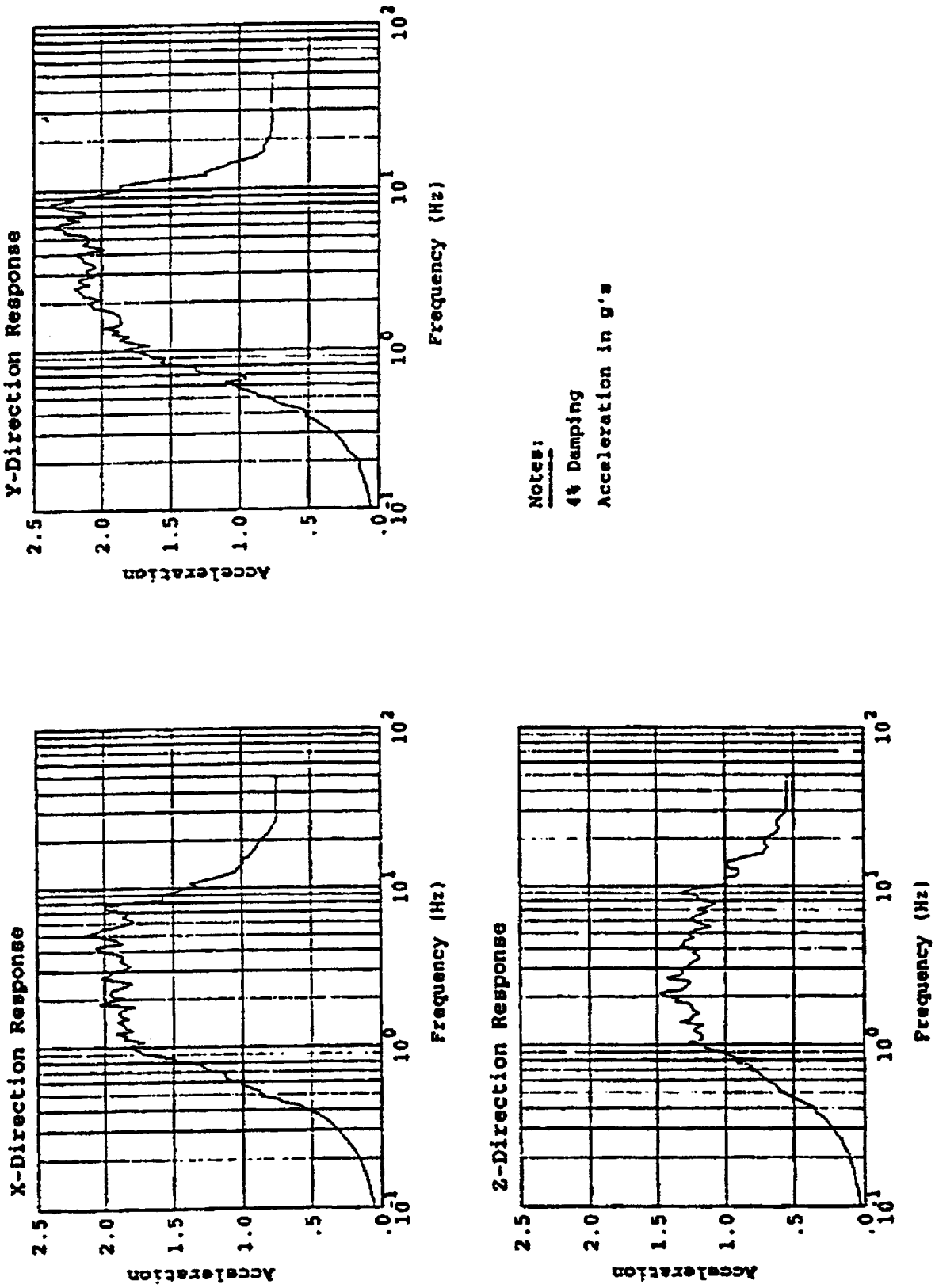

Figure 6-5: ISFSI SSI SASSI Solution: 100% Cask Mass, Envelope LB, BE, UB, LS Soil, X+Y+Z EQ, Envelope All Locations

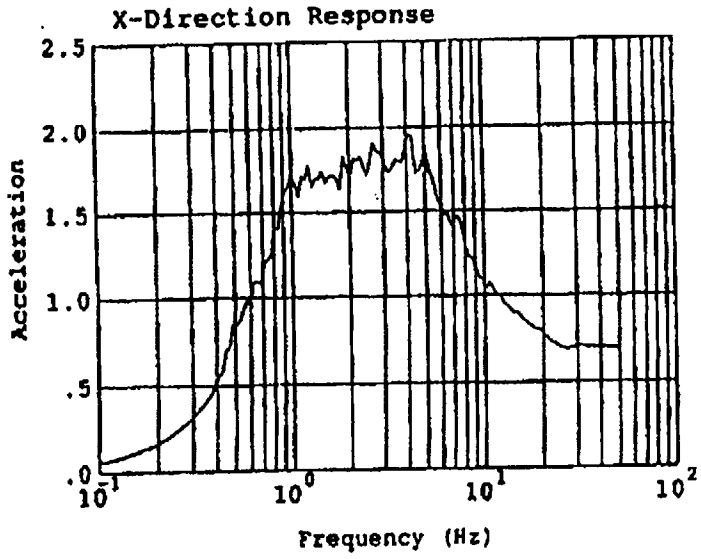

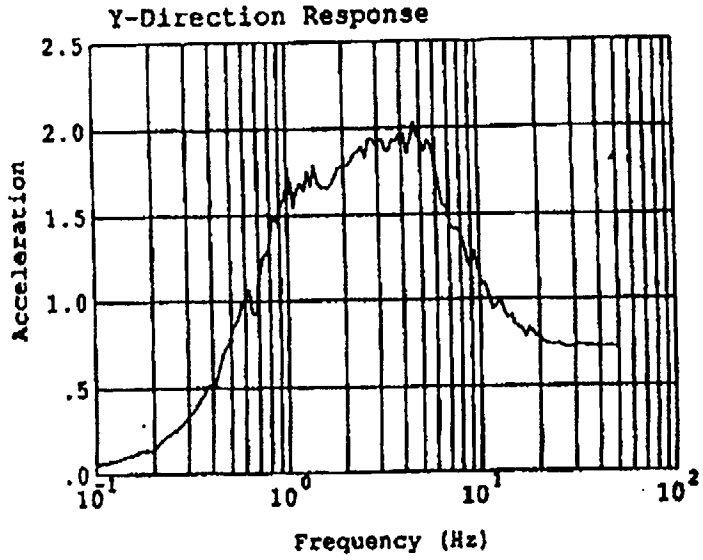

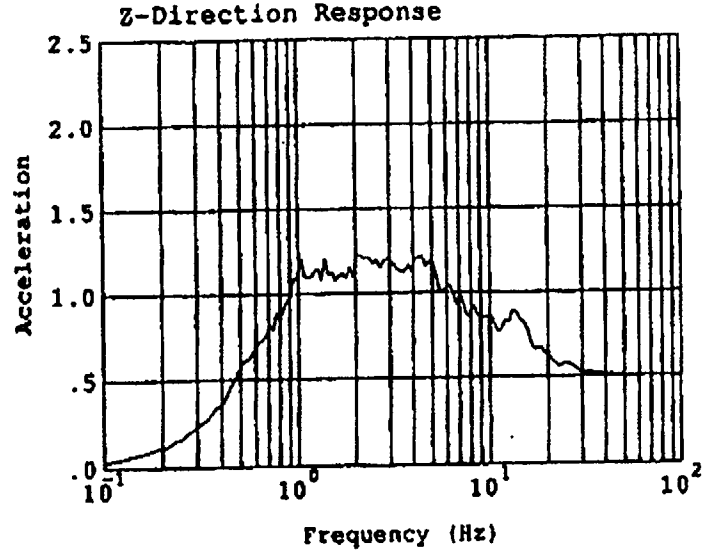

Notes:

4% Spectral Damping

Accelerations in g's

Figure 6-6: ISFSI SSI SASSI Solution: Hall Cask Mass, Best Estimate Soil, X+Y+Z EQ, Envelope All Locations

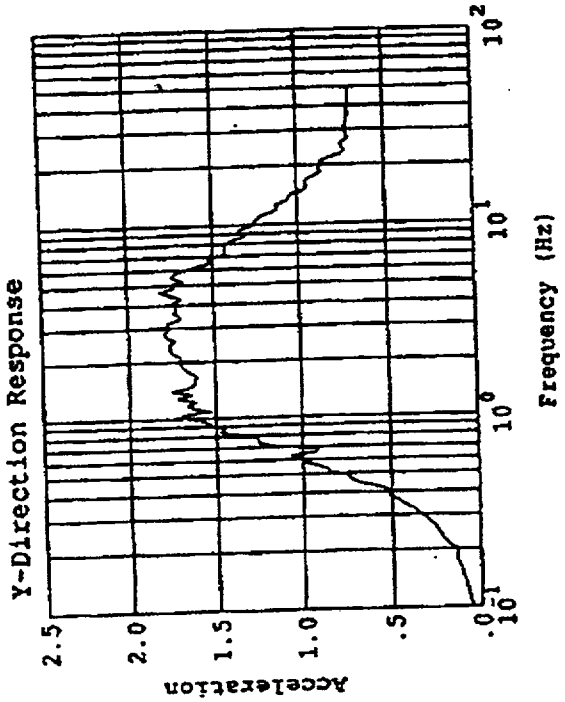

Notes:
4% Spectral Damping
Accelerations in g's

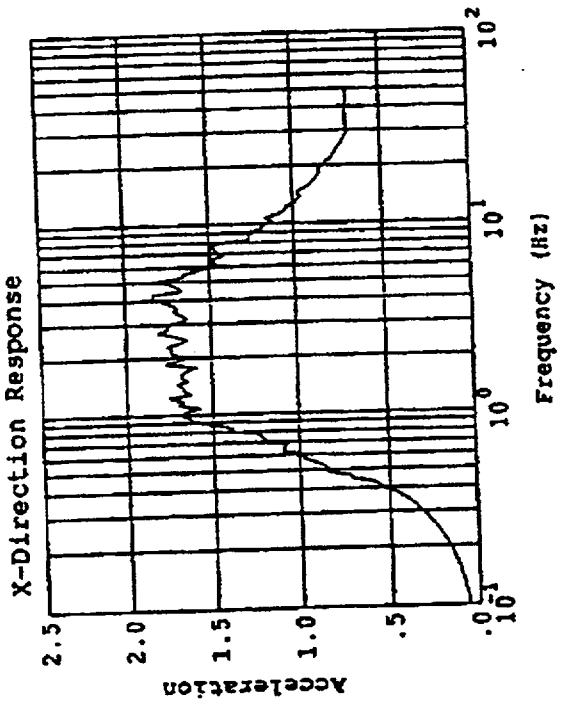

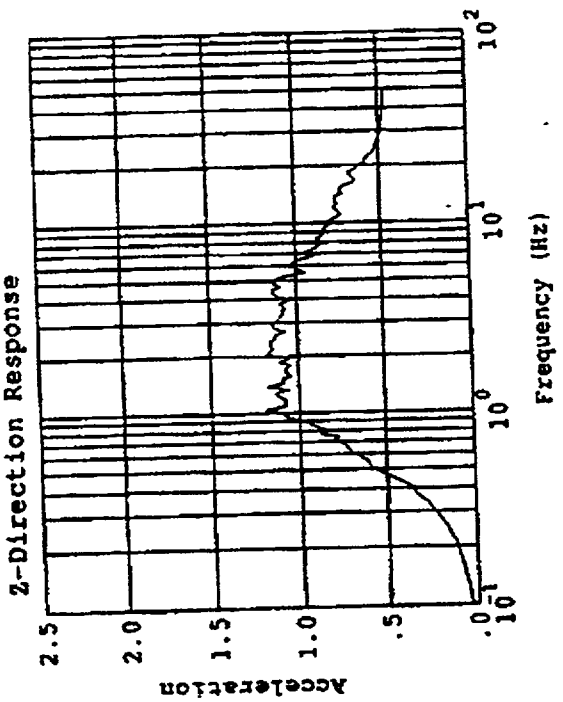

Figure 6-7: ISFSI SSI SASSI Solution: No Cask Mass, Best Estimate Soil, X+Y+Z EQ, Envelope All Locations

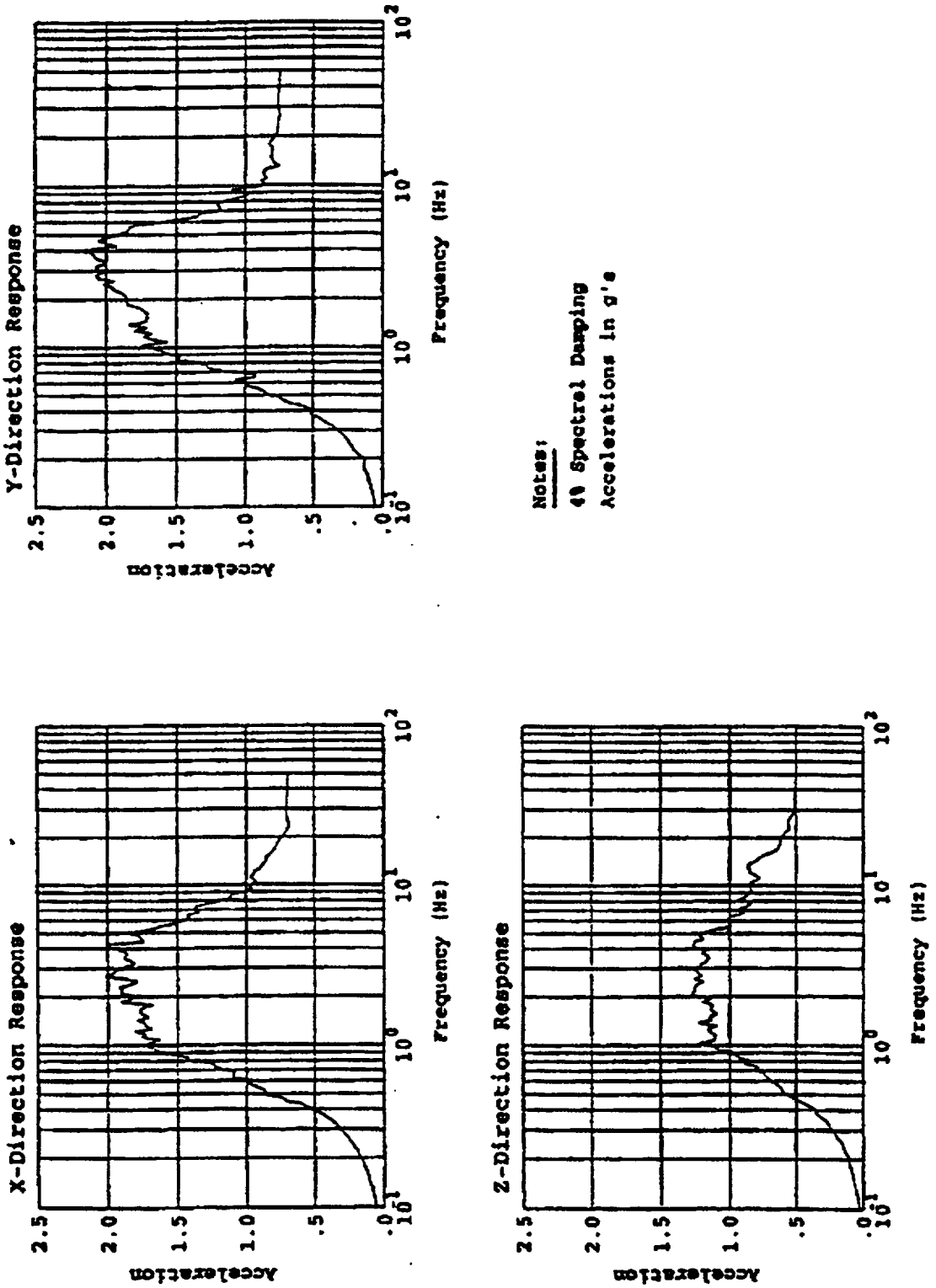

Figure 6-8: ISFSI SSI SASSI Solution: 100% Cask Mass, Rigid Pad, Best Estimate Soil, X+Y+Z EQ, Envelope All Locations

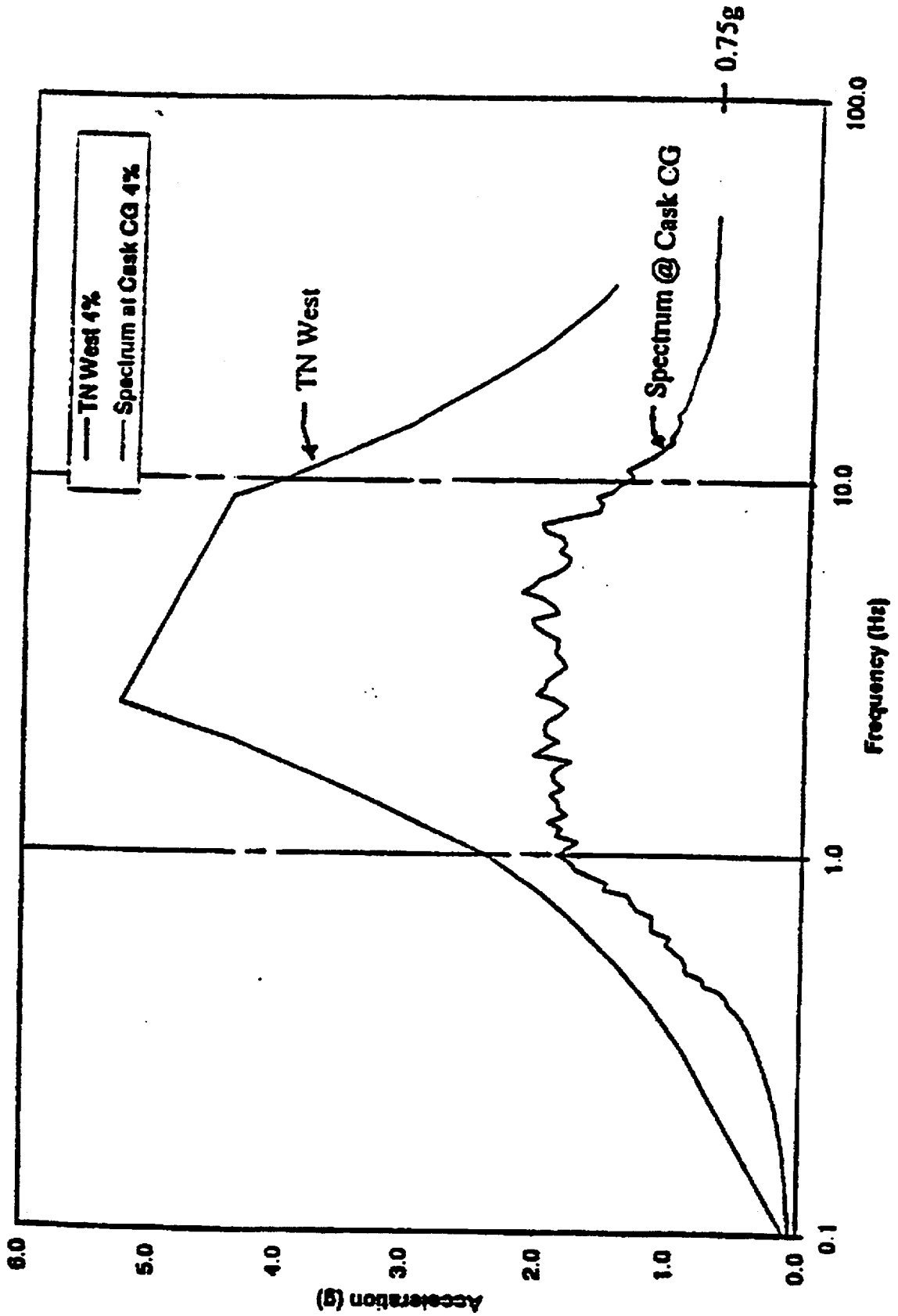

Figure 6-9a: TN West vs. SSE Casks CG Spectra – Horizontal Longitudinal Direction

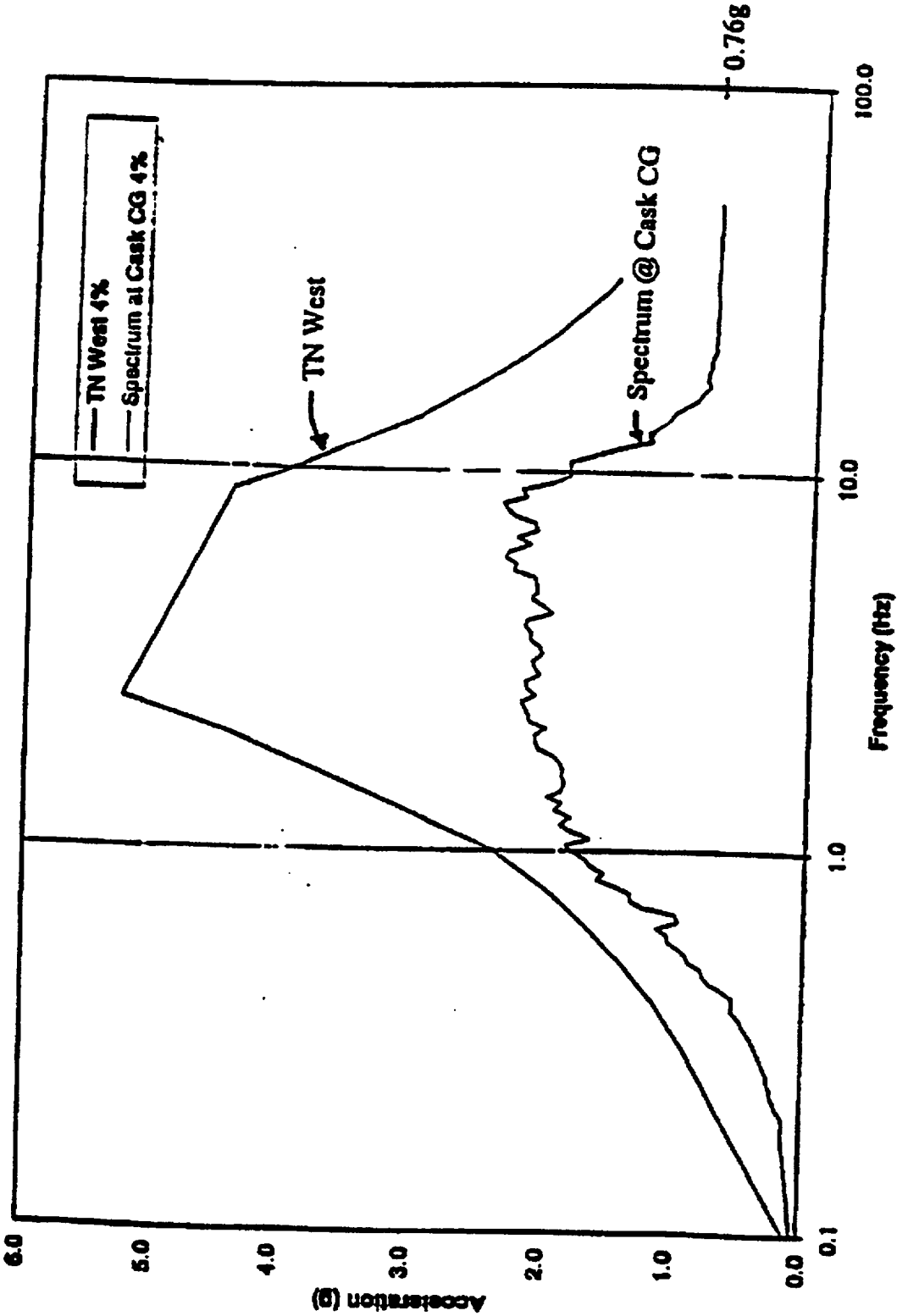

Figure 6-9b: TN West vs. SSE Casks CG Spectra – Horizontal Transverse Direction

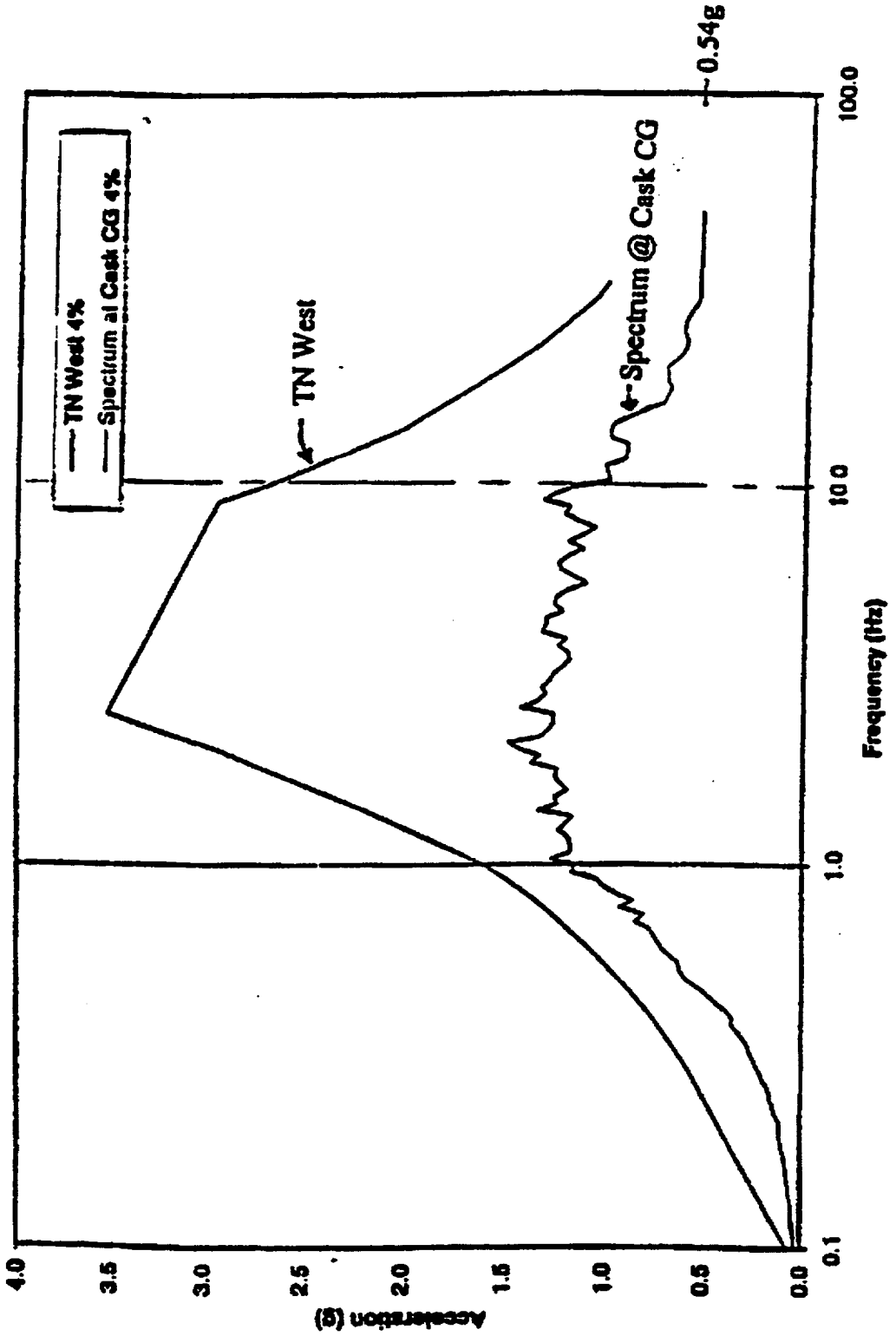

Figure 6-9c: TN West vs. SSE Casks CG Spectra – Vertical Direction